Chloroplast protein import in stress and disease

Robert G. Sowden

Magdalen College

Trinity term 2019



Contents

Acknowledgements 7

Abbreviations 8

0. Abstract 13

1. General introduction 15

1.1 Format 16

1.2 Introduction to chloroplasts 17

1.2.1 The plastids 17

1.2.2 Plastid biogenesis 18

1.2.3 Retrograde signalling coordinates biogenesis and stress responses 18

1.3 Plastid protein import pathways 20

1.3.1 Plastid protein targeting 20

1.3.2 The translocon at the outer chloroplast envelope membrane 21

1.3.3 The translocon at the inner chloroplast envelope membrane 22

1.3.4 The TOC-TIC supercomplex and peripheral components 23

1.3.5 Import of envelope proteins 25

1.3.6 Non-canonical import pathways 27

1.4 Organellar protein regulation by the ubiquitin-proteasome system 29

1.4.1 The ubiquitin-proteasome system 29

1.4.2 The 26S proteasome 30

1.4.3 Regulation of chloroplast protein import by ubiquitin 31

1.4.4 UPS regulation of organelle proteins 33

1.4.5 Chloroplast-associated protein degradation 36

1.5 Chloroplasts and oxidative stress 38

1.5.1 Chloroplasts cause oxidative stress 38

1.5.2 Avoidance and scavenging help to manage ROS 38

1.5.3 Turnover of damaged chloroplast components reduces ROS production 40

1.6 The plant immune system 42

1.6.1 The multiphase zig-zag model 42

1.6.2 *Pseudomonas syringae*: an important model pathogen 43

1.7 Phytohormones and immunity 45

1.7.1 Chloroplasts produce phytohormones to tailor immune responses 45

1.7.2 Retrograde signalling regulates hormone biosynthesis in immunity 47

1.7.3 Pathogens target phytohormone production to promote virulence 49

1.8 ROS dysregulation enhances plant immunity 50

1.8.1 Pathogen recognition initiates a ROS cascade 50

1.8.2 Disruption of ROS management promotes immunity 51

1.8.3 Apoplastic and chloroplastic ROS 52

1.9 Pathogens target the chloroplast compartment to achieve virulence 54

1.9.1 NECG expression is altered during immunity and virulence 54

1.9.2 Some effectors are imported into the chloroplast 56

1.9.3 Non-canonical import of effectors 57

1.9.4 Chloroplast proteins are targets of effectors 58

1.9.5 Effectors can alter host protein localisation 59

1.10 Aims 60

1.11 Figures 61

2. Effect of SP1 on immunity 71

2.1. Abstract 72

2.2. Introduction 73

2.3. Results 75

2.3.1. *sp1* mutant plants show enhanced immunity 75

2.3.2. *sp1* plants show increased chloroplastic ROS accumulation in disease 76

2.3.3. Dynamics of chloroplast oxidation during early stages of infection 78

2.3.4. ROS production during disease parallels abiotic stress 80

2.3.5. Generation of ROS by photosynthesis is necessary for the resistance phenotype of *sp1* 82

2.4. Discussion 84

2.4.1. The suppression of PTI by *Pst*DC3000 depends on an SP1-mediated pathway 84

2.4.2. The enhanced immune response of *sp1* is not constitutive 85

2.4.3. Persistent differential growth of the two bacterial strains suggests additional PTI signalling events 87

2.4.4. Timing of chloroplast ROS burst 88

2.4.5. Mechanism of SP1-mediated ROS avoidance 90

2.4.6. *P. syringae* activates a host system of stress tolerance inappropriately to facilitate infection 93

2.5. Figures and tables 95

3. Regulation of chloroplast protein import during infection 111

3.1. Abstract 112

3.2. Introduction 113

3.3. Results 115

3.3.1. Pathogenesis induces mislocalisation of a chloroplast-targeted probe 115

3.3.2. Chloroplast-targeted probe mislocalisation is not the result of a loss of chloroplast membrane integrity 116

3.3.3. A microscopy-based method for the comparison of the rates of chloroplast protein import 117

3.3.4. Rate of chloroplast protein import is reduced during ETS 119

3.3.5. The chloroplast-targeted probe mislocalisation induced by *Pst*DC3000 depends on SP1 119

3.3.6. The TOC machinery is targeted for turnover during infection in an SP1-dependent manner 120

3.4. Discussion 122

3.4.1. Explanation for and sequence of events in *Pst*DC3000-induced chloroplast-targeted probe mislocalisation 122

3.4.2. Biological considerations for the FRAP-based assay for import 124

3.4.3. Technical considerations for the FRAP-based assay for import 125

3.4.4. Commonality between PTI and ETS 127

3.4.5. Model for the role of SP1 in chloroplast protein import modulation during abiotic and biotic stresses 128

3.5. Figures 129

4. Photosynthesis during infection 145

4.1. Abstract 146

4.2. Introduction 147

4.2.1. Photosynthesis 147

4.2.2. Chlorophyll fluorescence 148

4.2.3. Photosynthesis during immunity 149

4.3. Results 152

4.3.1. Changes to chlorophyll fluorescence during infection 152

4.3.2. Frequency of chlorophyll fluorescence measurements affects photochemistry during infection 153

4.4. Discussion 154

4.4.1. The efficiency of photochemistry during infection 154

4.4.2. Significance of the *NPQ* parameter 155

4.4.3. Significance of F_v/F_m as a stress measurement 156

4.4.4. Role of NPQ in virulence 157

4.4.5. Reported changes to photosynthetic parameters during disease may represent loss of circadian entrainment 158

4.4.6. Pathogenesis suppresses photosynthesis but does not alter the efficiency of photochemistry 159

4.5. Figures 162

5. Metabolic changes during infection 164

5.1. Abstract 165

5.2. Introduction 166

5.2.1. Transmission of redox signalling 166

5.2.2. Metabolomics 167

5.3. Results 169

5.3.1. Identification of metabolites that are differentially abundant between *sp1* and the wild type 169

5.3.2. Interactions between the metabolic phenotypes of the *sp1* mutation and inoculation 171

5.3.3. Metabolic signatures of PTI and ETS 173

5.4. Discussion 176

5.4.1. Phytohormones and *sp1*-mediated immunity 176

5.4.2. Lipid metabolism and *sp1*-mediated immunity 177

5.4.3. Untargeted analysis of metabolic differences in immunity and disease..180
5.5. Figures and tables 182
6. Concluding remarks 196
6.1 Principal findings 197
6.2 Regulation of SP1 by *P. syringae* 198
6.3 Perception of the chloroplast ROS burst 202
6.4 Considerations for the engineering of stress tolerant crops 203
6.5 Figure 205
7. Methods 207
7.1 Plant growth conditions 208
7.1.1 Growth on soil 208
7.1.2 Growth on solid media 208
7.2 Bacterial inoculation 209
7.2.1 Bacterial growth 209
7.2.2 Dilution 209
7.2.3 Syringe inoculation 209
7.2.4 Determination of bacterial growth 209
7.3 Callose deposition 211
7.3.1 Plant material 211
7.3.2 Slide preparation 211
7.3.3 Microscopy 211
7.3.4 Analysis 211
7.3.5 Presentation 212
7.4 DCF fluorescence 213
7.4.1 Material 213
7.4.2 Slide preparation 213
7.4.3 Microscopy 213
7.4.4 Presentation 214
7.5 Redox fluorescent probe under biotic stress 215
7.5.1 Line crossing 215

7.5.2 Material 215
7.5.3 Microscopy 215
7.5.4 Analysis 216
7.6 Redox fluorescent probe under abiotic stress 217
7.6.1 Material 217
7.6.2 Visualisation 217
7.6.3 Analysis 217
7.7 Localisation of fluorescent probe 218
7.7.1 Plant transformation 218
7.7.2 Microscopy 218
7.8 Measuring import rates by photobleaching 219
7.8.1 Microscopy 219
7.8.2 Photobleaching 219
7.9 Protein assay 220
7.9.1 Protein extraction 220
7.9.2 Gel electrophoresis and western blotting 220
7.9.3 Quantification 220
7.10 Chlorophyll fluorescence measurements 221
7.10.1 Extraction and mass spectroscopy 222
7.10.2 Inoculation 221
7.10.3 Fluorescence imaging 221
7.11 Metabolomics analysis 222
7.11.1 Plant material 222
7.11.2 Analysis 222
8. Bibliography 224

Acknowledgements

I have benefited greatly from the combined expertise and guidance of Professors Paul Jarvis and Gail Preston throughout my DPhil studies. In particular, I would like to thank them for their very helpful feedback on drafts of this thesis.

I must thank all members of the Jarvis group, past and present, for the many contributions they have made to the understanding of chloroplast protein import that have made this project possible. In particular, I am grateful for the technical support of Na Li and Dr Qihua Ling, whom I must also thank for the insightful analysis he has often afforded me on my work as my project developed.

I would like to thank Naomi Cannell for her advice on using R; Dr Zhe Ji for his assistance with genotyping; Edward Smith for fielding my many questions about LC-MS; and Dr Tomáš Zeman for his advice on mathematics. I am grateful to Prof. Mark Fricker and the late Prof. Ian Moore for their advice and assistance with confocal microscopy.

⁂

Goodbye to everyone who has made my time at Oxford and Plant Sciences so colourful, including Tom King, James Whisker, and Dr Ellis O'Neill.

I do not know how to describe how much I have grown personally during the course of my studies here; instead I can only express my gratitude to everyone who has been part of this experience. I am indebted to my family and friends, in addition to those mentioned above, for all their support, advice, and patience, especially to Muriel and Richard Sowden, Stephen Blanchard, Dr Lottie Chapman, Dr Timothy Gao, Richard G. IL. Kendall, Liam Loan-Lack, Dr Noreen Masud, and Nicola Rae.

As I write now it is the week before the start of Michaelmas term. I am flooded with fond memories of all the people who helped me find my feet here, and all the ways they made Oxford become my home. I suddenly feel that I have come to the end of a journey, and am desperately envious of all those who are due, in one week's time, to start theirs.

Abbreviations

A

ABA: abscisic acid.

ACC: 1-aminocyclopropane-1-carboxylic acid.

AKR: ankyrin repeat.

ALB3: albino 3.

ANOVA: analysis of variance.

AOS: allene oxide synthase.

APG1: albino or pale green mutant 1.

ATG: autophagy-related.

ATP: adenosine triphosphate.

ATS: acyltransferase.

B

BAK1: brassinosteroid-associated kinase 1.

C

CAH1: α-carbonic anhydrase 1.

Cbl: casitas B-linease lymphoma.

CCA1: circadian clock associated 1.

Cdc48: cell division cycle 48.

CDPK: calcium-dependent protein kinase.

ceh1: *constitutively expressing HPL.*

ceQORH: chloroplast envelope quinone oxidoreductase homologue.

CFDA: carboxyfluorescein diacetate.

CFU: colony forming units.

CHIP: C-terminus of Hsc70-interacting protein.

CHLORAD: chloroplast associated protein degradation.

Clp: caseinolytic proteinase.

CoA: coenzyme A.

COI1: coronatine insensitive 1.

cpGFP: chloroplast-targeted GFP.

cpHsc: chloroplast heat sock cognate.

CPR1: consitutive expressor of pathogenesis related genes 1.

D

Da: Dalton.

DAG: diacylglycerol.

DAMP: damage-associated molecular pattern, 41

DAPI: 4′,6-diamidino-2-phenylindole.

DCF: dichlorofluorescein.

DCFH-DA: 2′,7′-dichlorodihydrofluorescein diacetate.

DCMU: 3-(3,4-dichlorophenyl)-1,1-dimethylurea.

Dfm1: derlin-like family member protein 1.

Doa1: degradation of alpha 1.

Doa10: degradation of alpha 10.

DUB: de-ubiquitinating isopeptidase.

E

EGAD: endosome and Golgi associated degradation.

ER: endoplasmic reticulum.

ERAD: ER-associated protein degradation.

ET: ethylene.

ETI: effector-triggered immunity.

ETS: effector-triggered susceptibility.

EX1, 2: executer 1, 2.

EXPA4: α-expansin 4.

F

FIJI: FIJI is not ImageJ.

FKBP73: FK506 binding protein 73.

FLS2: flagellin sensitive 2.

FRAP: fluorescence recovery after photobleaching.

FtsH: filamentous temperature sensitive H.

G

GA: gibberellic acid.

GaAsP detector: gallium arsenide phosphide detector.

GFP: green fluorescent protein.

GLI1: glycerol insensitive 1.

GLY1: plastidic GPDH.

GPDH: glycerol-3-phosphate dehydrogenase.

GPDHC1: cytosolic GPDH.

Grx1: glutaredoxin 1.

GTP: guanosine-5'-triphosphate.

GUN: genomes uncoupled.

H

HECT: homologus to E6AP C-terminal.

Hop: Hsp70/Hsp90 organising protein.

HPL: hydroperoxide lyase.

HR: hypersensitive response.

Hrd1: HMG-CoA reductase degradation 1.

HRP: hypersensitive-response pilus.

HSD: honestly significant difference.

Hsp: heat shock protein.

I

IBRDC2: in-between RING fingers-domain containing protein 2.

ICS: isochorismate synthase.

IEM: chloroplast inner envelope membrane.

IEP32: inner envelope protein 32.

IMP: *myo*-inositol monophosphatase.

IMPL1: IMP like 1.

INMAD: inner nuclear membrane associated degradation.

J

JA: jasmonic acid.

JAZ: jasmonate ZIM domain proteins.

L

LACS: long chain acyl-CoA synthetase.

LB: lysogeny broth.

LC-MS: liquid chromatography-mass spectrometry.

LDAD: lipid droplet associated degradation.

LHY: late elongated hypocotyl.

M

MAD: mitochondria associated degradation (aka OMMAD).

MAMP: microbe-associated molecular pattern (aka PAMP).

MAPK or MPK: mitogen-activated protein kinase.

Mdm2: mouse double minute 2 homologue.

MEcPP: 2-C-methyl-D-erythritol-2,4-cyclopyrophosphate.

mEosFP: monomeric EOS fluorescent protein.

MEP: methylerythritol 4-phosphate.

MIPS: *myo*-inositol phosphate synthase.

mitoTAD: mitochondrial protein translocation assocaited degradation.

MKK: MAPK kinase.

MORF2: multiple organellar RNA editing factor 2.

MS: Murashige and Skoog.

N

NADP+: nicotinamide adenine dinucleotide phosphate.

NCED: 9-*cis*-epoxycarotenoid dioxygenase.

NECG: nucleus-encoded chloroplast gene.

NECP: nucleus-encoded chloroplast protein.

NEDD8: neural precursor cell expressed developmentally downregulated 8, aka RUB.

NLR4: nucleotide binding leucine repeat protein 4.

Npl4: nuclear protein localisation 4.

NPQ: (Fm / $F`m$) - 1. ; non-photochemical quenching.

O

OEM: chloroplast outer envelope membrane.

OEP: outer envelope protein.

OMMAD: outer mitochondrial membrane associated degradation (aka MAD).

OMP85: outer membrane protein 85.

OOP: organellar oligopeptidase.

OPDA: 12-oxo-phytodienoic acid.

OPR3: 12-oxophytodienoate reductase 3.

Oxa1: oxidase assembly protein 1.

P

PA: phosphatidic acid.

PAMP: pathogen-associated molecular pattern.

PAP: phosphonucleotide 3'-phosphoadenosine 5'-phosphate.

PC: plastocyanin.

PCD: programmed cell death.

PDF1.2: plant defensin 1.2.

ppi1: *plastid protein import 1* (aka *toc33).*

ppi2: *plastid protein import 2* (aka *toc159).*

PQ: plastoquinone.

PR1: pathogenesis-related 1.

PreP: presequence protease.

PS I, II: photosystem I, II.

Pst: *Psuedomonas syringae* pv. *tomato.*

PTI: PAMP-triggered immunity.

PUB: plant U box.

PUX10: plant UBX containing protein 10.

pv.: pathovar.

R

R gene: resistance gene.

RbcS: rubisco small subunit.

RBOH: respiratory burst oxidative homologue.

RCB: Rubisco containing body.

RIN4: RPM1 interacting protein 4.

RING: really interesting new gene.

roGFP: TKTP-Grx1-roGFP2.

roGFP2: redox sensitive GFP 2.

ROS: reactive oxygen species.

RPM1: *P. syringae* pv. *maculicola* 1.

RSS: residual sum of squares.

RUB: related to ubiquitin, aka NEDD8.

S

SA: salicylic acid.

SEC2: secretory 2.

SEM: standard error of the mean.

SNC1: suppressor of *np1-1* constituive 1.

SOD: superoxide dismutase.

SP1: suppressor of *ppi1* locus 1.

SP1ox: SP1 overexpresson.

SP2: suppressor of *ppi1* locus 2.

SPP: stromal processing peptidase.

ssi2: *suppressor of SA insensitive 2.*

SUMO: small ubiquitin-like modifier.

T

T3SS: type III secretion system.

TAM: translocation and assembly module.

TCA: tricarboxylic acid.

TIC: translocon at the inner chloroplast envelope membrane.

TKTP: transketolase transit peptide.

TOC: translocon at the outer chloroplast envelope membrane.

TOM: translocon of the outer mitochondrial membrane.

U

UBA: ubiquitin-associated domain.

UBX: ubiquitin regulator X domain.

Ufd1: ubiquitin fusion degradation 1.

Ufd3: ubiquitin fusion degradation 3.

UPR: unfolded protein response.

UPRam: UPRmt activated by mistargeting of proteins.

UPRcp: chloroplast UPR.

UPRmt: mitochondrial UPR.

UPS: ubiquitin proteasome system.

V

VCP: valosin-containing protein (aka Cdc48).

Vms1: VCP-associated mitochondrial stress responsive 1.

W

WT: wild-type.

0. Abstract

There is a growing body of evidence that demonstrates that plants and pathogens compete over the chloroplast to activate or disable immunogenic signalling. A critical event in the initiation of immunity is the generation of a reactive oxygen species (ROS) burst in the chloroplast with energy diverted from photosynthesis.

Here, it is shown that model bacterial pathogen *Pseudomonas syringae* suppresses chloroplast protein import to subvert the chloroplast ROS burst and facilitate infection. This depends on a pathway mediated by suppressor of *ppi1* locus 1 (SP1) and requires the secretion of pathogen effector proteins. SP1 activity in times of stress promotes tolerance by suppressing photosynthesis, and antagonises the generation of ROS in the chloroplast. Its activation by pathogen effectors in disease antagonises the generation of the chloroplast ROS burst, thereby antagonising immunity and promoting susceptibility. In the absence of SP1, *P. syringae* cannot suppress basal plant immunity.

Thus, the pathogen suppresses the chloroplast ROS burst and basal plant immunity by activating SP1-mediated ROS avoidance. This demonstrates that the pathogen has evolved to exploit a native host system of stress tolerance to derail chloroplast-mediated immunogenic signalling, which may be an important consideration in the design of climate change resistant crops.

1. General introduction

Note on Authorship

§§1.5-1.9 contains text adapted from, and **Figure 1.3**-**Figure 1.5** are taken from, Sowden *et al.* [1]. Co-authors S. J. Watson and P. Jarvis contributed to the editing and proofing of that manuscript.

1.1 Format

This introduction covers four areas.

In **§§1.2-1.3**, the nature and biogenesis of the chloroplasts is introduced, including the mechanisms of plastid protein import.

In **§1.4**, the ubiquitin-proteasome system and how it can regulate organellar proteomes are explored.

In **§1.5**, the susceptibility of photosynthesis to abiotic stress and the generation of toxic by-products are discussed.

In **§§1.6-1.9**, the central involvement of chloroplast to plant-pathogen interactions is reviewed. **§1.6** provides an overview of the plant immune system. The immune response is tailored or disrupted by phytohormone synthesis, discussed in **§1.7**, and initiated and propagated by oxidative signalling, discussed in **§1.8**. Pathogens have evolved many ways of targeting the chloroplast to suppress immunity, reviewed in **§1.9**.

1.2 Introduction to chloroplasts

1.2.1 The plastids

Chloroplasts are the prototypical, photosynthetic members of the plastids, an organelle family found ubiquitously in plant cells [2]. They are derived from an ancient cyanobacterial endosymbiont [3], which has become tightly integrated into the eukaryote host ("organellogenesis" [4]). This eventually gave rise to new forms of plastid with many different functions beyond photosynthesis.

Other members of the plastid family can be divided into the chromoplasts—coloured plastids that accumulate carotenoids, typically involved in flower and fruit development [5]—and the leucoplasts—the white or colourless plastids, including the amyloplasts that accumulate starch and are involved in gravitropism [6], and the lipid-accumulating elaioplasts involved for example in pollen development [7].

In addition to performing photosynthesis, chloroplasts are productive centres of the plant cell, involved in the biosynthesis of amino acids, lipids, nucleotides, starch, and terpenoids [8]. As the site of both important phytohormone biosynthesis reactions and photosynthesis, chloroplasts are both hubs of stress signalling and targets of many stress tolerance processes.

During developmental transitions, plastids are converted from one type to another by changes to their proteomes [2]. For example, leaves grown in the dark develop etioplasts, which are pre-photosynthetic chloroplasts; when returned to the light, the leaves de-etiolate and etioplasts redifferentiate into chloroplasts. During leaf senescence, the photosynthetic machinery is carefully dismantled and chloroplasts transition into gerontoplasts. These changes reflect alterations to both gene expression and protein import and turnover.

1.2.2 Plastid biogenesis

The chloroplast is semi-autonomous, retaining a small genome of approximately 100 protein-coding genes [9]. Most of the endosymbiont genome has been eliminated or transferred to the nucleus. Thousands of other plastid proteins are expressed from genes in the nucleus (nucleus-encoded chloroplast genes; NECGs), and must be imported into the plastid post-translationally [2,10].

Chloroplast biogenesis and homeostasis require tight co-ordination between gene expression systems in the nucleus and in the organelle, mediated by anterograde (from the nucleus) and retrograde (to the nucleus) signalling pathways [2,11,12]. In fact, the chloroplasts integrate many signalling pathways, participating in metabolic cross-talk with each other, and with the mitochondria, the peroxisomes, and the ER [13].

1.2.3 Retrograde signalling coordinates biogenesis and stress responses

Chloroplasts participate in retrograde signalling pathways that alter cellular homeostasis. In addition to functioning in cell development (biogenic signalling), these signals allow the chloroplasts to act as stress sensors.

Retrograde signalling was first identified in 1979, when it was found that disruption of chloroplast gene expression in white areas of variegated leaves also perturbs NECG expression [14]. Suppression of photosynthesis-related NECGs can also be induced by damaging chloroplasts with herbicides like norflurazon. Mutants defective for this norflurazon-induced feedback are known as the *genomes uncoupled* (*gun*) mutants [15]. So far, six *gun* mutants have been identified. *gun2* to *gun6* are all mutants for tetrapyrrole biosynthetic enzymes, however the exact mechanism of the signal and identity of the signalling molecule remains unclear [12].

GUN1 is pentatricopeptide repeat protein, and has been suggested to integrate tetrapyrrole-based signalling with photosynthetic redox signals and plastome expression

signals [16]. Recently, GUN1 was found to interact with chloroplast heat shock protein (Hsp) 70 (also known as chloroplastic heat shock cognate 70-1, cpHsc70-1), a motor powering plastid protein import (see **§1.3.4**), during photomorphogenesis. It is not found in differentiated chloroplasts except when induced by stress, e.g. norflurazon treatment. It acts to maximise chloroplast import capacity in these conditions. In its absence, unimported preproteins accumulate and this promotes gene expression in the nucleus via cytosolic chaperone Hsp90, in a chloroplast analogue of the unfolded protein response (UPR) [17]. Tetrapyrrole biosynthetic enzymes are imported in a GUN1-dependent manner when chloroplast biogenesis is disrupted (e.g. with norflurazon) and accumulate in the cytosol in the *gun1* mutant: in this way, GUN1 activity is connected to tetrapyrrole biosynthesis-based signalling also [17]. It has also been suggested that GUN1 modulates tetrapyrrole biosynthesis-based signalling by direct binding of haeme [18]; and integrates retrograde signalling and plastome expression through interaction with multiple organellar RNA editing factor 2 (MORF2), which it inhibits to reduce RNA editing efficiency [19]. It may be the case then that GUN1 is a multifunctional protein.

Since the discovery of the *gun* mutants and biogenic signalling, a plethora of other retrograde signalling pathways have been proposed. These include pathways that are induced following stress perception in the chloroplast. For example, dysfunction of photosystem (PS) II is perceived by the chloroplast through singlet oxygen production and can initiate photooxidative stress tolerance transcriptional reprogramming, signalled by the carotenoid oxidation product β-cyclocitral [20], or programmed cell death (PCD), signalled by the proteolysis of executer 1/2 (EX1/2) [21,22]. Recently, new retrograde signals transmitted by the methylerythritol 4-phosphate (MEP) pathway intermediate 2-C-methyl-D-erythritol-2,4-cyclopyrophosphate (MEcPP or cMEPP) and by the phosphonucleotide 3'-phosphoadenosine 5'-phosphate (PAP) have been found that connect both abiotic and biotic stress responses [23–26]. These signals will be revisited in **§1.7.2**, while reactive oxygen species (ROS) will be discussed separately in **§1.5** and **§1.8**.

1.3 Plastid protein import pathways

1.3.1 Plastid protein targeting

The vast majority of nucleus-encoded chloroplast proteins (NECPs) are targeted to the chloroplast via cleavable, N-terminal signals called transit peptides, and are imported via the translocons at the outer and inner chloroplast envelope membranes (TOC-TIC). This is called the canonical protein import pathway.

Transit peptides are necessary and sufficient to target a protein to the plastid, but vary greatly in length, from 13 to 146 residues, and in sequence, possessing no obvious consensus motifs. Rather, they are the "perfect random coil", without regular secondary or tertiary structure [27,28]. One model, called the "multi-selection and multi-order" model, suggests that transit peptides consist of several motifs that each interact with different translocon components, but that each preprotein may only need to interact with some of the translocon components for import. These motifs may appear in different orders, reminiscent of promoter organisation [29]. Some transit peptide sequences have considerable commonality with mitochondrion-targeting presequences. Recently, it was found that an N-terminus multiple-arginine region was critical for preventing certain mitochondrial proteins from becoming targeted to the plastid [30].

As the transit peptide emerges from the ribosome during translation, it is recognised by chaperone proteins that recruit others to keep the preprotein unfolded and prevent aggregation [31]. These include cytosolic Hsp70, which may guide preproteins to the chloroplast independently or in co-operation with members of the 14-3-3 protein family [32], and Hsp90, which may associate with Hsp70/Hsp90 organising protein (Hop) and FK506 binding protein 73 (FKBP73) [33]. It is not clear to what extent these guidance complexes are essential, as mutation of Hsp70 binding sites in transit peptides or of the receptor for Hsp90/Hop/FKB73 in the chloroplast outer membrane does not perturb substrate import efficiency, at least under normal conditions [31].

Regardless of the exact mechanism, the preprotein is guided to the TOC complex for translocation into the chloroplast.

1.3.2 The translocon at the outer chloroplast envelope membrane

At the chloroplast outer envelope membrane (OEM), the preprotein is received by the TOC complex. The TOC complex is composed of multiple OEM proteins: a protein channel and two classes of preprotein receptors. TOC complex components are named for their weight in kDa. The pore of the complex is Toc75, and the two primary receptors are the GTPases Toc159 and Toc34. The exact stoichiometry of Toc34 to Toc75 to Toc159 has been estimated as 3:3:1 or 4-5:4:1 [34,35].

Multiple isoforms of the higher and lower molecular weight GTPases exist. In Arabidopsis, there are three additional isoforms of Toc159—Toc90, Toc120, and Toc132 [36]—and there is one additional isoform of Toc34—Toc33 [37]. The different isoforms of the large and small GTPases can associate with each other to create receptor complexes with affinities for different classes of transit peptides [36,37]. These different receptor complexes are developmentally regulated and create at least two distinct import routes, a "multilane GTPase highway" [38,39].

This allows the preferential import of different classes of preprotein. Photosynthetic preproteins are preferentially imported by Toc159 and Toc33, while the other isoforms prioritise non-photosynthetic proteins [36,37]. Separating plastid traffic in this way may allow the plant freedom to increase photosynthetic gene expression without the risk of out-competing the import of "housekeeping" proteins—less highly expressed but essential non-photosynthetic proteins [38,39].

Membrane translocation begins with the formation of an 'early import intermediate', where the preprotein is inserted into the Toc75 channel [40]. Although this process requires the availability of hydrolysable GTP [40], curiously, the ability of either Toc34 or Toc159 singularly to bind GTP is not essential, though it may improve import rates [41–

43]. Binding of the transit peptide to the Toc receptors promotes the exchange of GDP for GTP, the hydrolysis of which acts as a checkpoint before committing to translocation [43,44].

1.3.3 The translocon at the inner chloroplast envelope membrane

Import of preproteins is then completed by the TIC machinery, which has roles in protein translocation, internal routing, and quality control.

The exact membership of the TIC complex is the subject of considerable controversy [45,46]. Tic110 was proposed to act as the TIC channel, both recognising the preprotein and translocating it across the inner membrane [47,48]. This view was later challenged following the identification of a stable 1 MDa translocation complex at the chloroplast inner membrane which does not include Tic110. At the core of this complex is Tic20, a polytopic membrane protein that, in this model, is the main channel-forming protein. The other components of this complex are Tic56, Tic100, and Tic214 [44,49–51].

Following this model, Tic110 (together with another component called Tic40, which possesses characteristics of a cochaperone) was suggested to function later, after membrane translocation, in the recruitment of stromal chaperones to the preprotein as part of a protein import motor [52,53].

However, two lines of evidence suggests that 1 MDa complex component Tic214 is not essential for import. Firstly, Tic214 homologues are very variable or absent in several lineages of metaphyta, including the Poaceae [54]. Two other Tic components, Tic56 and Tic100, have also been lost in the Poaceae lineage, but are essential in Arabidopsis, so it may be the case that the TIC complex is greatly divergent in the grasses [2,43].

Secondly, Tic214 is plastome-encoded, unlike other translocon components, and its accumulation can be abrogated by the plastid translation inhibitor spectinomycin. It was found that Arabidopsis plants treated with the herbicide do not undergo

photomorphogenesis nor do they have detectable Tic214, but they still show import of some non-photosynthetic plastid proteins, like fatty acid export 1 [55]. Noting that Tic110 was present even after herbicide treatment, the study's authors [55] revived the Tic110 channel hypothesis.

Mutants lacking Tic20 [56,57], Tic56 or Tic100 [50] can grow heterotrophically on supplemented media, but otherwise will fail to undergo photomorphogenesis and die. Therefore, they must carry out housekeeping protein import. This has been used as evidence to suggest the existence of a second, semi-redundant TIC complex, which in the absence of major TIC components can continue to import housekeeping proteins [46]. Genetic analysis implicates Tic20-IV, the chromosome 4-encoded isoform of Tic20, as the channel in the secondary TIC complex, however, not Tic110 [50,56,57].

1.3.4 The TOC-TIC supercomplex and peripheral components

Unlike the protein translocation machinery at the two membranes of mitochondria, which only come together transiently during import, the inner and outer envelope chloroplast translocons are thought to form more stable supercomplexes [58]. The two complexes are held together by the IEM protein Tic236, which extends a large domain into the intermembrane space that interacts with Toc75, and promotes its association with Tic20 [59]. Tic236 is a homologue of bacterial translocation and assembly module (TAM) protein TamB [59], which is bound to the inner membrane of Gram-negative bacteria and interacts with outer membrane protein 85 (OMP85) proteins [60], a family that includes Toc75. This suggests that Tic236 and Toc75 derived from a homologous TAM couple in the cyanobacterial ancestor [59]. A soluble intermembrane space protein, Tic22, has also been implicated in bringing the TOC-TIC supercomplex into association. In Arabidopsis, there are two isoforms of Tic22, which act redundantly to promote protein import but are not essential [61,62].

The core TIC complex associates with a number of stromal proteins to complete the import process, including the quality control and the internal routing of the protein [2]. These proteins include the stromal processing peptidase (SPP), a metalloendopeptidase which cleaves the preprotein's transit peptide [63,64]. The cleaved peptides are then degraded by two oligopeptidases, the organellar oligopeptidase (OOP) and the presequence protease (PreP), which also degrade targeting signals in the mitochondrion [65]. They form part of a cascade with stromal aminopeptidases to recover free amino acids from the transit peptide [66]. The clean-up of transit peptides is important for the health of the plant. SPP is essential for viability, while mutation of OOP and PreP reduces growth and causes changes to plastid and mitochondrion ultrastructure [65,67]. Growth defects in Arabidopsis triple mutants for OOP and the two isoforms of PreP appear to be caused by constitutive activation of immune-related genes, suggesting that the accumulation of short peptides in the plastid and mitochondrion cause a "peptide stress response" linked to retrograde signalling [68].

Motive power for translocation through the TIC is provided by the hydrolysis of ATP in the stroma [69]. There have been several candidates considered for the motor protein, including stromal ATPase Hsp93, which was found both to co-immunoprecipitate with TOC-TIC supercomplex components and interact with preproteins in an ATP-dependent manner [70,71]. Additionally, Arabidopsis double mutants for both of the two chloroplastic *hsp93* isoforms have chlorotic phenotypes [72]—consistent with a role in import. However, recent evidence regarding Hsp93 now points to a role in quality control. Hsp93, also known as caseinolytic proteinase (Clp) C, is a component of the stromal protease complex Clp complex, which was recently found to associate with the IEM in the same proportion as stromal Hsp93. Hsp93's role in the Clp is in substrate recognition and unfolding. It is now thought that Hsp93 recruits the Clp to the IEM by binding Tic110, then recognises substrates during import and conducts them to the proteolytic Clp core [71,73].

A stronger candidate for the stromal ATP motor is cpHsc70. Mutation in Arabidopsis of either of the two isoforms of cpHsc70 (the double mutant is lethal), or of one of the two isoforms in Physcomitrella (Hsp70-2), has been shown to impair chloroplast protein import [74,75]. Additionally, cpHsc70 remains associated with the preprotein later in import even after the transit peptide has been cleaved, whereas Hsp93 only associates with preproteins and the TIC during the early stages of translocation [74,76]. This is more consistent with cpHsc70 acting as the motor, rather than Hsp93. Further evidence supporting the role of cpHsc70 comes from a kinetics study in Physcomitrella, where the ATP requirement for import was found to correlate with the affinity of Hsp70-2 for ATP, and could be increased by introducing a mutation to Hsp70-2 that enhanced its ATP binding affinity. [77].

A recent alternative view has been proposed involving an IEM-bound 2 MDa complex, which unlike cpHsc70 has been shown to associate directly with components of the 1 MDa TIC as well as preproteins [78]. This complex comprises Ycf2, a plastome-encoded ATPase, and five nucleus-encoded filamentous temperature sensitive H (FtsH) homologues, thought to form a hexameric ATPase ring [78]. It was argued that the Ycf2 complex must be the primary motor protein in IEM translocation, rather than cpHsc70, on the basis of two points: firstly, that the Ycf2 complex associates more strongly with the TOC-TIC supercomplex and preproteins than cpHSC70; and secondly, that when protein import is disrupted by supplying a non-hydrolysable ATP analogue to isolated chloroplasts, preproteins accumulated that were bound to the Ycf2 complex, but not to cpHsc70 [78]. However, key pieces of evidence, e.g. the consumption of ATP by the Ycf2 complex, still need to be determined.

1.3.5 Import of envelope proteins

Some NECPs, such as OEM proteins, do not have cleavable transit peptides. In the case of OEM proteins, targeting information is instead intrinsic to the transmembrane

domains of the protein, and this is recognised during translation by the N-terminal domains of the cytosolic chaperones ankyrin repeat (AKR) proteins AKR2A and AKR2B [79]. The C-terminal AKR domains additionally recognise the OEM by binding to a unique plastid lipid, monogalactosyldiacylglycerol [80]. Binding efficiency is enhanced by the binding of another lipid abundant in the OEM, phosphatidylglycerol, and by the co-factor Hsp17.8 which also interacts with the AKR domains [80].

Components of the TOC-dependent import pathway become involved at later stages, at the point of membrane insertion. For signal-anchored proteins liked outer envelope protein (OEP) 17, insertion into the OEM is mediated by Toc75 [81]. Insertion of tail-anchored proteins diverges into at least two routes: for some proteins it is mediated by Toc33 and Toc34, and is inhibited in chloroplasts isolated from mutants for those proteins; for others it is mediated by another OEM protein, perhaps Toc75 [82].

For inner envelope membrane (IEM) proteins, the canonical import pathway branches into two pathways for envelope insertion. Proteins may become integrated into the inner envelope either during or after import through the TIC complex, known as the stop-transfer and post-import mechanisms respectively.

In post-import integration, e.g. of Tic40, a soluble intermediate is formed in the stroma following transit peptide cleavage. A second processing event occurs on membrane integration, forming the mature protein. These substrates have a bipartite transit peptide, the N-terminus of which targets the preprotein to the chloroplast and is cleaved by SPP, the remainder is necessary for membrane targeting and is cleaved by an unknown peptidase [83]. Recently, membrane integration of post-import substrates like Tic40 was found to be mediated by the secretory 2 (SEC2) complex, composed of homologues for the bacterial Type II secretion system, known as Sec [84].

In the stop-transfer mechanism, import is halted at the TIC translocon and the substrate moves laterally into the membrane. In this mechanism, substrates do not form a soluble

intermediate and undergo only one processing event, the cleavage of the transit peptide. One such substrate is albino or pale green mutant 1 (APG1). Rather than using a bipartite transit peptide, an integral signal in the transmembrane domain of APG1 induces stop-transfer [85]. This is similar to the stop-transfer co-translational integration of membrane proteins into the ER [86].

In mitochondria, analogues of both the post-import and stop-transfer pathways are found—the former is known as the conservative sorting pathway [87]. There are however key differences between mitochondrion conservative sorting and chloroplast post-import pathways. In conservative sorting, membrane integration is dependent on oxidase assembly protein 1 (Oxa1), a homologue of YidC, part of an ancestral bacterial protein export mechanism [88,89]. The chloroplast Oxa1/YidC homologue, albino 3 (ALB3), mediates integration of thylakoid membrane proteins but is not found in the IEM [90], and the mitochondria do not possess Sec pathway components [88]. Thus, the conservative pathway in mitochondria and the post-import pathway of chloroplasts represent the neofunctionalisation of two different ancestral bacterial protein export systems.

Additionally, the transmembrane domains of mitochondrial proteins destined conservative sorting incorporate proline residues that prevent initiation of the stop-transfer pathway. These do not have the same role in distinguishing stop-transfer and post-entry insertion in chloroplasts [85].

1.3.6 Non-canonical import pathways

Non-canonical pathways of chloroplast protein import, that are TOC independent and do not involve cleavable transit peptides, have also been described.

For example, while the ten N-terminal residues of inner envelope protein 32 (IEP32) are necessary to ensure its proper import into the chloroplast, they are not cleaved on import and its import is independent of Toc33, Toc75, or Toc158 [91]. Its import proceeds

normally at low concentrations of ATP, suggesting that ATPase action is not required to drive import, unlike in the canonical pathway [91].

The IEM protein chloroplast envelope quinone oxidoreductase homologue (ceQORH) does not have a transit peptide and is imported independently of Toc75 and Toc159 [92,93]. Both the N- and C-termini of ceQORH were found to be dispensable for chloroplast import, suggesting that an internal sequence was necessary to convey targeting information [92]. Further analysis found that targeting of ceQORH relied on a central, soluble domain of 40 residues flanked by membrane-binding domains on either side [93]. Import of ceQORH requires greater concentrations of ATP than canonical import [93], which suggests it is imported by a different route to IEP32.

Finally, a small number of proteins are thought to be imported to the chloroplast by vesicular transport. This allows for the uptake of certain proteins that have first been routed to the Golgi apparatus for glycosylation, as is the case for α-carbonic anhydrase 1 (CAH1) [94] and nucleotide pyrophosphatase/phosphodiesterase 1 [95], or where there is a requirement to route proteins to both the plastid and the plasma membrane, as is the case for some α-amylases [96–98]. Endomembrane transport of plastid proteins is more common in algae, and it may represent an ancestral import pathway from before to the evolution of the canonical pathway [99]. In algae, plastid targeted proteins have a bipartite targeting sequence, resembling an ER signal sequence followed by a chloroplast transit peptide [99]. As proteins like CAH1 do not have algae-style bipartite targeting sequences, how they encode targeting information, and how mechanistically they become transported from the Golgi lumen to the plastid stroma, has yet to be elucidated.

1.4 Organellar protein regulation by the ubiquitin-proteasome system

1.4.1 The ubiquitin-proteasome system

The ubiquitin-proteasome system (UPS) is highly conserved nucleocytosolic system that serves to regulate the abundance and turnover of proteins in eukaryotes. Proteins are marked for destruction by the ligation of chains of ubiquitin—a small, 76-residue protein, named for its "ubiquitous" presence in cells [100]—at one or more lysine residues, and are subsequently received by the 26S proteasome, which degrades the protein and recycles the ubiquitin.

The ligation of ubiquitin to a substrate ("ubiquitination" or "ubiquitylation") is facilitated by a cascade of enzymes. Ubiquitin exists in an inactive form and so must first be activated by an ATP-dependent ubiquitin activating enzyme, or E1. Activated ubiquitin is then transferred to an E2 conjugating enzyme, which in the process recycles the E1. A substrate-specific E3 ligase then transfers the ubiquitin to the target protein, either directly from the E2 to the substrate, or via the E3 as an intermediary [101]. Ubiquitin monomers may themselves become ubiquitinated (at one or more internal lysine residues), enabling the formation of branched or linear chains, a process which may be assisted by ubiquitin chain elongation factors [102], or E4s. Ubiquitin modifications may also be removed by de-ubiquitinating isopeptidases (DUBs) [103].

E3s convey target specificity. Some E2-E3 interactions are specific, while certain E2s can interact with multiple E3s and vice versa [101]. There have been three classes of E3 ligases discovered in plants, of which really interesting new gene (RING)-domain and plant U-box (PUB)-domain E3 ligases directly transfer ubiquitin from the E2 to the substrate, while homologous to E6AP C-terminal (HECT)-domain ligases first become loaded with ubiquitin themselves [104,105].

Typically, there are just one or two types of E1 per cell, and there are more E2s and many more E3s; for example, in Arabidopsis, only two E1s are necessary to interact with all 41 E2s, which themselves interact with well over 1,000 E3s [105–107].

Ubiquitination can have other roles in addition to the marking of a protein for degradation. These may include modifications to protein translocation, activity, partner recruitment, or stabilisation [108–111]. As ubiquitin monomers may be joined together at multiple lysine residues, there are different ubiquitin chain topologies and these may convey different signals. Targeting to the proteasome typically requires the formation of a polyubiquitin chain of at least four ubiquitin monomers, covalently linked at the lysine 48 residue, while chains connected by ubiquitin's six other lysine resides are often associated with non-proteolytic functions, for example in activating kinases, DNA repair, or endocytosis [112–114]. Furthermore, branched chains or the monoubiquitination of a substrate at one or multiple sites (multi-monoubiquitination) can each encode different signals [115]. As they respectively lengthen and shorten ubiquitin chains, E4 enzymes and DUBs may also have a role in disambiguating signals encoded in different ubiquitin chain topologies [115].

1.4.2 The 26S proteasome

The 26S proteasome is a nucleocytosolic protein complex consisting of a core particle and two caps or regulatory particles. The core particle is comprised of a stack of four heteromeric rings—two α-rings and two β-rings—each formed from seven subunits. At the centre of the stack are the two proteolytic β-rings. Access to this proteolytic chamber is via the pores in the two α-rings, located either side of the β-rings, which in their default configuration are closed [116].

Opening of the α-ring pore is caused by the binding of the regulatory particle. Each regulatory particle consists of a base subcomplex, proximal to the α-ring, and a horseshoe-shaped lid subcomplex. The base subunit includes a heterohexameric ATPase ring, which

docks into α-ring at pockets formed at the junctions between the subunits of the α-ring, to bring about conformational changes to the α-ring and open the pore [116,117].

The regulatory particles ensure only polyubiquitinated substrates have access to the core particle. Access to the proteolytic core had been thought to be granted by the dynamic opening and closing of the α-ring as substrates were identified. This notion was brought into question by the observation that the binding of the regulatory and core particles obligatorily opens the α-ring [118]. However, in a recent cryo-electron microscopy study, the regulatory particle was found to exist mostly in intermediate states of docking and the α-ring pore was closed. Full docking, and opening of the α-ring, can only be achieved by stepwise reconfiguration of the lid and base subcomplexes [117]. This suggests that the regulatory particle does not become fully integrated, and open the α-ring for access, until the recognition of a substrate occurs. The regulatory particle also participates in protein unfolding and includes DUBs involved in ubiquitin recycling.

Proteasome activity is regulated at many additional levels, including via recruitment of the complex to sites of protein turnover, the synthesis and assembly of proteasome subunits, and the post-translational modification of proteasome subunits [119–121].

1.4.3 Regulation of chloroplast protein import by ubiquitin

The UPS helps regulate chloroplast protein import both in the cytosol and at the chloroplast OEM, which is important for both biogenesis and stress tolerance.

Preproteins in the cytosol are regulated by the chaperone heat shock cognate 70-4 (Hsc70-4), which binds to transit peptides and recruits the E3 ligase C-terminus of Hsc70-interacting protein (CHIP) [122–124]. Hsc70-4 and CHIP are induced by increased cytosolic abundance of chloroplast preproteins, which occurs both in the Arabidopsis mutant for Toc159, *plastid protein import 2*, which has a severe import defect, and in protoplasts transformed with Rubisco small subunit carrying a variant transit peptide that

is poorly imported. As unfolded proteins in the cytosol may form harmful aggregates, Hsc70-4/CHIP acts to remove unimported preproteins and prevent toxicity [124].

In addition, the Hsc70-4/CHIP system also targets for degradation FtsH and Clp proteolytic components, chloroplast proteases which are induced in abiotic stresses like high light. Constitutive over-expression of CHIP prevents stress-induction of these proteases [122,123,125]. This suggests that the Hsc70-4/CHIP system acts in both chloroplast proteome homeostasis and stress-induced remodelling.

TOC components have also been found to be under UPS regulation. The first E3 targeting the TOC was found in a mutant screen for suppressors of the Arabidopsis mutant for Toc33, *plastid protein import 1* (*ppi1*) [126]; *ppi1* mutants are less green than wild-type plants as chloroplast protein import is reduced [37,127]. The screen identified a second-site suppressor mutation, *suppressor of ppi1 locus 1* (*sp1*), that improves greening in the *ppi1* background, mediated by enhanced chloroplast protein import. SP1 was determined to be an OEM-bound ubiquitin E3 ligase that acts to target TOC components to the proteasome. In the *sp1 ppi1* mutants, TOC complexes accumulate to higher levels, partially compensating for the loss of Toc33 and restoring protein import efficiency [126].

As different TOC components promote the import of different classes of NECP, their reconfiguration provides another means to regulate plastid biogenesis in addition to transcriptional reprogramming and the proteolysis of imported proteins. Indeed, *sp1* plants fail or take longer to de-etiolate and have delayed senescence, whereas plants overexpressing SP1 (SP1ox) show more rapid de-etiolation and senesce faster [126].

By reducing the import of photosynthetic preproteins during senescence, SP1 acts to reduce photosynthetic development [126]. This ability is also important during abiotic stress [128]. SP1ox Arabidopsis plants show greater tolerance of osmotic, oxidative, and salt stress conditions than wild-type plants; whereas *sp1* mutants are more susceptible to these stresses than the wild type. In the proposed ROS-avoidance model, SP1 is stimulated

upon stress exposure to downregulate photosynthetic chloroplast protein import. This supresses photosynthesis, which would otherwise be liable to produce toxic ROS under such environmentally adverse conditions [128].

1.4.4 UPS regulation of organelle proteins

The UPS is utilised for the degradation of many different targets and participates in a wide range of different processes. These include phytohormone signalling (for example, gibberellin signalling relieves the transcriptional repression of DELLAs by targeting them to the proteasome); the oscillations of proteins that maintain the plant circadian clock; and the regulation of plant immune receptors [129–132]. In these examples, the proteins are soluble and readily available to proteasome complexes located in the nucleus and cytosol.

The UPS has also been shown to also act in the turnover of proteins that are not immediately accessible; that is, proteins either integrated into or held behind cellular membranes. These systems require additional components that facilitate the extraction and retrotranslocation of substrates prior to their degradation by the proteasome.

The first of these systems to be described facilitates the destruction of misfolded proteins in the endoplasmic reticulum (ER). Three variants of ER associated protein degradation (ERAD) have been described, which degrade lumenal misfolded proteins (ERAD-L) and membrane-bound proteins that are misfolded in their lumenal (ERAD-M) or cytosolic (ERAD-C) domains.

In ERAD, a membrane-bound E3 ligase ubiquitinates the substrate; this is HMG-CoA reductase degradation 1 (Hrd1) in ERAD-M and -L, and degradation of alpha 10 (Doa10) in ERAD-C [133]. These E3 ligases are also thought to form a channel for retrotranslocation with their extensive membrane spans. This notion was strongly supported by a recent cryo-electron microscopy study which found that Hrd1 dimerises and forms two funnels, each composed of six transmembrane spans. Each Hrd1 protein

contributes five transmembrane spans to one funnel and one transmembrane to the other [134].

Although Hrd1 mediates ubiquitination of membrane-bound and lumen proteins, its retrotranslocation activity is thought to only be critical in ERAD-L. A separate retrotranslocon, Derlin-like family member protein 1 (Dfm1) has been implicated in the extraction of integral membrane proteins ubiquitinated by either E3 ligase [135].

Extraction from the membrane is assisted by motive power from cell division cycle 48 (Cdc48), also known as p97 or valosin-containing protein (VCP). Cdc48 assembles into a multimeric cytosolic ATPase complex that, in ERAD, is associated with the polyubiquitin-targeting cofactors ubiquitin fusion degradation 1 (Ufd1) and nuclear protein localisation 4 (Npl4), and so it is sometimes referred to as the Cdc48-Npl4-Ufd1 complex.

Analogous systems of protein extraction and degradation involving Cdc48 have recently been identified in a number of other organelles and compartments, including outer mitochondrial membrane associated degradation (OMMAD or MAD) [136], lipid droplet associated degradation (LDAD) [137,138], inner nuclear membrane associated degradation (INMAD) [139], and endosome and Golgi associated degradation (EGAD) [140]. Schemes depicting some of these processes are presented alongside ERAD in **Figure 1.1**, p.61. Although not all of the components are known in every example, in comparing these systems some general principles of Cdc48-mediated protein degradation emerge: there must be a means of identifying an appropriate substrate, one or more E3 ligases, a retrotranslocon, and cofactors that recruit Cdc48 to provide motive power.

Several E2 and E3 ligases have been shown to act in OMMAD [141]. These may be cytosolic, like Parkin, or membrane-bound, like Mulan. In humans, Parkin is known to interact with four E2s [142], while Mulan interacts with a different set of four E2s [143]. While no direct analogue of ERAD lumenal substrate recognition proteins have been

identified in OMMAD, it is worth noting that the combination of diverse sets of E2 and E3 enzymes may offer a mechanism for specific targeting of different classes of substrates and thereby different pathways. Other E3s implicated in OMMAD include March5 [144,145], Mule [146], and in-between RING fingers-domain containing protein 2 (IBRDC2) [147].

No study has identified a retrotranslocon for OMMAD specifically. In fact, the activity of Cdc48 alone has generally been assumed to be sufficient to extract substrates from the mitochondrial membrane. However, the translocon of the outer mitochondrial membrane (Tom) 40 could be an interesting candidate. The Tom40 channel is part of the mitochondrial protein import apparatus, and it has recently been implicated in the retrotranslocation of misfolded proteins from the intermembrane space to the cytosol for proteasome degradation [148]. Although it has yet to be established if the two pathways converge, there is a tantalising possibility that the OMMAD E3 enzymes target intermembrane space proteins thus retrotranslocated, and that Tom40 assists in the retrotranslocation of membrane-bound OMMAD substrates.

This is further supported by the recent discovery that Cdc48, recruited by Ubx2, functions in the extraction of substrates from the Tom complex that have become arrested during import, a process christened mitochondrial protein translocation-associated degradation (mitoTAD) [149].

Adapter proteins that interact with both Cdc48 and the polyubiquitinated substrate assist in the recruitment of the chaperone to the relevant complex. In ERAD, localisation of Cdc48 to the complex can be mediated by the membrane protein Ubx2, which has an N-terminal ubiquitin associated (UBA) domain and a C-terminal ubiquitin regulatory x domain (UBX). It is hairpin-anchored within the ER membrane, presenting both domains to the cytosol. The UBA domain associates with the polyubiquitin tail of ERAD substrates, whereas the UBX domain interacts with the Cdc48 complex [150]. In addition to acting as a retrotranslocon, Dfm1 has been shown to act to recruit Cdc48

independently of Ubx2 [135]. One of the plant homologues of Ubx2, plant UBX domain-containing protein 10 (PUX10), is present in lipid droplets monolayers and has been shown to recruit Cdc48 for the extraction of oleosins in LDAD [137,138]. So far, this and Cdc48 are the only components identified in LDAD.

In OMMAD, recruitment of Cdc48 is assisted by degradation of alpha 1 (Doa1), also known as ubiquitin fusion degradation 3 (Ufd3). Although it is not a UBA/UBX protein, Doa1 still binds to both Cdc48, via its C-terminal domain, and ubiquitinated substrates, via two ubiquitin-binding domains [151]. Intriguingly, it is not inserted into the mitochondrial membrane, but nevertheless specifically promotes Cdc48 recruitment to the mitochondrion and not to the ER. Its specificity has been demonstrated by its mutation in *Saccharomyces cerevisiae*, which does not prevent the turnover of ERAD substrates or induce the UPR in susceptible mutant backgrounds (unlike mutants for ERAD components). However, this mutation does cause the accumulation of the mitochondrial OMMAD substrates fuzzy onions homologue 1 (a mitofusin) and mitochondrial distribution and morphology 34, and does increases sensitivity to mitochondrial oxidative stress [152]. These data suggest that Doa1 can recognise mitochondrial substrates specifically.

The Cdc48-Npl4-Ufd1 complex is known to be involved in both ERAD and OMMAD. However, a third cofactor has also been discovered in OMMAD: VCP-associated mitochondrial stress-responsive 1 (Vms1) [136]. Cdc48-Npl4-Ufd1 and Cdc48-Vms1 are thought to target different substrates in OMMAD [153].

1.4.5 Chloroplast-associated protein degradation

Recent advances can now put SP1 in a broader context as part of a chloroplast-specific system of Cdc48-mediated protein turnover, known as chloroplast-associated protein degradation (CHLORAD) [154].

SP1 does not have the extensive transmembrane sequences necessary to form a retrotranslocon like Hrd1. Instead, a separate channel protein, suppressor of *ppi1* locus 2 (SP2), provides the retrotranslocon. Like *sp1*, *sp2* was identified in an Arabidopsis mutant screen for suppressors of the mutant *ppi1*. SP2 is a β-barrel channel protein belonging to the OMP85 superfamily of proteins typically found in the outer membranes of Gram-negative bacteria and the endosymbiotic organelles. In the eukaryotes, OMP85 superfamily members include Sam50, required for correct assembly of mitochondrial outer membrane complexes including Tom, and Toc75, the main outer membrane channel of the canonical plastid protein import pathway which also assists in the assembly of the TOC complex [155,156].

In CHLORAD, SP1's intermembrane space domain recognises substrates and its RING domain ubiquitinates them [126]. Substrates are then retrotranslocated through SP2, and extracted by motive power generated by Cdc48 [154]. Recruitment of Cdc48 to the chloroplast is assisted by Ubx2 homologue PUX10 (unpublished data).

Unlike ERAD and OMMAD, which have both been connected to the turnover of misfolded proteins, so far CHLORAD has been found to act specifically in the regulation of TOC components. Whether there are other targets, perhaps mediated by different E2 and E3 enzymes, has yet to be shown. Similarly, questions remain as to the cofactors that recruit Cdc48 in CHLORAD.

1.5 Chloroplasts and oxidative stress

1.5.1 Chloroplasts cause oxidative stress

While necessary for phototrophic life, the photosynthetic machinery is potentially very dangerous as it can generate ROS. Although ROS have important signalling roles in the plant [13,157,158], they can also cause significant damage through toxic oxidation reactions with carbohydrates, lipids, nucleic acids, and proteins [159], and so their production must be tightly regulated.

When intercepted photon energy exceeds the ability of the chloroplast to fix carbon ("photon excess"), the surplus energy can drive the creation of ROS at PS I and II [160] (**Figure 1.2**, p.63). Under adverse environmental conditions that reduce carbon assimilation (e.g. abiotic stresses like drought), or under more intense light conditions, the tendency to produce ROS at the expense of photosynthesis is increased [160,161]. In this way, the chloroplast converts abiotic stresses into oxidative stress.

1.5.2 Avoidance and scavenging help to manage ROS

Many safety systems protect the plant from chloroplast dysfunction during abiotic stress. Together these represent systems of ROS management (**Figure 1.3** p.65) and are important contributors to abiotic stress tolerance. For example, when chlorophyll molecules are excited beyond the capacity for photosynthesis, the extra energy can be released as heat by non-photochemical quenching (NPQ). NPQ is rapidly induced and readily reversible, and accounts for the dissipation of up to half of intercepted light energy under field conditions [162–164].

Recently, it was shown that the import of photosynthetic preproteins into the chloroplast is reduced under stress conditions, thereby lessening energy interception and ROS production from photon excess. Initially, and during short-term stress exposure, this is controlled post-translationally by increasing turnover of the chloroplast protein import

machinery regulated by SP1 [165]. During longer-term stress, NECG related to photosynthesis become downregulated [166]. These represent strategies of ROS avoidance (**Figure 1.3A** p.65).

If such avoidance is insufficient—for instance, if NPQ is suppressed—the excited photosystems can react with oxygen and generate ROS instead (**Figure 1.2** p.63). The chloroplast has several ROS scavenging systems (**Figure 1.3B** p.65). In the water-water cycle, hydrogen peroxide is reduced to water by the oxidation of ascorbic acid, catalysed by stromal ascorbate peroxidase. The ascorbic acid is regenerated by electrons diverted from photosynthesis, therefore the water-water cycle is light-dependent [160]. In addition, there are a number of proteins present in the chloroplast that act in maintaining redox homeostasis. These include the glutaredoxins and the thioredoxins, two families of oxidoreductases that catalyse thiol-disulphide exchanges—that is, the reduction of oxidised cysteine residues [167–169]. There are two types of thioredoxin systems in chloroplasts, where reducing power is derived either from NADPH or ferredoxin, while glutaredoxins derive reducing power from the glutathione buffer pool [167]. In the chloroplast, there are five classes of soluble thioredoxin and a number of thylakoid membrane-bound thioredoxin-like proteins. These can target a wide number of substrates involved in many different plastid processes [168,169]. In particular, targets of thioredoxin regulation include enzymes involved in chlorophyll biogenesis and the Calvin cycle: in this way, the thioredoxin system contributes to the redox regulation of photosynthesis [168].

In addition, plants contain a number of peroxiredoxins that act to detoxify hydrogen peroxide and are themselves reduced by the glutaredoxin or thioredoxin systems. These include 2-cysteine peroxiredoxin, which can mediated water-water scheme detoxification during darkness and then be regenerated by thioredoxin [167,170]. Finally, if hydrogen peroxide accumulates to the point where it begins to diffuse into the thylakoids, lumenal catalases will act to decompose it [160].

Increased ROS production stimulates the production of more antioxidants, including β-carotene, non-photochemically active plastoquinol, and α-tocopherol [160,171,172]. For more information on ROS generation and strategies of scavenging, the reader is direct to [173].

1.5.3 Turnover of damaged chloroplast components reduces ROS production

When oxidative damage does occur, chloroplast proteins can be rapidly degraded by plastid-localised proteases (**Figure 1.3C** p.65). Eliminating damaged chloroplast components significantly contributes to oxidative stress tolerance [174]. The D1 core subunit of PS II is especially liable to accumulate oxidative damage. A specialist repair cycle operates in which damaged photosystems migrate away from the grana (stacks of thylakoid lamellae where PS II is concentrated) to the stromal thylakoid domains, are partially dissembled so that the D1 core subunit may be replaced, and then reassembled before migrating back to the grana [175]. The damaged protein is degraded by the plastid proteases FtsH and Deg [176].

Chloroplast proteins may also be turned over in the vacuole via autophagy and related processes (**Figure 1.3C** p.65). Vesicles called Rubisco containing bodies (RCBs) carry stromal proteins, including the Rubisco large subunit and glutamine synthetase, to the vacuole[177,178]. RCB-mediated autophagy represents a route for stromal proteins to be mobilised to the vacuole without degrading entire chloroplasts; thus, chloroplast number per cell is unaffected [178]. This could have utility in turning over stromal proteins damaged by oxidative stress, as well as downregulating photosynthetic development.

If the damage is extensive enough, the entire chloroplast may be sent for vacuolar degradation. This process, called "chlorophagy", follows extensive chloroplast membrane damage [179], which is both indicative of lipid peroxidation [180] and, by causing stromal protein leakage, could be causative of ROS accumulation. Evidence has been presented

that the selective vacuolar degradation of damaged chloroplasts can be signalled by extensive ubiquitination of OEM components by the E3 ligase PUB4 [181].

There are two pathways that facilitate autophagosome membrane formation during autophagy, which both feature similarities to ubiquitination. In one pathway, ubiquitin-like autophagy-related 12 (ATG12) becomes conjugated to ATG5 following sequential activation by E1 and E2 enzymes. In the other pathway, the ubiquitin-like ATG8 protein is sequentially activated by the same E1 and a different E2 enzyme, and then is conjugated to phosphatidylethanolamine, a membrane lipid, by E3 action of the aforementioned ATG12-ATG5 complex. Thus, both the ATG pathways are blocked by mutation of *atg5* [182]. The autophagy pathways, which are conserved in animals, fungi, and plants, have been recently reviewed [183].

Both RCB-mediated autophagy and whole-organelle chlorophagy are dependent on the ATG pathways. RCBs are studded with ATG8 proteins and do not form in *atg5* mutants [178,184]. Additionally, *atg5* mutants or others lacking the autophagy E1 cannot perform chlorophagy under high-light stress, and show leaf death, increased ROS generation, and reduced shoot growth under stress conditions [179]. ATG-mediated autophagy is known to be involved in the nutrient recycling of plastids in rice and wheat [185,186] as well as Arabidopsis [182], and so it seems likely that chlorophagy is a common strategy of chloroplastic ROS management.

If these mechanisms fail to alleviate the oxidative stress, the final gambit is PCD, initiated by chloroplastic ROS sensors EX1 and EX2, which during oxidative stress are degraded by FtsH in the granal margins to produce an as-yet unknown retrograde signal [22,187].

1.6 The plant immune system

During disease, the plant reprogrammes the chloroplast to produce immunogenic signals in the form of ROS, Ca^{2+} ions, and phytohormones. The pathogen survives by supressing the plant's immune programme and promoting signals beneficial to itself (**Figure 1.4**, p.67). The chloroplast, as a centre of immune signalling, is thus a valuable target for pathogen effectors (**Figure 1.5**, p.69).

1.6.1 The multiphase zig-zag model

Plant immune responses come in several forms. Recognition of microbe- or pathogen-associated molecular patterns (MAMPs or PAMPs), typically highly conserved microbe peptides like flagellin-22, initiates a programme of host defences known as PAMP-triggered immunity (PTI). PTI can also be initiated by recognition of host peptides indicative of damage (damage-associated molecular patterns, DAMPs) [188]. PTI is a basal immune response that excludes most microbes from exploiting the plant's resources, i.e. non-host resistance [189].

PAMP recognition by pattern recognition receptors such as flagellin sensitive 2 (FLS2) [190,191] is transduced through a network of Ca^{2+} ion signalling, ROS generation [192,193], and kinase cascades to extensively reprogramme the plant's transcriptome [194], leading to characteristic PTI responses like callose deposition, closure of the stomata, and extracellular alkalinisation [192,195]. Stomata, pores in the leaf epidermis that allow for gas exchange with the environment, are closed to reduce water loss in drought conditions [196], but in PTI, stomatal closure is thought to hinder pathogen penetration into the leaf [195]. Likewise, callose-rich papillae reinforce the cell wall and restrict pathogen penetration into the tissue [197].

Successful pathogenesis necessitates the suppression of PTI. Pathogens that are adapted to a certain host have evolved or acquired [198] a battery of effectors to disable the

immune system and allow them to exploit the host's resources (effector triggered susceptibility; ETS) [199]. However, effectors themselves may be recognised by plant Resistance (R) genes and elicit effector triggered immunity (ETI), i.e. host resistance [189]. Most R genes encode nucleotide binding leucine rich repeat proteins, and while there are some examples of R genes that recognise effectors directly [200,201], many more are thought to act by guarding host proteins that may be disrupted by effectors, thereby recognising effectors indirectly [202–204].

ETI is an amplified immune response where the plant employs the hypersensitive response (HR), a dramatic "scorched earth" tactic of widespread PCD, and readies defences in distal parts of the plant through systemic acquired resistance (SAR) [203,205]. Over time, an arms race ensues as the pathogen brings to bear new molecular weapons to subvert ETI and the plant evolves new R genes to recognise them. This is the basis of the zigzag model [203], which describes how plant interactions with bacterial and fungal pathogens evolve. A principally similar model has been put forward to describe plant immunity to viruses [206].

1.6.2 *Pseudomonas syringae*: an important model pathogen

Pseudomonas syringae is a model bacterial biotroph—a pathogen that feeds on living host tissue—that infects tomato and other plants like *Arabidopsis thaliana* [207]. Several strains of this pathogen have been instrumental in teasing apart different layers of plant immunity. Plants have different immune responses tailored to biotrophs and necrotrophs—which feed of dead tissue [208]. Some pathogens transition between biotrophic and necrotrophic feeding during their life cycle [209].

Of particular use are the *P. syringae* pv. *tomato* (*Pst*) DC3000 strain, which elicits ETS in Arabidopsis, and mutants with defects in the type III secretion system (T3SS) like *Pst*DC3000 *hrpA*$^-$, which lack the capability to deliver effectors and so only elicit PTI

[210,211]. Other strains, for example, *Pst*DC3000 *AvrRpm1*$^{+}$ and *Pst*DC3000 *AvrRps4*$^{+}$ [212,213], secrete effectors recognised by Arabidopsis R proteins, and thereby trigger ETI.

1.7 Phytohormones and immunity

1.7.1 Chloroplasts produce phytohormones to tailor immune responses

Plant hormones or "phytohormones" initiate gene expression programmes for plant development, stress tolerance, and disease. Complex interactions between different phytohormones allow the plant to prioritise responses to different sorts of stress (**Figure 1.4,** p.67). In disease, the interacting signalling cascades of phytohormones function to tailor the immune programme to resist different sorts of pathogenicity.

Several phytohormone biosynthetic pathways cross the plastid compartment: for example, abscisic acid (ABA) and gibberellic acid (GA) via the MEP pathway [214,215]; auxin, which is derived from chloroplast-synthesised tryptophan [216]; jasmonic acid (JA), which involves both the plastid and the peroxisome [217,218]; and salicylic acid (SA) via the isochorismate synthase (ICS) pathway [219].

Integration, either synergistic or antagonistic, of phytohormone signals tends to occur downstream of signal transduction. Unlike in the metazoans, where many signals may converge on a common receptor, targets of phytohormones rarely overlap [220]. Instead, multiple phytohormones can regulate common pathways by targeting different pathway members. Additionally, phytohormone targets often include genes involved in the biosynthesis or signal transduction of other hormones [220,221].

The two major hormone pathways induced in disease resistance are mediated by SA, or by JA and ethylene (ET). Both pathways involve signals synthesised in the chloroplast.

The SA-induced programme is active in resistance against biotrophs and may in some cases include the initiation of PCD to prevent the pathogen from feeding off living host tissue [222]. SA is produced from chorismate by one of two pathways: the phenylalanine ammonia lyase pathway and the ICS pathway. Only the ICS pathway is localised to the

chloroplast, but in abiotic and biotic stress, it is the major contributor to SA synthesis [219].

In contrast, JA and ET promote resistance against necrotrophs and herbivores [222], which feed off dead tissue so would not be inhibited by PCD. JA is derived from linoleic acid from thylakoid membrane galactolipids. A sequence of enzymatic steps in the chloroplasts, the allene oxide synthase (AOS) branch of the oxylipin pathway, generates the JA precursor 12-oxo-phytodienoic acid (OPDA). This precursor is saturated by a cytosolic enzyme and then undergoes β-oxidation in the peroxisome to produce JA [217,218]. JA is recognised by coronatine insensitive1 (COI1) in the nucleus, which initiates gene expression changes through the degradation of jasmonate ZIM domain (JAZ) proteins [223,224]. There are in fact several different JA derivatives with different activities [225]. The other branch of the oxylipin pathway, the hydroperoxide lyase (HPL) branch, is also chloroplast localised, and it generates aldehydes in response to wounding (i.e. to deter herbivores) [226–228]. ET is produced by enzymatic oxidation of 1-aminocyclopropane-1-carboxylic acid (ACC). The ACC pool, produced by ACC synthase from S-adenosylmethionine, is normally the limiting factor in ET biosynthesis [229].

The SA and JA-ET signalling pathways were thought to antagonise each other, allowing the plant to choose to activate resistance to biotrophs or to necrotrophs, with the trade-off that prioritising immunity to one increases susceptibility to the other [230]. However, this was hard to reconcile with evidence of SA and JA-ET synergy under certain conditions. There appears to be a more nuanced relationship between the two hormone systems depending on whether the plant is engaged in PTI or ETI. In response to PAMPs, SA suppresses JA accumulation by blocking the synthesis of OPDA [231], and application of either SA or JA inhibits the expression of JA or SA target genes, respectively [232,233]. In ETI, however, they act co-operatively: SA promotes JA biosynthesis and they synergistically enhance expression of target genes [234,235].

Another hormone, ABA, induces abiotic stress responses and acts to suppress both biotroph and necrotroph resistance [236]. ABA synthesis begins in the plastids via the MEP pathway. Xanthophylls are synthesised from isopentenyl diphosphate, and are cleaved by the plastid enzyme 9-cis-epoxycarotenoid dioxygenase (NCED) and released into the cytosol as ABA precursor xanthoxin for the final enzymatic steps [214]. GA, also a product of the MEP pathway, affects the balance between SA and JA signalling, but its role is ambiguous. In some systems, GA acts to promote SA-resistance to biotrophs at the expense of JA-resistance to necrotrophs, but in others GA promotes biotroph susceptibility [237].

1.7.2 Retrograde signalling regulates hormone biosynthesis in immunity

Regulation of plastidic hormone biosynthesis is mediated by both anterograde signalling, through the expression of NECGs, and retrograde signalling, via the PAP and MEcPP signals.

The chloroplast retrograde signal PAP is known to regulate resistance to high-light and drought stresses through ABA-mediated signalling [25,238]. PAP is synthesised in the cytosol but is transported into the chloroplast for degradation by the phosphatase SAL1 [239]. Recently, a new role of the PAP signal in regulating the SA and JA ratio in disease was uncovered [26].

The SAL-PAP system is involved both in the synthesis of SA and in SA signal perception. Arabidopsis *sal1* mutants have a lower basal level of SA, and during infection with the necrotroph *Pectobacterium carotovorum* they accumulate less SA and more JA than wild-type plants, suggesting PAP promotes SA signalling. The *sal1* mutants are less sensitive to SA, showing reduced expression of SA-induced genes encoding isochorismate synthase 1 (ICS1; the key enzyme in plastid-localised SA synthesis) and pathogenesis related 1 (PR1; involved in defence) in response exogenously applied SA [26].

Curiously, *sal1* mutants also show partial insensitivity to exogenous JA: methyl jasmonate induces both the genes encoding 12-oxophytodienoate reductase 3 (OPR3, involved in JA synthesis) and plant defensin 1.2 (PDF1.2, involved in defence) in wild-type and SAL1-overexpressor plants, but only *OPR3* (not *PDF1.2*) in *sal1* plants [26]. These data indicate that the PAP signal suppresses induction of both SA and JA immunity.

Arabidopsis *sal1* plants are more susceptible to avirulent, ETI-inducing *P. syringae*, but in *Pst*DC3000 infection where ETI is suppressed, they show increased symptoms but no additional bacteria growth compared to wild-type Arabidopsis. This implicates retrograde signalling in the induction ETI defences [26]. Given its established role in ABA-mediated signalling [25,238], the SAL-PAP pathway may represent a mechanism that calibrates defence responses between abiotic and biotic stress signalling [26].

As an intermediate in the MEP pathway [240], MEcPP is involved in the generation of isoprenoids, GA and ABA. MEcPP itself functions as a stress sensor, accumulating under stress conditions including high light and wounding, and integrates several stress pathways. It interacts with both SA and JA responses. MEcPP accumulation promotes the expression of *ICS1*, and accumulation of SA [23]. Enhanced MEcPP accumulation, as in the Arabidopsis *constitutively expressing HPL* (*ceh1*) mutant, which cannot catalyse the conversion of MEcPP to hydroxymethylbutenyl diphosphate (the next step in the MEP pathway), displays an elevated level of SA and enhanced resistance to biotrophs [23].

Despite constitutively higher SA levels, the *ceh1* mutant does not show reduced JA accumulation or JA-responsive gene expression compared to the wild type [24]. This seems to suggest that activated MEcPP signalling, while promoting SA, also prevents SA-induced suppression of JA signalling. The *ceh1* mutant induces the HPL branch of the oxylipin pathway, but does not alter the AOS branch [23]. Nevertheless, the increased MEcPP signal in *ceh1* promotes the synthesis by the AOS branch of plastid JA precursor OPDA, which may act to induce JA-responsive genes [24]. Finally, it is noteworthy that

the PAP and MEcPP retrograde signals are redox regulated, and so ROS overproduction may potentiate these signals [241].

1.7.3 Pathogens target phytohormone production to promote virulence

To render their host susceptible, pathogens interfere with phytohormone signalling and the induction of the appropriate stress responses. This can involve manipulation of the antagonism between SA and JA signalling. Necrotrophic fungi like *Alternaria solani* and *Botrytis cinerea* divert the plant's immune response to one against biotrophs, by secreting effectors that induce SA accumulation and boost expression of SA-responsive transcription factors [242,243]. This suppresses JA signalling and creates conditions favourable for necrotrophs. Fungal necrotroph *Gibberella fujikuro*, from which GA was first identified, secretes GA to inhibit JA-mediated resistance and promote the ineffective SA-mediated resistance instead [244]. Biotrophs, on the other hand, secrete effectors that promote JA gene expression. *P. syringae* secretes coronatine, a JA mimic that can activate COI [245], as can effectors secreted by the biotrophic fungus *Fusarium oxysporum* [246,247], while *P. syringae* effectors HopX1 and HopZ1a bypass COI to degrade JAZ proteins directly [248,249].

Both biotroph immunity and necrotroph immunity may be suppressed by ABA, which is a key regulator of drought and water stress response [250]. This can occur by releasing pathogen-derived ABA, as in infection by *B. cinerea* [251], or by upregulation of host ABA synthesis. *P. syringae* effectors induce increased expression of *NCED3*, the NECG that codes for the rate-limiting NCED enzyme, to promote the ABA pathway [252]. Pretreating Arabidopsis plants with ABA prevents deactivation of ROS management in *Pst*DC3000 *hrpA*$^{-}$ infection, suppressing the chloroplastic ROS burst and inducing susceptibility [253]. This is an example of the antagonism between pathways promoting immunity and promoting abiotic stress tolerance.

1.8 ROS dysregulation enhances plant immunity

1.8.1 Pathogen recognition initiates a ROS cascade

ROS were originally thought of only as toxic metabolic by-products that had utility as antimicrobials [254]. Increasingly, ROS are thought to have a more nuanced role. In fact, redox signalling underlies cell growth and organ patterning [13,157,158]. It is now clear that ROS contribute to immunity as signalling molecules.

PTI is associated with the generation of ROS [255] in the apoplast by plasma membrane-bound NADPH oxidases called respiratory burst oxidative homologues (RBOHs), particularly RBOH protein D (RBOHD) [256], and intracellularly by the peroxisomes and chloroplasts [157,257]. In photosynthetic tissues, chloroplasts and peroxisomes each generate twenty times more ROS than mitochondria do [157].

On PAMP recognition, the plant starts to disengage its own safety features to release the restraints preventing ROS generation. Within twenty minutes of PAMP exposure, NPQ is suppressed, driving more energy into photochemistry and increasing the production of ROS in the chloroplast [253,258]. This is achieved by downregulation of *PsbS* gene expression [193], which encodes the thylakoid sensor responsible for inducing NPQ [163].

NPQ suppression and enhanced photoproduction of ROS is a specific goal of the defence programme, and proceeds independently from apoplastic ROS generation [193]. The physiological importance of chloroplastic ROS generation during PTI was recently demonstrated in an experiment where it was inhibited by the herbicide 3-(3,4-dichlorophenyl)-1,1-dimethylurea (DCMU), which prevents plastoquinone binding at PS II, blocking electron transport and abolishing hydrogen peroxide production at PS I. This treatment prevented *Pst*DC3000 *hrpA*$^{-}$ eliciting a ROS burst and rescued its pathogenicity [253].

During infection, *Pst*DC3000 has been found to induce NPQ to dissipate more energy harmlessly as heat [253]. As infection continues, *Pst*DC3000 effectors, including coronatine [259], act to downregulate transcription of NECGs involved in light interception, and so depress photosynthetic efficiency [253,260]. In these ways, *Pst*DC3000 acts to reduce photon excess, thereby suppressing the critically timed PTI ROS burst.

1.8.2 Disruption of ROS management promotes immunity

Since the deactivation of ROS management strategies linked to abiotic stress tolerance promotes disease resistance, we might expect disease resistance to be enhanced in plant lines that show defective ROS management. Indeed, the *psb*S mutant of Arabidopsis, which is defective in NPQ, shows both ready overproduction of ROS [261] and enhanced expression of PTI-induced genes [193]. Moreover, autophagy mutants, which are defective in the chlorophagy-based ROS management system and show ROS overproduction in high-light stress [179], display enhanced resistance to powdery mildew, another biotroph, mediated by increased ROS production [262,263].

Recently, a negative regulator of ETI, constitutive expresser of pathogenesis related genes 1 (CPR1), was shown to be connected to chloroplast ROS management [264]. CPR1 is part of a cytosolic ubiquitin E3 complex that targets a number of proteins, including R proteins and chloroplast protein chaperones [265], for destruction. It acts in two independent pathways to suppress the activation of plant defences: by promoting expression of plastid antioxidants including 2-cysteine peroxiredoxin, and by ubiquitination of R proteins for turnover. The Arabidopsis *cpr1* mutants show enhanced chloroplastic ROS generation and SA accumulation, and the constitutive expression of ETI-related defence genes, even in the absence of pathogens. CPR1's role seems to be to prevent the inappropriate induction of immune responses that are costly to growth [264].

The example of *cpr1* suggests regulation of ROS scavenging, in addition to avoidance and reparation, may be important to the induction of defences.

In disease, RCB-mediated autophagy may facilitate ROS generation instead of restricting it. During infection by the avirulent, ETI-eliciting *Pst*DC3000 *AvrRps4*$^{+}$, which induces chloroplastic ROS generation, vacuole-targeted vesicles containing stromal proteins are formed [266], which resemble RCBs. Disruption of RCB-mediated autophagy in the a*tg5* mutant prevents vesicle formation during *Pst*DC3000 *AvrRps4*$^{+}$ infection and impairs ROS generation, correlating with the mutant's enhanced susceptibility [266]. These experiments illustrate a dual-role for the ATG pathways in disease. It seems that in the milder PTI, chlorophagy limits ROS generation and its disruption enhances resistance, whereas in ETI the more robust ROS burst is enhanced by RCB-mediated autophagic degradation of Rubisco, which would reduce carbon assimilation and so promote ROS photoproduction.

In summary, this suggests that abiotic stress tolerance systems to tolerate ROS antagonise immunity; that pathogens activate or enhance abiotic stress tolerance to promote virulence; and that disruption of these systems promotes resistance.

1.8.3 Apoplastic and chloroplastic ROS

The focus on the apoplast as the bulk source of ROS in plant pathology risks overlooking the contribution of intracellular ROS sources. It is becoming clear that the source of the ROS signal, not just the amount of ROS generated, is relevant to successful immunity. Chloroplastic ROS is critical to PTI in a way that apoplastic ROS may not be, but both contribute to HR in ETI; and the apoplastic ROS burst is important in establishing SAR.

The main RBOH involved in immunity, RBOHD, is activated by phosphorylation on PAMP recognition. The Arabidopsis *rbohd* mutant generates much less ROS, is impaired in stomatal closure, a feature of PTI [267], and shows a reduced HR in ETI [268]. However, these effects have no clear impact on immunity, neither enhancing nor

hindering resistance of *rbohd* to *Pst*DC3000 or *Pst*DC3000 *AvrRpm1*$^{+}$ [268] . In fact, the *rbohd* mutation has been studied with respect to resistance in a variety of biotrophic and necrotrophic interactions, and no clear consensus of its role in immunity emerges [268,269]. By contrast, prevention of chloroplastic ROS generation is a vital step in facilitating *Pst* infection in Arabidopsis [253]. Recently, it was suggested that the lack of an immunity phenotype in *rbohd* is because the complete absence of RBOHD—as in the null allele—may activate a compensatory form of immunity [267].

The apoplastic ROS signal has a less ambiguous role in systemic immunity. It travels at over eight centimetres per minute, propagating itself via ROS-activation of RBOHs along the way like a Mexican wave [270]. Consistent with the notion that the apoplastic ROS wave contributes to activation of SAR, the Arabidopsis *rbohd* mutant does not show increased resistance after priming [271].

Both chloroplastic and apoplastic ROS are implicated in the induction of HR. HR is reduced in *rboh* mutants for a number of plant-pathogen interactions, although exceptions exist where cell death is enhanced or unchanged [269]. HR is induced more strongly in the light than in the dark [272], suggesting the involvement of chloroplastic ROS; and tobacco plants expressing a chloroplast-targeted bacterial antioxidant, flavodoxin, show reduced chloroplastic ROS generation coupled with reduced cell death upon infection by the bacterial pathogen *Xanthomonas campestris* [273]. These experiments suggest either that ROS signalling is less critical in ETI than in PTI, or that in ETI apoplastic and chloroplastic ROS act redundantly.

1.9 Pathogens target the chloroplast compartment to achieve virulence

Pathogens implement changes to chloroplast homeostasis through modification of the chloroplast proteome. This is achieved in at least three different ways (**Figure 1.5**, p.69): by altering the expression of NECGs; by delivering effectors to the chloroplast that can interact with host chloroplast proteins; and by altering the targeting of cytosolic proteins, causing them to accumulate in the chloroplasts.

1.9.1 NECG expression is altered during immunity and virulence

In the example of flagellin-22 perception, the PAMP recognition signal is transduced by heterodimerization of the FLS2 receptor with brassinosteroid-associated kinase 1 (BAK1). The FLS2/BAK1 complex activates a cascade of phosphorylation by mitogen-activated protein kinases (MAPKs or MPKs) that rapidly brings about extensive transcriptome changes [194,274]. A cascade of calcium-dependent protein kinases (CDPKs) also induces transcriptomic changes, and works with the MAPK cascade to induce synergistically some target immunity genes [275]. It has been reported that in rice CDPK18 can directly phosphorylate MAPK, suggesting direct links between the two kinase cascades [276]. These signals are rapidly induced: CDPKs are activated by calcium ion influx within five minutes of elicitor treatment, remaining active for one to two hours [277], while MAPK activation begins one minute from PAMP perception and lasts no more than one hour [274].

A recent study revealed the extent of transcriptome remodelling in PTI. Recognition of *Pst*DC3000 *hrpA*$^-$ by Arabidopsis leads to regulatory changes to over 7,000 genes [278]. To suppress PTI, the pathogenic *Pst*DC3000 strain blocks the changes to just 525 of them, and induces sustained transcriptional changes in a core set of 182 genes not associated with PTI, i.e. ETI-related genes. These 182 regulatory changes ultimately drive the

differential expression of over 2,000 genes: an ETS transcriptomic signature which includes both targets of virulence reprogramming by effectors, and host ripostes to effector recognition [278].

A large number of the differentially regulated genes in PTI are NECGs [253]. Four hours into infection of Arabidopsis by *Pst*DC3000 *hrpA*$^-$, over five hundred NECGs are differentially regulated; twelve hours into infection, 473 NECGs are upregulated, particularly genes involved in chorismate, JA and tryptophan biosynthesis, and over 1,000 largely photosynthesis-related NECGs are downregulated. Initially, *Pst*DC3000 elicits the same changes to NECGs, but by three hours post-infection the transcriptome signature shows signs of divergence from the *Pst*DC3000 *hrpA*$^-$ response. By twelve hours post-infection with *Pst*DC3000, around 1,200 genes are differentially regulated compared to infection with *Pst*DC3000 *hrpA*$^-$. Surprisingly, effectors do not act just to suppress PTI-related gene expression changes, but also to enhance some changes: while the suppression of photosynthetic NECGs in PTI does not reduce photosynthetic efficiency, in ETS they are more strongly suppressed and photosynthetic efficiency declines [253].

Effectors can enhance or suppress PTI-related gene expression changes by targeting various stages of the kinase cascades. For instance, *P. syringae* effector HopF2 suppresses both BAK1 [279] and downstream MAPK kinases (MKKs) including MKK5 [280], while HopAI1 inactivates MPK3 and MPK6 [281]. Conversely, the effector AvrB activates MPK4 by phosphorylation [282], consistent with the observation that some ETS gene expression changes (e.g. suppression of photosynthetic NECGs) involve the enhancement, not subversion, of PTI-related expression changes [253].

Other effectors bring about ETS-related gene expression changes more directly, by targeting or mimicking transcription factors [283]. For example, *Pst*DC3000 effector HopD1 targets the Arabidopsis transcription factor NTL9 [284]; while *Xanthomonas* spp. transcriptional activator-like effectors translocate to the nucleus and bind specific

promoter sequences (e.g. AvrBs3 and Tal7 [285,286]). Some pathogen effectors are involved in chromatin reconfiguration, which can alter gene expression epigenetically [283,287].

1.9.2 Some effectors are imported into the chloroplast

While some effectors target pathways in the cytosol or nucleus, others are transported to the chloroplast. To reach the chloroplast stroma, effectors must pass across the chloroplast double envelope membrane. Delivering effectors to specific compartments presents the pathogen with a problem that the plant cell has already solved: the pathogen can exploit the cell's own transport machinery to traffic effector molecules to the chloroplast, mitochondria, and nucleus [288,289].

One hallmark of the canonical import pathway (see **§1.3)** is the presence of a cleavable N-terminal transit peptide. At least four effectors from *P. syringae*—AvrRps4, HopK1, HopO1-2 and HopR1—have been demonstrated to target the chloroplast using a cleavable transit peptide [253,290].

While the N-terminal regions of HopK1 and AvrRps4 do not show sequence homology with plant-derived chloroplast-targeted proteins, they are nevertheless necessary and sufficient to localise the proteins to the chloroplast, and are cleaved from the effector during import [290], a step that is characteristic of import through the TOC-TIC complexes [2]. This suggests that effector transit peptides have evolved to mimic chloroplast transit peptides, so as to be recognised by the host's protein import machinery. Interestingly, transit peptide mimicry has also been observed in fungal pathogens, for three effectors of the rust fungus *Melampsora larici-populina* [291,292], and in plant viruses, as in the cucumber necrosis virus coat protein [293].

As noted earlier, transit peptides are heterogeneous in relation to sequence and length, and possess no obvious consensus motifs [29], but predicting whether a sequence constitutes a transit peptide can be achieved by using neural network approaches, as in

the ChloroP software, which recognises the HopK1 and AvrRps4 N-terminal sequences as transit peptides [253,294].

In fact, these bioinformatics approaches suggest that transit peptide mimicry may be more common than was previously realised: a recent analysis of *Pst*DC3000 effector protein sequences using ChloroP identified a further 17 core effectors with putative chloroplast transit peptides. A remarkable 46% of the effector sequences from 56 species and pathovars analysed in this way are candidates for chloroplast targeting [253].

1.9.3 Non-canonical import of effectors

Other effectors seem to localise to the chloroplast through non-canonical routes, like *Pst* effectors HopI1 and HopN1. HopI1 is not predicted to have a chloroplast transit peptide by bioinformatic analysis [253], and neither HopI1 nor HopN1 undergoes N-terminal cleavage during import [295,296]. Nevertheless, both effectors are undoubtedly chloroplast targeted: they can be found in the chloroplasts isolated from infected plants, can be used to transport a fused fluorescence tag to chloroplasts [295,296], and interact with chloroplast-localised host proteins to promote virulence [296,297].

In these cases, the effectors may be exploiting one of host's supplementary chloroplast targeting pathways (**§§1.3.5-1.3.6**).

Alternatively, non-canonical targeting of effectors may employ pathways of localisation that are entirely novel to the pathogen. For example, potato virus X coat protein achieves chloroplast import without a transit peptide of its own by interacting with the transit peptide of the host plastocyanin preprotein. In the absence of plastocyanin, the coat protein cannot enter the chloroplast [298]. This is suggestive of a mechanism in which non-host proteins might be able to "share" the targeting information of host chloroplast-targeted proteins. Similarly, the chloroplast-localised *P. syringae* effector HopI1 binds to a chaperone component of a putative chloroplast preprotein guidance complex (see **§§1.3.1&1.9.5**) [31,299], raising the possibility that binding of guidance complex

components to parts of the protein other than transit peptides may facilitate plastid targeting.

1.9.4 Chloroplast proteins are targets of effectors

The targets of most confirmed chloroplast-localised effectors have yet to be identified. Those effectors that have been studied in this regard target the photosynthetic machinery and chloroplast-localised abiotic stress tolerance mechanisms.

HopN1 interacts with PsbQ, a component of the oxygen-evolving complex of PS II, and causes its proteolysis. This interferes with PS II activity, leading to reduced electron transport and oxygen production, and inhibition the chloroplastic ROS burst [296].

HopI1 targets chloroplast-localised Hsp70 isoforms [295,297]. In plants, Hsp70s can assist in chloroplast protein import (**§1.3.1**) and stromal Hsp70 isoforms are involved in correct PS II assembly and repair during chloroplast biogenesis and abiotic stress [300,301].

HopI1 forms large complexes with Hsp70 in the chloroplast, where it promotes virulence by activating Hsp70-mediated abiotic stress tolerance. Transgenic plants expressing HopI1 show increased heat shock tolerance; likewise, stimulation of Hsp70 ATP hydrolysis by abiotic stress (heat shock) restores susceptibility to the *P. syringae* pv *maculicola hopI1*$^{-}$ mutant strain. Arabidopsis plants overexpressing Hsp70 retain immunity to the *hopI1*$^{-}$ mutant even during heat shock, but are still susceptible to the HopI1-expressing strain [295,297]. Therefore, activation of Hsp70's role in abiotic stress tolerance, by heat shock or by interaction with HopI1, antagonises the induction of immunity. The HopI1-Hsp70 interaction also induces changes to thylakoid ultrastructure, and this may indicate a change in the PS II to PS I ratio caused by Hsp70's roles in PS assembly [295].

Chloroplast localisation of AvrRps4 and HopK1 has been shown to be necessary for their contribution to virulence, indicating that they have as-yet unidentified chloroplast localised targets [290]. Of the other *P. syringae* effectors with predicted transit peptides, most either do not have an identified mode of action, or have been shown to have activity outside the chloroplast. The latter point does not rule out the possibility that they have chloroplast targets, as some effectors have multiple independent roles in infection. HopF2, which is known to insert into the plasma membrane to target BAK1 [279], has an additional, independent role in preventing stomatal closure [302]. Although HopF2 has a predicted transit peptide [253], and stomatal closure is signalled via the chloroplast [303], it has not known if HopF2 performs its stomatal function by localising to the chloroplast.

1.9.5 Effectors can alter host protein localisation

The HopI1-Hsp70 complexes are composed of both chloroplastic Hsp70 and cytosolic Hsp70 isoforms. HopI1 interacts with cytosolic Hsp70 and promotes its translocation to the chloroplast [297]. This might function to enhance virulence by enhancing the HopI1-elicited activation of Hsp70-mediated abiotic stress tolerance in the chloroplast, or by sequestering Hsp70 away from its important functions in the cytosol, e.g. in the chloroplast guidance complex or the Hsp70/CHIP system (see §§**1.3.1**&**1.4.3**). Effector-induced recruitment of host proteins to different compartments is a mechanism known to promote ETI (e.g. [304,305]), but the HopI1-cytosolic Hsp70 interaction is interesting as it provides an example of induced relocalisation that promotes virulence.

1.10 Aims

The chloroplast stands at the crossroads of competing programmes of resistance to abiotic stresses and resistance to biotic stresses. The next century will be marked by extremes of temperatures, reduced water availability, poorer quality soil, emerging plant pathogens, and falling efficacy of herbicides and pesticides. How plants respond to these environmental challenges, and what the future of our planet will look like—including in terms of agricultural yields and world hunger, species biodiversity, and the biosequestration of carbon dioxide—will depend on reactions occurring in the chloroplast.

There is a complex interplay between abiotic stress, where multiple systems monitor the chloroplast to prevent toxicity, and biotic stress. Additionally, not only are there pathogen effectors that reprogramme the expression of NECGs, there are some that directly target and are imported into the chloroplast. This raises the intriguing possibility that regulation of the TOC machinery may also have a role to play during pathogenesis.

The objective of this thesis is to further the understanding of how chloroplasts regulate, and are affected by, stress and disease. In particular, it will elucidate the role of SP1, a regulator of chloroplast protein import, during infection by *Pst*.

In **§2**, SP1's role in immunity is investigated and the implications it has for how pathogens suppress basal resistance are discussed. In **§3**, the mechanism behind SP1's role in virulence and resistance is explored. In **§4**, the role of photosynthesis in disease is re-examined. Then, in **§5**, differences between immunity and susceptibility are examined in a broader metabolomic context.

1.11 Figures

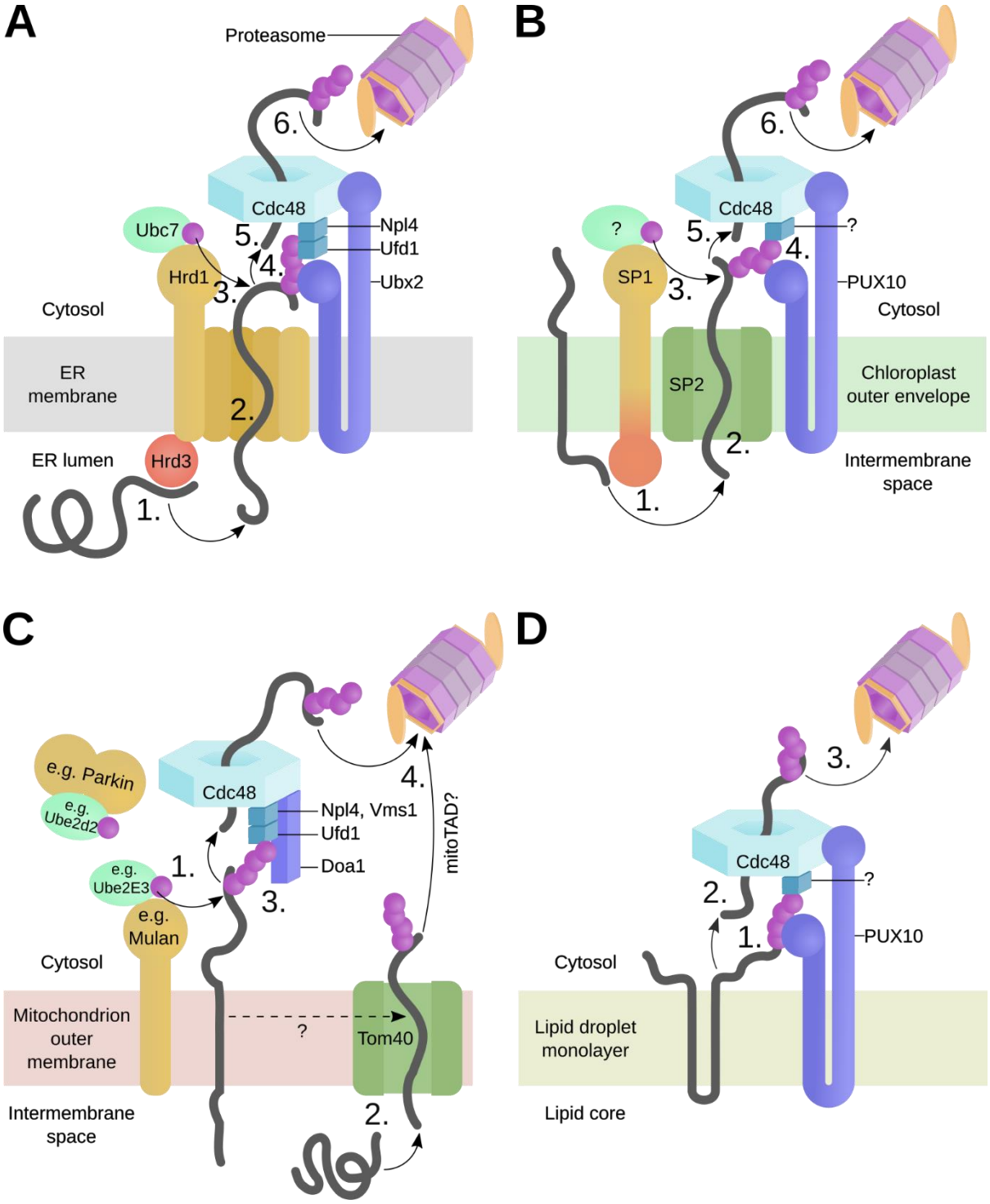

Figure 1.1 Analogous Cdc48-depdendent systems for the regulation of organelle proteins by the UPS.

A. Endoplasmic reticulum (ER)-associated protein degradation (ERAD). In this example, ERAD of lumenal proteins (ERAD-L) is shown. 1. Substrates (dark grey) are recognised by substrate recognition proteins including HMG-CoA reductase degradation (Hrd) 3. 2. Substrates are retrotranslocated via a funnel formed from the transmembrane loops of Hrd1 dimers. 3. The RING domain of the E3 ligase Hrd1, in concert with E2 ligase ubiquitin conjugating enzyme 7 (Ubc7), ligates ubiquitin (purple circles) to the substrate.. 4. The substrate's polyubiquitin chain is recognised by ubiquitin regulatory x (Ubx) 2, which assists in recruiting the ATPase cell division cycle 48 (Cdc48). 5. Cdc48, with ubiquitin recognising co-factors ubiquitin fusion degradation 1 (Ufd1) and nuclear protein localisation 4 (Npl4), provides the motive force to extract the substrate from the ER. 6. The substrate is thus available for degradation by the proteasome.
B. Chloroplast-associated protein degradation (CHLORAD). 1. Substrates are recognised by the intermembrane space domain of the E3 ligase suppressor of *ppi1* (SP) locus 1. 2. Retrotranslocation of substrates is assisted by the channel protein SP2. 3. Substrate is ubiquitinated by the RING domain of SP1 in concert with an unknown E2. The sequence of ubiquitination and retrotranslocation is not known. 4. The substrate's polyubiquitin chain is recognised by plant Ubx domain containing protein 10 (PUX10, unpublished data), a Ubx2 homologue, which assists in recruiting Cdc48. 5. Cdc48, with unknown cofactors, provides the motive force to extract the substrate from the chloroplast outer envelope membrane. 6. The substrate is thus available for degradation by the 26S proteasome.
C. Outer mitochondrion membrane-associated protein degradation (MAD or OMMAD). 1. Membrane bound (e.g. Mulan) or cytosolic (e.g. Parkin) E3 ligases ubiquitinate membrane-bound substrates. Target specificity might be achieved in part by the diverse range of E2 conjugases (e.g. Ube2d2 or Ube2E3) these E3s are known to interact with. 2. Intermembrane space substrates are retrotranslocated via the import channel translocon at the outer mitochondrial membrane 40 (Tom40); no retrotranslocon has been identified yet for membrane-bound substrates. 3. Cdc48 is recruited to the polyubiquitin chains by ubiquitin recognising cofactors including Doa1, and either Npl4 and Ufd1 or VCP-associated mitochondrial stress-responsive 1 (Vms1); and provides the motive force to extract the substrate from the mitochondrion outer membrane. 4. The substrate is is now available for degradation by the 26S proteasome.
D. Lipid droplet-associated protein degradation (LDAD). 1. Polyubiquitin chains of substrates are recognised by PUX10, which assists in recruiting Cdc48. 2. Cdc48, with unknown cofactors, provides the motive force to extract the substrate from the lipid droplet monolayer. 3. The substrate is now available for degradation by the 26S proteasome.

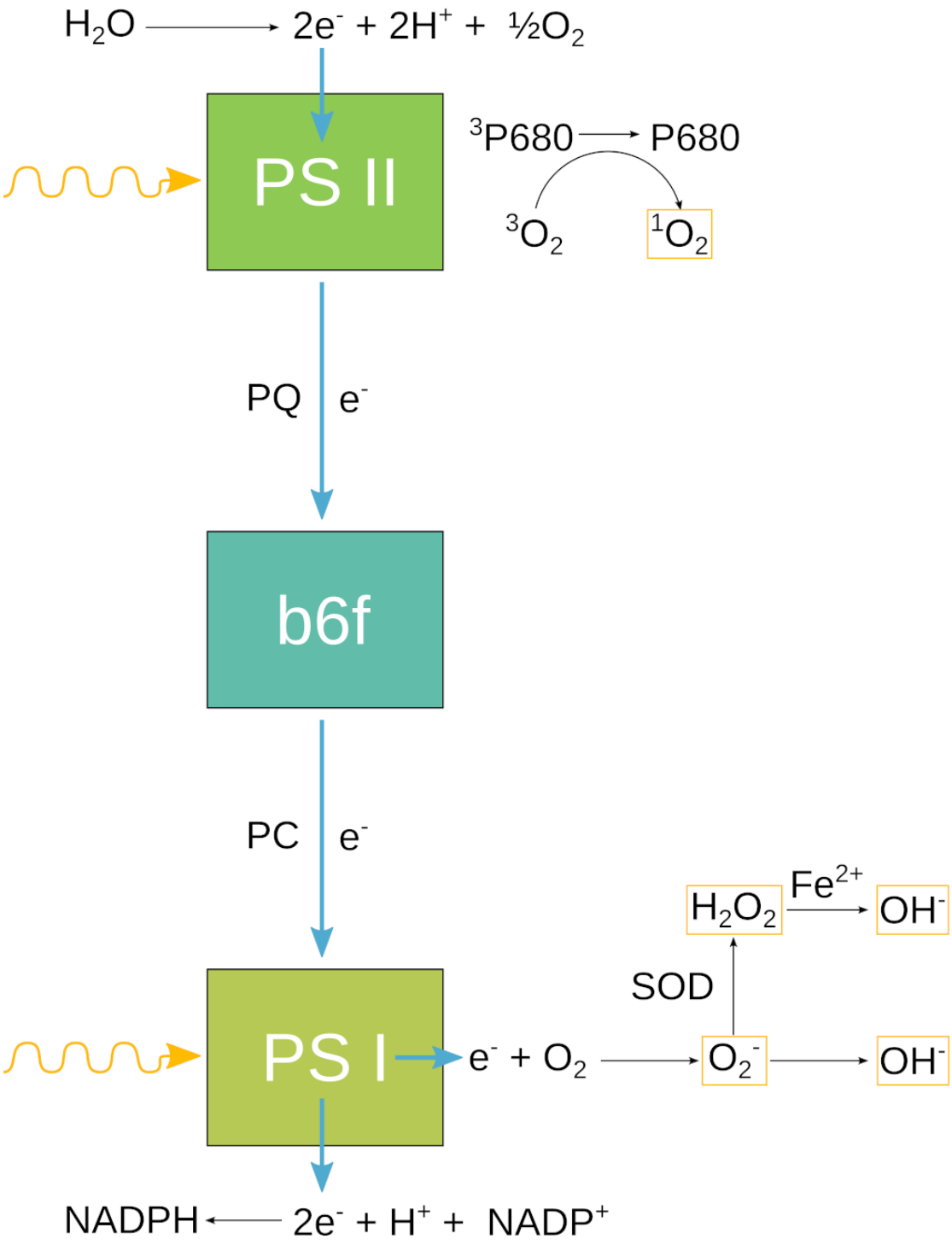

Figure 1.2 A simplified schematic of photosynthetic ROS generation.

During photosynthesis, electrons (e^-) from the splitting of water are passed through an electron transport chain from photosystem (PS) II to PS I, where they are safely employed in the reduction of $NADP^+$. Energy for this process is provided by the interception of photons (gold wavy lines) at each photosystem. In times of photon excess, this energy can instead drive the generation of reactive oxygen species (ROS, gold boxes). When overexcited, the primary donor of PSII (P680) enters a triplet state, and may react with oxygen ($^3O_2$ or O_2) to form highly reactive singlet oxygen ($^1O_2$). At PS I, electrons may react with O_2 to give rise to superoxide (O_2^-). Highly reactive superoxide is quickly converted to the longer-lived but less reactive hydrogen peroxide (H_2O_2) by superoxide dismutase (SOD). H_2O_2 may be decomposed into hydroxyl ions (OH^-) by an iron catalyst (Fe^{2+}), which may also arise from O_2^- directly.
Other abbreviations: b6f: cytochrome b_6f; PQ: plastoquinone; PC: plastocyanin.

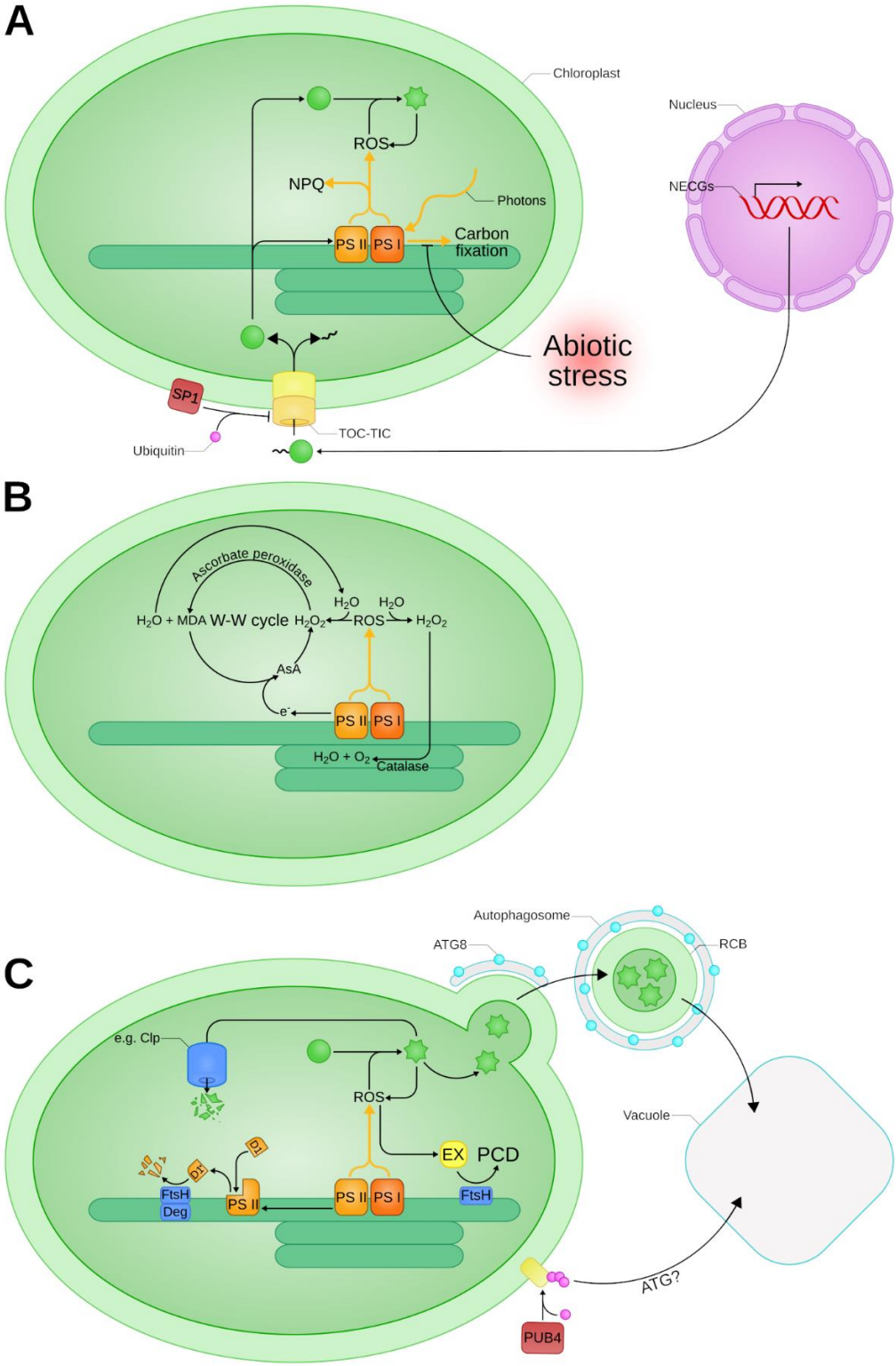

Figure 1.3 Strategies of chloroplast ROS management.

A. When the energy from intercepted photons exceeds the chloroplast's ability to use that energy to assimilate carbon, as is the case during abiotic stress, that energy may generate reactive oxygen species (ROS), which damage chloroplast components (star-shapes). Several mechanisms help avoid the generation of ROS. Surplus energy may be released as heat through non-photochemical quenching (NPQ). Additionally, photon excess may be reduced by reducing the import of photosynthetic preproteins. In the case of short-term stress, import is reduced by the ubiquitination of the translocon of the outer chloroplast membrane (TOC) complexes by suppressor of *ppi1* locus 1 (SP1), leading to their turnover by the proteasome. In acclimation to longer stress exposure, the expression of nucleus-encoded chloroplast genes (NECGs) becomes downregulated.
B. ROS once generated may be scavenged in a number of different ways. Represented here is the stromal water-water (W-W) cycle, where hydrogen peroxide (H_2O_2) is reduced by ascorbic acid (AsA), producing water and the monodehydroascorbate (MDA) radical. MDA is recycled to AsA with reducing power (e^-) diverted from photosynthesis. H_2O_2 that diffuses into the thylakoid lumen is decomposed by catalases.
C. Damaged chloroplast components must be turned over to prevent further ROS accumulation. This may be accomplished by chloroplast-localised proteases such as the caseinolytic peptidase (Clp). A specialist repair system services the core subunit (D1) of photosystem II (PS II). When D1 accumulates oxidative damage (D1*), PS II migrates away from the grana, is partially disassembled and its D1 subunit replaced. D1* is then degraded by thylakoid membrane-bound proteases FtsH and Deg. Rubisco-containing bodies (RCBs) traffic stromal components to the vacuole for degradation through an autophagy-related (ATG) pathway. Entire chloroplasts may be selectively degraded in the vacuole ("chlorophagy") in an ATG gene-dependent manner. Chlorophagy can be signalled by the ubiquitination of unknown outer membrane components by plant U-box 4 (PUB4). Finally, if ROS management fails, decomposition of executer 1 (EX) by FtsH generates an unknown retrograde signal that initiates programmed cell death (PCD).
Other abbreviations: ATG8: autophagy-related 8; PS I: photosystem I; TIC: translocon of the inner chloroplast membrane.

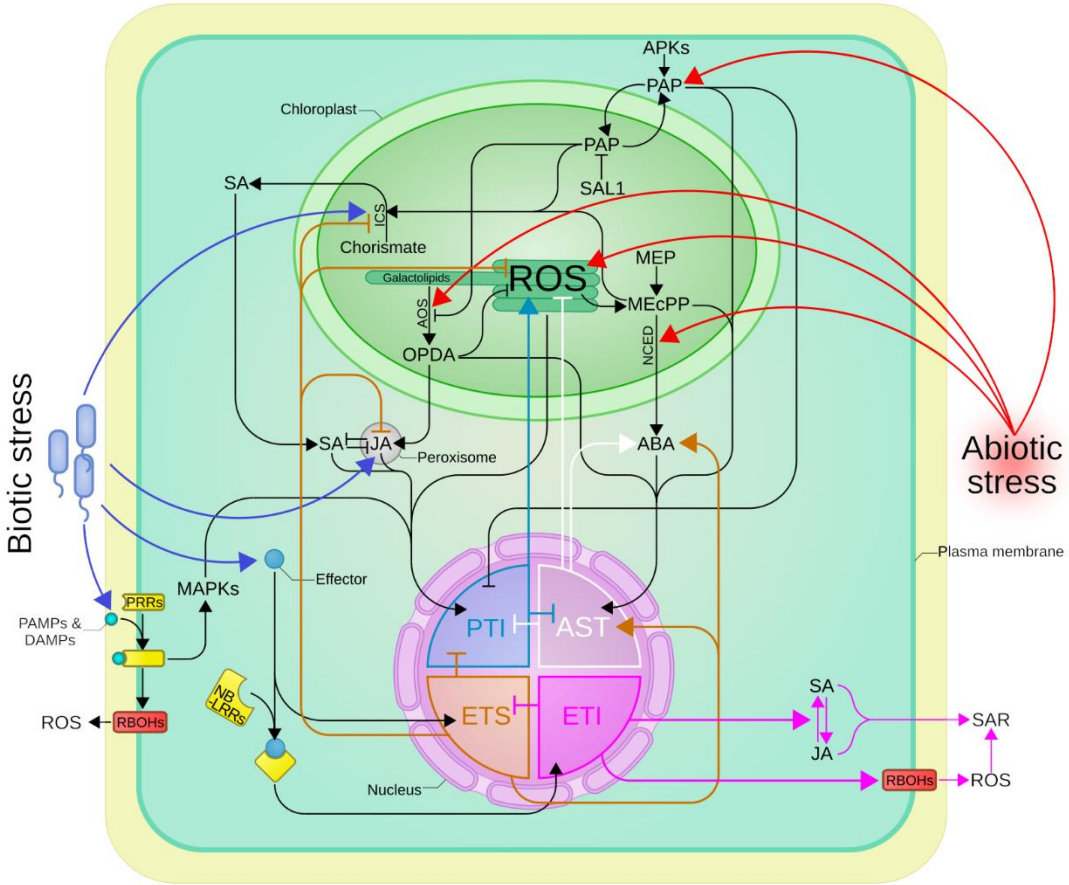

Figure 1.4 Stress and immunogenic signals are relayed and integrated through the chloroplast.

A simplified overview of some of the signalling pathways that involve the chloroplast, and the interaction of abiotic and biotic stresses on signalling. Abiotic stress tolerance (AST) programmes act to mitigate damaging reactive oxygen species (ROS) production in the chloroplast. Antagonism exists between AST and the basal immune programme (PAMP triggered immunity, PTI), triggered by perception of pathogen or damage associated molecular patterns (PAMPs & DAMPs) by plasma membrane pattern recognition receptors (PRRs). Pathogens secrete effectors to render the host susceptible (effector triggered susceptibility, ETS). In ETS, PTI is supressed and AST strategies are enhanced. However, in plants with a corresponding R gene, effectors may be recognised by nucleotide-binding leucine-rich repeat (NB-LRR) proteins and effector triggered immunity (ETI) is activated, suppressing ETS and leading to hypersensitive response (not shown) and systemic acquired immunity (SAR). Chloroplasts contribute to PTI and ETI through generation of reactive oxygen species (ROS), metabolic intermediates that function in retrograde signalling, and phytohormones. Salicylic acid (SA) and jasmonic acid (JA) both promote immunity, but antagonise each other during PTI, promoting resistance against either biotrophs or necrotrophs respectively. In ETI, SA and JA act synergistically to promote SAR.
Other abbreviations: ABA: abscisic acid; AOS: allene oxide synthase pathway; APKs: adenosine phosphosulphate kinases; ICS: isochorismate synthase pathway; MAPKs, mitogen-activated protein kinases; MEP: 2C-methyl-D-erythritol-4-phosphate; MEcPP: C-methyl-D-erythritol-2,4-cyclopyrophosphate; NCED: 9-cis-epoxycarotenoid dioxygenase; OPDA: 12-oxo-phytodienoic acid; PAP: 3`-phosphoadenosine 5`-phosphate; SAL1: aka FIERY1.

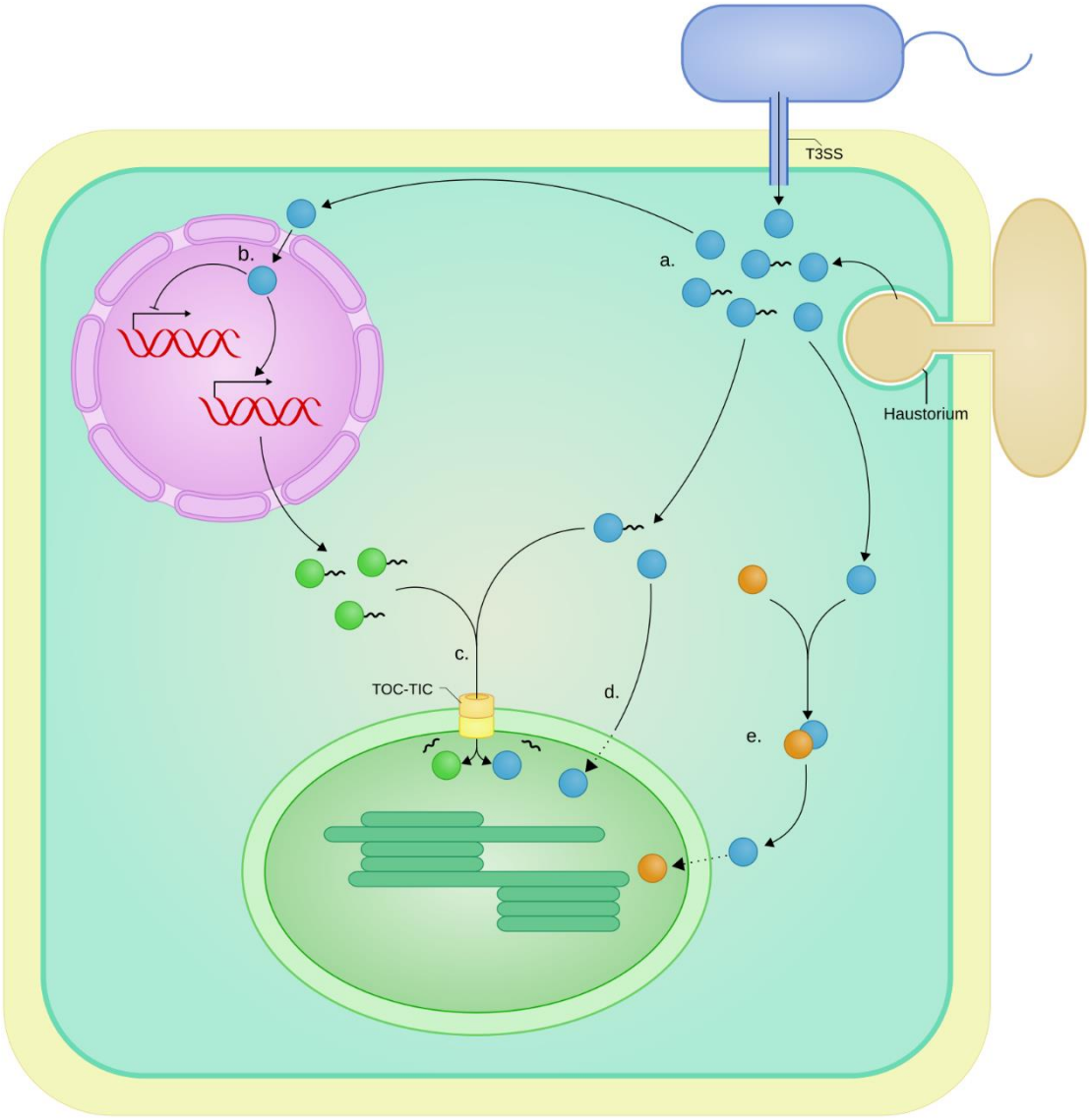

Figure 1.5 Pathogens use effectors to alter the chloroplast proteome.

a. Pathogens deliver effectors (blue circles) into plant host cells to derail plant immunity using structures like haustoria or the type III secretion system (T3SS). b. Some effectors are targeted to the nucleus, where they act to modulate gene transcription, including that of NECGs (green circles). c. Other effectors include imitation transit peptides. Host NECGs—which include enzymes for hormone biosynthesis and components of the photosynthetic machinery—and pathogen proteins with transit peptides are recognised by the canonical pathway mediated by the translocons of the outer and inner chloroplast membrane (TOC-TIC) complex. They are transported across the chloroplast double envelope and the transit peptide is cleaved away on import. d. At least one pathway of non-canonical import allows effectors without cleavable transit peptides to cross into the chloroplast. e. Effectors may also alter the localisation of non-chloroplastic host proteins (orange circles), causing them to be relocated to the chloroplast. Dotted branches of arrows indicate molecular mechanisms still to be unclear.

2.Effect of SP1 on immunity

Contributions

The TKTP-Grx1-RoGFP construct was provided by Prof. Markus Schwarzländer and was crossed into the SP1ox and *sp1* background by Dr Qihua Ling.

2.1. Abstract

Chloroplasts are central players in plant metabolism and are carefully regulated during abiotic stress. Additionally, they sit at a nexus of antagonistic signalling pathways involved in stress and disease, and there is a growing body of work that suggests pathogens directly target chloroplasts to cause disease.

In this chapter, a role in plant immunity for suppressor of *ppi1* locus 1 (SP1), a regulator of chloroplast biogenesis, is described. Plants overexpressing SP1 (SP1ox) or *sp1* mutants were respectively more susceptible or more resistant to infection by model pathogen *Pseudomonas syringae*. Using callose deposition as a biomarker of immune system output, it was shown that *sp1* activates a similarly strong immune response to pathogenic *P. syringae* as to a non-pathogenic strain. This demonstrated that *sp1* plants generate an immune response that is resilient to the suppression of basal immunity (that is, pathogen-associated molecular pattern-triggered immunity, PTI), by *P. syringae*.

In wild-type Arabidopsis, pathogenic *P. syringae* suppresses the chloroplast ROS burst, a key early event in PTI signal transduction, to promote virulence. This suppression was found to require SP1: the chloroplast ROS burst was not suppressed in *sp1* and was more strongly inhibited in SP1ox. Confirming the role of photosynthetic ROS production, it was shown that the enhanced immunity of *sp1* depends on photosynthesis: when photosynthesis was inhibited with a herbicide or by dark treatment, *P. syringae* suppressed PTI just as well in *sp1* as in wild-type plants.

These data suggests that *P. syringae* has evolved to activate a host system of abiotic stress tolerance, SP1-mediated ROS avoidance, inappropriately during infection, in order to reduce chloroplast immunogenic signally and supress immunity.

2.2. Introduction

Chloroplasts are essential plant organelles, derived from an ancient cyanobacterial endosymbiont [2]. They are productive centres of the plant cell, home not only to photosynthesis but also to the synthesis of amino acids, lipids, nucleotides, and phytohormones [8].

The chloroplast genome encodes only a small number of proteins [9]. Most chloroplast proteins are encoded in the nucleus and translated in the cytosol. These must be imported into the chloroplast, mainly through the TOC-TIC import pathway [2]. The TOC receptors are responsible for import substrate recognition, and different configurations of TOC receptor components favour the import of different classes of substrates. This allows chloroplasts to carefully balance photosynthesis with their other biosynthetic responsibilities [36–39]. They are reconfigured by SP1, a ubiquitin E3 ligase and component of the CHLORAD pathway [126,154].

Reconfiguration of the TOC complexes is important during photosynthetic development, as the import specificity of chloroplasts is changed to improve import of photosynthetic precursors. At the opposite end of development, during senescence, TOC complexes are reconfigured again to reduce photosynthetic protein import. These transitions are enhanced with greater expression of *SP1* and occur more slowly or fail to occur in *sp1* mutants [126].

Recently, reconfiguration of import by SP1 was found to be important during times of abiotic stress, where high rates of photosynthesis become disadvantageous to the plant due to the generation of toxic ROS. SP1 acts to reduced photosynthetic protein import during salt, osmotic, and oxidative stresses to reduce photon excess and avoid ROS production. Accordingly, stress tolerance is enhanced in plants with greater *SP1* expression and is reduced in *sp1* mutants [165].

Chloroplasts are important sources of signals that promote immunity and disambiguate different immunity programmes [23,26,222,230,232–235]. During resistance and disease, the plant and pathogens both bring about changes in gene expression that affect the chloroplast compartment. In fact, some pathogen effectors even target the chloroplast directly and are imported via the TOC-TIC system [253,290–293].

To study the role of the chloroplast and chloroplast protein import in pathology, the effect of SP1 on infection was investigated. Two strains of the model bacterium *P. syringae* pv. *tomato* were used. *Pst*DC3000 is a virulent strain: it secretes effectors that disable the host immune system and render it susceptible. The mutant strain *Pst*DC3000 *hrpA*$^-$ (referred to as *hrpA*$^-$ in the running text below) lacks the hrpA component of the T3SS. This makes it unable to deliver effectors so it cannot suppress host immunity. Therefore, the host engages in PTI, the basal immune defence [210,211]. The use of these two strains allows the dissection of different components of immunity and susceptibility.

2.3. Results

2.3.1. *sp1* mutant plants show enhanced immunity

Chloroplasts are known to be involved in pathways that regulate stress tolerance, immunity, and disease. As a regulator of chloroplast biogenesis, the SP1 protein was investigated here for its role in plant immunity.

To begin with, the resistance of the previously described [126] SP1 overexpression (SP1ox) line and T-DNA insertion mutant line *sp1-3* (herein, *sp1*) to bacteria was measured and compared to that of wild-type Arabidopsis. Rosette leaves of four-week-old plants were inoculated with a solution of 10^5 colony forming units (CFU) mL^{-1} of either *Pst*DC3000 or *hrpA*$^-$ bacteria. After four days, the bacterial growth was measured.

Growth of *Pst*DC3000 was enhanced in SP1ox, indicating greater susceptibility of the plant to infection, and suppressed in *sp1*, indicating greater resistance to infection, compared to the wild type. The *hrpA*$^-$ strain had greatly reduced growth in all genotypes, reflecting its inability to suppress basal immunity. As in *Pst*DC3000 infection, SP1ox plants were also more susceptible to *hrpA*$^-$ and *sp1* plants more resistant (**Figure 2.1A**, p.95).

These data indicate that SP1 activity enhances susceptibility to pathogens and that *sp1* plants have a more effective immune response.

One explanation for this trend could be that the *sp1* mutation passively makes the leaf environment more hostile to pathogen growth, and that with increased *SP1* expression the environment becomes more favourable. As a hemibiotroph, *Pst* assimilates carbon and nitrogen from the plant's apoplast in the form of amino acids, organic acids, and sugars [306]. These nutrients are synthesised by pathways that cross the chloroplast, and so conceivably their accumulation during infection could be disrupted or enhanced in plant lines with altered chloroplast biogenesis like *sp1* or SP1ox, respectively.

Alternatively, the data may reflect an inverse correlation between SP1 levels and the induction or strength of immunity. There is a growing body of evidence that chloroplasts have an active role in co-ordinating immunity, and are targeted by pathogens to render the plant susceptible (e.g. [253,307], for review see [1]). If this were the case, it would suggest that the *sp1* mutation makes chloroplasts more resilient to manipulation by the pathogen.

To test whether or not reduced bacterial growth in *sp1* is due to differences in the strength of the immune response, callose deposition, an immune output [197], was assayed 24 hours post infection. When elicited by *hrpA*$^-$, callose was extensively deposited in plant cell walls in all lines (**Figure 2.1B-C**, p.95). This indicates that the bacterium was recognised and PTI was induced. However, much less callose was deposited during the infections of the wild type and SP1ox by *Pst*DC3000, indicative of the suppression of immunity. In *sp1* mutant plants, however, similar levels of callose were induced by both strains (**Figure 2.1B-C**, p.95). This indicates that during infection of *sp1* plants, *Pst*DC3000 is unable to suppress the immune system, unlike during infection of the other lines.

2.3.2. *sp1* plants show increased chloroplastic ROS accumulation in disease

Recently, the appearance of chloroplast-localised hydrogen peroxide early in infection (the chloroplast ROS burst) was found to be important for inducing PTI [253,258]. As SP1 has previously been associated with the regulation of chloroplastic ROS under some abiotic stress conditions [165], the observed immunity phenotypes could be explained by SP1's effect on chloroplast ROS geneation. This was investigated in two ways: with a ROS-sensitive dye (this section), and with a transgenic redox sensor (**§2.3.3**).

Presence of hydrogen peroxide can be qualitatively measured by staining leaves with 2′,7′-dichlorodihydrofluorescein diacetate (DCFH-DA), which is membrane permeant and

when oxidised produces dichlorofluorescein (DCF), which can be visualised by fluorescence microscopy.

Consistent with previously reported results [253,258], DCF accumulated in wild-type Arabidopsis six hours post infection with *hrpA*$^-$ (**Figure 2.2**, p.97). In contrast, only a faint signal was seen during infection with *Pst*DC3000 (**Figure 2.3**, p.99); the difference between this result and that reported previously [253], where no DCF signal was seen, may be due to the increased sensitivity of the gallium arsenide phosphide (GaAsP) detector of the microscope used in this experiment.

Infection of the SP1ox line with either bacterial strain elicited no or negligible DCF signal (**Figure 2.2-2.3**, pp.97-99), however, whereas much stronger signals were visible in infection of the *sp1* mutant, relative to the wild type. This suggests that SP1 acts to reduce ROS accumulation during infection.

A stronger DCF signal is elicited in *sp1* after *Pst*DC3000 inoculation than the wild type, although like in the wild type, *hrpA*$^-$ inoculation elicits a higher DCF signal than *Pst*DC3000 in *sp1* (**Figure 2.2-2.3**, pp.97-99).

Although the probe could diffuse from where it is oxidised, a strong signal can be seen in the chloroplasts in wild-type plants after infection with *hrpA*$^-$, and in *sp1* plants after infection with *hrpA*$^-$ or *Pst*DC3000 (**Figure 2.2-2.3**, pp.97-99).

These data indicate that *sp1* is more liable to accumulate ROS in the chloroplast than wild-type or SP1ox plants after biotic challenge. This may be interpreted to mean that that the chloroplast ROS burst in *sp1* is more severe than in the other lines, reflecting the role of SP1 in mitigating oxidative stress in the chloroplast, leading to a stronger induction of PTI.

A slightly different interpretation is that there is a phase change in the induction of the ROS burst, i.e. that ROS accumulates more rapidly in *sp1*, leading to an earlier induction

of PTI, and more slowly in wild-type and SP1ox plants owing to the mitigating action of SP1, delaying but not eliminating PTI. This could explain why SP1ox has increased susceptibility to *hrpA*$^-$, compared to the wild type, despite generating similar levels of callose: PTI is still induced but later on when it is less effective. If ROS accumulation and therefore PTI is delayed but not eliminated in SP1ox, this would also explain why SP1ox is not equally susceptible to *hrpA*$^-$ and *Pst*DC3000.

2.3.3. Dynamics of chloroplast oxidation during early stages of infection

In order to further explore the chloroplast ROS burst, a plastid-targeted redox sensitive green fluorescent protein 2 (roGFP2) probe was crossed into the SP1ox and *sp1* backgrounds. This biosensor responds dynamically to oxidation and reduction by conformational changes that alter its excitation maxima. Green fluorescent protein (GFP) emission can be measured after excitation at both maxima, the ratio of which reflects the oxidation state of the cell or organelle [308]. It acts as a proxy measurement for the glutathione buffer pool. To increase its responsiveness, it is fused to glutaredoxin 1 (Grx1). A construct fusing Grx1-roGFP2 to the plastid-targeting transketolase transit peptide (TKTP) allows for chloroplasts specifically to be measured [309]. The TKTP-Grx1-roGFP2 (herein roGFP) construct was first transformed into wild-type Arabidopsis and then crossed into the *sp1* and SP1ox lines.

The roGFP construct allows for dynamic measurements to be taken, and as less preparation is needed before visualisation, it also allows for greater time-resolved measurements to be made than when samples must be first stained with DCFH-DA. Three time points were chosen for analysis: in addition to the six-hours post infection time point used in the DCF experiments, two hours before and after this point were also visualised.

In all lines, greater oxidation of the roGFP probe was seen six hours after infection with *hrpA*$^-$ than with *Pst*DC3000 (**Figure 2.4A**, p.101). In agreement with the DCF

fluorescence data (**§2.3.3**), chloroplasts of *sp1* plants showed the highest levels of oxidation of the three Arabidopsis lines at this time point. Similarly, during *Pst*DC3000 infection, high levels of oxidation were seen in *sp1*. Chloroplast oxidation was lower in both infections in SP1ox and wild-type plants, which at this time point show similar chloroplast oxidation.

In wild-type and SP1ox plants, *Pst*DC3000 acts to lower roGFP oxidation at six hours. Strikingly, this suppression is transient: the ratio of oxidised to reduced roGFP drops between four- and six-hours post infection but recovers by eight hours post infection (**Figure 2.5**, p.103). This implies that the ROS burst must be critically timed at six hours in order to be an effective immunogenic signal.

Regression analysis was employed to examine the different trends in chloroplast oxidation between the lines and inoculations.

The ability of two regression models to describe the change in the dependent variable may be compared by analysis of variance (ANOVA). The residual sum of squares (RSS) are compared to determine whether one model significantly better fits the data—a lower RSS indicates better fit. Using this approach, it is also possible to determine whether the trend significantly differs based on a particular factor, e.g. different Arabidopsis lines. Two models are compared, one with and without the factor in question: if the model is significantly improved by taking the factor into account, then the difference in trend between the groups is significant.

In this case, the polynomial regression model relating RoGFP oxidation to time, bacterial strain, and Arabidopsis line[1] significantly better describes the change in RoGFP oxidation

[1] Where x indicates time in hours, $\mathcal{A}$ indicates Arabidopsis line group coded as 0 = *sp1*, 1 = SP1ox, 2 = wild type and $\mathcal{B}$ indicates the bacteria line group coded as 0 = *Pst*DC3000 and 1 = *hrpA*⁻:
$y = -0.012x^2 + 0.003\mathcal{B}x^2 + 0.030\mathcal{A}_1x^2 + 0.030\mathcal{A}_2x^2 - 0.021\mathcal{B}\mathcal{A}_1x^2 - 0.21B\mathcal{A}_1x^2 + 0.139x + 0.032\mathcal{B}x - 0.377\mathcal{A}_1x - 0.372\mathcal{A}_2x + 0.255B\mathcal{A}_1x + 0.228B\mathcal{A}_2x + 0.331 - 0.039\mathcal{B} + 1.048\mathcal{A}_1 + 1.031\mathcal{A}_2 - 0.783\mathcal{B}\mathcal{A}_1 - 0.872\mathcal{B}\mathcal{A}_2$

than the model relating RoGFP oxidation to time and bacterial strain alone[2] (RSS 0.20 vs. 0.32, *P*=.005). Therefore, SP1 level significantly contributes to the trend in chloroplast oxidation over four to eight hours post inoculation.

In fact, SP1 level more profoundly affects chloroplast oxidation over this time period than which of the two strains of bacteria is used: including bacterial strain, time, and Arabidopsis line does not significantly improve the fit of the model over one including just time and Arabidopsis line[3] (RSS 0.20 vs. 0.25, *P*=.20).

These two lines of evidence, the DCF data and the roGFP data, agree that *SP1* expression antagonises the generation of the early ROS burst. This supports the notion that the increased immunity of the *sp1* mutant is due to stronger induction of chloroplast-mediated immunity, either in terms of earlier timing or increased intensity of the ROS burst, that leads to stronger PTI during *hrpA*$^-$ infection and increased resilience to effector-mediated suppression of PTI during *Pst*DC3000 infection.

While suppression of the ROS burst is typical of *Pst*DC3000 infection, SP1ox also exhibited impaired ROS production in the interaction with *hrpA*$^-$. This implies that the role of effectors are partially dispensable with higher levels of SP1, and invites conjecture that SP1 itself may be stabilised or induced by *Pst* effectors.

2.3.4. ROS production during disease parallels abiotic stress

Recently, increased expression of *SP1* was shown to both reduce ROS accumulation in seedlings grown on stressor media and contribute to seedling greening and survivorship when stressed [165].

This trend is reminiscent of the biotic stress ROS burst in SP1ox and *sp1*, but had not previously been visualised with the same methods. Therefore, complementary DCFH-DA

[2] $y = 0.006x^2 - 0.017x^2\mathcal{B} - 0.111x + 0.210x\mathcal{B} + 1.024 - 0.591\mathcal{B}$

[3] $y = -0.013x^2 + 0.020\mathcal{A}_1x^2 + 0.020\mathcal{A}_2x^2 + 0.155x - 0.250\mathcal{A}_1x - 0.234\mathcal{A}_2x + 0.311 + 0.656\mathcal{A}_1 + 0.595\mathcal{A}_2$

and roGFP experiments were performed under abiotically induced oxidative stress. The herbicide paraquat was used, which induces oxidative stress specifically in the chloroplast [310].

Rosette leaves of four-week-old wild-type, SP1ox, and *sp1* plants were syringe infiltrated with 5 μM or 10 μM paraquat and one day after treatment were stained with DCFH-DA. With the lower dose of paraquat, DCF fluorescence was much stronger in *sp1* plants than wild-type plants, and weaker in SP1ox plants (**Figure 2.6A**, p.105). This agrees with the previously reported results that SP1 has a protective effect against ROS accumulation [165]. At the higher dose, SP1ox leaves resembled wild-type leaves more closely, suggesting that the protective effect of the over-expression of *SP1* becomes overwhelmed, while *sp1* leaves showed dramatically more DCF fluorescence (**Figure 2.6B**, p.105).

The induction of roGFP oxidation tested in seedlings incubated in liquid culture with 1 μM or 10 μM paraquat was measured on a plate reader. When treated with 1 μM paraquat, the redox ratio of roGFP increased compared to mock treated seedlings; and the sensitivity of this response to paraquat was inversely correlated with *SP1* expression (**Figure 2.4B**, p.101). Treatment with the higher concentration of paraquat (10 μM) reduced the differential between SP1ox and wild-type plants, but further exacerbated ROS accumulation in *sp1* (**Figure 2.4C**, p.101). All three lines showed similar roGFP oxidation in mock treated seedlings (**Figure 2.4B-C**, p.101).

The similarity of these responses to those observed under biotic stress supports the notion that SP1's role in abiotic and biotic stresses is functionally similar, in both cases relating to the regulation of chloroplastic ROS generation.

2.3.5. Generation of ROS by photosynthesis is necessary for the resistance phenotype of *sp1*

The chloroplastic ROS burst is thought to require energy diverted from photosynthesis. However, it is conceivable that ROS are generated elsewhere and accumulate in the chloroplast, perhaps for signalling purposes. Additionally, the chloroplast ROS burst may be a by-product of enhanced immunity, rather than an initiator of PTI. To test the criticality of photosynthetically-generated ROS to the enhanced immunity phenotype of *sp1*, two experiments were performed.

Firstly, bacterial growth (as CFU per cm^2) was measured in plants kept in the dark for four days after inoculation to prevent photosynthesis. Without the ability to generate photosynthetic ROS, *sp1* plants were equally as susceptible as the wild type to *Pst*DC3000. Unexpectedly, SP1ox plants showed greater resistance to *Pst*DC3000 than the other two lines. Dark treatment eliminated the differences in resistance to *hrpA*$^-$ between the three lines, although *hrpA*$^-$ still grew less than *Pst*DC3000 (**Figure 2.7A**, p.107). Compared to incubation in long day conditions, dark incubation greatly increased the growth of both strains of bacteria in all lines except *Pst*DC3000 infection of SP1ox (cf. **Figure 2.1A**, p.95).

That *Pst*DC3000 should show reduced growth in SP1ox is doubly curious, as not only did SP1ox become more immune than *sp1*, in contrast to the trend under normal light cycle conditions, but whereas dark treatment improved bacterial growth in the other lines, here in SP1ox it reduced growth. This might be connected to senescence, which is induced by dark treatment in SP1ox plants more rapidly than in the wild type or *sp1* [126]. Not only is there overlap between genes induced in immunity and senescence [311], but there is some evidence that suggests dark-induced senescence promotes, at least transiently, ROS generation and lipid peroxidation [312,313]. On the other hand, despite undergoing senescence more slowly [126], *sp1* shows no greater susceptibility than the wild type. This

may be due to timing: the *sp1* senescence phenotype becomes apparent after five days dark treatment [126].

Secondly, bacterial growth was measured in plants treated with an inhibitor of photosynthesis, the herbicide 3-(3,4-dichlorophenyl)-1,1-dimethylurea (DCMU). DCMU competes for plastoquinone binding at PS II (**Figure 1.2**, p.63) and so prevents electron transport and the generation of hydrogen peroxide at PS I [314]. This has previously been shown to abrogate the early chloroplastic ROS burst during *hrpA*$^-$ inoculation and restore pathogenicity in wild-type Arabidopsis [253]. This approach allows plants to be incubated under normal, long day conditions while also inhibiting photosynthesis.

Co-inoculation with 10 μM DCMU increased the growth of *Pst*DC3000 and eliminated the differential in resistance between all the lines (**Figure 2.7B**, p.107, cf. **Figure 2.1**, p.95). Similar changes were seen in the growth of *hrpA*$^-$, although it remained less virulent than *Pst*DC3000.

These two different experimental approaches both support the hypothesis that the enhanced immunity of *sp1* requires photosynthetically generated ROS, and that the ability to carry out photosynthetic electron transport promotes immunity.

2.4. Discussion

2.4.1. The suppression of PTI by *Pst*DC3000 depends on an SP1-mediated pathway

In this chapter, a new role for the regulator of chloroplast biogenesis SP1 in plant pathology was discovered. Expression of *SP1* was found to correlate with susceptibility to *Pst*, a model bacterial pathogen. SP1 acts in the pathway by which *Pst*DC3000 suppresses PTI, where it downregulates photosynthetic ROS production and reduces the immunogenic chloroplast ROS burst. In *sp1* mutants, PTI is stronger (against *hrpA*$^-$) and more robust (resilient to suppression by *Pst*DC3000).

By examining the two strains of *Pst*, it is possible to tease apart the nature of the immune response. Typically, as in wild-type Arabidopsis, *hrpA*$^-$ elicits PTI. This restricts bacterial growth and is characterised by a chloroplast ROS burst and extensive callose deposition. *Pst*DC3000 elicits ETS by secreting effectors that derail PTI: the ROS burst and callose deposition are reduced, and bacterial growth is higher. On the other hand, infection of *sp1* by *Pst*DC3000 elicits a chloroplast ROS burst and high callose deposition, and bacterial growth is much lower than in the wild type (**Figure 2.1 & 2.3**, pp.95,99). This is more typical of PTI than ETS, and more closely resembles *hrpA*$^-$ infection of the wild type.

This shows that *Pst*DC3000 can inhibit PTI and render plants susceptible only when SP1 is present, as in the wild type or SP1ox. Either in the absence of SP1 (in the *sp1* mutant), or when *Pst* cannot secrete effectors (infection of all lines by *hrpA*$^-$), PTI is activated and plants show enhanced resistance. This indicates that *Pst*DC3000 secretes effectors that suppress immunity via an SP1-mediated pathway.

The resistance to both strains of bacteria in each of the three lines correlates with the strength of the chloroplast ROS burst, thought to be a key immunogenic signal inducing PTI (**Figure 2.2-2.4** pp.97-101). This suggests that the enhanced immune response of *sp1*

is caused by more robust immune activation, resilient to *Pst*DC3000's attempts to derail it, mediated by accumulation of ROS in the chloroplast.

When *SP1* is overexpressed, susceptibility to both strains of bacteria is increased (**Figure 2.1A**, p.95). In the SP1ox versus *hrpA*⁻ interaction, the constitutive overexpression of *SP1* partially compensates for the lack of effectors and impairs immunity. In the SP1ox versus *Pst*DC3000 interaction, this SP1-mediated immunity suppression pathway is induced faster or more strongly.

SP1's role in susceptibility is surprising, as its expression has a positive effect on tolerance to abiotic stresses [165] and might have been expected to also make a net positive contribution to immunity via the downregulation of import of chloroplast-targeted effectors. The abiotic and biotic stress tolerance paradox will be discussed in **§2.4.5**.

2.4.2. The enhanced immune response of *sp1* is not constitutive

An alternative explanation for SP1's role in immunity, as opposed to antagonising chloroplast-mediated immune signalling, is that it is involved in pathogen recognition. However, this does not appear to be the case.

There are examples of mutations in pathways that perceive pathogens that enhance immunity. These include gain-of-function mutations of NB-LRR proteins which recognise PAMPs or effectors, and loss-of-function mutations in proteins that are guarded by host R proteins (host proteins that trigger ETI) [315–317]. One example of the former pertains to the NB-LRR protein suppressor of *npr1-1* constitutive 1 (SNC1), which causes enhanced immunity either when affected by the *snc1* gain-of-function mutation (activating immunity even in the absence of PAMPs) [318] or when SNC1 turnover is prevented by the *cpr1* mutation. CPR1 is an F-box protein that normally regulates SNC1 protein levels as part of a SKP1-CULLIN-F-box E3 ligase complex [319]. This is an interesting case where mutation to an E3 ligase complex induces immunity by allowing its target to accumulate to higher protein levels.

An example of the latter is the RPM1 interacting protein 4 (RIN4), which is guarded by resistance to *P. syringae* pv. *maculicola* 1 (RPM1). RIN4 in guard cells is targeted by the effectors including AvrB and AvrRpm1, which cause its phosphorylation and negatively regulate immunity via changes to stomatal opening. RPM1 also interacts with RIN4, and initiates the HR if RIN4 levels are disrupted. However, RPM1 cannot distinguish between the depletion of RIN4 by pathogen effectors and its loss in the *rin4* mutant [320–322].

Given these examples, one might wonder if SP1, like fellow E3 ligase CPR1, might direct the UPS turnover a protein that initiates immunity as it accumulates, and in so doing antagonise immunity; or one might wonder if, like RIN4, SP1 is guarded against pathogen manipulation by an R protein that triggers immunity in the *sp1* knockout.

However, mutations like these cause immunity to be activated constitutively. The enhanced immune response of *sp1* is not constitutive, as only low levels of callose, similar to the wild type, are induced by mock (without a bacterial inoculum) infiltration of SP1ox and *sp1* (**Figure 2.1B-C**, p.95). This is consistent with its appearance under normal growth conditions, where it is indistinguishable from wild-type Arabidopsis. Constitutive activation of immunity typically causes severe defects not seen in *sp1*, including spontaneous lesion formation or dwarfism [323,324]: for example *cpr1* has a dwarf phenotype [264] and *rin4* plants show both dwarfism and, in older leaves, spontaneous lesion formation [321].

Thus, SP1 does not appear to initiate immunity by regulating the perception of PAMPs or effectors themselves, and the hypothesis that it acts downstream in signal induction, via the chloroplast ROS burst, stands.

An alternative hypothesis was mentioned above (**§2.3.1**) that the effect of the *sp1* mutation might be to make the leaf environment less hospitable for pathogens, e.g. by changes to nutrient synthesis in the chloroplast. It should be mentioned although PTI is induced more strongly and robustly inversely with *SP1* expression, this does not rule out

that nutrient availability in the apoplast is also disturbed by changes to *SP1* expression, which would need to be tested separately, e.g. by comparing bacterial growth in leaf apoplastic fluid extracted from the different Arabidopsis genotypes [306].

2.4.3. Persistent differential growth of the two bacterial strains suggests additional PTI signalling events

While the chloroplast ROS burst is connected with the induction of PTI, its abrogation does not completely restore the virulence of *hrpA*$^-$ to the levels seen in *Pst*DC3000. This suggests that there are additional PTI induction pathways that partially compensate for the missing chloroplast ROS burst; or that *Pst*DC3000 effectors target other aspects of immunity in addition to the chloroplast ROS burst; or both. Redundant immune signalling may prevent the total elimination of immunity when the chloroplast ROS burst is abrogated.

It has been observed that bacterial growth of *hrpA*$^-$ when co-inoculated with 10 μM DCMU is similar to that of *Pst*DC3000 alone [253]. This might suggest that elimination of chloroplast hydrogen peroxide production completely abolishes PTI. However, it is noteworthy that when *Pst*DC3000 is co-inoculated with DCMU, a difference in growth between the two strains re-emerges (**Figure 2.7B**, p.107). Likewise, there remains a difference in growth between the two strains in dark treatment or in the infection of SP1ox, both of which are also conditions that impair the chloroplast ROS burst. If elimination of the chloroplast ROS burst completely eliminated PTI, we would expect both strains to be equally virulent when co-inoculated with DCMU.

This discrepancy may reflect two factors. Firstly, the combination of each of these treatments with *Pst*DC3000's effectors may have a synergistic effect on the suppression of photosynthetic ROS production, leading to increased growth of *Pst*DC3000.

Secondly, there are likely to be additional roles for *Pst*DC3000 effectors other than the disruption of chloroplast ROS for which DCMU treatment, for example, does not compensate. There are likely to be additional pathways for immune induction, partially redundant with respect to the chloroplast ROS burst, that are targeted by other effectors. For example, the effector HopG1 is targeted to the mitochondria and reduces PTI by disrupting respiration [325]. Similarly, some *P. syringae* effectors may promote virulence in ways other than directly antagonising immune induction, for example by enhancing the secretion of nutrients to the apoplast [326] or the water-soaking response [327]. We would not expect effectors that mediate these mechanisms to be compensated for the disruption of chloroplast ROS generation by DCMU co-inoculation or similar treatments

In this way, in the absence of the chloroplast ROS burst, some aspects of immunity are still initiated, but *Pst*DC3000 has evolved effectors to target these as well. In other words, the treatments that prevent photosynthetic ROS production compensate for the loss of some but not all of the effectors that cannot be secreted during *hrpA*$^-$ infection.

This would also explain why *Pst*DC3000 is still slightly more virulent that *hrpA*$^-$ in *sp1* plants (**Figure 2.1A**, p.95), despite neither pathogen being able to utilise the SP1-mediated pathway of immune suppression: *Pst*DC3000 has additional strategies for suppressing immunity that are unaffected by the *sp1* mutation and which are absent in *hrpA*$^-$. Similarly, redundant (but less effective) means of inducing PTI would explain why callose deposition is still initiated in the SP1ox versus *hrpA*$^-$ interaction, even though the chloroplast ROS burst is mitigated.

2.4.4. Timing of chloroplast ROS burst

The roGFP probe reveals dynamic changes to the chloroplast redox state that differentiate PTI and ETS and suggest that the timing of ROS accumulation, as well as its severity, may be important to immunity (**Figure 2.5**, p.103).

At the four hours timepoint, chloroplast oxidation in the wild type is similar in both *Pst*DC3000 and *hrpA*$^-$ inoculation. This is surprising, since the accumulation of chloroplast ROS is associated with immunity and the *hrpA*$^-$ infection. Chloroplast oxidation in response to the two strains only clearly diverges around six hours, where chloroplasts become more oxidised in *hrpA*$^-$ infection and more reduced in virulent *Pst*DC3000 infection. This indicates that it is ROS generated around this time that are critical for the initiation of immunity.

Accordingly, in *sp1*, which responds to both strains with a strong immune reaction, the reduction of chloroplast redox associated with virulence in the wild type vs. *Pst*DC3000 interaction does not occur. Chloroplast oxidation in *sp1* follows a similar trend in *Pst*DC3000 or *hrpA*$^-$ inoculation, though in agreement with the DCF evidence, oxidation peaks more highly in the latter.

Likewise, by the eight hours timepoint, the importance of chloroplast ROS accumulation for immunity may largely have passed. At this time point in the wild type interaction, chloroplast oxidation in both infections has begun to converge: the importance of chloroplast oxidation in eliciting immunity to *hrpA*$^-$, and the importance of reducing chloroplast redox in eliciting virulence during *Pst*DC3000 infection, both seem to have passed.

It appears that *Pst*DC3000 can suppress the induction of PTI so long as oxidation is reduced at six-hours post inoculation, as it is in SP1ox and wild type lines, regardless of the level of oxidation at four- and eight-hours post inoculation. Despite the differential immunity of the lines, all three genotypes show similar chloroplast oxidation at four hours post inoculation with *Pst*DC3000. Therefore, if *Pst*DC3000 induces SP1 to reduce chloroplast oxidation, it does not do so until between four- and six-hours post inoculation.

It is curious that chloroplast oxidation does not remain suppressed indefinitely in *Pst*DC3000 infection. This has very intriguing implications: perhaps the six-hour time point represents a vital window that allows *Pst*'s effectors to disable host defences. As long as chloroplast ROS accumulation is prevented during that small window, then it can be allowed to increase again by eight hours post infection but without the risk that it may provoke an immunogenic signal.

In agreement with expectations, chloroplast oxidation after inoculation with *hrpA*$^-$ (or *Pst*DC3000) peaks both earlier and higher in *sp1* than chloroplast oxidation in the wild type after *hrpA*$^-$ inoculation. However, the hypothesis that in SP1ox the chloroplast ROS burst isn't eliminated but delayed has not been borne out. In fact, chloroplast oxidation in this interaction trends downwards across the time course.

2.4.5. Mechanism of SP1-mediated ROS avoidance

A previous study found association between SP1 and abiotic stress tolerance: the ROS overaccumulation phenotype of *sp1* is associated with increased sensitivity to salt and osmotic stress conditions, whereas SP1ox plants are more tolerant of stress [165]. The mechanism by which SP1 reduces oxidative stress may therefore shed light on the mechanism by which it suppresses the chloroplast ROS burst in disease.

On the surface, there appears to be a paradox concerning SP1's roles in abiotic and biotic stresses—promoting tolerance to the former but susceptibility to the latter. However, the underlying phenotype of chloroplast ROS accumulation is the same. In both abiotic and biotic stresses, SP1 acts to reduce levels of oxidation in the chloroplast; the paradox of whether SP1 helps or harms plant tolerance to stress arises from the dual role that chloroplast ROS has: a harmful by-product and an immunogenic signal.

Plastids from plants with higher *SP1* expression undergo more rapid chloroplast transitions, including both photomorphogenesis and senescence, mediated by the turnover of TOC components and reconfiguration of import specificity [126]. During

abiotic stress, the TOC components were also found to be reconfigured in an SP1-dependent manner, and the import efficiency of photosynthesis-related substrates was reduced [165]. This was interpreted to indicate that SP1 acts in stress conditions to downregulate photosynthetic preprotein import, as it does during senescence. This reduces the capacity for photosynthetic ROS generation and allows plants to avoid stress ("ROS avoidance"). In SP1ox lines, this reconfiguration happens more rapidly and plants generate less ROS, but in *sp1* mutant lines it happens more slowly and plants overproduce ROS [165].

There are two other interpretations that are interesting enough to mention.

One alternative, highlighted by the recent discovery of the CHLORAD pathway [154], is that ubiquitination by SP1 mediates the removal of ROS-damaged or misfolded proteins (i.e. ROS remediation). This occurs in the analogous ERAD pathway, where misfolded proteins are removed from the membrane or lumen of the ER. Accumulation of misfolded proteins in the ER is called ER stress, and can both cause and be caused by ROS [328]. In plants, the relief of ER stress has been shown to be important for salt tolerance [329]. Turnover of ROS-damaged chloroplast components contributes to stress tolerance and reduce ROS accumulation (e.g. [174,178]), so perhaps SP1 helps relieve oxidative stress in this way. However, it has yet to be shown either that SP1 mediates the ubiquitination of proteins other than the TOC components, or that CHLORAD acts to remove other proteins.

A related possibility worth entertaining relates to the UPR. If ER stress is not relieved, it triggers the UPR, a feedback system that acts to reduce ERAD's workload and if sustained triggers apoptosis. UPR arrests protein translation and induces chaperones that assist in correct protein folding [330]. There is now known to be a homologous response in the mitochondria, called mitochondrial UPR (UPRmt), which upregulates ROS detoxification and mitochondrial chaperone genes. UPRmt may be induced by many diverse stresses in the mitochondria, but they all have the common effect of inhibiting

mitochondrial protein import. This inhibition is perceived by changes to the localisation of a transcription factor (activating transcription factor associated with stress 1) from the mitochondria to the nucleus, where it then induces UPRmt [331]. Other related systems also respond to disruption of mitochondrial protein import. A heat shock factor 1 (Hsf1)-mediated mechanism suppresses expression of mitochondria-targeted genes if the availability of chaperones falls [332]. Hsf1 also triggers UPRmt activated by mistargeting of proteins (UPRam), a system by which unimported proteins become turned over by the UPS [333], not unlike CHIP.

Recently, there have been several suggestions made that there also exists a chloroplast UPR (UPRcp). In the absence of chloroplast proteases ClpP or FtsH2, there is strong induction of genes involved in ROS detoxification, chloroplast chaperones, and chloroplast proteases, which is analogous to the UPR and UPRmt responses [334,335]. Although premature, it is interesting to speculate that the signalling pathway for UPRcp, like that for UPRmt and UPRam, might involve the disruption of protein import; in which case, it might be enhanced by the turnover of TOCs by SP1.

Nevertheless, the ROS avoidance model, that SP1 reduces ROS by downregulation of photosynthetic protein import [165], is appealing because it is parsimonious with SP1's previously reported roles [126], and with the down-regulation of photosynthesis-associated NECGs that abiotic stress treatment also induces [336,337].

Similar to in abiotic stress, *Pst*DC3000 is known to cause extensive changes to gene expression, including downregulating photosynthesis-associated NECGs [253]. SP1 may represent another mechanism by which *Pst*DC3000 suppresses photosynthesis: effectors may induce or stabilise SP1 to downregulate photosynthetic protein import and avoid ROS generation, as in abiotic stress. This will be explored further in **§4**.

2.4.6. *P. syringae* activates a host system of stress tolerance inappropriately to facilitate infection

The implication of the above results is that effectors from *Pst*DC3000 activate an SP1-mediated oxidative stress tolerance mechanism as a means to promote pathogenesis.

Plants must carefully balance how their resources are allocated to the competing demands for growth, abiotic stress tolerance and biotic stress tolerance, as mediated by interactions between stress signalling pathways [338]. It has often been recognised that plants under stress conditions become more susceptible to disease [339–341]. As plants in field conditions are frequently exposed to combinatorial stress, the interaction between abiotic and biotic stress pathways is of growing concern. These interactions include antagonism of abiotic stress tolerance by immune receptors, and of immunity genes by abiotic stress tolerance [1].

Some immunity proteins have been shown to reduce stress tolerance, including NB-LRR proteins like nucleotide binding leucine repeat protein 4 (NLR4) and SNC1. NLR4 acts in PTI induction but reduces osmotic stress tolerance [342], while SNC1 is thought to be involved in triggering ETI but reduces tolerance to high temperatures [318,343]. Other immunity proteins have more complex effects, reported to impair tolerance to some abiotic stresses but improving tolerance to others [344–346], indicating that factors promoting immunity can also alter the balance of susceptibility to different abiotic stresses.

Complementarily, systems to tolerate abiotic stress can cause downregulation of immunity. The most prominent example is the antagonism of SA- and JA-induced immunity by the phytohormone ABA, which is produced under many abiotic stresses, including drought, salinity, low temperature, and high light [214,236]. A recent, curious example is that of α-expansin 4 (EXPA4) in *Nicotiana tabacum*. Expansins like EXPA4

reshape the cell wall to improve tolerance to drought and salinity, but this also makes cells more susceptible to infection by tobacco mosaic virus and *Pst* [347].

Conversely, mutants with impaired abiotic stress tolerance systems may show increased immunity. As discussed in **§1.8.2**, these include mutants for chloroplast oxidative stress tolerance, such as mutants for the autophagy pathways, which have enhanced immunity but greater sensitivity to high-light stress [179,262,263], and the *cpr1* mutant which has reduced chloroplast antioxidant expression but constitutive activation of immunity genes [264]. An example from outside of the chloroplast is *aba2*, a mutant for ABA synthesis, which has enhanced or constitutive activation of immunity [348,349].

The trade-off between resistance to pathogens and tolerance of abiotic stress suggests that pathogens could evolve to target abiotic stress pathways to facilitate disease. Indeed, some pathogens have been shown to induce host plants to upregulate ABA synthesis, or even secrete ABA themselves, to facilitate infection [242,252].

During *Pst*DC3000 infection, the bacterium faces the challenge of suppressing the chloroplast ROS burst in order to impair PTI. The results presented in this chapter suggest that, rather than evolving a novel mechanism to do so, it co-opts an existing host system of abiotic stress tolerance, activating SP1-mediated ROS avoidance inappropriately and for its own benefit.

In **§3**, changes to chloroplast protein import during infection, the mechanism by which SP1 may prevent the chloroplast ROS burst, are explored.

2.5. Figures and tables

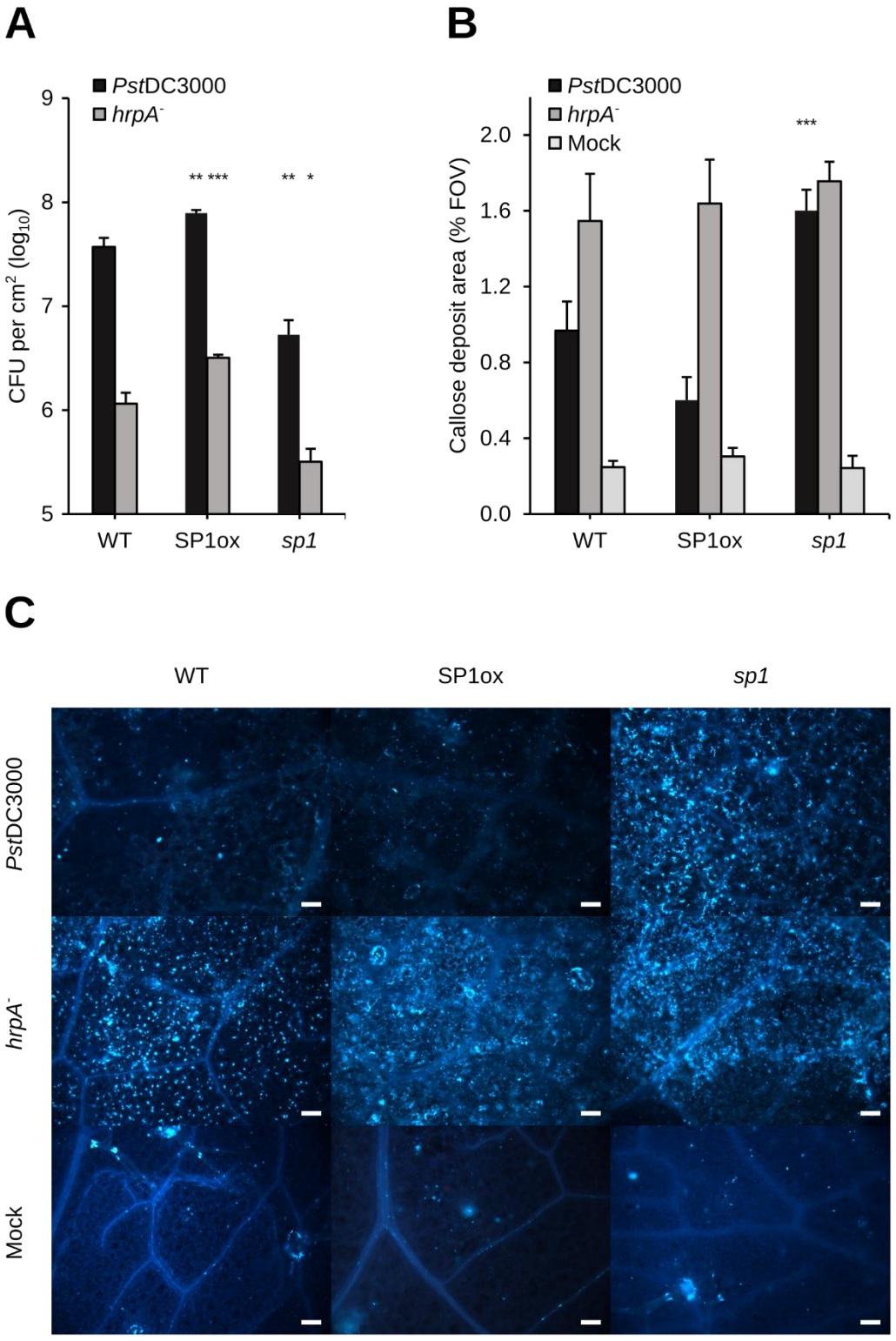

Figure 2.1 The *sp1* mutation promotes immunity.

A. Growth of *Pst* is impaired in *sp1* but enhanced in SP1ox relative to wild type. Bacterial growth was measured in colony forming units (CFU) per cm^2 four days after inoculation with pathogenic (*Pst*DC3000) or non-pathogenic (*hrpA*$^-$) bacteria (at a concentration of 10^5 CFU mL^{-1}). Error bars indicate the SEM (n=4).
B. Both *Pst*DC3000 and *Pst*DC3000 *hrpA*$^-$ elicit similar levels of callose in *sp1*. Callose deposition was analysed by aniline blue staining in the indicated genotypes 24 hours following inoculation with bacterial cultures (at a concentration of 10^7 CFU mL^{-1}) or a mock infiltration solution ($MgCl_2$). The values show the extent of staining as a percentage of field of view (FOV). Error bars indicate the SEM (n=6 for bacterial inoculations, n=5 for mock).
C. Representative micrographs of leaves stained for callose as in **B**. Scale bar = 100 μm.
Asterisks indicate significant difference from corresponding wild-type treatment as calculated by Holm-corrected pairwise T test at $P<.05$ (*), $P<.01$ (**), or $P<.001$ (***).

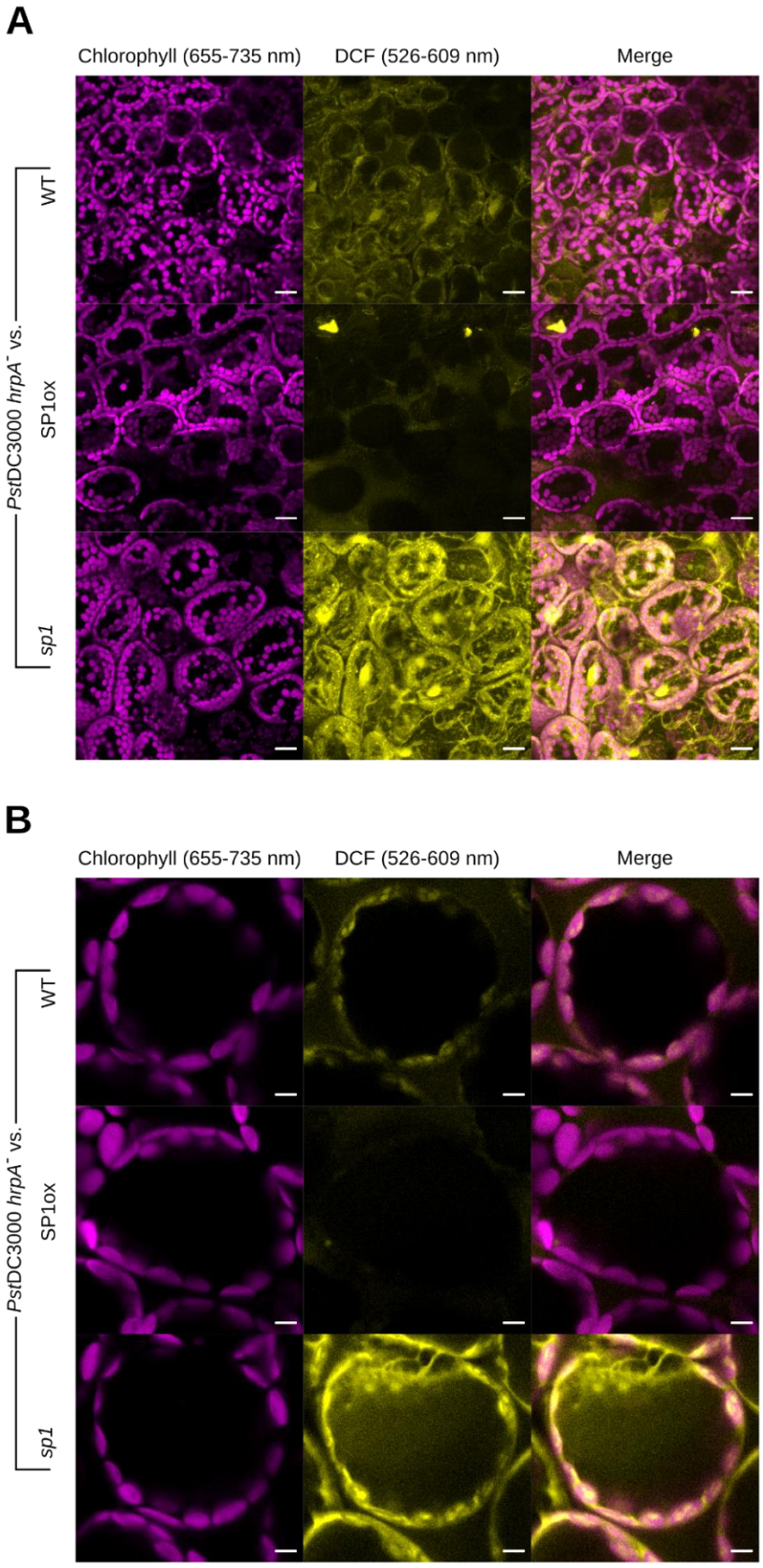

Figure 2.2 Detection of ROS by DCF staining during infection by *Pst*DC3000 *hrpA*$^-$.

Conversion of membrane permeant 2′,7′-dichlorodihydrofluorescein diacetate to fluorescent marker dichlorofluorescein (DCF) was used to monitor the accumulation of an important ROS molecule (H_2O_2) in wild-type (WT), SP1ox, and *sp1* Arabidopsis plants 6 hours post inoculation with *hrpA*$^-$ (10^7 CFU mL^{-1}).

A. DCF staining inversely correlates with *SP1* expression. Representative maximum intensity orthogonal projections of leaves six hours post inoculation of the indicated genotypes are shown. The DCF signal can be seen in the treatment of wild-type (WT) and *sp1* plants. Scale bar = 20 μm.

B. The DCF signal colocalises with chloroplasts in WT and *sp1* plants. The chlorophyll autofluorescence signal indicates the positions of the chloroplasts. Colocalization of the DCF and chlorophyll signals can be clearly seen in the Merge panels. Scale bar = 5 μm.

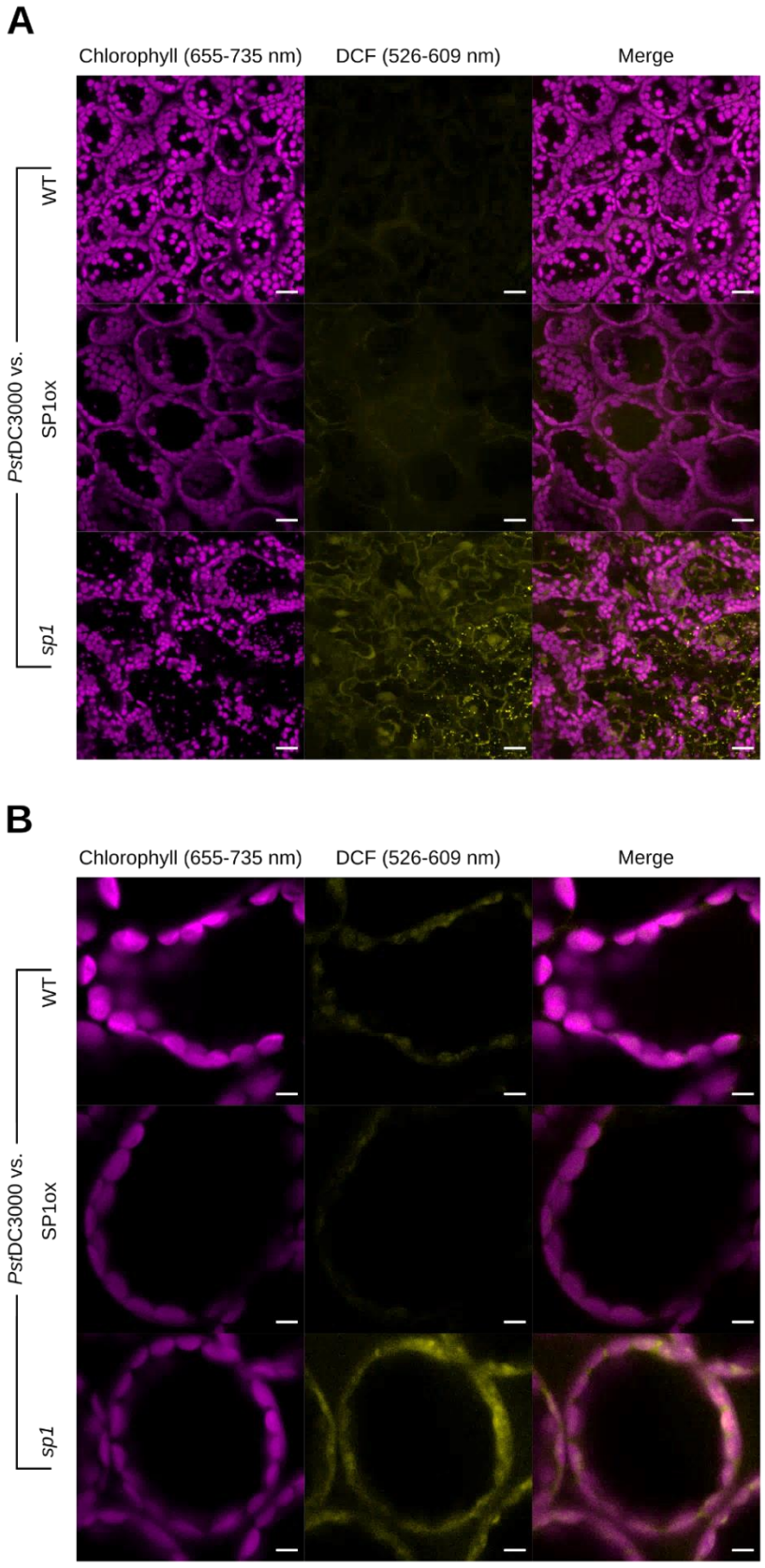

Figure 2.3 Detection of ROS by DCF staining during infection by *Pst*DC3000.

Conversion of membrane permeant 2′,7′-dichlorodihydrofluorescein diacetate to fluorescent marker dichlorofluorescein (DCF) was used to monitor the accumulation of an important ROS molecule (H_2O_2) in wild-type (WT), SP1ox, and *sp1* Arabidopsis plants 6 hours post inoculation with *Pst*DC3000 (10^7 CFU mL^{-1}).

A. DCF staining inversely correlates with *SP1* expression. Representative maximum intensity orthogonal projections of leaves six hours post inoculation of the indicated genotypes are shown. The DCF signal can be seen in the treatment of wild-type (WT) and *sp1* plants. Scale bar = 20 μm.

B. The DCF signal colocalises with chloroplasts in WT and *sp1* plants. The chlorophyll autofluorescence signal indicates the positions of the chloroplasts. Colocalization of the DCF and chlorophyll signals can be clearly seen in the Merge panels. Scale bar = 5 μm.

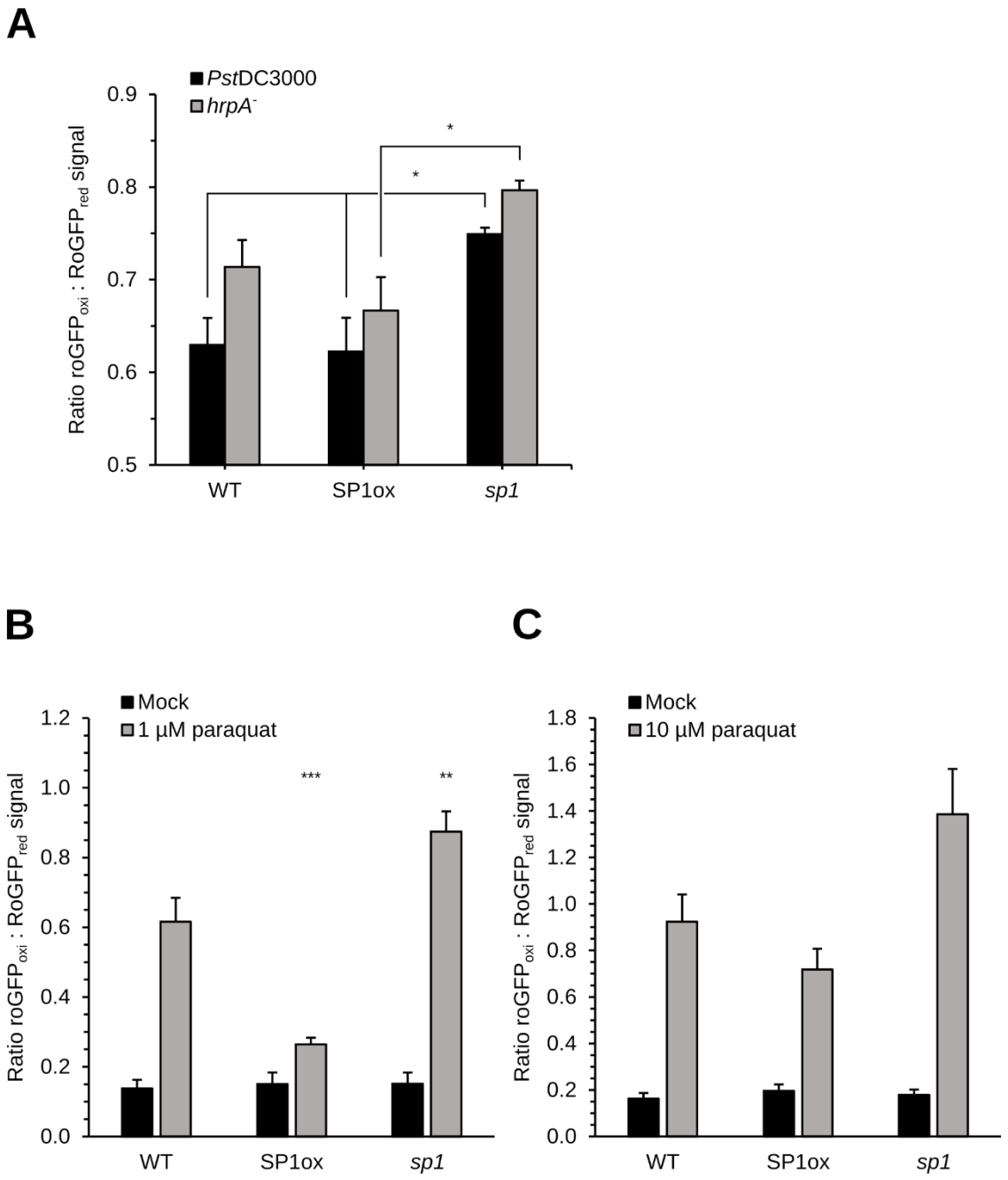

Figure 2.4 Measurement of chloroplast redox state *in planta* using a redox-sensitive probe.

Wild-type (WT), SP1ox, and *sp1* plant lines expressing a chloroplast-targeted redox-sensitive GFP probe (roGFP) were subjected to biotic (**A**) and abiotic (**B**, **C**) stress treatments, and fluorescence was measured by confocal microscopy (**A**) or using a plate reader (**B**, **C**). The ratio of oxidised ($roGFP_{oxi}$) to reduced ($roGFP_{red}$) roGFP was calculated as a measure of chloroplast oxidation.

A. Chloroplast oxidation is more strongly induced in *sp1*. Six hours post inoculation with *Pst*DC3000, chloroplasts in *sp1* plants were more strongly oxidised than chloroplasts in WT and SP1ox plants. Chloroplast oxidation six hours post $hrpA^-$ inoculation was also more strongly induced in *sp1* than SP1ox. Error bars indicate the SEM (n=4 per time point).

B-C. Expression of SP1 reduces response to a herbicide that induces chloroplast oxidative stress. The roGFP ratio was measured in seedlings incubated for two days with or without paraquat (**B** -1 μM, **C** - 10 μM). At the higher paraquat concentration (**C**), the protective effect of SP1 seen at the lower concentration (**B**) becomes overwhelmed and roGFP oxidation converges. Error bars indicate the SEM (n=4 to 8).

Asterisks indicate significant differences from corresponding treatment in WT (**B** and **C**) or as indicated by brackets (**A**) as calculated by Holm-corrected pairwise T test at $P<.05$ (*), $P<.01$ (**), or $P<.001$ (***).

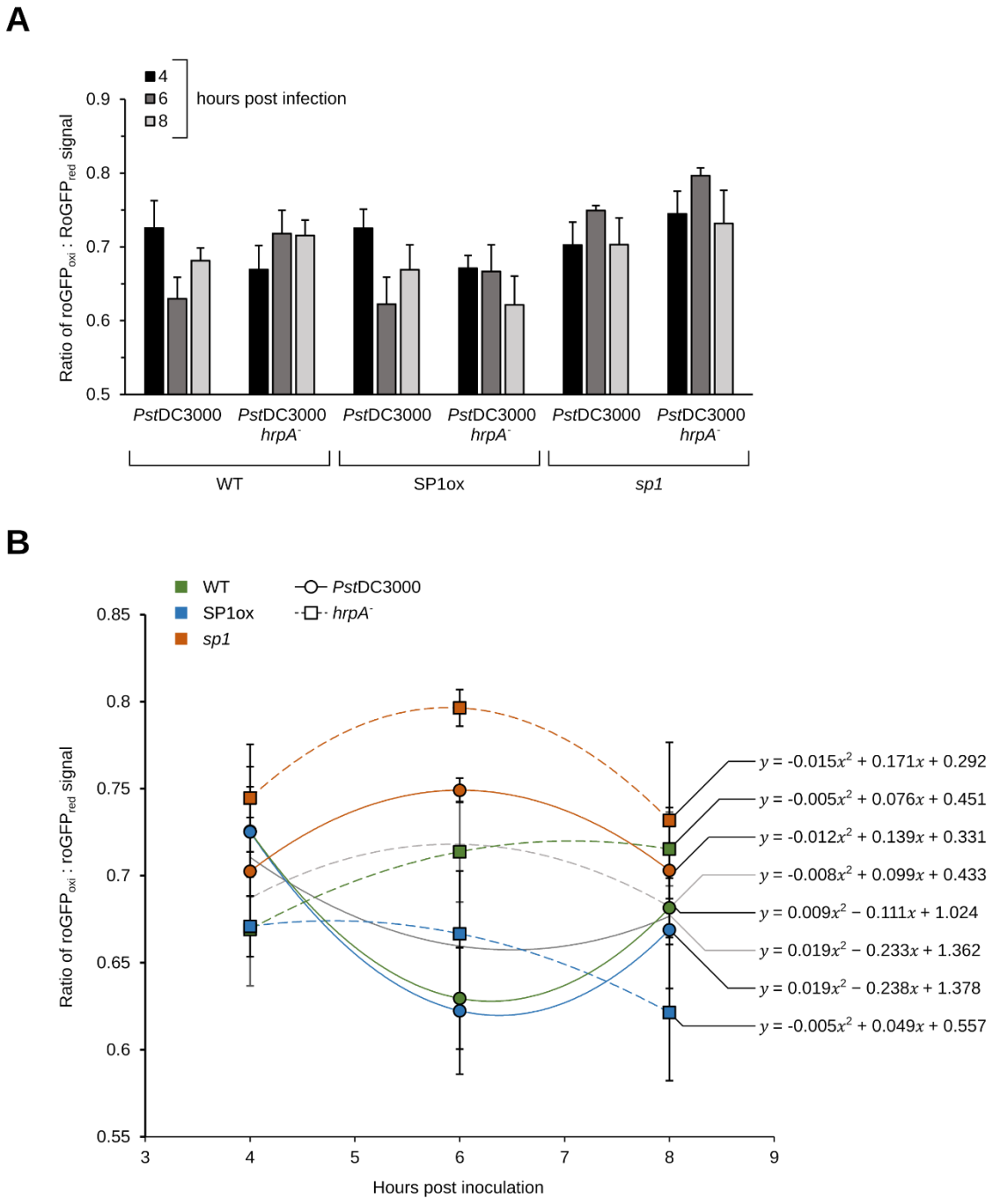

Figure 2.5 Chloroplast oxidation over 4 to 8 hours post inoculation reveal distinct dynamics for different bacterial strains and Arabidopsis lines.

Fluorescence in wild-type (WT), SP1ox, and *sp1* plant lines expressing a chloroplast-targeted redox-sensitive GFP probe (roGFP) was measured four, six, and eight hours post inoculation with either *Pst*DC3000 or *hrpA*$^-$. The ratio of oxidised ($roGFP_{oxi}$) to reduced ($roGFP_{red}$) roGFP was calculated as a measure of chloroplast oxidation. The same six hour data presented in **Figure 2.4A**, p.101 is shown here in broader temporal context.

A. Differences in chloroplast oxidation between pathogenic and non-pathogenic infection are clearest at critical six-hour timepoint. Chloroplast oxidation is transiently induced following *hrpA*$^-$ inoculation and transiently suppressed following *Pst*DC3000 inoculation. *hrpA*$^-$ induces an oxidative burst around six hours post infection in WT plants, but this induction is reduced in SP1ox plants and enhanced in the *sp1* plants. *Pst*DC3000 suppresses the oxidative burst in WT and SP1ox plants, instead shifting the redox state towards reduction at six hours post inoculation; but fails to do so in *sp1* plants. Error bars indicate the SEM (n=4 per time point).

B. Regression analysis showing trends in the response of chloroplast oxidation to bacterial inoculation. Grey trendlines were calculated from the polynominal regression model that fit roGFP ratio to time point and bacterial strain, and show general response of chloroplast oxidation over time to *Pst*DC3000 (solid line) and *hrpA*$^-$ (broken). The coloured trendlines were calculated form a regression model that also included Arabidopsis genotype. This model significantly better fit the data than the first (see running text). Inoculation with *hrpA*$^-$ caused 'hump' shaped trends with a $-x^2$ term. Inoculation with *Pst*DC3000 typically caused 'valley' shaped trends with a $+x^2$ term, except for in *sp1*, where response resembled that to *Pst*DC3000. Error bars indicate the SEM (n=4).

The equations for each line are shown. For the overall equations of each model, see the running text. Circles: *Pst*DC3000; squares: *hrpA*$^-$; green: WT; blue: SP1ox; orange: *sp1*.

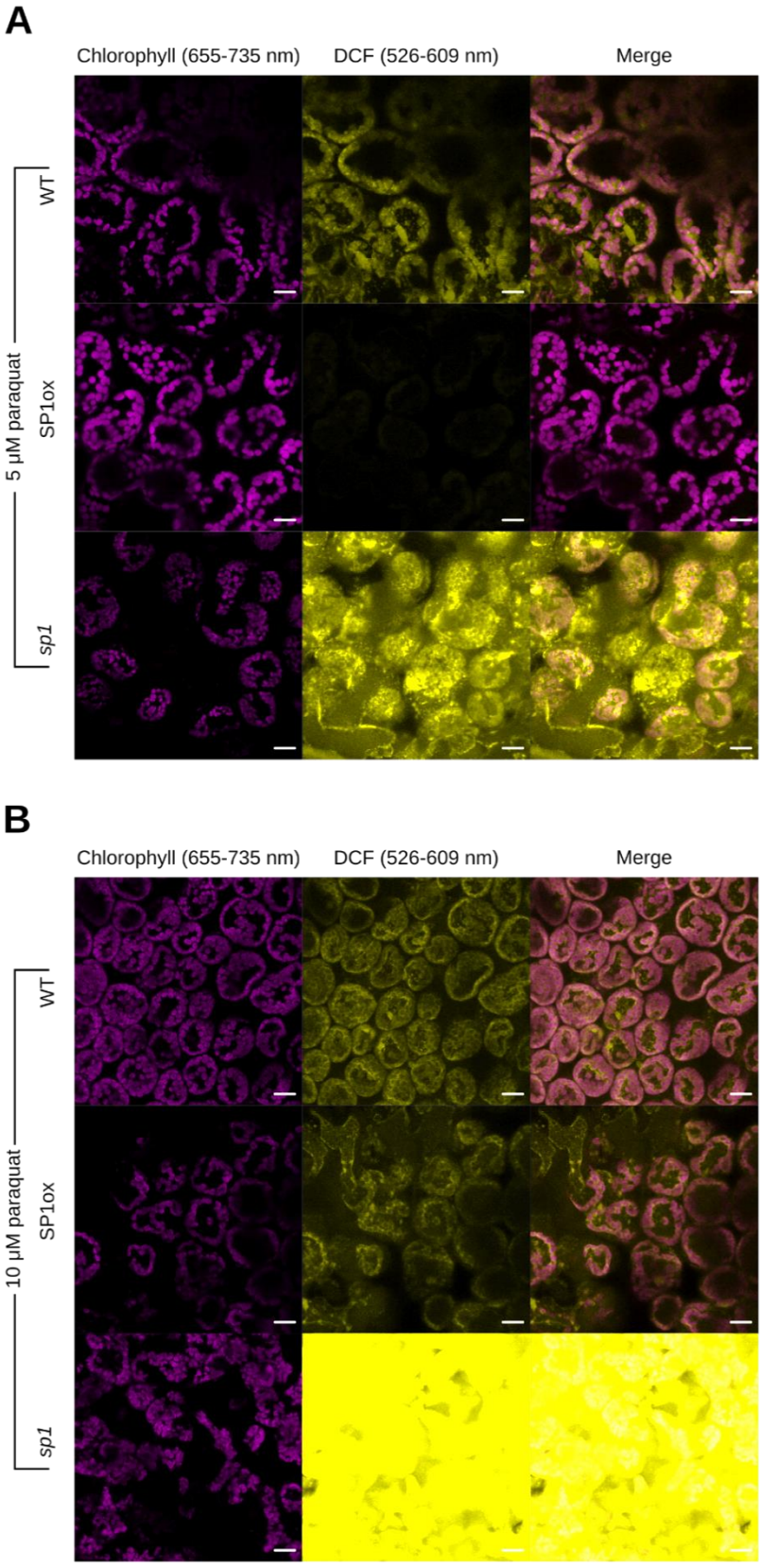

Figure 2.6 Detection of ROS by DCF staining during oxidative stress.

Conversion of membrane permeant 2′,7′-dichlorodihydrofluorescein diacetate to fluorescent marker dichlorofluorescein (DCF) was used to monitor the accumulation of an important ROS molecule (H_2O_2) in wild-type (WT), SP1ox, and *sp1* Arabidopsis plants after treatment for one day with two different concentrations of paraquat (5 μM, **A**; 10 μM, **B**).

A. DCF staining in response to the low paraquat concentration inversely correlates with *SP1* expression. Representative maximum intensity orthogonal projections of leaves of the indicated genotypes are shown. Paraquat treatment (5 μM) elicits a DCF signal in wild-type plants and a stronger signal in *sp1* plants, but the signal is abrogated in the SP1ox line. Scale bar = 20 μm.

B. At the higher paraquat concentration, the protective effect of SP1ox becomes overwhelmed, while *sp1* plants show very high ROS accumulation. Representative maximum intensity orthogonal projections of leaves of the indicated genotypes are shown. Paraquat treatment (10 μM) elicits a DCF signal in all genotypes, but this response is dramatically exacerbated in the *sp1* mutant. Scale bar = 20 μm.

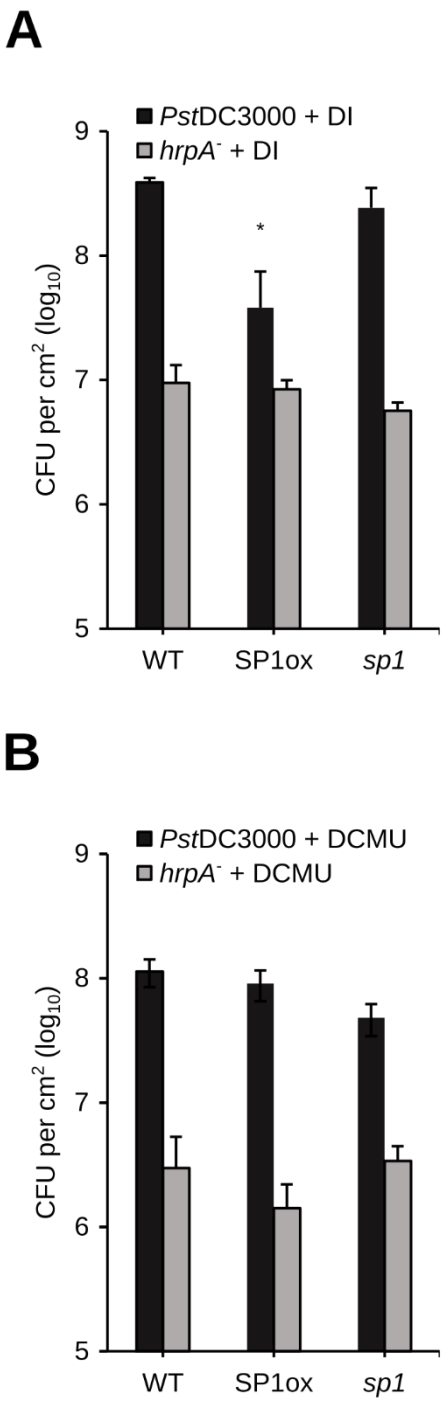

Figure 2.7 Enhanced immunity of *sp1* depends on photosynthesis.

Bacterial growth, measured as colony forming units (CFU) mL^{-1}, was determined four days after inoculation of the indicated plant genotypes with *Pst*DC3000 or *hrpA*$^-$ (10^5 CFU mL^{-1}) using one of two different treatments to disrupt photosynthesis.

A. Effect of disrupting photosynthesis by dark treatment on immunity. After inoculation, plants were kept incubated in the dark (DI) for four days before measuring bacterial growth. This changed the trend of resistance compared to light incubation (**Figure 2.1A**, p.95). In this condition, wild type (WT) and *sp1* were equally susceptible to *Pst*DC3000 and *Pst*DC3000 *hrpA*$^-$, whereas SP1ox showed increased resistance, relative to the wild-type to *Pst*DC3000 but not *hrpA*$^-$. Error bars indicate the SEM (n=3).

B. Effect of disrupting photosynthesis with a chemical inhibitor on immunity. Plants were co-inoculated with the bacterial solutions and 10 μM 3-(3,4-dichlorophenyl)-1,1-dimethylurea (DCMU). WT, SP1ox, and *sp1* are similarly susceptible to *Pst*DC3000 and to *hrpA*$^-$ four days post inoculation. *SP1* expression does not regulate immunity when photosynthesis is inhibited by co-inoculation of 10 μM DCMU. Error bars indicate the SEM (n=3).

Asterisk indicates significant difference ($P<.05$) from corresponding wild-type treatment as calculated by Holm-corrected pairwise T test.

Table 2.1 Summary of *P* values relating to figures in §2

2.1A (CFU)		*P*=	
*Pst*DC3000	WT vs SP1ox	.0015	**
	WT vs *sp1*	.0039	**
hrpA⁻	WT vs SP1ox	.00027	***
	WT vs *sp1*	.029	*
2.1B (Callose)			
*Pst*DC3000	WT vs SP1ox	.36	
	WT vs *sp1*	.000016	***
hrpA⁻	WT vs SP1ox	.62	
	WT vs *sp1*	.62	
Mock	WT vs SP1ox	.082	
	WT vs *sp1*	.082	
2.4A (RoGFP)			
*Pst*DC3000	WT vs SP1ox	.86	
	WT vs *sp1*	.028	*
	SP1ox vs *sp1*	.028	*
hrpA⁻	WT vs SP1ox	.254	
	WT vs *sp1*	.124	
	SP1ox vs *sp1*	.026	*
2.4B-C (RoGFP)			
1 µM PQ	WT vs SP1ox	.00049	***
	WT vs *sp1*	.0011	**
10 µM PQ	WT vs SP1ox	.30	
	WT vs *sp1*	.059	
Mock (B)	WT vs SP1ox	.99…	
	WT vs *sp1*	.99…	
Mock (C)	WT vs SP1ox	.99…	
	WT vs *sp1*	.99…	
2.7A (CFU)			
*Pst*DC3000 + DI	WT vs SP1ox	.033	*
	WT vs *sp1*	.18	
hrpA⁻ + DI	WT vs SP1ox	.89	
	WT vs *sp1*	.89	
2.6B (CFU)			
*Pst*DC3000 + DCMU	WT vs SP1ox	.52	
	WT vs *sp1*	.29	
hrpA⁻ + DCMU	WT vs SP1ox	.99…	
	WT vs *sp1*	.99…	

3.Regulation of chloroplast protein import during infection

Contributions

The chloroplast-targeted fluorescent probe lines were provided by Professor Masanori Izumi, and were crossed into the SP1ox and *sp1* backgrounds by Dr Qihua Ling.

3.1. Abstract

Nucleus-encoded proteins must become imported into the plastid during the remodelling or maintenance of the plastid proteome during biogenesis and homeostasis. Import is regulated during development and during abiotic stress, and the efficiency of this regulation has consequences for the efficacy of developmental transitions and tolerance to stresses.

In this chapter, the regulation of chloroplast protein import during immunity and pathogenesis is explored. The localisation of chloroplast-targeted probes was found to become disrupted during ETS after inoculation with virulent *Pst*DC3000, but maintained during PTI after inoculation with *hrpA*$^{-}$. The cytosolic and vacuolar localisation of the chloroplast targeted probes during ETS could not be attributed to a loss of chloroplast membrane integrity; rather it appeared to arise from a disruption to import.

To visualise the changes to chloroplast protein import in infection, a fluorescence recovery approach was devised. The *ppi1* mutation of Toc33, which constitutively reduces plastid protein import, caused reduced recovery of the fluorescent probe signal after mild photobleaching of the plastid compared to wild-type plants. Likewise, inoculation with *Pst*DC3000 but not *hrpA*$^{-}$ similarly impaired the recovery of fluorescent signal in the chloroplast, confirming that *Pst*DC3000 specifically has an effect on plastid protein import.

Given that the regulator of plastid protein import, SP1, was found to control the immune response by antagonising the chloroplast ROS burst (see **§2**), a possible role for SP1 in modulating chloroplast protein localisation during infection was investigated. Plastid localisation after *Pst*DC3000 inoculation was found to be restored by the *sp1* mutation, indicating that the activity of SP1 is necessary for the protein import defect phenotype. Accordingly, protein levels of Toc159 were found to be reduced in ETS in an SP1-dependent manner.

3.2. Introduction

The plastid proteome must be remodelled during development as plastids proliferate and take on new roles. In addition to the transcriptional control of nucleus- and plastome-encoded gene expression, which is mediated by anterograde and retrograde signalling [350], this is under post-translational control through the import of new proteins and the degradation of old ones. Consequently, differentiation is often perturbed in mutants defective in the import (e.g. *ppi1* [37], *ppi2* [351], and the *toc75* mutants [352]) or turnover (e.g. mutants for a number of Clp components [353]) of plastid proteins, which show chlorotic phenotypes or embryo lethality.

The import and turnover of proteins is also vital for maintaining plastid homeostasis. Several novel systems of turnover have been identified to act in the chloroplast, where the photosynthetic machinery is particularly liable to cause damage, especially during stress. These include the efficient replacement of the D1 subunit of PS II, which easily becomes photodamaged, by a specialised repair cycle mediated by the Deg and FtsH proteases [176]. There are 20 classes of plastid-localised proteases that act in the quality control of proteins in the stroma and internal membranes. Many of these are prokaryotic in origin, or have eukaryotic embellishments to a prokaryotic core, for example, the plastid Clp protease [354,355].

The degradation of photodamaged components has also been shown to be mediated by the vacuole in at least two processes active under high-light stress. In one, stroma-containing vesicles, RCBs, bud off from the plastid for autophagic destruction [178]; in the other, entire photodamaged chloroplasts are transported to the vacuole instead [179]. The turnover of damaged proteins is an important remedial step in preventing further stress damage, and plants that are mutants for these systems tend to be more stress sensitive

Of course, the turnover of damaged components must be complemented by the import of new replacements, but it was recently found that protein import can become downregulated during stress, mediated by SP1, to assist stress tolerance [165]. In the SP1 ROS-avoidance model, the reduction in import of photosynthesis-related precursors downregulates photosynthesis during abiotic stress, reducing the accumulation of toxic ROS by-products of photosynthesis [165]. Thus, plastid protein import not only has an important role in remodelling the plastid proteome in development, it is critical for the reconfiguration of the organellar proteome in response to environmental cues.

It is well established that the chloroplast is a signalling nexus in both abiotic and biotic stresses [1,350]. However, the role of plastid protein import in disease has received limited attention. Pathogens like *P. syringae* can cause alteration of the chloroplast proteome at both the transcriptional and post-translational levels [1], and it is known for example that certain pathogen effectors that target the chloroplast become imported into the organelle through the host's import machinery, e.g. HopK1 and AvrRps4 [290].

To complement the work presented in **§2**, where SP1 was discovered to have a role during pathogenesis and immunity, in this chapter the effect of pathogenesis and immunity on the import into chloroplasts of host proteins is examined. The results afford new insight into the mechanistic basis by which SP1's activity suppresses the immunogenic chloroplast ROS burst.

3.3. Results

3.3.1. Pathogenesis induces mislocalisation of a chloroplast-targeted probe

The import of preproteins into the chloroplast is a critical step in chloroplast biogenesis and homeostasis, and in stress tolerance. To test whether chloroplast protein import is affected by disease, the localisations of two chloroplast-targeted fluorescent probes were studied.

Two different transgenic plant lines expressing a chloroplast-targeted fluorescent marker were used. One line carried a construct encoding GFP fused downstream of a chloroplast recA transit peptide (cpGFP), under the control of the constitutive *35S* promoter [178]. The other line carried a construct encoding full-length Rubisco small subunit (RbcS) tagged C-terminally with GFP (RbcS-GFP), under the control of the native *RBCS* promoter. The recombinant RbcS-GFP protein is able to correctly integrate with Rubisco large subunit proteins to form the Rubisco holoenzyme [178].

Rosette leaves from both lines were infiltrated with either *Pst*DC3000, *hrpA*$^-$, or a mock inoculum, and the localisation of the GFP probe was visualised one and two days post inoculation. By one day post inoculation, both probes correctly localised to the chloroplast in all treatments (data not shown). However, by two days post inoculation, both probes lost chloroplast localisation in *Pst*DC3000-infiltrated plants, but not in *hrpA*$^-$ - or mock-infiltrated plants (**Figure 3.1**, p.129). These data show that the localisation of chloroplast-targeted proteins can be disrupted as part of ETS, but not PTI.

In the *Pst*DC3000-inoculated plants, the GFP signal was seen to accumulate either alongside chloroplasts, in the cytosol but not in the vacuole; or uniformly throughout the cell in the cytosol and vacuole (**Figure 3.2**, p.131). This suggests a sequence of events in the mislocalisation of the GFP probes.

3.3.2. Chloroplast-targeted probe mislocalisation is not the result of a loss of chloroplast membrane integrity

Loss of the chloroplast-targeted probe from the stroma could be caused by membrane damage, causing the probe to passively leak out. Membrane integrity can be lost by lipid peroxidation; in fact, cellular lipid peroxidation and electrolyte leakage are characteristic of the hypersensitive response during ETI [356,357]. It would be surprising if this was the case here, however, in light of the fact that *Pst*DC3000 elicits lower levels of ROS in the chloroplast than *hrpA*$^-$: therefore if *Pst*DC3000 inoculation causes extensive enough lipid peroxidation to cause membrane leakage, one would expect to membrane leakage after *hrpA*$^-$ inoculation also.

To determine whether mislocalisation could be the result of membrane damage, chloroplast membrane integrity was assayed with the dye carboxyfluorescein diacetate (CFDA). Carboxylesterases present in the stroma hydrolyse the dye, and fluorescent 5-carboxyfluorescein (5-CF) accumulates in chloroplasts. If membrane integrity is damaged, or if the chloroplast membranes have broken and resealed, these carboxylesterases are lost and chloroplasts do not show 5-CF signal [358].

Protoplasts were isolated from the leaves of wild-type Arabidopsis two days after infiltration with *Pst*DC3000, *hrpA*$^-$, or a mock inoculum. These were incubated with CFDA and visualised by epifluorescence microscopy. Protoplasts that were subjected to high-light stress (500 µmol m^{-2} s^{-1} actinic light for 10 minutes) prior to staining were used as a control. Fluorescence of 5-CF in the chloroplasts could be seen in all treatments except for the high-light control (**Figure 3.3**, p.133), confirming that chloroplast membranes retain integrity during both *Pst*DC3000 and *hrpA*$^-$ infections. It is unlikely, therefore, that the mislocalisation of the chloroplast-targeted probes seen during *Pst*DC3000 infection was caused by membrane leakage.

3.3.3. A microscopy-based method for the comparison of the rates of chloroplast protein import

It is possible that the GFP probes become mislocalised because import into the chrooplast is disrupted. To examine this hypothesis, a novel fluorescence microscopy assay was developed to allow the measurement of import rates under suitable conditions following infection.

Rates of protein import into chloroplasts may be measured by isolating chloroplasts from plants via density gradient centrifugation, and then incubating the organelles with a radiolabelled preprotein. This approach has allowed the nature of mutations like *ppi1* [37], and the recovery of protein import in the *sp1 ppi1* double mutant [126], to be characterised. However, this technique, though amenable for studying mutations in the import apparatus with constitutive and early phenotypes, is not suitable for studying the effect of biotic stress on import, for several reasons.

Firstly, isolated chloroplast yields decrease as the plant material ages, meaning the technique is most suitable for studying seedlings and not chloroplasts from mature rosette leaves as used here. A method for the infection of Arabidopsis seedlings has been published [359], but despite best attempts it has not proven possible to replicate this procedure. Secondly, as starch crystals can rupture the chloroplasts during isolation, plants must be kept in an extended dark period before chloroplasts are isolated; such dark treatment exacerbates infection and alters the resistance and susceptibility phenotypes of *sp1* and SP1ox (**Figure 2.7**, p.107).

Thus, in this section, an alternative system for comparing rates of chloroplast protein import was devised. In this approach, some of the fluorescent signal of the probe is photobleached and fluorescence recovery is quantified over time to provide a measure of protein import. This is based on a similar fluorescence recovery after photobleaching (FRAP) approach that was used previously to study protein trafficking through stromules,

stroma-filled tubules that extend from chloroplasts [360–363]. FRAP has also been used in the chloroplast to study thylakoid membrane protein dynamics [364].

Briefly, Arabidopsis lines that express chloroplast-targeted GFP (the cpGFP construct, as above) are visualised by confocal microscopy and the accumulated GFP signal in their chloroplasts is reduced via photobleaching. The subsequent recovery of the fluorescence signal represents the maturation [365] of the GFP molecules that have been imported from the cytosol. In this method, an entire cell in a field of view is lightly bleached, sufficient to reduce the total GFP signal of the cell by approximately 10%. Another cell in the same field of view is used as a control cell and is not bleached. Recovery of the signal from the bleached cell, relative to the signal of the unbleached cell, can be measured over time.

To determine how appropriate this system is for comparing rates of protein import, the rates of fluorescence recovery were compared between wild-type and *ppi1* Arabidopsis lines expressing the cpGFP construct. The *ppi1* mutation, which causes loss of Toc33, was previously shown to reduce the rate of protein import into chloroplasts isolated from seedlings using the traditional *in vitro* assay [37,126]. In accordance with those published results, the *ppi1* mutation reduced the rate of fluorescence recovery relative to wild type, in seedlings (**Figure 3.4A**, p.135). In mature rosette tissue, fluorescence recovery in *ppi1* was even poorer, relative to the wild type, than in seedlings, and began to decline later on in the time course (**Figure 3.4B**, p.135). The difference in fluorescence recovery between *ppi1* seedlings and rosette leaves may reflect the different import capacities of seedlings undergoing photomorphogenesis and fully differentiated leaves.

These results show that defects in chloroplast protein import can be measured by the rate of recovery of a fluorescent probe.

3.3.4. Rate of chloroplast protein import is reduced during ETS

The newly-established FRAP-based assay for chloroplast protein import (**§3.3.3**) was then used to determine whether protein import is altered during infection in a way that could account for the GFP mislocalisation phenotype.

Leaf discs from cpGFP-expressing plants were taken one day after inoculation with either *Pst*DC3000 or *hrpA*$^{-}$. At this time point, cpGFP was still localised to the chloroplast compartment. Chloroplasts were bleached as described above and the rates of fluorescence recovery were then compared to assess chloroplast protein import.

Consistent with the idea that the mislocalisation seen after *Pst*DC3000 infection was caused by a suppression of protein import, fluorescence recovery was greatly reduced in leaves inoculated with *Pst*DC3000 (**Figure 3.5A**, p.137). In fact, the data closely resembled those obtained for mature *ppi1* leaves. Comparatively, fluorescence recovery in leaves that had been infected with *hrpA*$^{-}$ was much higher (**Figure 3.5A**, p.137).

This indicates that chloroplast protein import is not suppressed during PTI, but that *Pst*DC3000 suppresses it during ETS. This supports the hypothesis that the mislocalisation phenotype described in **§3.3.1** is caused by a failure to properly import the probe.

3.3.5. The chloroplast-targeted probe mislocalisation induced by *Pst*DC3000 depends on SP1

Because *Pst*DC3000 suppresses chloroplast protein import during pathogenesis, and because SP1 both regulates the rate of chloroplast protein import and is required for pathogenesis, the available evidence suggests that *Pst*DC3000 may utilise SP1 to suppress protein import. This could provide a mechanistic explanation for the subversion of the chloroplast ROS burst observed in **§2**. To test this, SP1ox cpGFP (**Figure 3.6A** p.139) and *sp1* cpGFP lines (**Figure 3.6B**, p.139) were generated and visualised during infection.

If *Pst*DC3000 utilises SP1 to suppress protein import, it would be expected that in *sp1*, chloroplast-targeted probes would retain their localisation. Accordingly, two days after inoculation with *Pst*DC3000 as above, *sp1* cpGFP plants still showed chloroplast localisation of the probe (**Figure 3.6B**, p.139).

When analysed in the SP1ox background, the cpGFP probe became mislocalised two days after inoculation with *Pst*DC3000, as in the wild type (**Figure 3.6A**, p.139). Interestingly, inoculation of these plants with *hrpA*$^-$ induced a GFP 'halo' phenotype not seen in the other plant lines or after mock infiltration (**Figure 3.7**, p.141). This suggests that some cpGFP may be retained in the cytosol in this condition, also; that is to say, overexpression of SP1 during PTI causes some reduction in chloroplast protein import even in the absence of proteinaceous effectors.

3.3.6. The TOC machinery is targeted for turnover during infection in an SP1-dependent manner

SP1 regulates chloroplast protein import through the UPS-dependent turnover of TOC components [126,154,165]. If *Pst*DC3000 accomplishes the suppression of import via SP1, we would expect to see this reflected in TOC protein abundancy.

To confirm that the import changes above reflect differences to the TOC components, total protein was extracted from rosette leaves of wild-type, SP1ox and *sp1* plants two days after infiltration with *Pst*DC3000, *hrpA*$^-$, or a mock inoculum. The abundance of the major TOC component Toc159 was determined by western blotting and normalised to Histone 3.

In the wild type, Toc159 levels were slightly reduced during infection with *hrpA*$^-$ but much more strongly reduced during *Pst*DC3000 infection. In *sp1*, however, Toc159 levels were similar in all treatments (**Figure 3.8A**, p.143). This indicates that regulation of Toc159 during infection requires SP1. In SP1ox, Toc159 was heavily suppressed even in the *hrpA*$^-$

infection, and almost undetectable after infection with *Pst*DC3000, even when the samples were overloaded (**Figure 3.8C**, p.143). These results support the conclusion that chloroplast protein import is suppressed during pathogenesis by the depletion of the TOC apparatus in an SP1-dependent manner. Furthermore, they support the notion that an excess of SP1 enhances pathogenesis, even in the absence of proteinaceous effectors, by TOC depletion.

3.4. Discussion

3.4.1. Explanation for and sequence of events in *Pst*DC3000-induced chloroplast-targeted probe mislocalisation.

Two chloroplast-targeted probes, including a tagged native protein under its native promoter, lose their plastid localisation in mesophyll cells specifically two days after inoculation with *Pst*DC3000 but not *hrpA*$^-$. This implies that chloroplast protein import is disrupted during ETS as part of pathogenesis, but not during PTI.

Apart from a failure to import the preprotein, a defect in the chloroplast localisation of a chloroplast-targeted protein could in principle be brought about by passive or active release of the protein from the chloroplast. That chloroplasts retain membrane integrity during infection (**Figure 3.3**, p.133) would seem to rule out passive leakage.

There are two known mechanisms of chloroplast protein quality control that could conceivably release GFP from the stroma. Firstly, entire chloroplasts may be turned over autophagically in the vacuole during stress (chlorophagy), which could account for vacuole-localised GFP. However, this has only been shown to occur after extensive lipid peroxidation and membrane damage [179], which was not apparent in *Pst*DC3000 infection. Additionally, it would not explain the observed localisation of GFP in the cytosol but not the vacuole in some cells (**Figure 3.2**, p.131).

Secondly, stromal proteins may be exported from the chloroplast to the vacuole for degradation in vesicles called RCBs. RCBs can be made visible with a stromal fluorescent probe like cpGFP or RbcS-GFP, and are identified as small particles exhibiting Brownian motion in the vacuole [177,178]. Therefore, they would be expected to be visible in the above experiments if present. No such particles were visible during *Pst*DC3000 infection. Interestingly, similar particles have previously been reported during ETI but not ETS, although they were not identified at the time as RCBs [266].

It is unlikely, then, that the observed mislocalisation was caused by these processes. Furthermore, neither chlorophagy nor RCB-mediated autophagy would account for the accumulation of fluorescent signal in the cytosol, but not vacuole, in some cells. The interpretation that is most consistent with all of the available data is that the mislocalisation comes from a suppression of chloroplast protein import, even before considering that, by the same timepoint, Toc159 abundance has greatly declined during *Pst*DC3000 infection, or that preceding the mislocalisation, inoculation with *Pst*DC3000 impairs the recovery of chloroplast fluorescence after photobleaching,

When the cpGFP or RbcS-GFP probes have become mislocalised following *Pst*DC3000 infection, fluorescence can be seen in the cytosol exclusively or more uniformly within the cell. This suggests a sequence of events, where GFP first begins to fill the cytosol around the chloroplasts, and then later accumulates in the vacuole also (**Figure 3.2**, p.131).

For the GFP or GFP-tagged preproteins to become fluorescent in the cytosol, they must have completed protein folding and the autocatalytic cyclisation necessary to form the chromophore [365]. Normally, cytosolic chaperones prevent the folding of preproteins in the cytosol (see **§1.3.1**), and so if this is the case it suggests that the capacity of the available chaperones was exceeded. Expression of chaperones might be downregulated in parallel with the reduction in chloroplast import efficiency during infection; or, the chaperone supply may have simply become exhausted due to an excess of preproteins that have failed to import. The second scenario seems likely to occur when import is prevented in photosynthetic cells, given that the import of highly expressed native photosynthetic proteins will be affected in addition to that of the probe.

Unimported preproteins are normally turned over by the UPS via CHIP (see **§1.4.3)**, but that system is clearly insufficient to clear the fluorescent probes in this case. The later appearance of GFP in the vacuole suggests that, with cytosolic turnover having been

found to be inadequate, the GFP eventually becomes the substrate of an autophagic process (e.g. microautophagy [366]).

3.4.2. Biological considerations for the FRAP-based assay for import

In this chapter, a novel assay for organellar protein import based on FRAP was described. To properly interpret the results generated by this method, it is important to consider what the recovery of the chloroplast-localised fluorescence signal during the assay represents biologically.

FRAP experiments are normally used to study the diffusion of probes; for example, one might bleach an area of probes from part of the plasma membrane and measure how rapidly they are replaced from other parts of the membrane. This may reveal that the repopulation of the probe is a result of passive diffusion or active transport, or it may reveal that barriers to diffusion exist that restrict probes to different areas [367].

In the measurement of chloroplast protein import by FRAP, what is being measured is not the movement of a fluorescent probe from one compartment to another—e.g. from the cytosol to the chloroplast—but the maturation of new GFP in the stroma. Wild-type GFP may take as long as 53 minutes to mature, but maturation time can greatly vary depending on temperature and the organism in which it is expressed. Modified GFPs like enhanced GFP or GFPmut3 tend to mature faster, in under 14 minutes and under eight minutes, respectively, *in vitro* [368]. Maturation time is the time taken to complete several processes: the transcription, translation, and folding of GFP, followed by its cyclisation. Cyclisation is autocatalytic and involves an oxidation and dehydration reaction to produce the fluorescent core [365].

There are no available data on maturation times for GFP in the chloroplast, or for the plant-enhanced variety of GFP used here (S65TmGFP4; it possess a serine-to-threonine point mutation at the 65th residue that greatly enhances fluorescence, and modified codon usage for enhanced expression in Arabidopsis [369]). However, given that pre-fluorescent

GFP in the stroma will already have been transcribed and translated, and that its folding is assisted by the import apparatus and associate chaperones, we may only be measuring the cyclisation, oxidation[4], and dehydration steps. It can be assumed, then, that maturation in this assay will be complete in the order of minutes. Therefore, the amount of GFP signal that matures during the time-course reflects how much protein was imported a few minutes earlier.

Bleaching of this cpGFP construct has previously been used to study movement of proteins from the stroma of an unbleached chloroplast to a bleached one via stromules [360–363]. In the experiments presented here, this phenomenon was controlled for by bleaching and measuring whole cells, rather than one chloroplast in a cell. Furthermore, while stromules are induced during ETI, where they interface with the nucleus, they are not apparent in mesophyll cells during ETS or PTI as elicited with *Pst*DC3000 or *Pst*DC3000 *hrcC*$^-$ [370], another HRP mutant defective in T3SS effector secretion like *hrpA*$^-$. Similarly, they were not observed during *Pst*DC3000 or *hrpA*$^-$ infection here. It is unlikely, therefore, that the observed fluorescence recovery could represent remobilisation of already imported GFP from one chloroplast to another.

3.4.3. Technical considerations for the FRAP-based assay for import

These measurements take place over a longer timescale than normal FRAP experiments, which typically measure diffusion in under a minute. This in itself should not cause a problem. To study some systems, even longer timescales have been used, such as the replacement of aquaporins in root plasma membranes measured over half an hour [371]. However, the maximum possible timescale here is limited by Z-axis drift. Chloroplasts tend to reposition themselves in response to light stimuli such as the scanning laser. Consequently, measurements of recovery after longer time periods become more error

[4] In fact, the bleaching itself may trigger oxidation in the chloroplast that encourages the chromophore oxidation step. This could explain why GFP fluorescence seems to jump after bleaching (see first two timepoints in **Figure 3.4A&B**, p.28).

prone as the chance of chloroplasts drifting away in the Z-axis increases. This is apparent in the growing size of the error bars after 200 s in **Figure 3.5A**, p.137.

Initially, Z-axis movement in the test and control cells is similar as they are both scanned by the laser. This controls for small amounts of Z-axis drift. However, eventually chloroplasts will drift out of focus and the signal detected from them is lost: as this occurs, the signal detected in the test and control regions would both approach the detection floor, inflating the apparent recovery.

Several optimisations have been made to reduce this effect. Firstly, by only mildly bleaching the test cell so that the signal was reduced by just 10-15%, the duration of the experiment could be much shorter than if the signal had been completely bleached. Secondly, a large pinhole was used, which both increased the section size so as to keep chloroplasts in focus for longer, and, by increasing the amount of light hitting the detector, meant that a weaker scanning laser could be used, stimulating less chloroplast movement. An additional consideration in only partially bleaching the test cells was the desire to elicit less photodamage than would occur by completely bleaching the entire cell area. It also allowed the movement of chloroplasts in the X- and Y-axes to be tracked and adjusted for if necessary.

An alternative approach that would allow longer term measurements would be to use a chloroplast-targeted photoconvertible fluorescence probe. Photoconvertible probes shift their fluorescence emission after being excited by a certain wavelength; for example, the Kaede family of probes including monomeric Eos fluorescent protein (mEosFP) fluoresce green until photoconverted by ultraviolet light, after which they fluoresce red [372]. mEosFP is suitable for expression in plants, and can rapidly be photoconverted either by a 405 nm laser on a confocal microscope or simply by illuminating the sample for a few seconds on an epifluorescence microscope with a DAPI filter [373]. Like cpGFP, mEosFP could be fused to a transit peptide to target it to the chloroplast, and after

photoconversion, the ratio of red to green fluorescence could be measured over time to determine how long the complete replacement of the probe in the chloroplast takes.

3.4.4. Commonality between PTI and ETS

Interestingly, Toc159 levels appear to be reduced during PTI as elicited by *hrpA*$^-$ as well as during ETS as elicited by *Pst*DC3000. However, the smaller reduction of Toc159 in PTI does not cause the chloroplast import suppression phenotype of *Pst*DC3000 infection[5]. This joins a short list of similarities between the effects of *hrpA*$^-$ and *Pst*DC3000 inoculations, relative to mock infiltration, which contribute to pathogenesis only in *Pst*DC3000 inoculation where the changes are of a greater magnitude.

Inoculation with *hrpA*$^-$ or *Pst*DC3000 causes similar gene expression changes, relative to mock-treated leaves, including the downregulation of photosynthesis-related NECGs and the upregulation of genes related to the biosynthesis of jasmonic acid, chorismate and tryptophan. However, these genes are more strongly down- or upregulated in *Pst*DC3000 infection [253]. This might indicate that *hrpA*$^-$ can still release non-proteinaceous effectors, for example coronatine [374], that on their own are capable of eliciting weak (and insufficient) changes to the host.

Alternatively, it might point to some commonality between immunity and pathogenesis: perhaps during PTI the plant redirects some resources from growth to immunity (from photosynthesis to defence); while in ETS the pathogen more completely undermines the plant metabolism by suppressing photosynthesis. Metabolomic changes induced in PTI and ETS are the subject of **§5**.

Intriguingly, the downregulation of photosynthetic genes by neither *hrpA*$^-$ nor *Pst*DC3000 prevented the expression of the RbcS-GFP probe, which is driven by the

[5] Mild depletion of TOC components often does not cause a noticeable phenotype: for example, SP1ox or SP2 overexpression lines both have reduced Toc159 levels relative to the wild type, but do not have a different macroscopic phenotype under normal growth conditions.

native *RBCS* promoter. This suggests that post-translational regulation, the reprogramming of import, may be more key to antagonising photosynthesis during infection than the reprogramming of gene expression.

Commonality in the induction of NPQ in PTI, ETS, and ETI is discussed briefly in **§4.4.4**.

3.4.5. Model for the role of SP1 in chloroplast protein import modulation during abiotic and biotic stresses

In **§2**, SP1 was found to have an important role in mediating the suppression of host immunity by *Pst*DC3000. It was proposed that this role is related to the strength of an early immunogenic signal, the chloroplast ROS burst, which is antagonised by SP1. After a pathogen is detected, in the absence of the delivery of pathogen effectors or in plants with the *sp1* mutation, the burst is generated. In the presence of both pathogen effectors and SP1, this burst is abrogated. In the absence of effectors, mutation of *sp1* further enhances the chloroplast ROS burst, while SP1ox compensates for the absent effectors and reduces the ROS burst. The similarities between this and SP1's role during abiotic stress were noted but the mechanism of its action in disease was still to be determined.

This chapter reveals that chloroplast protein import is suppressed by *Pst*DC3000 during pathogenesis. This suppression depends on SP1 and is linked to reduced levels of important TOC component, Toc159. This supports a model in which SP1 acts in pathogenesis to avert the chloroplast ROS burst by the suppression of chloroplast protein import (**Figure 6.1**, p.205). As in the abiotic stress tolerance model [165]l, in this model the suppression of chloroplast protein import downregulates photosynthesis, reducing the capacity to generate ROS photochemically; this averts the immunogenic ROS burst.

In **§4**, photosynthesis during infection, and a previously-proposed mechanism to account for the suppression of the chloroplast ROS burst by *Pst*DC3000 [253], are examined.

3.5. Figures

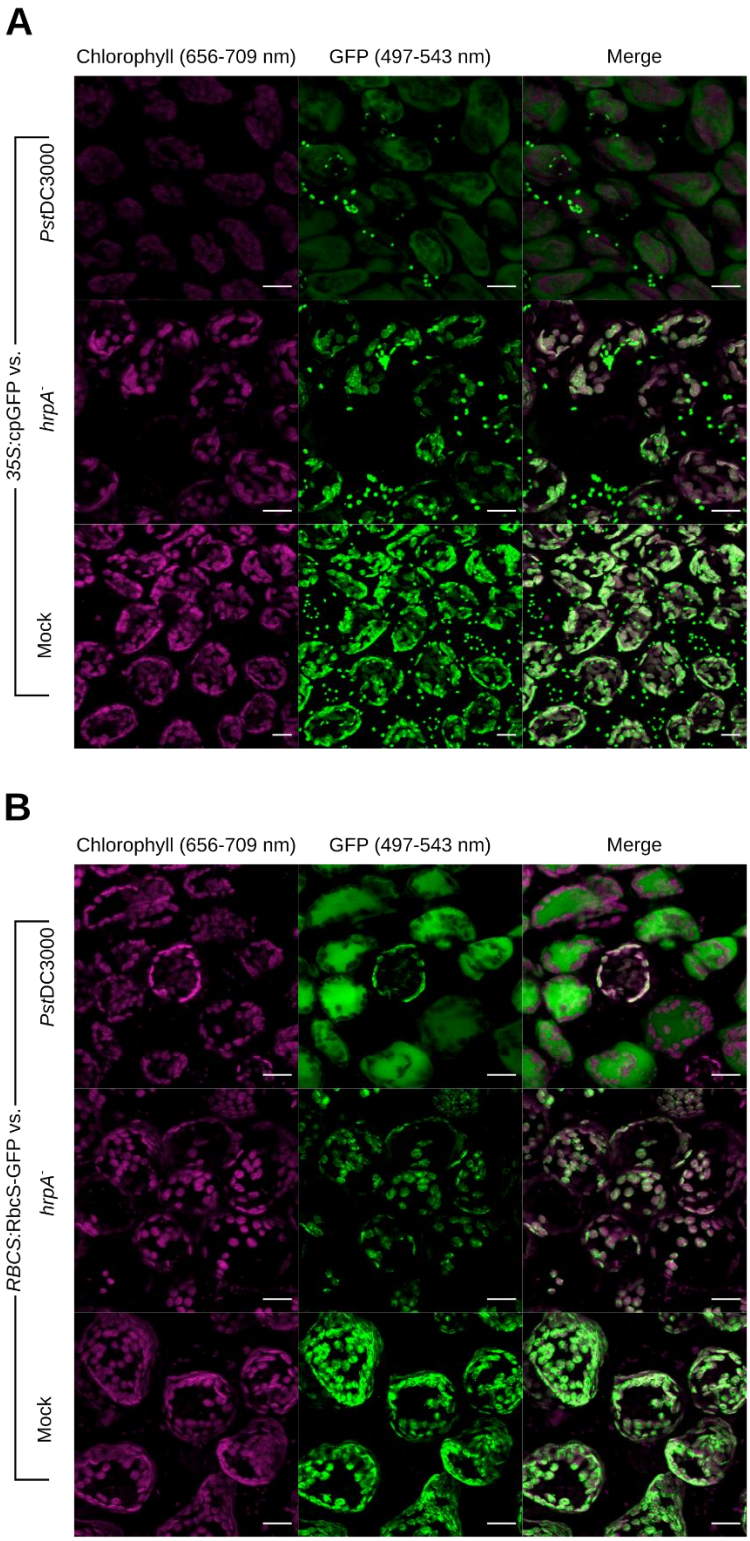

Figure 3.1 Mislocalisation of two chloroplast-targeted GFP probes during *Pst*DC3000 infection.

Maximum intensity Z-projections from plants expressing one of two chloroplast-targeted green fluorescent protein (GFP) probes, two days after infiltration with *Pst*DC3000, *hrpA*$^-$, or a mock inoculum ($MgCl_2$). Probes were correctly targeted to the chloroplast after *hrpA*$^-$ or mock infiltration, as shown by colocalization with the chlorophyll signal. Two days after inoculation with *Pst*DC3000, however, the probes localised outside of the chloroplast. Scale bars = 20 μm.

A. Inoculation with *Pst*DC3000 specifically induces chloroplast-targeted GFP probe to accumulate outside of the chloroplast. Leaves from plants constitutively expressing the probe (*35S*:cpGFP) were infiltrated and visualised as above. GFP was also seen in epidermal plastids, which are smaller and show little or no chlorophyll fluorescence.

B. Inoculation with *Pst*DC3000 specifically induces a fluorescently tagged native protein to accumulate outside of the chloroplast. Leaves from plants expressing the probe under a native promoter (*RBCS*:RbcS-GFP) were infiltrated and visualised as above. Unlike the *35S* promoter in **A**, the *RBCS* promoter used here is not expressed in epidermal cells and no epidermal plastid fluorescence is seen.

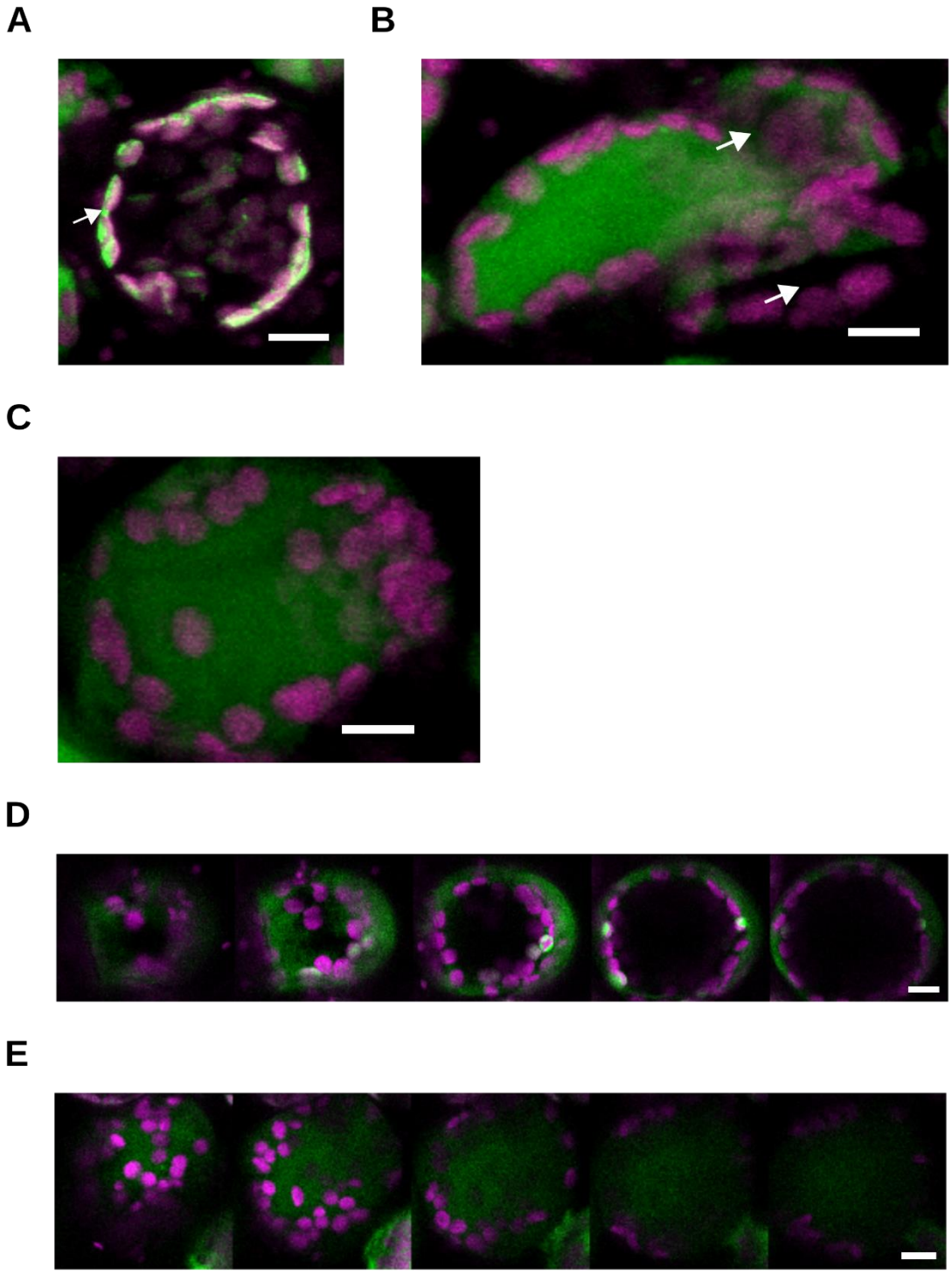

Figure 3.2 The mislocalised GFP probe accumulates in the cytosol or cytosol and vacuole after inoculation with *Pst*DC3000.

A-C. Proposed sequence of events in GFP mislocalisation. Two days after inoculation with *Pst*DC3000, GFP was seen in the cytosol immediately outside of the chloroplast (**A**, arrow), filling the cytosol but not the vacuole (**B**, arrow indicates vacuole lacuna), or uniformly filling the cytosol and vacuole (**C**). Images shown are detail from **Figure 3.1B**, maximum intensity Z-projections after inoculation of *RBCS*:RbcS-GFP with *Pst*DC3000. Similar cells can be seen in the 35S:cpGFP line (not shown). Scale bar = 10 μm.
D. Mislocalised RbcS-GFP can accumulate in the cytosol separately from the vacuole. Z-planes from a *RBCS*:RbcS-GFP expressing cell two days after inoculation with *Pst*DC3000 are shown. The vacuole is the void circled by chloroplasts and GFP signal. Scale bar = 10 μm.
E. Mislocalised RbcS-GFP can fill the cytosol and vacuole uniformly. Z-planes from a *RBCS*:RbcS-GFP expressing cell two days after inoculation with *Pst*DC3000 are shown. No lacuna in the GFP signal indicative of the vacuole is apparent. Scale bar = 10 μm.

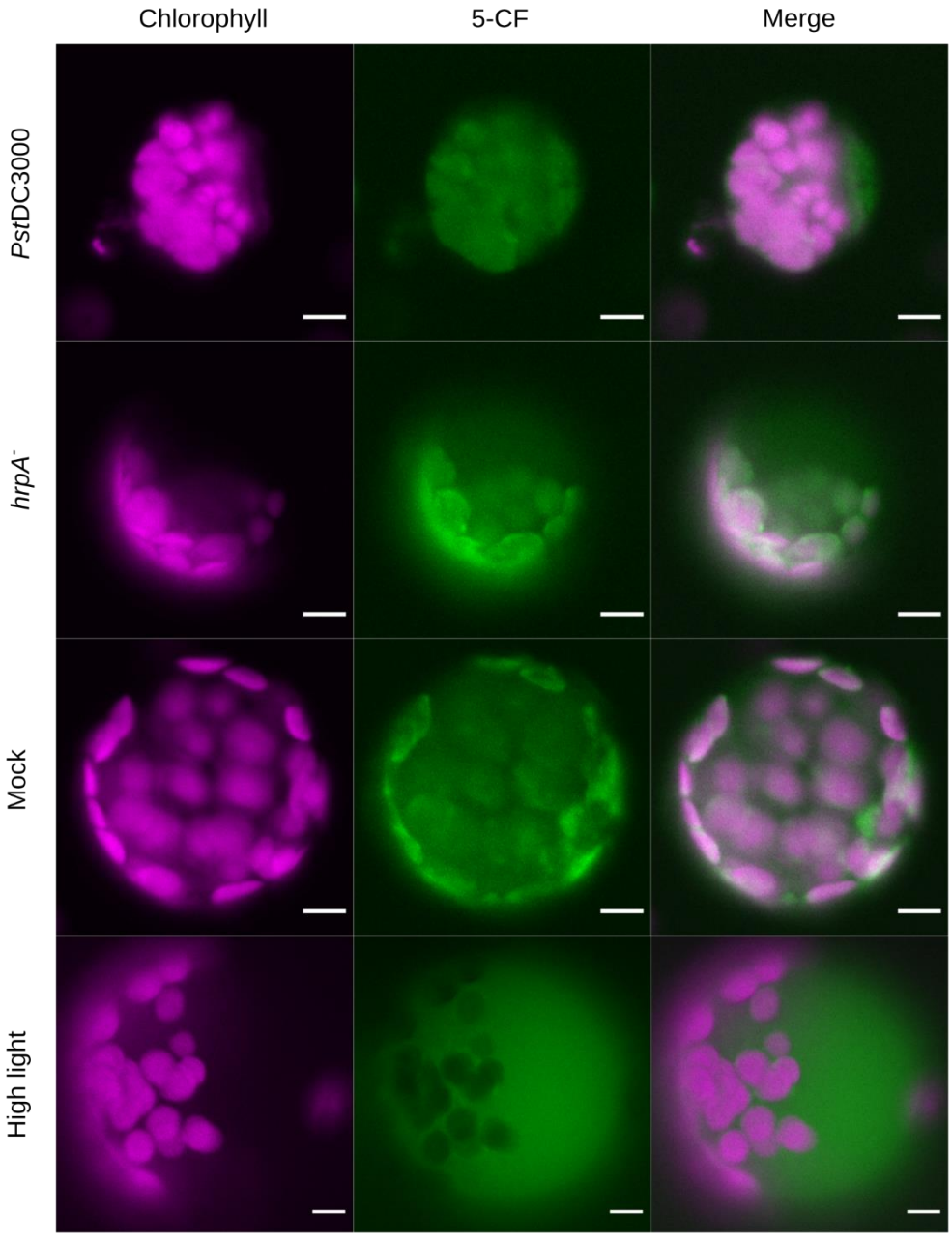

Figure 3.3 Chloroplast membrane integrity is maintained after inoculation with either *Pst*DC3000 or *hrpA*$^{-}$.

Protoplasts were isolated from wild-type Arabidopsis leaves two days after infiltration with *Pst*DC3000, *hrpA*$^-$, or a mock inoculum, incubated with carboxyfluorescein diacetate (CFDA) then visualised by epifluorescence microscopy. CFDA is converted to fluorescent 5-carboxyfluorescin (5-CF) in chloroplasts only when they have retained membrane integrity. Chloroplast membrane damage and consequentially absence of 5-CF signal are typical of high-light stress, as shown here in protoplasts treated with 500 μmol m^{-2} s^{-1} actinic light for 10 minutes after isolation but before CFDA treatment. However, chloroplast 5-CF fluorescence was maintained in protoplasts from plants treated with *hrpA*$^-$ or *Pst*DC3000, as in protoplasts from mock-treated plants ($MgCl_2$), implying that chloroplast membrane integrity is not compromised during inoculation with either the pathogenic or non-pathogenic bacteria. Scale bars = 5 μm.

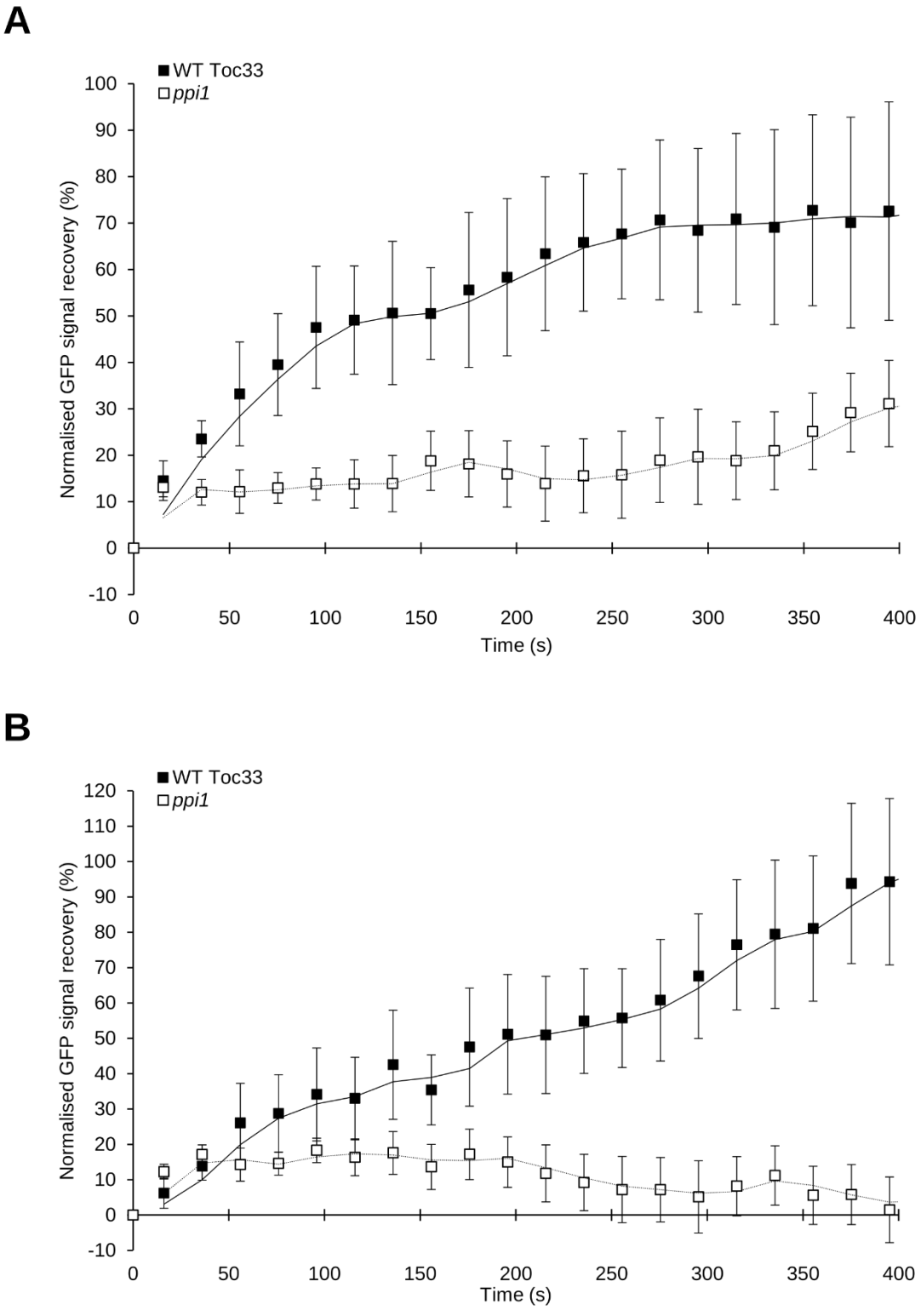

Figure 3.4 Effect of the *ppi1* mutation on chloroplast protein import as measured by fluorescence recovery.

Recovery of the cpGFP fluorescence signal in photobleached cells, normalised to unbleached cells, as a measure of chloroplast protein import rate. The cpGFP probe was analysed in both wild type (WT Toc33) and *plastid protein import 1* (*ppi1*) mutant backgrounds. Trend lines indicate the moving average for WT Toc33 (solid) and *ppi1* plants (dotted). 100% signal corresponds to the average normalised signal for 4-5 measurements taken 20 s apart before bleaching.

A. In seedlings, the fluorescent signal recovered in WT Toc33 cells much more quickly than it did in *ppi1* cells. Leaves from 10-day-old seedlings were analysed. Error bars indicate the SEM (n=4 from three biological replicates).

B. In mature rosette leaves, the fluorescent signal in *ppi1* did not appreciably recover over 400 seconds. Recovery was still observable in WT Toc33 cells. Leaves from 4-week-old plants were analysed. Error bars indicate the SEM (n=5 from three biological replicates).

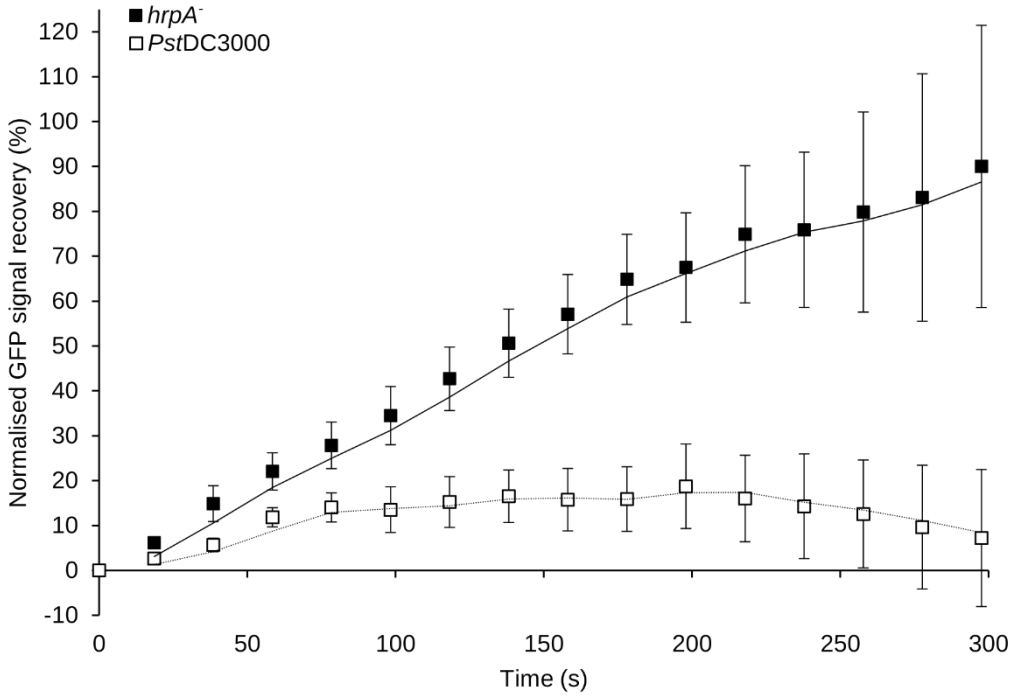

Figure 3.5 Rate of import during infection by *hrpA*⁻ or *Pst*DC3000 as measured by photobleaching.

Recovery of the cpGFP fluorescence signal in photobleached cells, normalised to unbleached cells, as a measure of chloroplast protein import rate. Trend lines indicate the moving average after *hrpA*$^-$ (solid) or Pst*DC3000* (dotted) inoculation. 100% signal corresponds to the average normalised signal for 4-5 measurements taken 20 s apart before bleaching. Fluorescence was seen to recover after infection with *hrpA*$^-$, but recovery was greatly reduced after infection with *Pst*DC3000. Error bars indicate the SEM (n=3).

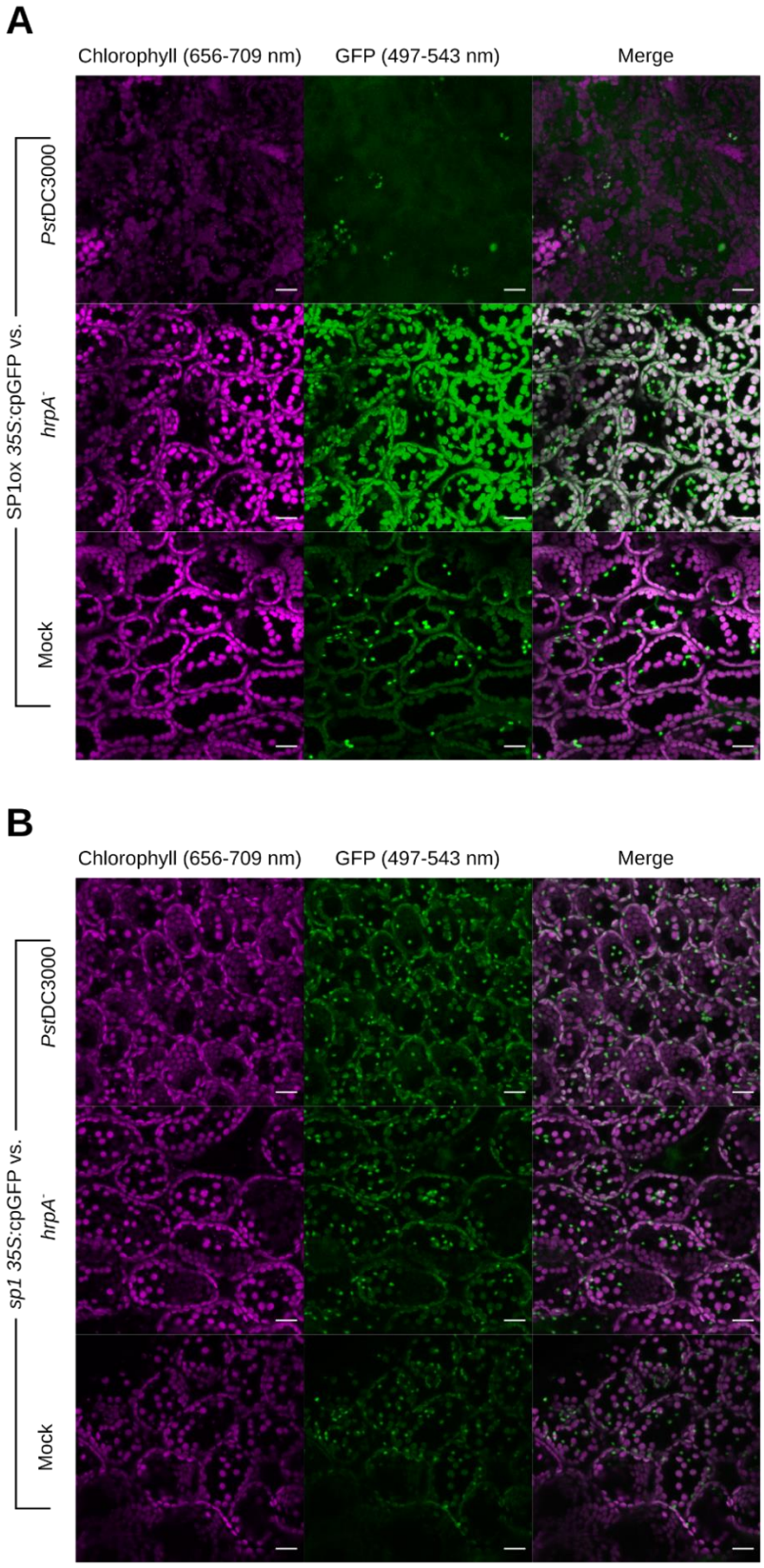

Figure 3.6 Localisation of the cpGFP probe during infection in the SP1ox and *sp1* backgrounds.

Maximum intensity Z-projections from plants expressing cpGFP two days after infiltration with *Pst*DC3000, *hrpA*$^-$, or a mock inoculum ($MgCl_2$). Scale bars = 20 μm.
A. *Pst*DC3000 induces mislocalisation of the GFP probe in the SP1ox background. As in the wild type (**Figure 3.1**, p.129), cpGFP accumulated outside the chloroplasts in SP1ox plants two days after infection with *Pst*DC3000. After infection with *hrpA*$^-$, the cpGFP probe still appeared in the chloroplasts, but also occurred in a halo around the chloroplasts (see detail in **Figure 3.7** p.141; cf. early stages of mislocalisation during *Pst*DC3000 infection of wild-type, shown in **Figure 3.2A&D**, p.131).
B. Localisation of the GFP probe in the *sp1* background is not altered during infection with either strain of bacteria. In *sp1* mutant plants, cpGFP retained chloroplast localisation two days post inoculation with *Pst*DC3000 and *hrpA*$^-$.

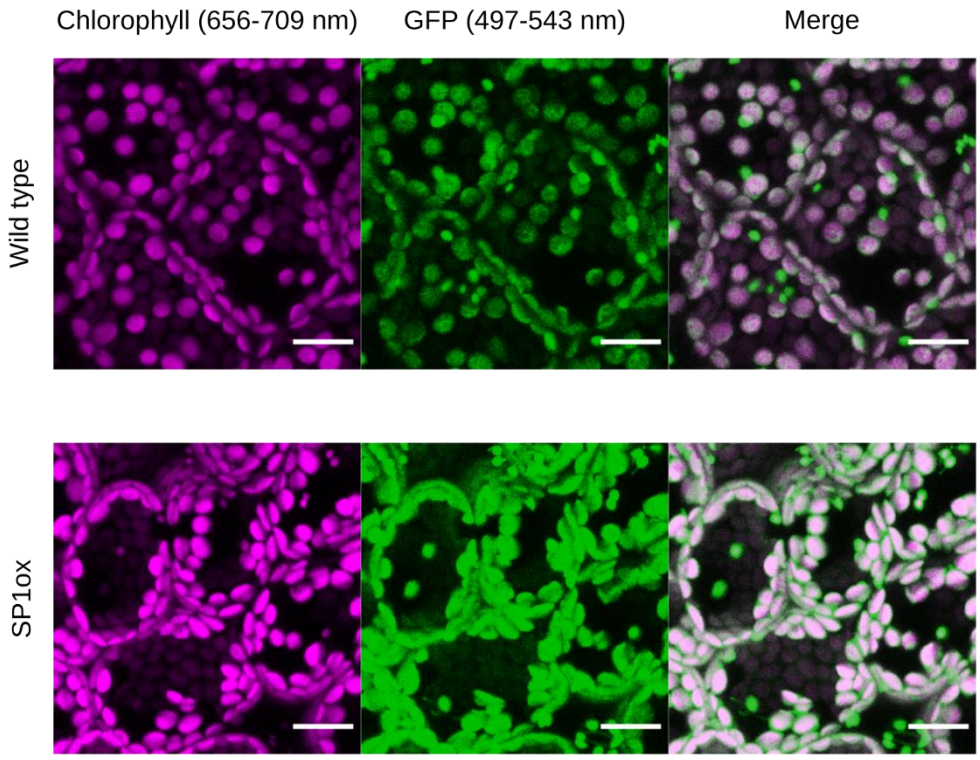

Figure 3.7 The 'halo' appearance of the cpGFP fluorescence signal in SP1ox plants.

Detail showing cpGFP localisation two days after *hrpA*$^-$ inoculation in the wild-type and SP1ox plant backgrounds.
The cpGFP probe accumulated in the chloroplasts, as shown by co-localisation with the chlorophyll signal, in wild-type plants after inoculation with *hrpA*$^-$. In similarly inoculated SP1ox plants, in addition to the fluorescence signal colocalising with the chlorophyll signal, a distinctive 'halo' phenotype was seen around the periphery of chloroplasts, suggesting partial retention of the probe in the cytosol.
The data shown are maximum intensity Z-projections. Scale bar = 20 μm.

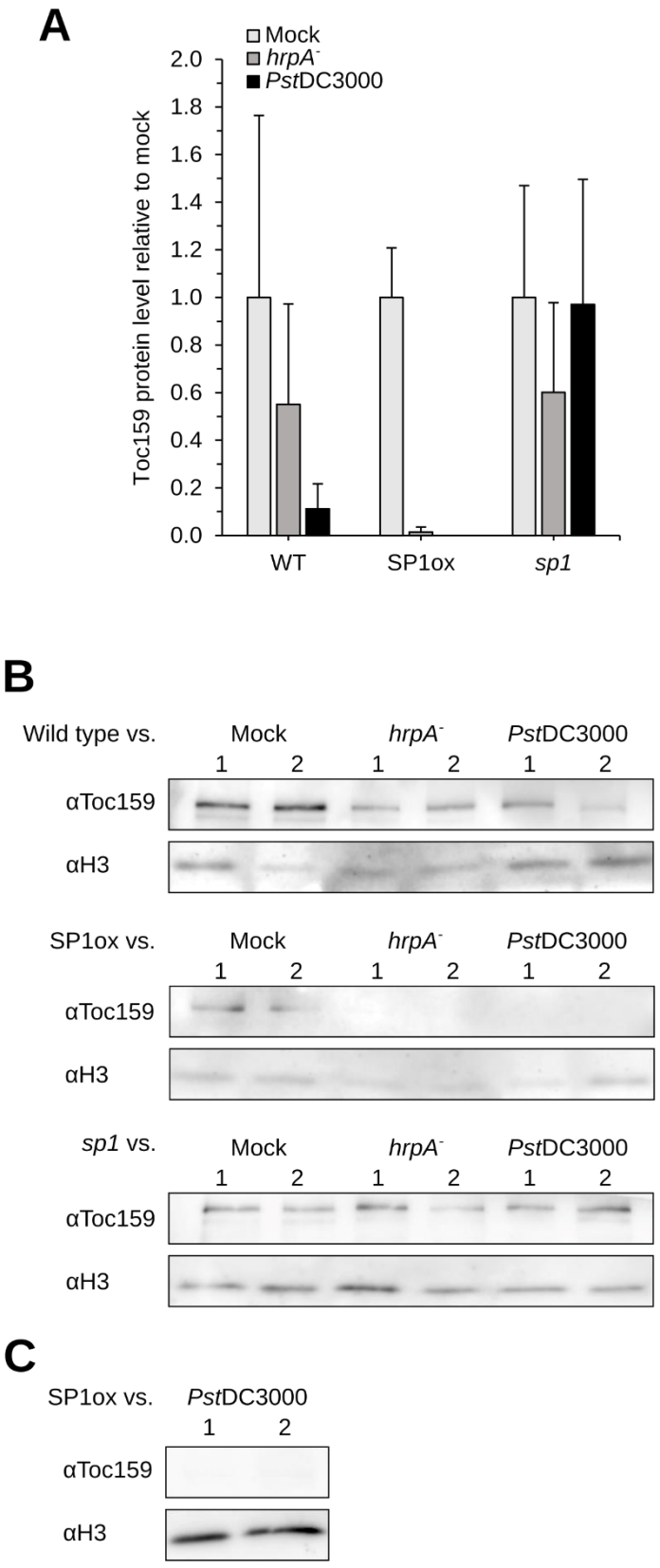

Figure 3.8 Regulation of Toc159 protein levels during infection.

A. Toc159 protein levels are reduced upon infection in an SP1-dependent manner. Toc159 abundance in the indicated genotypes, two days after different bacterial inoculations, was analysed by immunoblotting. The bands were quantified and normalised to equivalent histone 3 (H3) data, and then expressed relative to the corresponding mock infiltration value (set to 1). The data show that Toc159 was reduced after inoculation with *hrpA*$^{-}$, relative to mock inoculation, in each plant line, but most strongly so in SP1ox. Toc159 abundance was further reduced by *Pst*DC3000 infection in wild-type plants, and more strongly so in SP1ox plants; but it was unchanged by inoculations in *sp1*. Error bars indicate the SD, n=2.
B-C. Membrane images from A., showing anti-Toc159 (αToc159) and anti-H3 (αH3) bands for two biological replicates. The protein samples were from wild-type, SP1ox, and *sp1* plants. The plants had been infiltrated with *hrpA*$^{-}$, *Pst*DC3000, or a mock inoculum. Toc159 was undetectable in SP1ox after *Pst*DC3000 treatment (B). Even when the protein samples were overloaded, the Toc159 band was only barely detectable in SP1ox (**C**).

4.Photosynthesis during infection

4.1. Abstract

The chloroplast ROS burst, an event around six hours into infection, is an immunogenic signal that prevents infection by PTI-eliciting bacteria like *hrpA*$^-$. It is averted in part during infection by virulent *Pst*DC3000 in wild-type Arabidopsis, an effect that has previously been explained by disruption of photosynthesis. Based on chlorophyll fluorescence measurements, it was reported that *Pst*DC3000 effectors disrupt photosynthesis during infection by targeting PS II and promoting NPQ [253].

In one proposed explanation [253], here called the photochemistry efficiency model, *Pst*DC3000 increases NPQ, dissipating intercepted light energy as heat and preventing it from being used in ROS generation. An alternative explanation based on data presented in this thesis (**§§2-3**) is that changes to import reduce the total capacity for light interception and therefore ROS generation.

In this chapter, the reproduction of the chlorophyll fluorescence observations was attempted. The significance of chlorophyll fluorescence measurements is discussed, and the previously reported results are reinterpreted. It is argued that they do not show an increase in the dissipation of energy by NPQ or the reduction in the efficiency of photochemistry. Additionally, it is found that *Pst*DC3000 did not cause the reported changes to chlorophyll fluorescence parameters during normal incubation conditions. It is proposed that the previously observed effect was due to the disruption of circadian entrainment by the measurement technique used.

Therefore, the results described here and those previously reported are not consistent with a model in which *P. syringae* averts the chloroplast ROS burst during pathogenesis by lowering the efficiency of photochemistry. However, they do not preclude the possibility that the downregulation of photosynthesis overall, e.g. by reduction in import of photosynthetic precursors, reduces the rate of energy passed to ROS generation and therefore suppresses PTI.

4.2. Introduction

4.2.1. Photosynthesis

Chloroplasts are the site of photosynthesis, where light energy is converted into chemical energy for the plant. Photosynthesis consists of light-dependent "light reactions" and light-independent "dark" or "carbon reactions". Briefly, in the light reactions, light energy is intercepted at chlorophyll-containing photosystems and used to energise electrons. Starting at PS II, the electrons move along an electron transport chain, giving up some of their energy as they go, before reducing NADP+ to NADPH at the end of the chain. The energy they lose as they pass through the chain is used to create a proton gradient that drives the production of ATP from ADP. This is represented by the Z-scheme [375,376]. Later, in the dark reactions, the energy stored in ATP and NADPH is used to power the synthesis of carbohydrates from carbon dioxide by the enzyme Rubisco (in the Calvin cycle [377]).

When energy is absorbed by the photosystems, it may have one of three fates: it could be released as fluorescence, or be released as heat, or be used to energise electrons that are used in photochemistry. However, not all of the energised electrons will fully participate in the light reactions[6]. Some may instead react with molecular oxygen to produce radicals and ROS, including hydrogen peroxide. The photosynthetic production of hydrogen peroxide by the chloroplast was first recognised by Alan Mehler [378], after whom the reaction is sometimes named.

The tendency for photochemistry to create ROS instead of ATP and NADPH is a result of photon excess—where more light energy is intercepted than can be used in the light reactions—which is increased during times of stress [160]. ROS thus generated may

[6] For the sake of clarity, the phrase 'light reactions' will be used when necessary to distinguish the photochemistry that synthesises ATP and NADPH—i.e. what we typically mean by 'photosynthesis'—from the synthesis of ROS by light energy.

damage cellular components, or be scavenged by antioxidants or processes like the water-water cycle [160,171,172].

The photosynthetic production of ROS can be limited by reducing the transfer of light energy to electrons, thereby reducing photon excess. For example, if more of the intercepted light energy is dissipated as heat, less becomes available for photochemistry. Heat dissipation can be promoted by NPQ. The importance of NPQ as a photoprotective mechanism is clear in that it exists in some form in all clades of photosynthetic organisms; in the metaphyta it is regulated by the PS II subunit PsbS [379,380]. Dissipating more intercepted energy as heat lowers the rate at which the absorbed photons are used to energise electrons at PS II—that is, the quantum yield of PS II (ϕ_{PSII}) is reduced—and so less energy is available for ROS production or the light reactions.

4.2.2. Chlorophyll fluorescence

If not released as heat or used to energise electrons, the third fate for intercepted light energy is to be re-emitted as fluorescence. The measurement of chlorophyll fluorescence is a popular technique for inferring the activity of the photosystems [381–383]; in fact, NPQ was termed as such for its effect of quenching chlorophyll fluorescence.

The amount of chlorophyll fluorescence emitted from PS I that is shorter than 700 nm in wavelength is thought to be negligible, so filtering out fluorescence at longer wavelengths allows PS II fluorescence to be measured specifically. Many parameters can be derived from four measurements of fluorescence: before or after a saturating pulse of light, from leaves that are dark- or light-adapted. These respectively correspond to fluorescence when the PS II reaction centres are "open" (F_o) or "closed" (F_m) in dark adapted leaves, and "partially open/closed" (F') or "closed" (F'_m) in light adapted leaves. Fluorescence when PS II reaction centres are fully open in light-adapted leaves (F'_o) can also be recorded by first treating leaves with far-red light that specifically excites PS I [381].

This allows non-invasive and rapid monitoring of photosynthetic efficiency, including the quantum yield of PS II (ϕ_{PSII}), *NPQ*[7], and the maximum quantum efficiency of PS II (F_v/F_m, where F_v is the difference between F_o and F_m). F_v/F_m is a popular measurement as it is very responsive to stress treatment [381]: as a crude approximation, 81% of the 155 articles featuring F_v/F_m indexed by Web of Science in 2018 were about stress tolerance.

4.2.3. Photosynthesis during immunity

Chloroplasts have an important role in plant immunity, where they generate signals that promote immunity and disambiguate different immunity programmes [1,23,26,222,230,232–235]. Recently, a chloroplast ROS burst was identified as an early immunogenic signal [253]. In the infection of Arabidopsis by the non-pathogenic *hrpA*$^-$ mutant, which elicits PTI, a chloroplast ROS burst was found six hours post infection. The chloroplast ROS burst was suppressed in pathogenic *Pst*DC3000 infection, and chemical abrogation of the ROS burst enhanced the virulence of the *hrpA*$^-$ strain [253].

The report by de Torres Zabala *et al.* [253] proposed a mechanism by which the chloroplast ROS burst and PTI are suppressed by effector-driven reprogramming of photosynthesis. As *Pst*DC3000 but not *hrpA*$^-$ was found to target photosynthetic processes, in particular causing a decline in carbon assimilation and leaf F_v/F_m, the authors proposed that PS II is targeted by effectors to inhibit electron transport. Less energy is therefore available for either the light reactions or photosynthetic ROS generation.

The inhibition of electron transport could result from the activation of NPQ: de Torres Zabala *et al.* [253] also observed that *NPQ* transiently increased between four to ten hours post inoculation with *Pst*DC3000, which the authors interpreted as increased dissipation of excitation energy as heat. Here, the suppression of the ROS burst by effector-driven

[7] *NPQ*, in italics, here stands for the parameter calculated as $\frac{F_m}{F_m'} - 1$ [381], a non-linear estimation of non-photochemical quenching (given as NPQ in Roman type) which is different from the quantum yield of NPQ (see explanation in **§4.4.2**).

induction of NPQ, leading to reduced electron transport, is called the photochemistry efficiency model.

Alternatively, the inhibition of electron transport may reflect the suppression of photochemistry as a whole, rather than a change in the *efficiency* of photochemistry. Based on the results described in the previous chapters, the proposed function of SP1 during infection by *Pst*DC3000 is to lessen the chloroplast ROS burst (**§2**) by the suppression of chloroplast protein import (**§3**). In this model, as in the SP1 model of ROS avoidance during abiotic stress [165], the reduced import of photosynthetic apparatus preproteins reduces total photosynthesis: less energy is intercepted in the chloroplast and therefore less energy is available for photochemistry, either for the light reactions or for the generation of ROS.

A simple analogy can be made to throttling, a safety mechanism of a computer's central processing unit where its cycle frequency is reduced if the processor is inadequately cooled. Throttling reduces how much heat is generated, preventing the processor from overheating and suffering permanent damage, at the cost of lowering its capacity for processing. In SP1-mediated ROS avoidance, chloroplasts "throttle" photosynthesis to prevent ROS damage at the expense of photosynthetic productivity.

Hence, there are two possibilities for how *Pst*DC3000 accomplishes the suppression of the chloroplast ROS burst: either by reducing the efficiency of photochemistry, or by reducing photosynthesis as a whole. These raise the question of whether SP1 might in fact mediate ROS suppression through the NPQ mechanism instead.

In the following sections, the measurement of chlorophyll fluorescence to gauge photochemistry during infection are repeated, and important confounding factors in the experimental design are discussed. The photochemistry efficiency model is revisited, first *prima facie* and then in light of the new results. Finally, the consequences of these

arguments on the model that SP1 suppresses photosynthesis by the downregulation of import during disease are discussed.

4.3. Results

4.3.1. Changes to chlorophyll fluorescence during infection

Suppression of the chloroplast ROS burst had previously been attributed to changes in the efficiency of photochemistry. It was found to correlate with a transient induction of *NPQ* (see footnote p.149) concomitant with the a decline in F_v/F_m after inoculation with *Pst*DC3000 relative to *hrpA*$^-$ [253]. In this model, *Pst*DC3000 reduces photosynthetic efficiency to divert energy away from photochemistry, including both the light reactions and the photosynthetic generation of ROS including hydrogen peroxide.

To explore this model, the reproduction of the experiment in wild type Arabidopsis as described [253] over 20 hours post infection was attempted. The measurements for each time point were calculated from fluorescence measurements taken over a 59-minute cycle, which was repeated twenty times.

Values for F_v/F_m began to diverge between infection by *Pst*DC3000 and *hrpA*$^-$, although the magnitude of this effect was much lower than that described previously. In the experiment presented here, F_v/F_m was reduced by 6% relative to F_v/F_m in *hrpA*$^-$ after 17 hours, compared to an effect size of approximately 25% in the experiment reported previously (**Figure 4.1A**, p. 162; cf. figure 2c in [253]). *NPQ* also showed a similar transient increase following *Pst*DC3000 infection, but thereafter *NPQ* values continued to diverge over the course of the experiment (**Figure 4.1C**, p. 162; cf. figure 2g in [253]).

However, the quantum yield of PS II (ϕ_{PSII}) measurements after *Pst*DC3000 and *hrpA*$^-$ inoculation did not begin to diverge, unlike in the previously reported experiment where they began to diverge after 15 hours (**Figure 4.1E**, p. 162; cf. figure 2e in [253]).

4.3.2. Frequency of chlorophyll fluorescence measurements affects photochemistry during infection

When taking measurements hourly as above, the infected plants must be kept in the measurement chamber for the course of the experiment. To collect light- and dark-adapted fluorescence measurements, each cycle of measurements involves 39 minutes of illumination followed by 20 minutes of darkness. This is repeated every hour. Consequently, the plants experience unusual incubation conditions.

In order to control for this, wild-type plants were treated with bacteria as above, and then only three cycles of measurements were made: at the beginning of the time course, after seven hours (when *NPQ* was reported to have peaked in [253]), and after 24 hours. Between measurements, plants were returned to long day (16 hours light, 8 hours darkness) conditions.

These plants showed no divergence in F_v/F_m, ϕ_{PSII}, or induction of *NPQ* over 24 hours with respect to either inoculum or the first time point (**Figure 4.1B**, **D, & F**, p. 162). This suggests that such changes in infection as were previously reported are caused by the unusual lighting conditions inherent in taking repeated light- and dark-adapted fluorescence measurements.

4.4. Discussion

4.4.1. The efficiency of photochemistry during infection

Here and in §§**4.4.2-4.4.4**, the interpretation of the previously published observations, the replication of which was attempted in **Figure 4.1A**, **C**, & **E**, p.162, will be discussed *prima facie*. Then in §**4.4.5**, the implications of the further experiments, in **Figure 4.1B**, **D**, & **F**, p.162, will be discussed.

In the photochemistry efficiency model, suppression of the chloroplast ROS burst is attributed to the inhibition of photosynthetic electron transport by NPQ [253]. This accorded with the observation that infection of Arabidopsis with *Pst*DC3000, but not *hrpA*$^-$, caused a decline in F_v/F_m beginning around six hours after infection concomitant with induction of *NPQ* [253].

The crux of the proposed [253] photochemistry efficiency model is that NPQ reduces the rate at which photons are used for photochemistry. This would be reflected in a fall in ϕ_{PSII}[8] . However, this is not the case. ϕ_{PSII} did not fall following infection by *Pst*DC3000 relative to *hrpA*$^-$ either until 15 hours post infection (in the previously reported results)—well after the ROS burst is timed, and after the transient increase in *NPQ* had elapsed—or at all (in the results presented here; see figure 2e in [253], where ϕ_{PSII} is labelled as F'_q/F'_m and **Figure 4.1E**, p. 162). In fact, in both experiments, and in infections with both strains, ϕ_{PSII} remained fairly stable.

Therefore, as the rate of energy being passed into photochemistry is unchanged, there cannot be an increase to the amount of energy being dissipated as heat during this stage of pathogenesis. The efficiency of photochemistry does not become downregulated and so NPQ cannot be the mechanism by which the ROS burst is averted.

---

8 which may be calculated [381] for light-adapted leaves from the fluorescence before (F') and after (F'_m) the saturating flash as, $\phi_{PSII} = \frac{F'_m - F'}{F'_m} = \frac{F'_q}{F'_m}$

4.4.2. Significance of the *NPQ* parameter

This may seem to contradict the changes in the *NPQ* parameter (see footnote p.149), which appear to report that NPQ is induced transiently within the first seven hours of inoculation with *Pst*DC3000. However, care must be taken not to overinterpret this parameter, and it is not appropriate to use here due to confounding changes F_v/F_m.

NPQ is not a measurement of the rate at which photon energy at PS II becomes dissipated as heat. That would be the quantum yield of NPQ, which can be described as the sum of two other parameters that are mathematically distinct from *NPQ*. These are the quantum yield of light-induced (or regulated) NPQ (ϕ_{NPQ}), and the quantum yield of non-light-induced (or non-regulated) NPQ (ϕ_{NO})[9], which is also known as non-regulated energy dissipation [381–383]. Biologically speaking, ϕ_{NPQ} represents energy lost as heat due to the protective and reversible inhibition of photochemistry as mediated by PsbS, and ϕ_{NO} represents constitutive energy losses to heat due to damage and photoinhibition.

Instead, the parameter of *NPQ* is a non-linear estimation for the change in the rate constant for decay by heat loss (at PS II) between light and dark adaptation. As it compares the maximal fluorescence in dark and light adapted plants, it can only be compared for leaves that have similar dark-adapted fluorescence character (that is, similar F_v/F_m) [381]. This is not the case during infection by *Pst*DC3000 compared to infection by *hrpA*$^-$, or indeed for the same leaf in *Pst*DC3000 infection over time, and so *NPQ* is not an appropriate parameter to use here.

[9] The fluxes ϕ_{PSII}, ϕ_{NPQ}, and ϕ_{NO} combined account for the entire quantum yield of intercepted light. Therefore, ϕ_{NPQ} may be determined [381,383], where F is fluorescence from dark-adapted leaves, F' is fluorescence from light-adapted leaves, m is maximum fluorescence, o is minimum fluorescence, v is the variable fluorescence ($m - o$), and q is the quenched fluorescence ($F'_m - F'$), as, $\phi_{NPQ} = 1 - \frac{F'_q}{F'_m} - \frac{1}{\frac{Fm-F'_m}{F'_m}+1+\frac{F'_q}{F'_v}\times\frac{F'_o}{F'}\times\left(\frac{Fm}{Fo}-1\right)}$ i.e. $\phi_{NPQ} = 1 - \phi_{PSII} - \phi_{NO}$

Furthermore, even were ϕ_{PSII} to show changes during the early stages of infection, Baker [381] advises that,

> "changes in *NPQ* do not allow evaluation of the proportion of changes in PS II operating efficiency [ϕ_{PSII}] that are attributable to changes in nonphotochemical quenching."

Therefore, it is not correct to say that the changes in *NPQ* reflect that NPQ is induced and more excitation energy becomes dissipated.

The designation of this parameter as "*NPQ*", while it does differentiate it from other fluorescence measurements like F_v/F_m, may itself cause confusion. In this author's opinion, the parameter should be referred to as "$\frac{F_m}{F'_m} - 1$", as "*NPQ*" gives the false impression that it is a direct measurement of NPQ or equivalent to ϕ_{NPQ} (or to the sum of ϕ_{NPQ} and ϕ_{NO}).

4.4.3. Significance of F_v/F_m as a stress measurement

It is helpful to clearly demark the difference between ϕ_{PSII} and F_v/F_m. Although F_v/F_m is often reported as the "photosynthetic efficiency", it is an estimate of the *maximum* possible quantum yield of PS II, measured from dark-adapted leaves: under normal light conditions, ϕ_{PSII} would be much lower than this upper limit anyway, so when F_v/F_m decreases, this is not necessarily reflected in the efficiency of the photosynthesis being carried out by the plant [381]. Thus, ϕ_{PSII} is a more appropriate measurement of how efficiently light energy actually becomes apportioned for photochemistry.

Nevertheless, F_v/F_m declines during *Pst*DC3000 infection, which does imply that there is some interaction with photosynthesis. F_v/F_m is a popular chlorophyll fluorescence parameter to measure as it is very responsive to many abiotic and biotic stresses. However, its significance is at risk of being overplayed. Reduction in F_v/F_m cannot be attributed to a

specific biological cause, and may reflect changes to a number of factors including NPQ, photoinhibition, and oxidative damage to PS II [381].

In this case, the fall in F_v/F_m could simply be attributed to pathogen-induced cell damage caused by the virulent *Pst*DC3000 strain, but not by the *hrpA*$^-$ bacteria. In a study from Bonfig *et al.* [384] on the effects of *Pst* on photosynthesis, F_v/F_m was also reduced in infection by both *Pst*DC3000 and avirulent *Pst*DC3000 *avrRpm1*$^+$ (inducing ETI) after 48 hours. This, and an increase in ϕ_{NO} flux, was attributed to irreversible cellular damage and programmed cell death that preceded chlorosis visible to the naked eye.

4.4.4. Role of NPQ in virulence

It is surprising that the rate of NPQ does not increase (that is, ϕ_{PSII} does not fall) during the aversion of the ROS burst in *Pst*DC3000 infection. As it was shown that plants downregulate the expression of NPQ initiator *PsbS* when flg-22 is perceived [193], there was good reason to believe that NPQ might antagonise immunity. If this is so, then it is conceivable that it might be promoted during ETS.

However, it is uncertain if a reduction in NPQ necessarily promotes immunity. When the Arabidopsis *npq1 npq4* double mutant, which has constitutively low NPQ, is treated with flg-22, it shows stronger expression of two defence-related transcription factors, *WRKY2* and *WRKY29*, but shows abolished expression of two others, *PATHOGENESIS RELATED 1* and *5* [193]. This implies that the suppression of NPQ could reduce immunity or alter its specificity.

Furthermore, in the study by Bonfig *et al.* [384], ϕ_{NPQ} was reported to be reduced after either infection with *Pst*DC3000 (i.e. in ETS) or *Pst*DC3000 *avrRpm1*$^+$ (i.e. in ETI). Consequently, suppression of NPQ may in fact be inconsequential to the induction of PTI, ETS, and ETI. The importance of NPQ in stress-aversion is unequivocal, but whether it has a role in biotic stress tolerance still requires clarification.

4.4.5. Reported changes to photosynthetic parameters during disease may represent loss of circadian entrainment

An unintended interaction between the experimental method and plant immunity may preclude interpretation of the observed changes in F_v/F_m during infection in relation to infection by *Pst*DC3000.

The changes to chlorophyll fluorescence parameters could only be seen when measuring hourly, which required rapid cycling of dark and light incubation periods, and not when plants were incubated in normal growth conditions (**Figure 4.1B** & **D**, p. 162).

Lighting periodicity is important for entraining and resetting the plant circadian clock [385]. Several aspects of plant immunity are now accepted to be under circadian control [386]. For instance, pattern recognition genes *FLS2* and *EF-TU RECEPTOR* are more strongly expressed in the circadian morning [387]. This has an appreciable effect on the induction of PTI: Arabidopsis induces PTI-related transcription factor *WRKY29* and callose deposition more strongly when infected with *hrpA*$^-$ in the circadian morning than in the evening [387]. Both overexpression lines for, and the double mutant of, the circadian clock regulators circadian clock associated 1 (CCA1) and late elongated hypocotyl (LHY) have greater susceptibility to *P. syringae*, suggesting maintaining periodicity is important for immunity [388]. Additionally, infection by *P. syringae* in wild-type Arabidopsis acts to shorten the circadian period, perhaps by targeting the circadian oscillator glycine-rich RNA binding protein 7 (which acts downstream of CCA1 and LHY) with the effector HopU1 [388,389].

As the act of measuring F_v/F_m hourly necessitates rapid cycling of lighting conditions and bright measurement pulses, we can expect it to disrupt circadian entrainment (e.g. [390]), which is at the least beneficial to *P. syringae* and may be a goal of the infection programme. This could inadvertently enhance virulence and result in a disease phenotype not typical of infection with a given concentration of bacteria in normal growth conditions. Indeed,

plants measured in this analysis did appear to have more advanced disease symptoms after 24 hours than plants kept in normal conditions (data not shown). It is also worth mentioning that dark treatment increases the virulence of both strains of bacteria (compare **Figure 2.1A**, p.95 to **Figure 2.7A**, p.107).

4.4.6. Pathogenesis suppresses photosynthesis but does not alter the efficiency of photochemistry

The evidence previously reported [253] and repeated here is not consistent with the hypothesis that *Pst*DC3000 suppresses the efficiency of photochemistry during the early stages of infection. There is no reduction in ϕ_{PSII} during the critical period, indicating that energy is passed into photochemistry at the same rate after inoculation and there is no increase in the rate it is dissipated as heat (**§4.4.1**). The measurement of parameter *NPQ* is confounded by changes to the dark-adapted character of the leaf, F_v/F_m (**§4.4.2**), the changes to which may only represent cellular damage caused by the pathogenic strain but not the non-pathogenic strain (**§4.4.3**). Therefore, pathogen-induced reduction to the efficiency of photochemistry cannot be the cause of the suppression of the chloroplast ROS burst or consequently of PTI by *Pst*DC3000.

It may now have been established to the reader's satisfaction that there is no evidence that *Pst*DC3000 reduces efficiency of photochemistry, or indeed that chlorophyll fluorescence measurements taken in rapidly cycling light conditions may not be biologically relevant at all. However, it is important to emphasise that this does not mean that photosynthesis is not affected by pathogenesis, nor does it contradict the evidence for the chloroplast ROS burst.

Firstly, de Torres-Zabala *et al.* [253] also observed, under continuous light conditions, that carbon dioxide assimilation was reduced by *Pst*DC3000 relative to *hrpA*$^-$ at six hours post infection. As this was not alleviated by increasing carbon dioxide partial pressure,

the authors ruled out changes to stomatal conductance [253]. Therefore, pathogenesis must impair the light or dark reactions of photosynthesis.

Secondly, although ϕ_{PSII} can tell us something about the efficiency of photochemistry in the leaf, it cannot tell us how much of the energy being passed on from PS II is used for ROS production later on in the electron transport chain (this is also why ϕ_{PSII} is not reduced by the generation of ROS six hours after inoculation with *hrpA*$^-$). Indeed, the inability to untangle the productive light reactions from ROS generation has limited the utility of fluorescence measurements in the monitoring of plants in the field, where they are exposed to many stresses [391]. The similarity of ϕ_{PSII} between *Pst*DC3000 and *hrpA*$^-$ infection does not contradict the observation of a chloroplast ROS burst in response to the latter only. The question therefore remains as to how *Pst*DC3000 abrogates the chloroplast ROS burst.

The reduction in carbon dioxide assimilation during infection with *Pst*DC3000 [253] could be accounted for by a. a reduction in photochemistry efficiency e.g. by induction of NPQ; b. a reduction in the amount of light intercepted; or c. a decline in the productivity of the Calvin cycle (e.g. due to downregulation of the enzyme Rubisco).

In the first case, as discussed, the fall in carbon dioxide assimilation cannot be attributed to a reduction in photochemistry efficiency as ϕ_{PSII} does not fall over the relevant time period. In the second case, if the photosystems are operating at an unchanged efficiency but there are fewer of them, the amount of energy passed on to photochemistry would be reduced. This might occur for instance if the supply of chlorophyll biosynthetic enzymes or electron transport system components was restricted by downregulation of their expression or chloroplast import. In the context of ROS generation, this would function to reduce the photon excess. This is consistent with the proposed SP1 ROS-avoidance model of virulence.

Regarding the third possibility, involving downregulation of the dark reactions, it is noteworthy that the small subunit of Rubisco is imported into the chloroplast by the canonical TOC-dependent pathway that is subject to regulation by SP1 [126].

If less light energy is intercepted by the photosystems, then less photochemistry—both light reactions and ROS synthesis—would occur. This would not be reflected in the value of ϕ_{PSII}: the proportion of intercepted light energy which energises electrons for photochemistry would not change. Therefore, the observation that ϕ_{PSII} is static and carbon assimilation declines after *Pst*DC3000 inoculation is consistent with the model that *Pst*DC3000 induces the reduction of total photosynthesis, as in SP1-mediated ROS avoidance [165], to achieve pathogenesis.

Finally, *Pst*DC3000 was reported to cause extensive transcriptomic changes and in particular the suppression of NECGs associated with photosynthesis. Photosynthesis-associated NECGs were suppressed in both *hrpA*$^-$ and *Pst*DC3000 infection relative to mock infiltration, but they were more strongly suppressed by *Pst*DC3000 by 12 hours post-infection. This suggests that in the longer term, *Pst*DC3000 suppresses photosynthesis transcriptionally, but must use another mechanism to suppress photosynthesis and the chloroplast ROS burst at six hours post infection. Something remarkably similar occurs in the case of ROS avoidance during abiotic stress: SP1 acts to suppress photosynthesis in the short term after stress exposure, with longer term stress exposures causing transcriptional downregulation of photosynthesis-associated NECGs [128]. Additionally, impaired photosynthetic preprotein import is known to downregulate photosynthesis-associated NECG expression by retrograde signalling, for example as in the *ppi1* mutant [37,127], which suggests that the inhibition of protein import by SP1 may itself assist *Pst*DC3000 in transcriptional reprogramming.

4.5. Figures

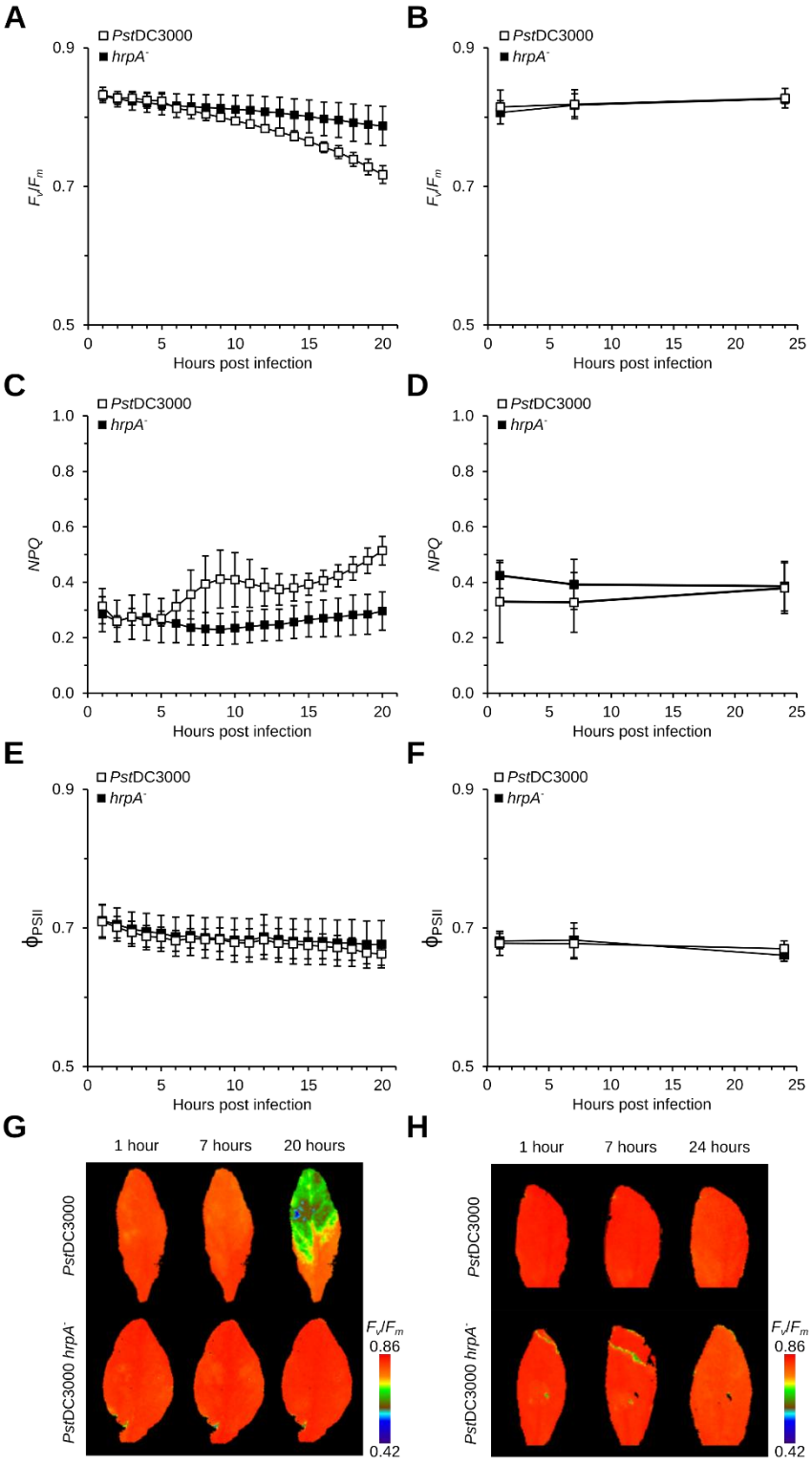

Figure 4.1 Measurements of chlorophyll fluorescence parameters during infection may be influenced by incubation conditions.

Chlorophyll fluorescence parameters in wild-type plants infected with *Pst*DC3000 or *hrpA*$^-$ (0.5×10^8 CFU mL^{-1}) were recorded. Plants in panels on the left (**A**, **C**, **E**, & **G**) were measured hourly, undergoing repeated cycles of 20 minutes darkness and 39 minutes light in the measurement chamber. Plants in the panels on the right (**B**, **D**, **F**, & **H**) were measured only three times, at the start of the experiment, once during the experiment (to coincide with the timing of the chloroplast ROS burst), and at the end of the experiment; in between measurements they were kept under long-day conditions.

A-B. Measurements of the maximum quantum efficiency of PS II (F_v/F_m). The F_v/F_m parameter responded more strongly to pathogenic *Pst*DC3000 infection than to non-pathogenic *hrpA*$^-$ infection, as has previously been reported [253], when the plants were exposed to short light cycling conditions (**A**), but did not when they are kept under long-day conditions (**B**). Error bars indicate the SD (n=3).

C-D. Measurements of non-photochemical quenching as estimated by (F_m/F'_m) – *1* (*NPQ*). The *NPQ* parameter increased following *Pst*DC3000 infection but not *hrpA*$^-$ infection, as has previously been reported [253], when the plants were exposed to rapid light cycling conditions (**C**), but did not when they were kept under long-day conditions (**D**). Error bars indicate the SD (n=3).

E-F. Measurements of the quantum yield of photosystem II (ϕ_{PSII}). Infection with neither *Pst*DC3000 nor *hrpA*$^-$ elicited an apparent change in ϕ_{PSII}, irrespective of the incubation conditions. Error bars indicate the SD (n=3).

G-H. Heat map images of the maximum quantum efficiency of PS II (F_v/F_m). Typical leaves inoculated with *Pst*DC3000 or *hrpA*$^-$ were imaged for F_v/F_m at the indicated time points, and representative examples are shown. The images reflect the data shown in **A** and **B** respectively.

5.Metabolic changes during infection

Contributions

Metabolite extraction, liquid chromatography, and mass spectrometry analysis were performed by Dr David Hauton, who also identified the metabolites and performed the initial statistical analysis which forms the basis for **Figure 5.1**, **Table 5.1**, and **Table 5.2**.

5.1. Abstract

In the previous chapters, the *sp1* mutation was found to heighten resistance to *P. syringae* by preventing the suppression of an early immunogenic signal, the chloroplast ROS burst, which *P. syringae* may suppress by using SP1 to downregulate chloroplast protein import. However, questions remain as to how the chloroplast ROS burst becomes integrated with the programme of immunity, and what other effects the regulation of chloroplast protein import may have.

In this chapter, the metabolome of wild-type and *sp1* Arabidopsis during infection is explored. Metabolites from leaves after infiltration with *Pst*DC3000 (causing disease), *hrpA*$^{-}$ (causing immunity), or a mock inoculum were extracted and analysed by liquid chromatography-mass spectrometry. Using two forms of chromatography, over 8,000 metabolites were detected.

The data indicated that the enhanced immunity of *sp1* relative to wild type is not mediated via changes in the levels of the classical immunity phytohormones salicylic acid (SA) or jasmonic acid (JA). However, the *sp1* mutation did affect levels of *myo*-inositol, which may lead to increased sensitivity to SA.

Glycerol-3-phosphate was also affected by *sp1* during disease. This suggests that lipid signalling may help to relay the oxidative burst. Additionally, the *sp1* mutation may alter the distribution of different fatty acids, which has previously been implicated in immunity.

Surprisingly, the metabolic signature of PTI, in either wild type or *sp1*, is entirely encompassed within the corresponding ETS metabolic signature, suggesting that the plant and the pathogen do not compete over the same metabolites. The data allowed a key set of metabolites that are associated with the success or failure of the chloroplast ROS burst to be identified.

5.2. Introduction

5.2.1. Transmission of redox signalling

In **§2**, SP1 was found to antagonise immunity and the chloroplast ROS burst, which is thought to be a key early immunogenic signal. It was determined that during pathogenesis, *Pst*DC3000 suppresses chloroplast protein import in an SP1-dependent manner (**§3**). This can suppress photosynthetic ROS production in the chloroplast by the downregulation of photosynthesis (**§4**). Lacking this mechanism, the *sp1* mutant displays an immune response that is more robust: *sp1* plants show greater resistance to *P. syringae* and can generate the chloroplast ROS burst even during *Pst*DC3000 infection.

However, it is yet to be determined how the chloroplast ROS burst signal integrates with the plant immune programme. While it has been shown that hydrogen peroxide from the chloroplast can be transported directly to the nucleus to regulate the hypersensitive response, this transport takes place via stromules that bridge the chloroplast and nucleus and are only induced in ETI (as elicited by avirulent bacteria like *Pst*DC3000 AvrRpm1 or *Pst*DC3000 AvrRps4 which express effectors that the plant can recognise [370]). They are not seen in mesophyll cells during PTI or ETS [370] (see also **Figure 3.1**, p.129). Instead, the chloroplast ROS burst could be communicated to the nucleus indirectly. Indirect ROS signalling molecules could arise from chloroplast components that have become oxidised (e.g. β-cyclocitral signalling arises from the antioxidant activity of carotenoids [20]) or from the activity of redox-sensitive proteins [392].

A protein's activity may be regulated by a number of post-translational redox modifications. Cysteine residues especially can be modified in multiple ways depending on the degree of oxidation [392]. There are several examples of immunity-related proteins that have redox-sensitive activity; for example, S-nitrosylation of the immunity transcription factor TGA1 (named for binding to TGACG sequences) enhances its binding activity [392]. Post-translational redox modification may also alter protein

localisation; for example, reduction or oxidation of cysteine residues in NPR1 regulates its localisation to the cytosol or nucleus, respectively [392]. Oxidative modification of proteins in immunity may be extensive: a recent proteomics study identified over 800 redox-sensitive proteins associated with ETI [393].

Alternatively, a change in the chloroplast redox state may become reported to the nucleus by inhibition or enhancement of other chloroplast signalling pathways. The two classical immunity regulators, the phytohormones JA and SA, are both synthesised by pathways that cross the chloroplast. They are thought to promote immunity to necrotrophs and biotrophs, respectively, and to antagonise each other, at least in PTI [1]. It is already thought that cellular ROS production and phytohormone signalling interact: SA production and ROS production may drive each other in a positive feedback loop, while high and low concentrations of JA may promote or antagonise ROS generation, respectively [394]. Treatment with JA or SA also affects the cellular glutathione pool, respectively reducing or increasing both the amount of glutathione and the ratio of reduced to oxidised glutathione [392]. Additionally, two other chloroplast metabolites, MEcPP and PAP, have recently been identified to act as retrograde signals that interact with JA, SA, and redox signalling pathways [23,26,395].

5.2.2. Metabolomics

In this chapter, the metabolomes of *sp1* and wild-type plants after inoculation, as determined by liquid chromatography-mass spectrometry (LC-MS), are analysed to address whether the enhanced immunity phenotype of *sp1* may be linked to changes in known plastid signals. In addition to measuring the abundance of specific compounds of interest, like JA and SA, the LC-MS analysis of whole plant leaf extracts allowed for the determination of a comprehensive leaf metabolome.

One challenge in metabolomics is that different metabolites have disparate physical properties. Ensuring that a metabolomics snapshot captures a large portion of the

metabolites in a sample often means employing multiple sample preparation techniques, such as different types of chromatography. An advantage of analysing the entire metabolome is that, by not presupposing what metabolites are critical to a phenotype, the analysis may generate interesting and unexpected leads.

The analysis of the whole metabolome may be particularly rewarding for the study of the nature of PTI and ETS. Whereas ETI is characterised by specific gene-for-gene resistance, where the immunity phenotype can arise from the possession of a single R gene; in PTI the strength of an immune response and whether a given biotic interaction results in pathogenesis, may depend on the cumulative actions of multiple plant and pathogen genes.

This leads to a continuum of immune responses of differing strength known as quantitative disease resistance. There is a renewed interest in quantitative disease resistance as crop breeders seek to enhance basal plant immunity (i.e. PTI), which has the benefits of being more broad-spectrum than ETI and, as a multi-locus trait, harder for a pathogen to overcome [396–398].

As it is a mutant with an enhanced immunity phenotype, *sp1* may be used to unravel the biochemical changes associated with immunity and susceptibility: for example, there might be certain critical metabolites that enhance PTI in *sp1* compared to the wild type, or certain metabolites that are only affected by ETS in the wild type and not in *sp1*. This could lead to promising new targets in the research of basal immunity.

Furthermore, the suppression of plastid protein import during ETS may not only suppress photosynthesis and the chloroplast ROS burst, but also the import of proteins involved in other metabolic pathways. As this suppression occurs in wild-type but not *sp1* plants, metabolomic differences between the two lines after *Pst*DC3000 inoculation may illuminate other alterations in the chloroplast metabolome associated with the suppression of import, thereby helping to illuminate the role of SP1 in disease.

5.3. Results

5.3.1. Identification of metabolites that are differentially abundant between *sp1* and the wild type

Several metabolites that are synthesised by pathways that pass through the chloroplast compartment have been associated with enhanced or impaired immune responses. By altering the chloroplast proteome, the activity of SP1 in impairing import could alter the synthesis of these metabolites. To explore this possibility, the metabolomes of *sp1* and wild-type leaves two days after infiltration with *Pst*DC3000, *hrpA*$^-$, or a mock inoculum were analysed by an LC-MS approach.

Samples were separated with two different types of chromatography: reverse phase chromatography, with a C_{18} column, and ion-exchange chromatography (also known as TCA chromatography as it is used for identifying tricarboxylic acid intermediates). A total of 5,430 metabolites were detected after C_{18} separation, and 2,597 metabolites were detected after TCA separation. The metabolites were identified by comparison with a database of standards and by cross-referencing with the Human Metabolome Database [399], which includes many compounds originating from plants in the human diet. It was only possible to positively identify a minority of the detected metabolites in this way (see below).

First, each compound was analysed to find those significantly differently abundant by ANOVA between the *sp1* and wild-type samples ($P<.05$). Tukey's honestly significant difference (HSD) test was then employed to determine between which inoculations the differences arose (**Table 5.1**, p.182). The majority of these differentially regulated metabolites were not positively identified, including those that showed the highest fold changes.

Several of the differentially regulated metabolites (**Table 5.2**, p.183) have been connected with immunity or stress response. Amongst those compounds identified were *myo*-inositol (**§5.4.1**) and glycerol-3-phosphate (discussed in **§5.4.2**), which are of interest to the effect of *sp1* in immunity as they are both known to be associated with immunity and the chloroplast (**Figure 5.1A&B**, p.184).

Several of the other differentially abundant identified compounds are known to be plant stress biomarkers (including pantothenic acid [400] and arabinonic acid [401]), or are associated with antioxidants and so might be connected to ROS overproduction in *sp1* (galacturonic acid is a precursor to ascorbic acid [402,403], while *para*-coumaric acid [404] and raffinose [405] are thought to have antioxidant activity themselves). *Myo*-inositol also contributes to the synthesis of raffinose and the related antioxidant galactinol [405].

Glucose, not sucrose, in the apoplast is the main source of energy for *P. syringae* [406]. Therefore, the lower levels of gluconic acid—the oxidation product of glucose—in *sp1* during *Pst*DC3000 infection probably does not represent a difference in Arabidopsis metabolism but reflects reduced bacterial growth, and therefore utilisation of glucose, in *sp1* leaves. Its production by *Pseudomonas* spp. can also act as an antifungal [407,408].

A previous study identified several metabolites that strongly discriminate the Arabidopsis PTI and ETS metabolomes early in infection (12 hours after inoculation with *hrpA*$^{-}$ or *Pst*DC3000) [409]. These include gluconic acid and raffinose, which have also been identified here as differentially abundant between *sp1* and the wild type. The alteration in the accumulation of these biomarkers caused by the absence of the *sp1* mutation is not unexpected given SP1's role in disease.

Surprisingly, at this time point there were no significant differences in the accumulation of JA or SA between the two lines (**Figure 5.1C** p.184). Although standards for MEcPP and PAP, two recently identified chloroplast retrograde signalling molecules which have

been linked to JA and SA cross-talk and signal induction [23,26], could be detected by the mass spectrometer, they were not detectable in the samples after either C_{18} or TCA chromatography.

The following analysis presented in **§§5.3.2-5.3.3** is based on only the TCA dataset.

5.3.2. Interactions between the metabolic phenotypes of the *sp1* mutation and inoculation

The entire TCA dataset was then examined to assess the scale of metabolomic reprogramming associated with *sp1* or with the different inoculations, and how many targets of the different reprogramming responses were shared.

Whether each factor—Arabidopsis line, inoculation, and the interaction of Arabidopsis line:inoculation—had a significant ($P<.05$) effect on the abundance of each metabolite was determined via regression analysis. The interaction of Arabidopsis line:inoculation signifies whether the difference in the abundance of a metabolite between *sp1* and wild type is dependent on the type of inoculation, i.e. if there is synergy. Even though many of the metabolites detected by LC-MS could not be identified as a particular compound, it is still possible to compare these metabolites across the different samples as they are uniquely distinguished in the dataset by their retention time (on the chromatography column) and their mass-charge ratio.

The number of metabolites in the TCA dataset found to differ with each factor are summarised in **Figure 5.2**, p.186. In total, 263 metabolites were found to differ based on the *sp1* mutation, corresponding to some 10.1% of all detected compounds. Of these, 83 differed only with respect to the *sp1* mutation and were not regulated during infection (group a in **Figure 5.2**, p.186). A total of 890 metabolites (34.3%) were found to differ with respect to the type of inoculation; these included metabolites that were up- or downregulated as part of resistance or susceptibility, or in response to either bacteria

relative to the mock infiltration. Of these, 500 differed only with respect to inoculation and not with respect to *sp1* (group c in **Figure 5.2**, p.186). This suggested that a large part of the metabolic changes brought on by bacterial inoculation was not affected by the *sp1* mutation (group c, 500 metabolites comprising 19.3% of all those detected).

A total of 430 metabolites (16.6%) were found to show synergistic differences with respect to Arabidopsis line:inoculation (with respect to the *sp1* mutation dependent on different inoculations). Not all of these metabolites also showed differences with respect to Arabidopsis line alone or inoculation alone. For 56 metabolites, differences between *sp1* and the wild type were entirely dependent on the different inoculation and *vice versa* (group e in **Figure 5.2**, p.186).

The abundances of another 46 metabolites were significantly different with respect to the *sp1* mutation and Arabidopsis line:inoculation (the difference caused by the *sp1* mutation significantly diverged in some inoculations) but did not show a difference between inoculations alone (group f in **Figure 5.2**, p.186); and the abundances of 256 others were significantly different with respect to inoculum and Arabidopsis line:inoculation (the difference between inoculations significantly diverged between *sp1* and wild-type plants) but did not show a difference between *sp1* and wild-type plants alone (group d in **Figure 5.2**, p.186).

Only 62 metabolites were significantly different with respect to inoculations and with respect to the *sp1* mutation, but did not differ with respect to Arabidopsis line:inoculation (group b in **Figure 5.2**, p.186). For these metabolites, the relative difference in abundance between *sp1* and wild type plants stayed the same even though the metabolite was significantly more strongly changed in some inoculations than others.

Finally, 72 metabolites were significantly different with respect to all factors: their abundance was changed by the *sp1* mutation and between certain inoculations, and the

effect on the metabolite under those inoculations was greater in one of the two genotypes (group g in **Figure 5.2**, p.186).

The 62 metabolites that were significantly different between both inoculation and the *sp1* mutation (group b) may represent pro-immunity or pro-susceptibility pathways that are already favoured or disfavoured by the *sp1* mutation, relative to the wild type. Intriguingly, the abundances of a further 328 metabolites (groups d and g) that are changed by bacterial inoculation show synergy with the *sp1* mutation. Biologically, these may be the result of pro-immunity or pro-susceptibility signalling that is more effective in *sp1* or wild-type plants.

5.3.3. Metabolic signatures of PTI and ETS

The LC-MS dataset also allowed differences in metabolism associated with PTI or ETS in *sp1* and wild-type Arabidopsis to be explored. This was of interest as it was envisaged that it could provide insight into the nature of the differences between pathogenesis and immunity programming.

Again using the TCA dataset, the differences between of metabolites that were increased or decreased between PTI and ETS were determined. Taking the metabolites that were significantly differently abundant between mock and *hrpA*$^{-}$ inoculation (for PTI) or mock and *Pst*DC3000 inoculation (for ETS), the fold up- or downregulation for each metabolite were determined for *sp1* and wild-type plants, separately.

First, metabolites regulated in the wild type were compared (**Figure 5.3**, p.188). All the metabolites that were regulated in PTI were also regulated in ETS (**Figure 5.3A**, p.188). During PTI, there were 69 metabolites upregulated and 67 downregulated, and during ETS, there were 188 upregulated and 176 downregulated (**Figure 5.3B**, p.188). Surprisingly, all the metabolites that are up- or downregulated in PTI were also respectively up- or downregulated in ETS. The metabolites that are regulated only in ETS

may be members of metabolic pathways that are disturbed by the suppression of plastid protein import by *Pst*DC3000.

Next, metabolites regulated in *sp1* were compared (**Figure 5.4**, p.190). As in the wild type, all the metabolites that were regulated in PTI were also regulated in ETS (**Figure 5.4A**, p.190). More metabolites were found to be regulated in *sp1* than in the wild type: 134 metabolites were upregulated and 158 metabolites downregulated during PTI, and 362 metabolites were upregulated and 397 metabolites downregulated during ETS (**Figure 5.4B**, p.190). Again, as in the wild type, all the metabolites that were up- or downregulated during PTI were also correspondingly up- or downregulated in ETS.

Then, the differences in the metabolite signatures of *sp1* and wild type were examined. There was surprisingly little overlap during PTI (**Figure 5.5A**, p.192). For most metabolites that were induced or repressed in PTI, the change only occurred in one of the genotypes. Only 23 metabolites were similarly changed in PTI in both *sp1* and wild type. Moreover, a small number of metabolites, 17, were regulated in opposite directions during PTI in *sp1* and the wild type (**Figure 5.5**, p.192).

In ETS, there was a greater degree of overlap than in PTI (22.5% regulated metabolites shared vs 10.3%) between the metabolite signatures of the two Arabidopsis lines type (**Figure 5.6A**, p.194). Interestingly, in addition to the 158 metabolites that were only regulated in the wild type, there were 82 metabolites that were regulated in opposite directions in *sp1* and the wild type (**Figure 5.6**, p.194). These are changes associated with ETS that require the SP1-dependent suppression of import.

If the 553 metabolites only regulated during ETS in *sp1* but not the wild type substantially overlapped with the metabolites associated with PTI in *sp1*, they might represent that a PTI-style response continues during ETS in *sp1*, caused by the failure to suppress import and the chloroplast ROS burst. Indeed, of the 553 metabolites regulated during ETS in

sp1 alone, 36.5% of those upregulated and 40.7% of those downregulated were also up- or downregulated respectively during PTI in *sp1*.

However, metabolites that were up- or downregulated during PTI for each genotype were found across all the different categories of ETS-associated metabolites (up- and downregulated in *sp1* or wild type). Similar proportions of metabolites that were regulated in ETS in both the wild type and *sp1* were also regulated during PTI in *sp1* (39.3% of those upregulated and 36.1% of those downregulated were also up- or downregulated during PTI in *sp1*). It does not appear to be the case, then, that the difference in ETS-associated metabolites between *sp1* and the wild type represents extensive conservation of the PTI response.

Furthermore, the PTI response is not especially more conserved during ETS in *sp1* than in the wild type: metabolites regulated during PTI in the wild type similarly appear across all the different categories of ETS-associated metabolites (up- and downregulated in *sp1* or wild type). Of the metabolites regulated during ETS in the wild type alone, 43.1% of those upregulated and 31.0% of those downregulated were also up- or downregulated respectively during PTI in the wild type. As in *sp1*, many metabolites that were regulated during ETS in both the wild type and *sp1* were also regulated during PTI in the wild type (26.2% of those upregulated and 52.5% of those downregulated were also up- or downregulated during PTI in the wild type).

Among the metabolites that are regulated in ETS only in the wild type and not in *sp1*, and those that are oppositely regulated during ETS in *sp1* and the wild type, may be compounds that form the basis of susceptibility to *P. syringae* following the disruption of chloroplast-mediated immune signalling.

5.4. Discussion

5.4.1. Phytohormones and *sp1*-mediated immunity

One of the surprising findings of the metabolomic analysis is that the mutation of *sp1* does not significantly alter the abundance of JA or SA. As the classical regulators of plant immunity, one might have expected SA and JA to be induced to higher and lower levels, respectively, during *sp1*'s heightened immune response. Unfortunately, with data from only one timepoint, it is impossible to visualise the dynamics of SA and JA accumulation after inoculation. This would potentially be informative, as it is possible that in *sp1*, SA accumulates faster than in the wild type and drives an earlier immune response, but by 48 hours post inoculation (the time-point measured here) this difference has disappeared.

Although *sp1* and the wild type do not differ in SA and JA accumulation, it is possible that they may still respond differently to phytohormone signalling. Mutant *sp1* plants have constitutively reduced (i.e. reduced in the mock infiltration) levels of *myo*-inositol. Increased cellular *myo*-inositol reduces sensitivity to SA and reduces resistance to *Pst*DC3000 [410]; in fact, the *myo*-inositol synthesis mutant *myo-inositol-3-phosphate synthase* (*mips*) *1* undergoes spontaneous cell death [411,412], a phenotype that is similar to that of plants with constitutive immune response. This suggests that even though there is no increase in SA in *sp1* plants compared to the wild type, *sp1* plants may be more sensitive to SA, leading to a heightened immune response.

Like SA, synthesis of *myo*-inositol in plants occurs in both the cytosol and the plastid. The *myo*-inositol precursor, *myo*-inositol-3-phosphate, is synthesised by MIPS from glucose-6-phosphate. Then, the conversion of *myo*-inositol-3-phosphate to *myo*-inositol is catalysed either by cytosolic *myo*-inositol monophosphatase (IMP) 1 or plastidic IMP like 1 (IMPL1) [413]. The plastid enzyme is thought to facilitate the recovery of *myo*-inositol from recycled phosphatidylinositol [414]. This appears to be a critical process as the Arabidopsis *impl1* knockout is seedling lethal [414]. As a plastid-localised process, it is

conceivable alteration of the plastid proteome by *sp1* may impair it and cause the reduction of the *myo*-inositol pool and increased responsiveness to SA.

5.4.2. Lipid metabolism and *sp1*-mediated immunity

Another compound identified in the dataset that is associated with both the chloroplast and immunity is glycerol-3-phosphate. Glycerol-3-phosphate is an important player in the cell's lipid metabolism, forming the backbone of many lipids [415]. In plants, lipid and fatty acid biosynthesis occurs predominantly in the plastid [416], which suggests it could be affected by chloroplast proteome changes caused by the *sp1* mutation. As discussed below, both the cell's level of glycerol-3-phosphate and fatty acid composition have been connected to plant immunity.

Glycerol-3-phosphate may arise either by the dehydrogenation of dihydroxyacetone phosphate by glycerol-3-phosphate dehydrogenase (GPDH; there are cytosol-localised and plastid-localised GPDH enzymes in Arabidopsis, encoded by *GPDHC1* and *GLY1*, respectively); or by the phosphorylation of glycerol by a glycerol kinase (in the cytosol, encoded by *GLI1* in Arabidopsis). Glycerol-3-phosphate becomes acylated by acyltransferase (ATS) 1 and 2 with fatty acids to produce phosphatidic acid (PA), which can then be dephosphorylated to produce diacylglycerol (DAG). PA and DAG are the two precursors of plastid lipid synthesis [416,417].

Briefly, *de novo* synthesis of fatty acids, required for the production of PA, begins with the carboxylation in the plastid of acetyl-coenzyme A (CoA) by acetyl-CoA carboxylase, followed by a cascade of reactions culminating in the generation of 16:0 (that is, a carbon chain length of 16, with zero double bonds) and 18:0 fatty acids, the latter of which is desaturated to 18:1. One of each of the 16:0 and 18:1 fatty acids is used to acylate glycerol-3-phosphate to produce PA. Afterwards, less-saturated 16:1-3 and 18:2-3 fatty acid chains may be generated by fatty acid desaturases [416,417].

Changes to glycerol-3-phosphate metabolism have previously been connected to plant stress and disease responses. The Arabidopsis *gly1* and *gli1* mutants have reduced accumulation of glycerol-3-phosphate and are more susceptible to the hemibiotrophic fungus *Colletotrichum higginsianum* than wild-type plants, while the overexpressor of *GLY1* or the *ats1* mutant both have increased glycerol-3-phosphate accumulation and enhanced resistance [418].

If glycerol-3-phosphate levels are positively correlated with immunity, it is surprising that they are lower in the more-resistant *sp1* mutant than the wild type. There may be several explanations for this.

Glycerol-3-phosphate may have a more nuanced role in immunity. For instance, pathogenesis of *C. higginsianum* in (the susceptible) wild-type Arabidopsis also elevates glycerol-3-phosphate levels, suggesting that increased glycerol-3-phosphate may in some cases be part of pathogenesis, or at least is not always capable of inducing immunity [418].

The subcellular localisation of glycerol-3-phosphate may be important to its effect on immunity: loss of the cytosolic GPDH (in the Arabidopsis *gpdhc1* mutant), also causes reduced glycerol-3-phosphate levels but this does not impair immunity [418]. The relative contribution of the chloroplast and cytosol to the total cellular pool of glycerol-3-phosphate cannot be determined from the LC-MS data described here, and so it cannot be ruled out that the reduction seen in *sp1* is caused only by changes to cytosolic glycerol-3-phosphate, which would not be expected to affect immunity.

Greater insight into the complex role of glycerol-3-phosphate in immunity may be found by examining the immunity effects of fatty acid metabolism.

Modulation of the cellular ratios between different fatty acids has been associated with different immunity phenotypes. Mutants of the desaturase that converts 18:0 to 18:1, *suppressor of SA insensitive 2* (*ssi2*), have a reduced pool of 18:1 fatty acid, and have constitutively active immunity and greater resistance to biotrophs (but greater

susceptibility to necrotrophs) [419,420]. These phenotypes are suppressed, and biotroph susceptibility is restored, by second-site mutations that increase the level of 18:1 [421]. These suppressor mutations include either of the above-mentioned *ats1* and *gly1* mutations [421], which increase the cellular 18:1 pool by preventing the 18:1 acylation reaction of glycerol-3-phopshate: this reduces the conversion of 18:1 to 18:2-3 fatty acids, as once bound to the glycerol backbone, in PA or DAG, 18:1 can be further desaturated by fatty acid desaturase enzymes.

This is interesting because it demonstrates immunity can be antagonised both by a mutation that increases the glycerol-3-phosphate pool (*ats1*) or by one that decreases it (*gly1*, upstream of ATS1): the critical feature is the effect this has on 18:1.

Without information on the flux through glycerol-3-phosphate, it cannot be determined unequivocally whether the reduction in the glycerol-3-phosphate pool in *sp1* during *Pst*DC3000 inoculation is due to reduced synthesis of glycerol-3-phosphate (as in the *gly1* mutant), which is correlated with deficient immunity; or increased utilisation of glycerol-3-phosphate for PA synthesis, which would reduce the 18:1 pool and promote biotroph immunity. However, there were no significant differences between *sp1* and wild type in the levels of either glycerol or dihydroxyacetone phosphate, the two possible precursors of glycerol-3-phosphate, in any of the treatments. This could be taken as an indication that glycerol-3-phosphate synthesis is not impaired in the *sp1* mutant.

SP1 might affect the glycerol-3-phosphate supply by mediating the import of chloroplast fatty acid metabolism enzymes like GLY1. This would be an interesting example of the effect of SP1-mediated import regulation on the uptake of preproteins not related to photosynthesis. Another possibility is that SP1 may affect lipid metabolism by directly targeting certain lipid enzymes or transporters for degradation. OEM-localised lipid enzymes such as long chain acyl-CoA synthetase (LACS) 8 and LACS9 [422], could be 'non-canonical' targets of SP1 subject to regulation by CHLORAD [154].

Alternatively, the reduction in the glycerol-3-phosphate pool could represent an increased demand for membrane lipid synthesis to remediate lipid oxidation. In fact, chloroplast trienoic fatty acids may act as ROS-signal carriers during *P. syringae* infection [423]. Therefore, fatty acids may be more greatly depleted in *sp1* due to the increase of chloroplast ROS generation in the mutant, necessitating their replacement and causing the exhaustion of the cellular glycerol-3-phosphate supply. With respect to immunogenic lipid signalling, it is worth nothing that phosphatidylinositol signalling is associated with ETI [424]. Given that they are *myo*-inositol derived lipids, phosphatidylinositols may also be altered in *sp1*.

It cannot be simply stated that enhanced levels of 18:1 always antagonise immunity. The relative contribution of different fatty acids to the cellular fatty acid pool is important for the immunity effect: in transgenic plants transformed with the yeast Δ-9 desaturase, other desaturated fatty acids, 16:1 and 16:3, are commensurately increased with 18:1, and these lines in fact show increased resistance to biotrophs [425,426]. It would be immensely informative, therefore, to determine the relative contributions of different fatty acids to the cellular pool in *sp1* and the wild type during infection through a lipidomics LC-MS approach.

5.4.3. Untargeted analysis of metabolic differences in immunity and disease

There is a high degree of commonality between the metabolism in PTI and ETS. The ETS metabolic signature entirely encompasses the PTI metabolic signature. There are no metabolites that, for example, are upregulated to promote immunity in PTI that must be downregulated (or at least prevented from being upregulated) to prevent immunity during ETS.

This suggests that the pathogen has not evolved to directly compete with the plant for regulation of the certain immunity-related metabolites. Immune pathways that are

initiated in PTI may instead be overridden in ETS by the manipulation of other, discrete parts of those pathways. Of course, this does not take into account whether certain metabolites that are upregulated or downregulated in both PTI and ETS may be more strongly induced or repressed in one than the other.

In this experiment, both PTI and ETS were induced by closely related strains of bacteria. Both *Pst*DC3000 and *hrpA*$^{-}$ will produce the majority of the same PAMPs that the plant may recognise, and this presumably is the basis for the overlap between the PTI and ETS metabolic patterns.

That the metabolic signatures of PTI in the wild type and *sp1* are distinct is intriguing. The additional 252 metabolites regulated only in *sp1*, and the 113 metabolites regulated differently in *sp1* than in the wild type, could be caused by the stronger induction of PTI in the mutant. Without charting the metabolic changes over time, it is not possible to say whether this might, for example, represent an earlier PTI metabolic response that is sustained for longer in one of the lines, or an entirely distinct phenotype.

Regarding the distinct metabolic signatures of ETS in the two genotypes, it is tempting to conclude that the strength of the immune response in *sp1* may be linked to effects on the 240 metabolites that are up- or downregulated in the wild type alone. Perhaps the changes in the levels of these metabolites are the result of the manipulations of *Pst*DC3000 that enable pathogenesis to which *sp1* is resistant (i.e. a signature of pathogenesis specifically caused by the subversion of the ROS burst).

5.5. Figures and tables

Table 5.1 Summary of compounds showing significantly different abundance in *sp1* leaves relative to wild-type leaves.
Number of metabolites that are significantly differently abundant between *sp1* and wild-type leaves (ANOVA, $P<.05$) detected after ion-exchange (TCA) or reverse-phase (C_{18}) chromatography, broken down by treatments in which they differed. Only a small number of these metabolites were positively identified in the reference databases, including the HMDB [399].

		№ differently abundant compounds ($P<.05$)	
Inoculum	**Method**	**… detected in total**	**… identified**
Mock	TCA	297	8
	C_{18}	60	0
hrpA$^-$	TCA	390	16
	C_{18}	227	22
*Pst*DC3000	TCA	280	9
	C_{18}	242	2

Table 5.2 Compounds significantly differently abundant in *sp1* relative to wild type after different inoculations.

Compounds identified after TCA chromatography that are significantly differently abundant in *sp1* leaves relative to wild-type leaves in at least one inoculation type. Fold change values (for *sp1* compared to wild type) are listed only for those inoculations where abundance was significantly different ($P<.05$).

	Fold change following inoculation with		
Compound	**Mock**	***hrpA*⁻**	***Pst*DC3000**
2,5-Dihydroxybenzoic acid	—	-2.15	—
2-Hydroxyglutarate	—	—	-1.26
3,3-Dimethylglutaric acid	—	-1.44	—
3,4-Dihydroxyphenylacetic acid	—	-1.73	—
3-Hydroxybutyric acid	—	1.25	—
Adenosine diphosphate	—	1.35	—
Adenosine monophosphate	—	-1.52	—
Arabinonic acid	-1.31	—	—
Dihydroxyacetone	-2.40	—	—
Galacturonic acid	—	+1.18	—
Gluconic acid	—	—	-1.18
Glycerol-3-phosphate	—	-1.42	-1.14
Glycolic acid	—	-1.15	—
Guanosine diphosphate	—	+1.63	—
Guanosine monophosphate	—	-2.14	—
Itaconic (methylene succinic) acid	—	—	-1.23
myo-Inositol	-1.25	—	-1.16
N-Acetyl-*L*-phenylalanine	—	—	—
N-Acetylvaline	—	—	-1.46
N-Methyl-*D*-aspartic acid	-1.17	—	-1.69
Pantothenic acid	-0.05	—	-1.39
para-Coumaric acid	—	-1.65	—
Phosphorylcholine chloride	—	-2.10	+1.26
Protocatechuic acid	+1.21	—	—
Raffinose	—	-1.26	—
Ribose	-1.20	—	—
Uridine 5'-monophosphate	—	+1.34	—
Xanthurenic acid	—	-1.52	—
α-Aminobutyric acid	-1.21	—	—

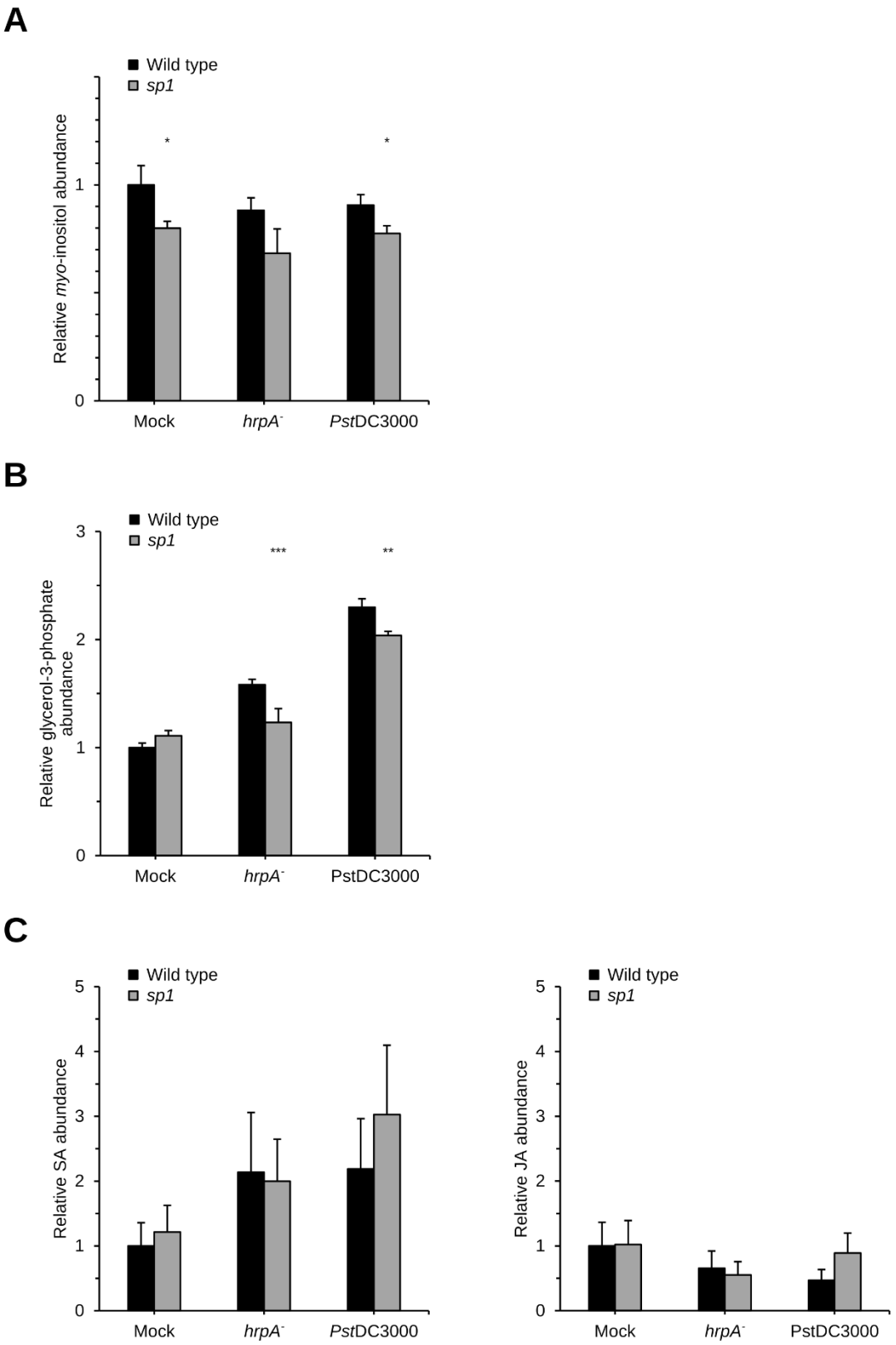

Figure 5.1 Accumulation of immunity-related metabolites.

The data show fold changes in metabolite levels, relative to the average in the wild type after mock infiltration, for wild-type and *sp1* plants two days after mock infiltration ($MgCl_2$) or inoculation with pathogen *Pst*DC3000 or the non-pathogenic mutant *hrpA*$^-$.
A. Levels of *myo*-inositol. The wild type accumulated greater levels of *myo*-inositol after a mock infiltration or after inoculation with *Pst*DC3000 than *sp1*.
B. Levels of glycerol-3-phsophate. The wild type accumulated greater levels after inoculation with *hrpA*$^-$ or *Pst*DC3000 than *sp1*.
C. Levels of phytohormones jasmonic acid (JA, right) and salicylic acid (SA, left). JA and SA, classical immunity signals, did not accumulate to statistically significant different amounts in *sp1* relative to wild type.
Asterisks indicate significant difference from corresponding wild-type treatment, as determined by ANOVA at $P<.05$ (*), $P<.01$ (**), or $P<.001$ (***). Error bars indicate the SEM (n=7 to 8).

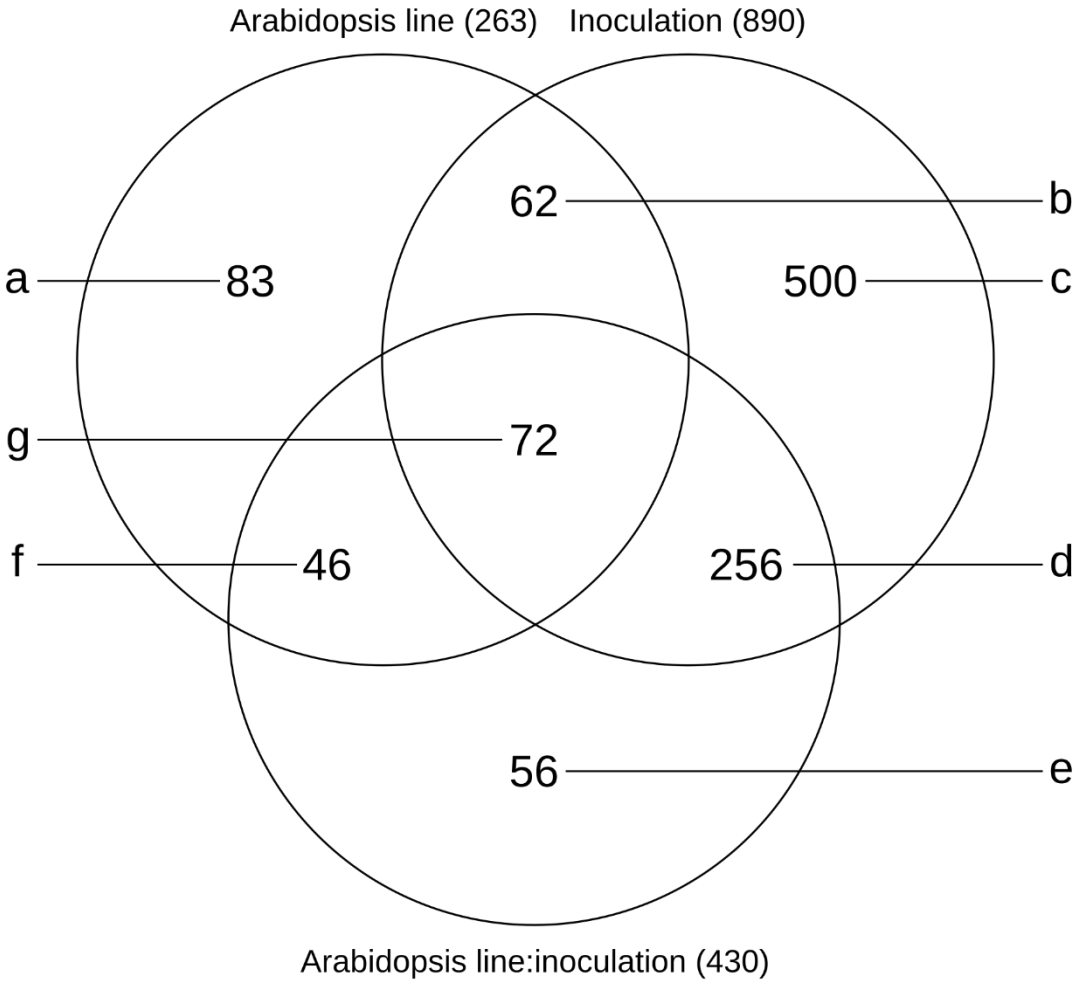

Figure 5.2 The numbers of metabolites for which abundance is influenced by genotype, inoculation, and genotype dependent on inoculation.

The Venn diagram shows the numbers of metabolites from the TCA dataset that statistically significantly differed ($P<.05$) in abundance with respect to at least one of three factors: Arabidopsis line (*sp1* or wild type), inoculation (mock infiltration, *hrpA*$^-$, or *Pst*DC3000), and the interaction of Arabidopsis line with inoculation (Arabidopsis line:inoculation). Total numbers affected by each factor are displayed in brackets. Seven sub-categories of changed metabolites are shown, and these can be defined as follows:

a. 83 metabolites were significantly different between *sp1* and the wild type but not with respect to inoculation.

b. 62 metabolites were significantly different between the Arabidopsis genotypes and also between inoculations, but this difference did not synergise.

c. 500 metabolites were significantly different between mock, *hrpA*$^-$, and/or *Pst*DC3000 inoculations but not with respect to Arabidopsis genotype.

d. The effect of Arabidopsis line on the abundance of 256 metabolites was dependent on inoculation. These metabolites also showed significant differences with respect to inoculation alone, but not with respect to Arabidopsis genotype alone. That is to say, there were significant differences in metabolite abundance between the inoculations, and these were enhanced or reduced by the *sp1* mutation.

e. The effect of inoculation on the abundance of 56 metabolites was entirely dependent on the Arabidopsis genotype. That is, these 56 showed no significant differences with respect to inoculation or Arabidopsis genotype alone. Differences only emerged in some combinations of Arabidopsis genotype and inoculation.

f. The effect of inoculation on the abundance of 46 metabolites was dependent on the Arabidopsis genotype. The abundance of these 46 metabolites also showed significant differences with respect to Arabidopsis genotype alone, but not with respect to inoculation alone. That is to say, there were significant differences in metabolite abundance between the Arabidopsis lines, and these were enhanced or reduced by certain inoculations.

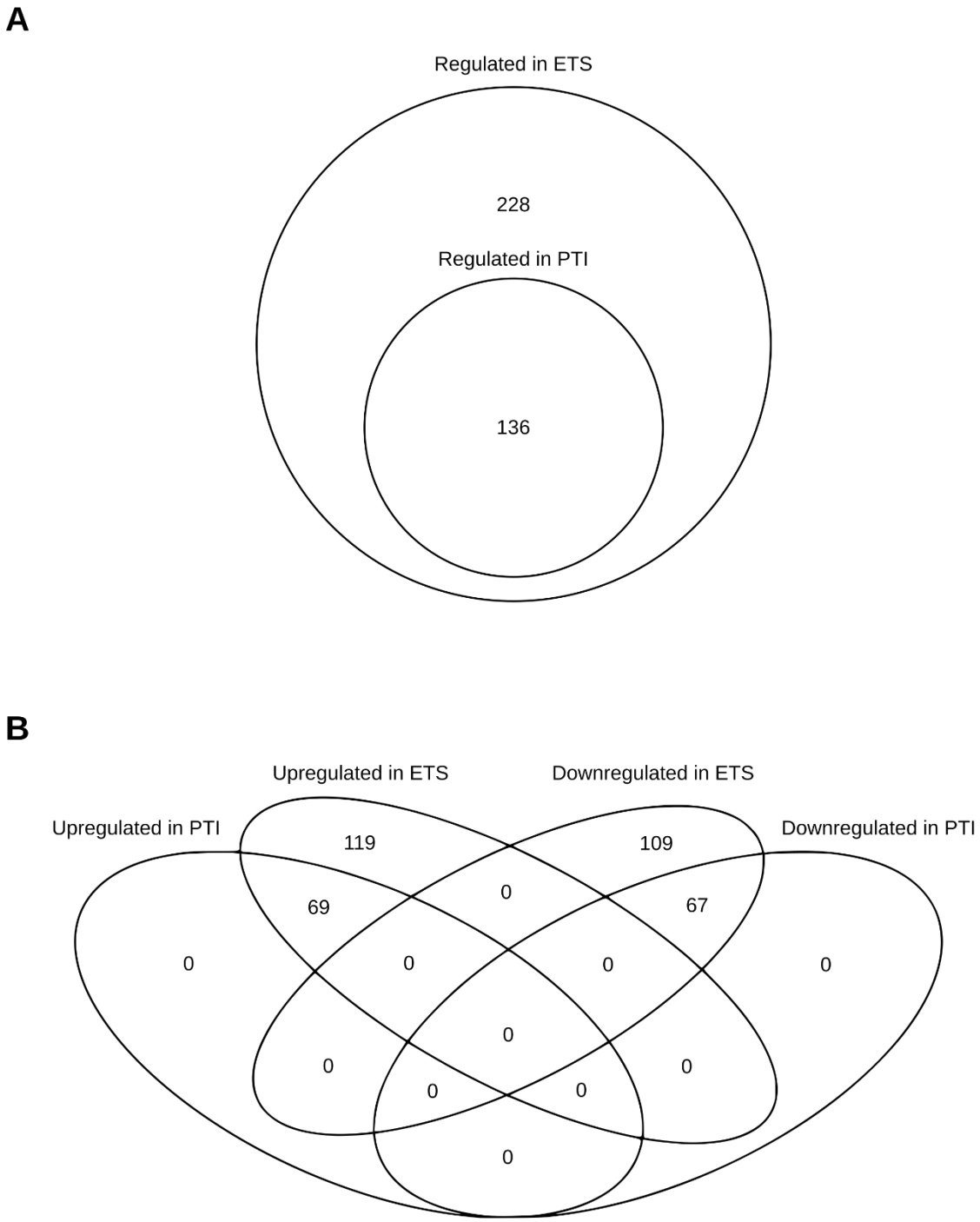

Figure 5.3 Metabolomic changes during infection of wild-type Arabidopsis.

The Venn diagrams compare the metabolomic changes (P<.05) induced in wild-type Arabidopsis during pathogen associated molecular pattern-triggered immunity (PTI) and during effector triggered susceptibility (ETS), two days after inoculation with either *hrpA*$^-$ or *Pst*DC3000 relative to mock inoculation ($MgCl_2$).

A. Comparison of all metabolites that were altered in abundance (showing either up- and downregulation) during PTI with those that were similarly altered during ETS. All metabolites that were regulated during PTI were also regulated during ETS. An additional 228 metabolites were regulated during ETS that showed no change during PTI.

B. Comparison of all metabolites showing up- or downregulation during PTI with those that were similarly regulated during ETS. All metabolites that were regulated during PTI were regulated in the same direction during ETS.

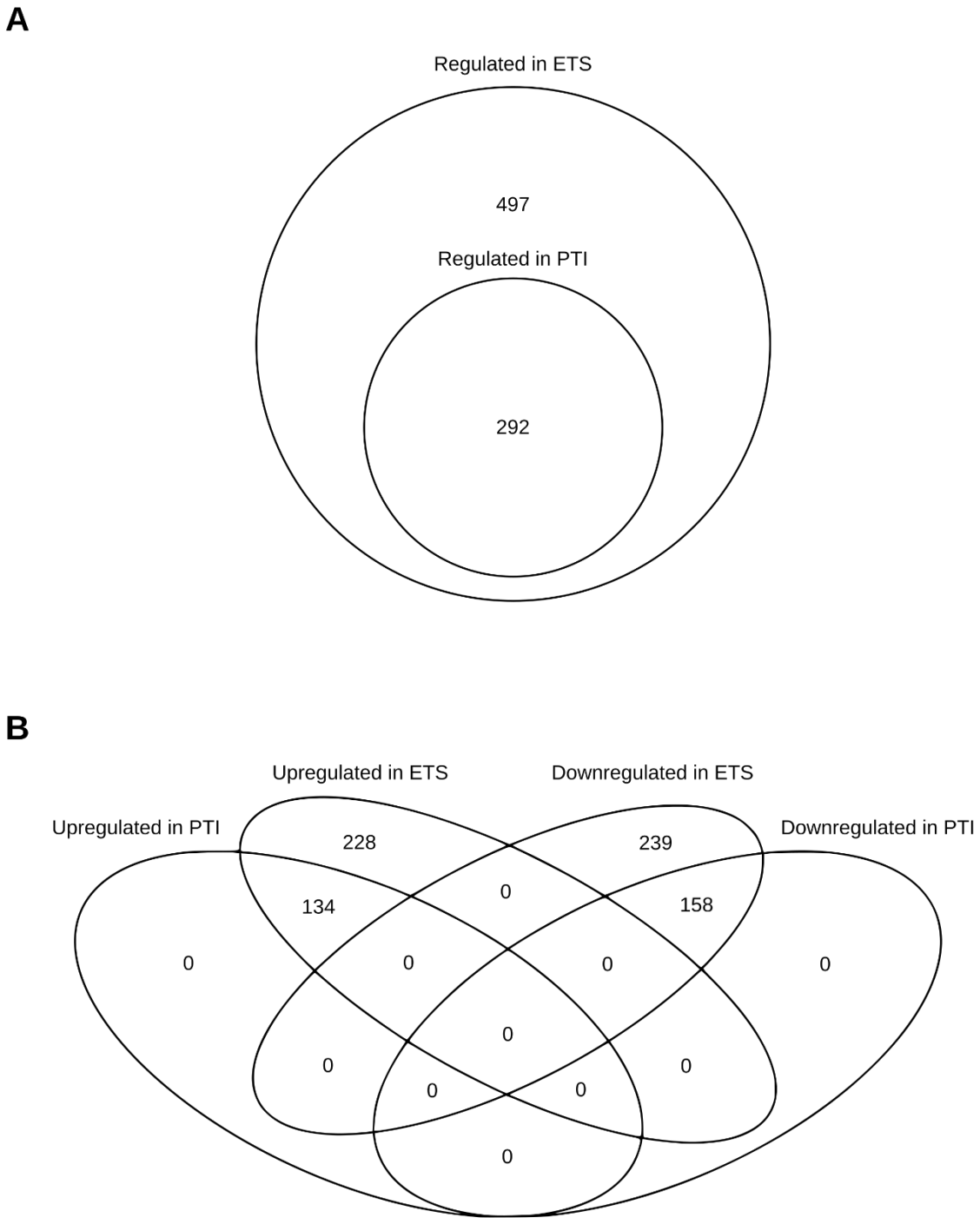

Figure 5.4 Metabolomic changes during infection of *sp1* mutant Arabidopsis.

The Venn diagrams compare the metabolomic changes (P<.05) induced in *sp1* Arabidopsis during pathogen associated molecular pattern-triggered immunity (PTI) and during effector triggered susceptibility (ETS), two days after inoculation with either *hrpA*$^{-}$ or *Pst*DC3000 relative to mock inoculation ($MgCl_2$).

A. Comparison of all metabolites showing regulation (both up- and downregulation) during PTI with those that were similarly regulated during ETS. All metabolites that were regulated during PTI were also regulated during ETS. An additional 497 metabolites were regulated during ETS that showed no change during PTI.

B. Comparison of all metabolites showing up- or downregulation during PTI with those that were similarly regulated during ETS. All metabolites that were regulated during PTI were regulated in the same direction during ETS.

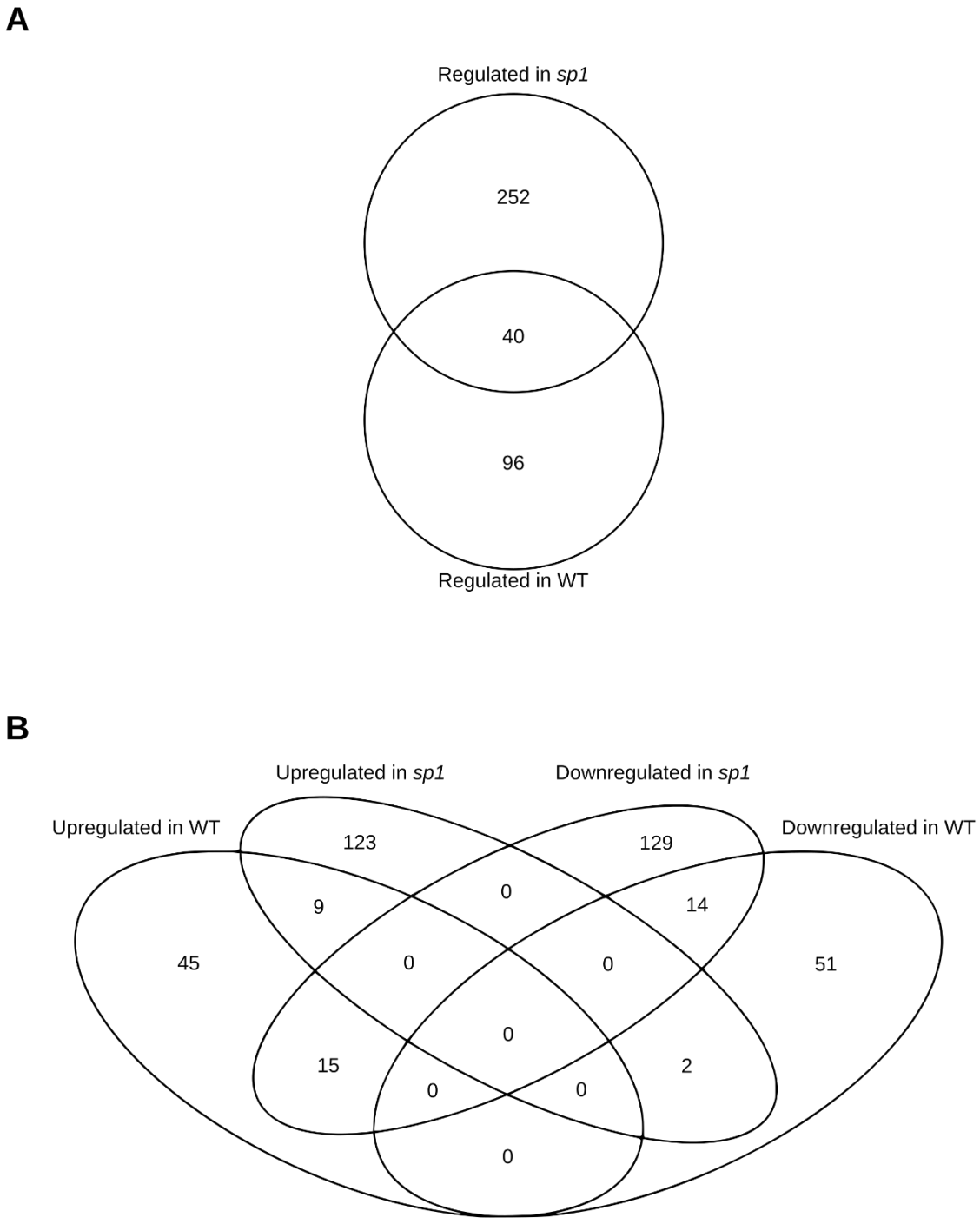

Figure 5.5 Comparison of metabolomic regulation during PTI between *sp1* and wild-type Arabidopsis.

The Venn diagrams compare the metabolomic changes (P<.05) induced during pathogen associated molecular pattern-triggered immunity (PTI) in *sp1* to those induced in wild-type (WT) Arabidopsis, two days after inoculation with *hrpA*$^{-}$ relative to mock inoculation ($MgCl_2$).

A. Comparison of all metabolites showing regulation (both up- and downregulation) during PTI in *sp1* or WT. Only a minority, 40, of the regulated metabolites were regulated in both *sp1* and WT.

B. Comparison of all metabolites showing up- or downregulation during PTI in *sp1* with those that were similarly regulated during PTI in WT. Metabolites regulated in both *sp1* and wild type during PTI are split both between those that are regulated in the same direction in both (23) and those that are regulated in opposite directions (17).

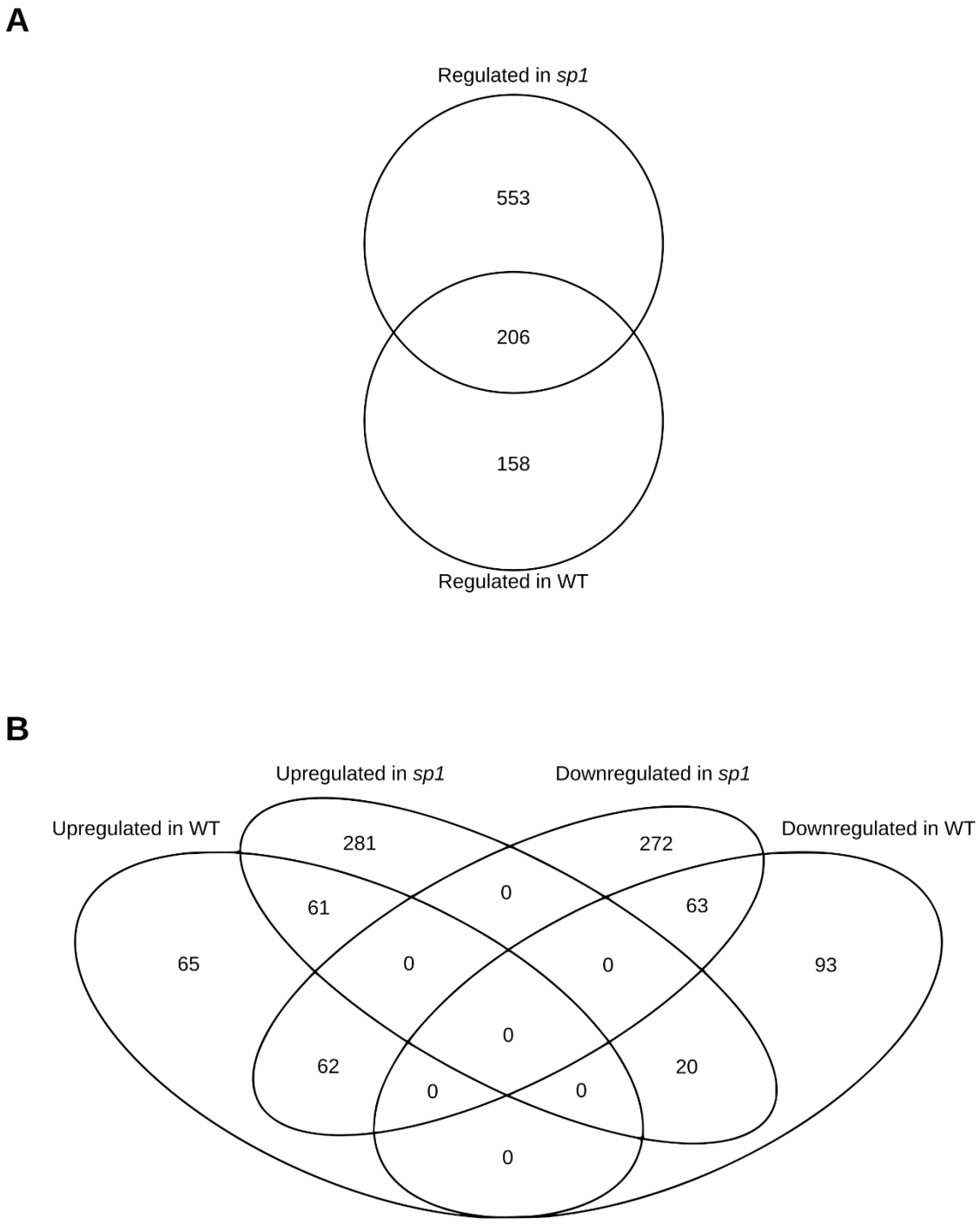

Figure 5.6 Comparison of metabolomic regulation during ETS between *sp1* and wild-type Arabidopsis.

The Venn diagrams compare the metabolomic changes (P<.05) induced during effector-triggered susceptibility (ETS) in *sp1* to those induced in wild-type (WT) Arabidopsis, two days after inoculation with *Pst*DC3000 relative to mock inoculation ($MgCl_2$).

A. Comparison of all metabolites showing regulation (both up- and downregulation) during ETS in *sp1* or WT. Most metabolites regulated during ETS in WT are also regulated in *sp1*. However, many more are regulated in *sp1* only.

B. Comparison of all metabolites showing up- or downregulation during ETS in *sp1* with those that were similarly regulated during ETS in WT. Metabolites regulated in both *sp1* and wild type during PTI are split both between those that are regulated in the same direction in both (124) and those that are regulated in opposite directions (82). The ETS-regulated metabolites that are up- or downregulated in the wild type but not *sp1* might form the underlying metabolic phenotype of susceptibility.

6. Concluding remarks

6.1 Principal findings

The findings presented in this thesis underscore the important role that the chloroplast plays in biotic stress, in addition to its established roles in abiotic stress, development, and homeostasis. It highlights the interplay between abiotic stress and biotic stress, and uncovers a new role for SP1 and chloroplast protein import during infection.

An early immunogenic signal is the photosynthetic generation of a ROS burst in the chloroplast. During pathogenesis, *Pst*DC3000 must suppress the chloroplast ROS burst to impair PTI. In this thesis, it has been argued that it has co-opted a host system of abiotic stress tolerance to do so.

A new feature of pathogenesis by *P. syringae* was found. Virulent *Pst*DC3000 downregulates chloroplast protein import. Suppression of chloroplast protein import depends on both the secretion of effectors via the T3SS, as it is not a feature of inoculation with the *hrpA*$^-$ mutant, and the presence of SP1, a host protein that regulates the abundance of TOC translocon components.

The suppression of chloroplast import by SP1, in both abiotic and biotic stress, functions to antagonise the generation of ROS in the chloroplast. *P. syringae* utilises this system to suppress the immunogenic chloroplast ROS burst. Mechanistically, the reduction in the import of photosynthesis preproteins may reduce ROS generation by reducing light interception and thereby photon excess.

SP1ox further antagonises the chloroplast ROS burst, enhancing infection by *Pst*DC3000 and reducing immunity to *hrpA*$^-$, while the *sp1* mutant generates a stronger ROS burst that enhances immunity to *hrpA*$^-$ and is resilient to suppression by *Pst*DC3000, reducing susceptibility.

6.2 Regulation of SP1 by *P. syringae*

The model that *P. syringae* suppresses chloroplast protein import via the SP1-mediated turnover of TOC components raises questions as to how T3SS effectors may interact with this pathway. *P. syringae* might enhance the activity or stability of SP1, or target TOC proteins to make them more susceptible to turnover.

Little is known about the manner in which SP1 is itself regulated by the plant. However, the activity of many E3 ligases are known to be regulated at the post-translational level by a number of modifications including phosphorylation, ubiquitination, and ubiquitin-like modifications. *P. syringae* could enhance TOC turnover by either preventing modifications that reduce SP1 activity or promoting modifications that enhance it.

Several E3 ligases require phosphorylation to become active: this allows them to remain inert and only function following specific cues [427]. For example, phosphorylation of a linker region in RING-type E3 casitas B-lineage lymphoma (Cbl) causes a conformational change necessary to bring the E2 enzyme bound to the RING domain into proximity with the substrate binding domain, allowing the transfer of ubiquitin to target proteins, receptor tyrosine kinases [428].

Many E3 ligases are themselves regulated by ubiquitination. This may reduce the E3 ligase's activity by causing its UPS-dependent turnover, but in some instances it has been found to increase its activity. An example of the latter is the regulation by ubiquitin of proto-oncogene E3 ligase mouse double minute 2 homologue (Mdm2) [429]. Autoubiquitination of Mdm2 improves E2 enzyme recruitment because of affinity between the ubiquitin binding domains of the E2 enzymes and the polyubiquitin chain on Mdm2. This is thought to enhance Mdm2's processivity, leading to enhanced ubiquitination of its substrate, p53 [429]. The idea that autoubiquitination may activate E3 enzymes (by increasing E2-E3 affinity) is a fascinating one, as autoubiquitination could act as its own negative feedback regulator via UPS-turnover—though it should be

noted though that autoubiquitination can produce chains linked at residues other than lysine 48 [430], so does not necessarily induce turnover (ubiquitin chain topology is discussed in **§1.4.1**).

Other ubiquitin-like modifications can also affect (ubiquitin) E3 ligase function, including neddylation, the ligation of neural precursor cell expressed developmentally downregulated 8 (NEDD8; known in plants as related to ubiquitin, RUB) [431], which acts as a conformational switch to activate cullin-family E3 ligases [432]. Another example is sumoylation, the ligation of small ubiquitin like modifier (SUMO), of Mdm2 which can alter its subcellular localisation or prevent its autoubiquitination [433,434].

It is likely that SP1 is also regulated by post-translational modifications. SP1 itself can become ubiquitinated and may be subject to turnover by the UPS, as treatment with a proteasome inhibitor elevates SP1 protein level [126]. Therefore it is possible that *P. syringae* interferes with regulatory pathways to induce or suppress the post-translational modification of SP1—for example its ubiquitination—to stabilise it or modulate its activity.

P. syringae effectors themselves might even directly target SP1 for post-translation modification. There are many examples of bacterial effectors that manipulate host proteins by causing post-translational modifications, including dephosphorylation, phosphorylation, and desumoylation [435]. Some effectors are even capable of ubiquitination: the *P. syringae* effector AvrPtoB is a structural mimic of a RING-type E3 ligase and has an E2 binding domain [436]. Its E3 activity is necessary for its ability to suppress immunity, as this ability is lost when its RING domain or E2 binding domain is mutated [436,437]. It targets for degradation certain host kinases implicated in immunity, including Fen in tomato and chitin elicitor receptor kinase 1 in Arabidopsis [437,438]. It is especially intriguing how this may have arisen, as bacteria do not have a UPS of their own and so this cannot represent neofunctionalisation of a bacterial regulatory protein.

In fact, AvrPtoB does not possess sequence identity with plant E3s, rather it has convergently evolved to mimic the RING domain structure in order to interface with the host UPS [436]. This is not unlike transit peptide mimicry, described in **§1.9.2**. Since the discovery of the E3 ligase activity of AvrPtoB, a number of other effectors from a range of bacteria have been found to mimic RING- or HECT-family E3 ligases [439,440], so this may not be uncommon. Additionally, some bacterial effectors, including two *Chlamydia trachomatis* effectors [441], have deubiquitinating enzyme activity.

Instead of enhancing the activity or stability of SP1, *P. syringae* might promote the SP1-mediated turnover of TOC by targeting the TOC components themselves, for example through phosphorylation. Post-translational modifications like phosphorylation can change how amenable substrates are to ubiquitination. Phosphorylation of substrates can promote or prevent turnover by encouraging or hindering interaction with E3 ligases [442]. In the TOC complex, the Toc34 and Toc159 isoforms can become extensively phosphorylated [443,444]. The phosphorylation of Toc34 hinders its association with other TOC components: this has been described as a mechanism by which different Toc34 isoforms can be separated from and swapped out of the complex [444]. Perhaps disassociation from the TOC complex by phosphorylation makes the components more accessible to SP1, and if so, perhaps *P. syringae* causes the phosphorylation of TOC components to enhance this process.

It is of course possible that *P. syringae* enhances SP1 activity at the transcriptional level. As is established from the SP1ox line, increased expression of SP1 is correlated with increased SP1 activity [126]. However, alone, the high level of expression in the SP1ox line is insufficient to suppress chloroplast protein import in the absence of *Pst*DC3000, after mock or *hrpA*$^{-}$ inoculation. Therefore, it is unlikely that transcriptional upregulation of SP1 could on its own account for the suppression of import seen after inoculation with *Pst*DC3000.

There are several approaches that might give greater insight into the regulation of SP1 in plant development generally and in disease. It would be informative to learn to what extent SP1 might be post-translationally modified, and then whether these modifications are affected by immunity or disease. This might be achieved through a mass-spectrometry approach, where post-translational modifications of a protein are detected by mass shift [445]. Another direction from which to approach this problem would be to determine SP1's interacting partners, which might reveal by which proteins it is regulated. This might be possible with a tandem affinity purification and mass spectrometry approach [446].

6.3 Perception of the chloroplast ROS burst

However it is accomplished, once *Pst*DC3000 effectors have succeeded in utilising SP1 to downregulate chloroplast protein import, the chloroplast ROS burst, and immunity, is prevented. However, one of the features of immunity that remains unclear is how exactly the chloroplast ROS burst functions as an immunogenic signal.

There are several possible ways in which the chloroplast ROS signal may be relayed to the nucleus. One promising candidate identified here are chloroplast lipids. The plastid is the primary source of fatty acid biosynthesis in the cell, and the thylakoids of the chloroplast have a distinctive galactolipid composition. Given that the metabolomic analysis suggests that lipid biosynthesis might be altered in *sp1*, it may be worth revisiting lipids as a potential mediator of the chloroplast immunogenic signal.

The generation of ROS in the chloroplast is also likely to cause the activation or inhibition of redox sensitive enzymes by post-translational modification. There are many possible redox protein modifications, including hydroxylation, nitrosylation, and the formation of disulphide bridges. Additionally, redox changes may indirectly alter protein modifications: for example, activation or deactivation of a redox-sensitive kinase could cause a cascade of phosphorylation differences in other proteins. As they are highly nucleophilic, cysteine residues in particular can be subject to ROS-modification in the form of S-nitrosylation [392].

Modification of redox sensitive proteins may integrate chloroplast ROS generation with other retrograde signals. For example, the cysteine residues of SAL1 are required for its activity to become downregulated during oxidative stress: in this way redox can integrate with the SAL1-PAP retrograde signal [395]. It would be informative to chart the role of chloroplast oxidation in the redox regulation of sensitive proteins through profiling hyper reactive cysteines in wild-type, SP1ox, and *sp1* plants during disease and immunity.

6.4 Considerations for the engineering of stress tolerant crops

As autotrophs, plants must perform photosynthesis to survive. However, environmental challenges can turn the productive photosynthesis machinery into an engine for generating oxygen radicals and ROS, highly reactive byproducts that have the potential for toxicity. There are a number of mechanisms in place by which ROS generation can be mitigated or reduced during stress, including the downregulation of chloroplast protein import [165].

The effect of SP1 on immunity may not apply to all pathogens. *P. syringae* is used as a model biotroph, a pathogen that derives nutrition from living tissue [207]. Typical biotroph immune responses, which are associated with SA and include PCD, are often not effective against necrotrophs, which can depend on cell death for virulence [208]. It cannot be assumed therefore that the chloroplast ROS burst in early biotroph immunity contributes to necrotroph immunity: this would have to be examined separately.

Nevertheless, if the role of SP1 is generalisable for other plant-pathogen interactions, the criticality of the chloroplast ROS burst in the initiation of immunity is concerning. Plants activate ROS avoidance and mitigation programmes under abiotic stress to promote tolerance, but the results presented here suggest this may come at the expense of resistance to pathogens. In fact, this may be the basis of combinatorial stress and disease susceptibility [339–341].

If global food security is to be maintained in the face of a changing climate, the creation of new crop lines that are more resistant to abiotic stress is vital. To prevent the deleterious effects of stress on photosynthesis, plant lines with improved photosynthetic ROS avoidance or damage remediation must be engineered. Worryingly, however, the role of SP1 in immunity described here suggests that plants that have been engineered to be constitutively less liable to produce photosynthetic ROS are likely to be constitutively immunocompromised, more susceptible to opportunist and specialist pathogens due to

impaired induction of PTI. This should be an important consideration in crop engineering.

6.5 Figure

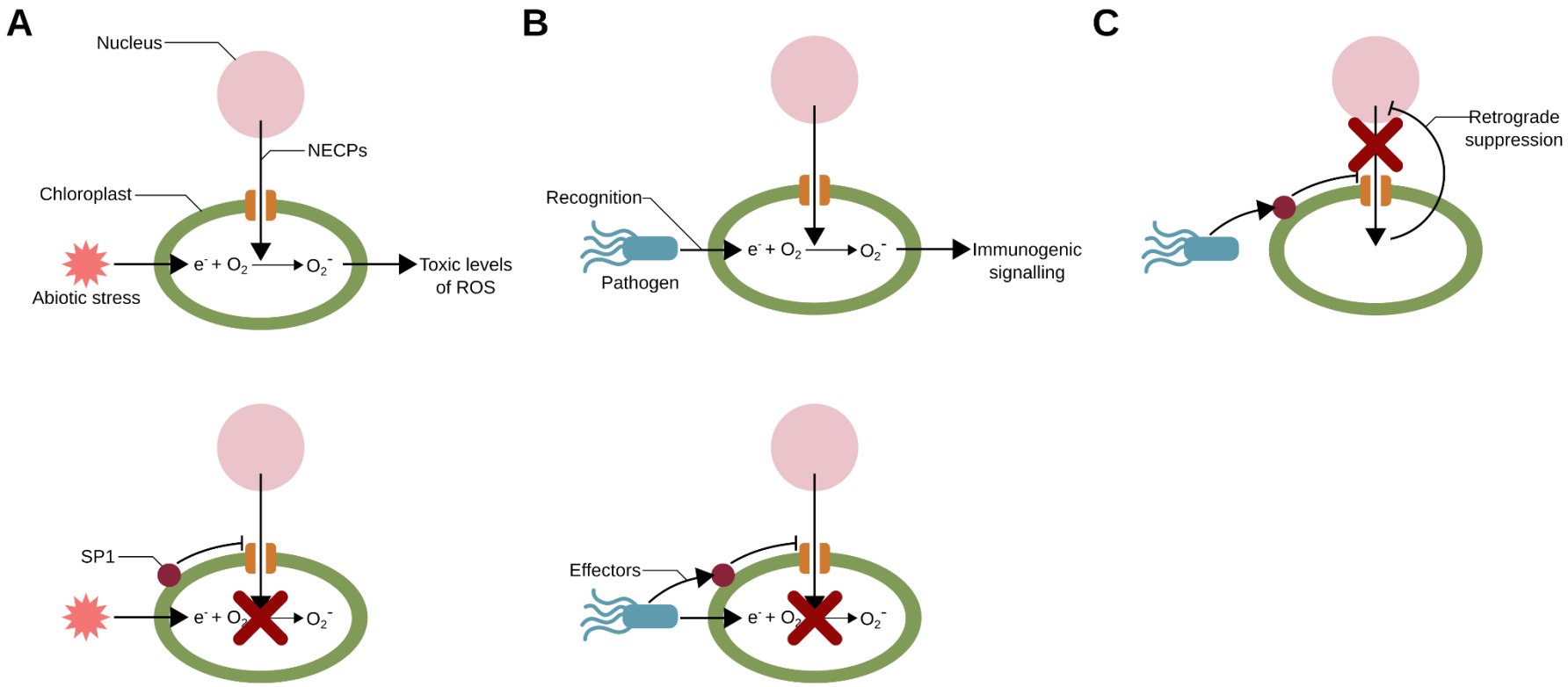

Figure 6.1 Schematics of the SP1-mediated ROS avoidance model in abiotic and biotic stress

A. Model for SP1-mediated ROS avoidance during abiotic stress. Abiotic stress encourages the reduction of oxygen in the chloroplast, dependent on photosynthesis and the import of photosynthesis-related nucleus encoded chloroplast proteins (NECPs), which can lead to toxic levels of ROS. SP1-mediated turnover of the TOC complex (orange) reduces the import of NECPs, thereby preventing the accumulation of toxic levels of ROS.
B. Model for SP1-mediated ROS avoidance during biotic stress. Pathogen recognition triggers the reduction of oxygen in the chloroplast, dependent on photosynthesis and the import of photosynthesis-related NECPs, which acts as an immunogenic signalling. Pathogens can secrete effectors that active SP1-mediated turnover of the TOC complex reduce the import of NECPs, thereby averting the immunogenic signal.
C. Suppression of photosynthesis-related gene expression in the nucleus, as caused by pathogens like *P. syringae*, could be caused by the suppression of chloroplast protein import. Suppression of the import of photosynthesis-related NECPs into the chloroplast, as caused by effector activation of SP1, could cause retrograde signalling that suppresses photosynthesis-related gene expression. Retrograde suppression of photosynthesis-related gene expression is a feature of constitutive chloroplast protein import deficient mutants like *ppi1* [37].

7. Methods

7.1 Plant growth conditions

7.1.1 Growth on soil

For most experiments, plants were grown on soil. Seed was vernalised at 4°C in water and the dark for at least three days before sowing directly onto soil (one part vermiculite to three parts Levington M2 compost) in 0.1% phytoagar solution. Soil was treated with Imidasect 5GR (Sinclair Pro) to prevent scarid fly. Plants were either sown two seeds per 6 cm^2 pot, or sown at a higher density and reduced to two per pot after germination. Germination was encouraged using a clear plastic propagator hood. Seedlings transferred from media to soil were also covered in a propagator hood for several days after transplantation to encourage re-rooting.

7.1.2 Growth on solid media

For experiments involving seedlings or where lines needed to be screened by a herbicide, seed was surface sterilised in ethanol and then sown on ½ strength Murashige and Skoog medium with 0.5% (w/v) sucrose, adjusted to pH 5.7, and 0.8% (w/v) phyotoagar. They were then vernalised on the plates at 4°C in the dark for at least three days.

7.2 Bacterial inoculation

7.2.1 Bacterial growth

Bacteria were streaked from -80°C glycerol stocks directly onto 1% agar (w/v) lysogeny broth (LB) plates (1% tryptone, 0.5% yeast extract, 0.5% NaCl) with rifampicin (dissolved in methanol, 20 $ng.mL^{-1}$ final concentration) added before pouring. For inoculation, colonies were taken from these plates and subcultured in liquid LB with rifampicin overnight at 26°C.

7.2.2 Dilution

Concentration of the overnight cultures was estimated on a spectrophotometer, with an optical density at 600 nm of 0.02 taken as equivalent to 10^7 $CFU.mL^{-1}$. Bacteria were diluted in 10 mM $MgCl_2$ inoculation buffer before use. A concentration of 1×10^5 $CFU.mL^{-1}$ was used for measuring bacterial growth four days post inoculation. A concentration of 1×10^7 $CFU.mL^{-1}$ was used for experiments with shorter directions, including measuring ROS by DCFH-DA staining or roGFP fluorescence, the FRAP experiments involving chloroplast protein import during infection, and the metabolite analysis. For chlorophyll fluorescence measurements, 0.5×10^8 was used.

7.2.3 Syringe inoculation

1 hour before inoculation, plants were misted with distilled water, and again immediately before inoculation, to encourage stomatal opening. Inoculation was performed with a syringe through the abaxial surface of the leaf. To minimise circadian affects, inoculation was performed at approximately the same time in all bacterial experiments.

7.2.4 Determination of bacterial growth

After four days of incubation, infected leaves were removed from the plants. Two leaf discs (treated together as one biological replicate) were punched per leaf with a cork borer,

area 0.393 cm^2 each, and homogenised with a microcentrifuge tube pestle with 1 mL 10 mM $MgCl_2$ buffer solution. The homogenate was serially diluted (normally to 1×10^{-7} for *Pst*DC3000 and 1×10^{-5} for *hrpA*$^-$), and 10 uL spot replicates made on LB plates (as in **§7.2.1**). Colonies were counted after two days incubation at 26°C. CFUs in the undiluted of homogenate were calculated and are given per cm^2 area of leaf.

7.3 Callose deposition

7.3.1 Plant material

Four-week-old wild-type, SP1ox, or *sp1-3* Arabidopsis rosette leaves were syringe inoculated with a mock inoculum, *Pst*DC3000, or *hrpA*$^{-}$, as described above (**§7.2**).

For each experiment, 5-6 biological replicates were prepared. Samples were taken 24 hours after inoculation.

7.3.2 Slide preparation

Callose deposition staining was based on an established protocol [447]. Whole Arabidopsis leaves were fixed and destained of chlorophyll in 1:3 solution of acetic acid and ethanol overnight, then the solution was replaced and left to destain for another three hours. They were then washed in 150 mM K_2HPO_4 aqueous solution for 30 minutes at 50 rpm. The samples were stained for callose with aniline blue (0.01% aniline blue in 150 mM K_2HPO_4 aqueous solution) for 3 hours in the dark. Leaves were mounted on slides in 40% glycerol solution and sealed with clear nail varnish.

7.3.3 Microscopy

Slides were visualised under epifluorescence on an Olympus B201 microscope with a WU fluorescence cube (excitation filter BP330-385 nm, barrier BA420 nm). Six to eight micrographs were taken per biological replicate in areas distal from the wound site (where syringe inoculation occurred, which invariable showed a strong signal) with a QICAM Fast 1394 colour camera.

7.3.4 Analysis

A macro was written to automate image analysis in FIJI (a distribution of ImageJ, available from `https://fiji.sc`) [448,449]. Each micrograph was separated into its colour channels from which the green channel was taken. A gaussian blurred copy of that

channel was subtracted from original channel image to remove the background signal. Deposits were then identified by IsoData thresholding [450], and deposit area measured.

Two additional conditions were applied to improve data collection. Firstly, where the computed threshold was less than thirty, it was increased to thirty before deposit area was measured. This was necessary for some mock infection micrographs where very little callose signal was detected, as in these cases the computed IsoData threshold would be too low in order to distinguish the *bone fide* deposits from background fluorescence.

Secondly, trichome autofluorescence may also be counted by this macro. As the trichome area was several orders of magnitude higher than legitimate callose deposits, these could easily be recognised in the data set and were removed from the analysis.

7.3.5 Presentation

For presentation in this thesis (but not analysis), the brightness and contrast of the whole image set has been enhanced so that it is more clearly rendered in print and on screen.

7.4 DCF fluorescence

7.4.1 Material

For biotic stress experiments, four week old rosette leaves were inoculated (**§7.2**). For abiotic stress experiments, plants were syringe inoculated with 10 mM $MgCl_2$ with or without paraquat (5 µM or 10 µM).

7.4.2 Slide preparation

Based on a described method [253], material was stained in a solution of 10 µM 2′7′-dichlorodihydrofluorescein diacetate (DCFH-DA) in 10 mM $MgCl_2$ for two hours, then washed in 10 mM MgCl2 for at least twenty minutes before imaging.

DCFH-DA staining was conducted in the light, as dark treatment during staining reduced signal production in wild type plants challenged with *Pst*DC3000 *hrpA*$^-$ compared to light treatment during staining. This does not seem to be the result of photooxidation of DCFH-DA, as an A/B comparison of DCF signal production in leaves infiltrated with H_2O_2 solution and stained either in the light or in the dark did not show noticeable differences (data not shown), but instead is indicative of increased photosynthetic ROS generation by keeping the plants in the light for two additional hours.

Leaves were mounted in perfluorodecalin for visualisation [451].

7.4.3 Microscopy

Images were taken on a Zeiss 880 Airyscan confocal microscope using a 40x water immersion objective. Samples were excited with a 488 nm argon laser. DCF signal was collected at 512-527 nm on a gallium arsenide phosphide (GaAsP) detector, and chlorophyll signal at 656-709 nm on a standard photomultiplier tube (PMT).

7.4.4 Presentation

For presentation in this thesis, the brightness and contrast of the whole image set has been enhanced equally so that it is more clearly rendered in print.

7.5 Redox fluorescent probe under biotic stress

7.5.1 Line crossing

The TKTP-Grx1-roGFP2 (that is, roGFP) construct was provided by Prof. Markus Schwarzländer, and crossed into the *sp1* and SP1ox backgrounds by Dr Qihua Ling.

7.5.2 Material

Seedlings were germinated on MS agar and screened for fluorescence under a UV stereomicroscope at 10 days. Positive seedlings were transferred to soil and inoculated (**§7.2**) at three weeks old. This was one week earlier than in the DCF fluorescence experiments but is developmentally comparable, as plants transferred to soil tended flower approximately a week earlier than plants germinated on soil (four weeks old versus five).

7.5.3 Microscopy

Leaf discs from treated plants were punched shortly before the time point and floated in perfluorodecalin [451]. At the time point they were taken to dark conditions, mounted on slides and visualised as quickly as possible.

Samples were visualised on a Zeiss 880 Airyscan confocal microscope using a 40x water immersion objective. GFP fluorescence was collected between 497-543 nm on a GaAsP detector after excitation with a 405 nm diode laser and a 488 nm argon laser. Tracks were switched every line. Chlorophyll fluorescence was collected between 656-687 nm after excitation with the 488 nm laser, and autofluorescence was monitored by collecting emissions between 415-475 nm after excitation with the 405 nm laser.

7.5.4 Analysis

The chloroplast roGFP ratio for each biological replicate (one leaf disc) was determined from three to five technical replicates, each one consisting of a tile scan comprised of four adjacent images.

A macro was written to automate image analysis in FIJI [448,449]. Briefly, chloroplasts were located in each imager by smoothing the chlorophyll channel, IsoData thresholding [450], and watersheding the result. Individual chloroplasts locations were then identified by the `Analyze Particles` function, with very small (< 8.5 μm^2) or large (> 34.7 μm^2) – i.e. noise or chloroplasts that were not individually resolved – particles ignored.

The ratio of roGFP signals when excited by each laser (ex 405 nm : ex 488 nm) was then determined for each located chloroplast in the image, and the average ratio for that image determined. The average of these for all four of the images in a tile scan was taken for each technical replicate. The average of three to five technical replicates was taken for each biological replicate.

Four biological replicates were taken per interaction (i.e. each combination of Arabidopsis and *P. syringae* genotype at each of three time points). For each biological replicate, a total of 4,130-8,333 chloroplasts were measured.

7.6 Redox fluorescent probe under abiotic stress

7.6.1 Material

Seedlings were germinated on solid media, before being transferred to liquid MS media at 10 days old and allowed to adjust to the new media for one day with agitation. Paraquat or a mock treatment was added to the culture liquid, and the seedlings were returned to the shaker for two days.

7.6.2 Visualisation

After treatment, seedlings were transferred to fresh liquid MS media in a black 96 well plate, one seedling per well. Measurements were performed on a Beckmann DTX 880 plate reader. Top GFP fluorescence was recorded from each loaded well after illumination at 405 nm and 485 nm light to give measurements for $roGFP_{red}$ and $roGFP_{oxi}$. Four technical replicates were taken per well. Four wells with only the media were also recorded to provide a background measurement.

7.6.3 Analysis

The average fluorescence readings of $roGFP_{oxi}$ and $roGFP_{red}$ were taken from the media only wells to provide a background measurement, which was subtracted from the average of the technical replicates for $roGFP_{oxi}$ and $roGFP_{red}$ for each biological replicate. The background-corrected ratio of the $roGFP_{oxi}$:$roGFP_{red}$ was determined for each biological replicate and the mean averages presented.

7.7 Localisation of fluorescent probe

7.7.1 Plant transformation

Prof. Masanori Izumi provided the cpGFP and RbcS-GFP lines, which were crossed into the *sp1*, SP1ox, and *ppi1* backgrounds by Dr Qihua Ling. Lines homozygote for SP1ox and for *sp1* were identified by hygromycin resistance and gDNA PCR [126] respectively, and seedlings selected for GFP fluorescence under a Leica M-series UV stereomicroscope at ten days old.

7.7.2 Microscopy

Leaves taken one- or two-days post infection (as indicated) were mounted in perfluorodecalin and visualised by confocal microscopy with a Zeiss LSM 510, a Leica SP5, or a Zeiss 880 Airyscan confocal microscope. Samples were excited with a 488 nm argon laser to collect GFP and chlorophyll fluorescence (respectively 497-543 nm and 656-709 nm on Leica SP5 and Zeiss 880 Airyscan).

7.8 Measuring import rates by photobleaching

7.8.1 Microscopy

Leaf discs from treated four week old plants (for measuring *ppi1* and biotically stressed plants) or from ten day old seedlings (*ppi1* and control only) were mounted in perfluorodecalin. In order to minimise chloroplast movement during measurement, the leaf discs were dark adapted for approximately 20 minutes before visualisation.

Slides were visualised on a Zeiss 880 Airyscan confocal microscope with a 40x water immersion objective and excited with a 488 nm argon laser to collect GFP fluorescence between 497-543 nm on a GaAsP detector and chlorophyll fluorescence between 656-709 nm.

7.8.2 Photobleaching

Two regions were created in each field of view containing a test and a control cell of similar size. 4-5 scans were taken to give an average pre-bleach measurement. Then, the test region was bleached with twenty passes of the laser at 0.8 times power, which was sufficient to reduce GFP signal by approximately 10%. GFP signal in the test region relative to the control region was measured over the recovery period and given as a percentage of the pre-bleach measurement. If necessary, drift in the x and y axes was corrected by scale-invariant feature transformation for linear stack alignment [452].

7.9 Protein assay

7.9.1 Protein extraction

Leaf samples were flash-frozen in liquid nitrogen and stored at -80°C until use. Tissue was homogenised with metal beads in a Qiagen TissueLyser and protein was extracted in a protein extraction buffer (100 mM Tris-HCl at pH 6.8, 10% glycerol, 1% SDS, 0.1% Triton X-100, 5 mM EDTA, 10 mM DTT, 1 × Roche Protease Inhibitor Cocktail).

7.9.2 Gel electrophoresis and western blotting

Aliquots of protein were diluted in Laemmli buffer and heated to 90°C for five minutes for denaturation. They were then run in pre-cast 10% SDS-PAGE gels (Bio-Rad Mini-PROTEAN) in TGS running buffer (25 mM Tris, 192 mM glycine, 0.1% SDS), for 35-40 minutes at 180 volts. For Western blotting, protein was then transferred to nitrocellulose membranes in transfer buffer.

Membranes were blocked in a 5% skimmed milk powder solution in TBS-T (10 mM Tris-HCl at pH 8.0, 150 mM saline, 1% Tween 20), cut into pieces based on expected protein size and incubated in the primary antibody overnight at 4°C. Membranes were incubated with appropriate secondary antibodies ligated to horseradish peroxidase for at least an hour at room temperature.

To normalise sample loading, equal volumes of the samples were first run on a gel and stained for protein with InstantBlue Coomassie stain (Sigma-Aldrich). The entire lane was then quantified to estimate equal loading. Sample loading was adjusted again based on the anti-Histone 3 (αH3; Abcam) band used as a Western blot loading control.

7.9.3 Quantification

Bands on membranes were visualised with ECL Select (General Electrics Healthcare) and photographed with a LAS 4000 series ImageQuant (General Electrics Healthcare). Band quantification, normalised to αH3, was performed in FIJI [448] with the gel analyser tool.

7.10 Chlorophyll fluorescence measurements

7.10.1 Inoculation

Four-week old Arabidopsis on soil were syringe inoculated with bacteria before imaging (**§7.2**).

7.10.2 Fluorescence imaging

Imaging was conducted with a CF Imager (Technologica Ltd, Colchester, UK), as in [253] with some modifications. Briefly, minimal fluorescence was collected following a 0.8s pulse of 6,349 μmol $m^{-2}s^{-1}$ actinic light after a 20 minute dark incubation, and maximal fluorescence was collected during a 39 minutes light incubation period. This cycle must be repeated for every timepoint.

Measurements were collected in two ways, either as in [253] where plants were the cycle of measurements was repeated immediately, gathering a measurement for ever hour, or where plants were measured after inoculation (giving a one hour post inoculation measurement), after six hours (giving a seven hours post inoculation measurement), and after 23 hours (giving a 24 hours post inoculation measurement). In the second case, plants were returned to normal growth conditions between measurements.

7.11 Metabolomics analysis

7.11.1 Plant material

Four-week-old Arabidopsis rosette leaves were inoculated as above, and harvested 48 hours post inoculation, frozen immediately in liquid nitrogen and freeze dried before analysis. Seven-eight biological replicates were measured per interaction, wild type versus *Pst*DC3000, wild type versus *hrpA*$^-$, *sp1-3* versus *Pst*DC3000, and *sp1-3* versus *hrpA*$^-$.

7.11.2 Extraction and mass spectroscopy

Metabolite extraction and liquid chromatography-tandem mass spectroscopy (LC-MS/MS) analysis was performed by Dr David Hauton. Extracts were separated by two different chromatography methods to improve detection of different metabolites: C_{18} reverse phase chromatography, and ion exchange chromatography.

Metabolites were identified by cross-reference to a list of authentic standards and the Human Metabolome Database (`http://www.hmdb.ca`), which also lists many plant-specific compounds that are found in humans due to diet [399].

7.11.3 Analysis

Analysis was performed with R [453] in the RStudio environment [454], using the agricolae [455] car [456], and VennDiagram [457] packages.

Lists of compounds that differed ($P<.05$) between wild type and *sp1* for each inoculation were determined by ANOVA by Dr David Hauton.

To determine the scale metabolomic reprogramming targets and the overlap of targets in the TCA dataset, type III ANOVAs with unweighted means were performed with the linear model that metabolite abundance changes with Arabidopsis line (*sp1* or wild type), inoculation (mock, *hrpA*$^-$, or *Pst*DC3000) and the interaction between Arabidopsis line and inoculation (Arabidopsis line:inoculation, i.e. if the change in abundance of the

metabolite between *sp1* and wild type is dependent on the inoculation). Where this relationship was significant ($P<.05$) for each metabolite it was followed by a Tukey's honestly significant differences test to determine which factor or factors had a significant effect on the abundance of each metabolite. The number of metabolites regulated by each factor was determined. This did not distinguish between positive or negative regulation or between different types of inoculation.

To determine the metabolic signatures in PTI and ETS, a type III ANOVA with unweighted means modelling abundance changes with inoculation was performed for each metabolite with respect to the wild type samples and *sp1* samples separately. Where the relationship was significant ($P<.05$), a Tukey's honestly significant differences test to determine between which inoculations the difference occurred. Those metabolites that were differently abundant between mock and *hrpA*$^-$ inoculation, and mock and *Pst*DC3000 inoculation, were recorded to determine metabolites regulated during PTI and ETS respectively. For metabolites that were regulated in PTI or ETS, the means for abundance between mock and *hrpA*$^-$ or mock and *Pst*DC3000 inoculation were compared to determine if it was upregulated or downregulated.

8. Bibliography

[1] Sowden R.G., Watson S.J., Jarvis P. (2018) The role of chloroplasts in plant pathology. *Essays Biochem.* **62**, 21–39

[2] Jarvis P., López-Juez E. (2013) Biogenesis and homeostasis of chloroplasts and other plastids. *Nat. Rev. Mol. Cell Biol.* **14**, 787–802

[3] Margulis L. (1970) The origin of eukaryotic cells. New Haven: Yale University Press; 1970.

[4] Keeling P.J. (2010) The endosymbiotic origin, diversification and fate of plastids. *Philos. Trans. R. Soc. Lond. B Biol. Sci.* **365**, 729–748

[5] Sadali N.M., Sowden R.G., Ling Q., Jarvis R.P. (2019) Differentiation of chromoplasts and other plastids in plants. *Plant Cell Rep.* **38**, 1–16

[6] Nakamura M., Nishimura T., Morita M.T. (2019) Gravity sensing and signal conversion in plant gravitropism. *J. Exp. Bot.* **70**, 3495–3506

[7] Suzuki T., Tsunekawa S., Koizuka C., Yamamoto K., Imamura J., Nakamura K., et al. (2013) Development and disintegration of tapetum-specific lipid-accumulating organelles, elaioplasts and tapetosomes, in Arabidopsis thaliana and Brassica napus. *Plant Sci.* **207**, 25–36

[8] Rolland N., Curien G., Finazzi G., Kuntz M., Marechal E., Matringe M., et al. (2012) The biosynthetic capacities of the plastids and integration between cytoplasmic and chloroplast processes. *Annu. Rev. Genet.* **46**, 233–264

[9] Daniell H., Lin C.S., Yu M., Chang W.J. (2016) Chloroplast genomes: Diversity, evolution, and applications in genetic engineering. *Genome Biol.* **17**, 1–29

[10] Tanz S.K., Castleden I., Hooper C.M., Vacher M., Small I., Millar H.A. (2013) SUBA3: a database for integrating experimentation and prediction to define the SUBcellular location of proteins in Arabidopsis. *Nucleic Acids Res.* **41**, D1185–D1191

[11] Woodson J.D., Chory J. (2012) Organelle signaling: how stressed chloroplasts communicate with the nucleus. *Curr. Biol.* **22**, R690–R692

[12] Chan K.X., Phua S.Y., Crisp P., Mcquinn R., Pogson B.J. (2016) Learning the Languages of the Chloroplast : Retrograde Signaling and Beyond. *Annu. Rev. Plant Biol.* **67**, 25–53

[13] Bobik K., Burch-Smith T.M. (2015) Chloroplast signaling within, between and beyond cells. *Front. Plant Sci.* **6**, 1–26

[14] Bradbeer J.W., Atkinson Y.E., Börner T., Hagemann R. (1979) Cytoplasmic synthesis of plastid polypeptides may be controlled by plastid-synthesized RNA.

Nature. **279**, 816–817

[15] Susek R.E., Ausubel F.M., Chory J. (1993) Signal transduction mutants of Arabidopsis uncouple nuclear CAB and RBCS gene expression from chloroplast development. *Cell.* **74**, 787–799

[16] Hernández-Verdeja T., Strand Å. (2018) Retrograde Signals Navigate the Path to Chloroplast Development. *Plant Physiol.* **176**, 967–976

[17] Wu G.-Z., Meyer E.H., Richter A.S., Schuster M., Ling Q., Schöttler M.A., et al. (2019) Control of retrograde signalling by protein import and cytosolic folding stress. *Nat. Plants.* **5**, 525–538

[18] Shimizu T., Mochizuki N., Nagatani A., Watanabe S., Shimada T., Tanaka K., et al. (2019) GUN1 regulates tetrapyrrole biosynthesis. *bioRxiv Preprint.*

[19] Zhao X., Huang J., Chory J. (2019) GUN1 interacts with MORF2 to regulate plastid RNA editing during retrograde signaling. *Proc. Natl. Acad. Sci. USA.* **116**, 10162–10167

[20] Ramel F., Birtic S., Ginies C., Soubigou-Taconnat L., Triantaphylides C., Havaux M. (2012) Carotenoid oxidation products are stress signals that mediate gene responses to singlet oxygen in plants. *Proc. Natl. Acad. Sci. USA.* **109**, 5535–5540

[21] Lee K.P., Kim C., Landgraf F., Apel K. (2007) EXECUTER1- and EXECUTER2-dependent transfer of stress-related signals from the plastid to the nucleus of Arabidopsis thaliana. *Proc. Natl. Acad. Sci. USA.* **104**, 10270–10275

[22] Dogra V., Duan J., Lee K.P., Lv S., Liu R., Kim C. (2017) FtsH2-Dependent Proteolysis of EXECUTER1 Is Essential in Mediating Singlet Oxygen-Triggered Retrograde Signaling in *Arabidopsis thaliana. Front. Plant Sci.* **8**, 1–7

[23] Xiao Y., Savchenko T., Baidoo E.E., Chehab W.E., Hayden D.M., Tolstikov V., et al. (2012) Retrograde signaling by the plastidial metabolite MEcPP regulates expression of nuclear stress-response genes. *Cell.* **149**, 1525–1535

[24] Lemos M., Xiao Y., Bjornson M., Wang J.-Z., Hicks D., De Souza A., et al. (2016) The plastidial retrograde signal methyl erythritol cyclopyrophosphate is a regulator of salicylic acid and jasmonic acid crosstalk. *J. Exp. Bot.* **67**, 1557–1566

[25] Estavillo G.M., Crisp P.A., Pornsiriwong W., Wirtz M., Collinge D., Carrie C., et al. (2011) Evidence for a SAL1-PAP chloroplast retrograde pathway that functions in drought and high light signaling in *Arabidopsis. Plant Cell.* **23**, 3992–4012

[26] Ishiga Y., Watanabe M., Ishiga T., Tohge T., Matsuura T., Ikeda Y., et al. (2017) The SAL-PAP chloroplast retrograde pathway contributes to plant immunity by regulating glucosinolate pathway and phytohormone singaling. *Mol. Plant.*

Microbe. Interact. **30**, 829–841

[27] von Heijne G., Nishikawa K. (1991) Chloroplast transit peptides the perfect random coil? *FEBS Lett.* **278**, 1–3

[28] Jarvis P. (2008) Targeting of nucleus-encoded proteins to chloroplasts in plants (Tansley Review). *New Phytol.* **179**, 257–285

[29] Li H.M., Teng Y.S. (2013) Transit peptide design and plastid import regulation. *Trends Plant Sci.* **18**, 360–366

[30] Lee D.W., Lee S., Lee J., Woo S., Razzak M.A., Vitale A., et al. (2019) Molecular Mechanism of the Specificity of Protein Import into Chloroplasts and Mitochondria in Plant Cells. *Mol. Plant.* **12**, 951–966

[31] Flores-Pérez U., Jarvis P. (2013) Molecular chaperone involvement in chloroplast protein import. *Biochim. Biophys. Acta.* **1833**, 332–340

[32] May T., Soll J. (2000) 14-3-3 proteins form a guidance complex with chloroplast precursor proteins in plants. *Plant Cell.* **12**, 53–64

[33] Fellerer C., Schweiger R., Schongruber K., Soll J., Schwenkert S. (2011) Cytosolic HSP90 cochaperones HOP and FKBP interact with freshly synthesized chloroplast preproteins of Arabidopsis. *Mol. Plant.* **4**, 1133–1145

[34] Schleiff E., Soll J., Küchler M., Kühlbrandt W., Harrer R. (2003) Characterization of the translocon of the outer envelope of chloroplasts. *J. Cell Biol.* **160**, 541–551

[35] Kikuchi S., Hirohashi T., Nakai M. (2006) Characterization of the preprotein translocon at the outer envelope membrane of chloroplasts by blue native PAGE. *Plant Cell Physiol.* **47**, 363–371

[36] Ivanova Y., Smith M.D., Chen K., Schnell D.J. (2004) Members of the Toc159 import receptor family represent distinct pathways for protein targeting to plastids. *Mol. Biol. Cell.* **15**, 3379–3392

[37] Kubis S., Baldwin A., Patel R., Razzaq A., Dupree P., Lilley K., et al. (2003) The Arabidopsis *ppi1* mutant is specifically defective in the expression, chloroplast import, and accumulation of photosynthetic proteins. *Plant Cell.* **15**, 1859–1871

[38] Kubis S., Patel R., Combe J., Bédard J., Kovacheva S., Lilley K., et al. (2004) Functional specialization amongst the Arabidopsis Toc159 family of chloroplast protein import receptors. *Plant Cell.* **16**, 2059–2077

[39] Kessler F., Schnell D.J. (2006) The function and diversity of plastid protein import pathways: a multilane GTPase highway into plastids. *Traffic.* **7**, 248–257

[40] Young M.E., Keegstra K., Froehlich J.E. (1999) GTP promotes the formation of

early-import intermediates but is not required during the translocation step of protein import into chloroplasts. *Plant Physiol.* **121**, 237–244

[41] Aronsson H., Combe J., Patel R., Agne B., Martin M., Kessler F., et al. (2010) Nucleotide binding and dimerization at the chloroplast pre-protein import receptor, atToc33, are not essential in vivo but do increase import efficiency. *Plant J.* **63**, 297–311

[42] Agne B., Infanger S., Wang F., Hofstetter V., Rahim G., Martin M., et al. (2009) A Toc159 import receptor mutant, defective in hydrolysis of GTP, supports preprotein import into chloroplasts. *J. Biol. Chem.* **284**, 8670–8679

[43] Paila Y.D., Richardson L.G.L., Schnell D.J. (2015) New insights into the mechanism of chloroplast protein import and its integration with protein quality control, organelle biogenesis and development. *J. Mol. Biol.* **427**, 1038–1060

[44] Richardson L.G., Small E.L., Inoue H., Schnell D.J. (2018) Molecular topology of the transit peptide during chloroplast protein import. *Plant Cell.* **30**, 1789–1806

[45] Bölter B. (2018) En route into chloroplasts: preproteins' way home. *Photosynth. Res.* **138**, 263–275

[46] Nakai M. (2018) New Perspectives on Chloroplast Protein Import. *Plant Cell Physiol.* **59**, 1111–1119

[47] Heins L., Mehrle A., Hemmler R., Wagner R., Küchler M., Hörmann F., et al. (2002) The preprotein conducting channel at the inner envelope membrane of plastids. *EMBO J.* **21**, 2616–2625

[48] Balsera M., Goetze T.A., Kovács-Bogdán E., Schürmann P., Wagner R., Buchanan B.B., et al. (2009) Characterization of Tic110, a channel-forming protein at the inner envelope membrane of chloroplasts, unveils a response to Ca2+ and a stromal regulatory disulfide bridge. *J. Biol. Chem.* **284**, 2603–2616

[49] Kikuchi S., Oishi M., Hirabayashi Y., Lee D.W., Hwang I., Nakai M. (2009) A 1-megadalton translocation complex containing Tic20 and Tic21 mediates chloroplast protein import at the inner envelope membrane. *Plant Cell.* **21**, 1781–1797

[50] Kikuchi S., Bédard J., Hirano M., Hirabayashi Y., Oishi M., Imai M., et al. (2013) Uncovering the protein translocon at the chloroplast inner envelope membrane. *Science*. **339**, 571–574

[51] Kovács-Bogdán E., Benz J.P., Soll J., Bölter B. (2011) Tic20 forms a channel independent of Tic110 in chloroplasts. *BMC Plant Biol.* **11**, 133

[52] Bédard J., Kubis S., Bimanadham S., Jarvis P. (2007) Functional similarity between

the chloroplast translocon component, Tic40, and the human co-chaperone, Hsp70-interacting protein (Hip). *J. Biol. Chem.* **282**, 21404–21414

[53] Chou M.L., Chu C.C., Chen L.J., Akita M., Li H.M. (2006) Stimulation of transit-peptide release and ATP hydrolysis by a cochaperone during protein import into chloroplasts. *J. Cell Biol.* **175**, 893–900

[54] de Vries J., Sousa F.L., Bölter B., Soll J., Gould S.B. (2015) YCF1: A Green TIC? *Plant Cell.* **27**, 1827–33

[55] Bölter B., Soll J. (2017) Ycf1/Tic214 Is Not Essential for the Accumulation of Plastid Proteins. *Mol. Plant.* **10**, 219–221

[56] Kasmati A.R., Töpel M., Patel R., Murtaza G., Jarvis P. (2011) Molecular and genetic analyses of Tic20 homologues in Arabidopsis thaliana chloroplasts. *Plant J.* **66**, 877–889

[57] Hirabayashi Y., Kikuchi S., Oishi M., Nakai M. (2011) In vivo studies on the roles of two closely related arabidopsis Tic20 proteins, AtTic20-I and AtTic20-IV. *Plant Cell Physiol.* **52**, 469–478

[58] Chen L.-J., Li H. (2017) Stable megadalton TOC-TIC supercomplexes as major mediators of protein import into chloroplasts. *Plant J.* **92**, 178–188

[59] Chen Y.-L., Chen L.-J., Chu C.-C., Huang P.-K., Wen J.-R., Li H. (2018) TIC236 links the outer and inner membrane translocons of the chloroplast. *Nature.* **564**, 125–129

[60] Selkrig J., Mosbahi K., Webb C.T., Belousoff M.J., Perry A.J., Wells T.J., et al. (2012) Discovery of an archetypal protein transport system in bacterial outer membranes. *Nat. Struct. Mol. Biol.* **19**, 506–510

[61] Rudolf M., Machettira A.B., Groß L.E., Weber K.L., Bolte K., Bionda T., et al. (2013) In vivo function of Tic22, a protein import component of the intermembrane space of chloroplasts. *Mol. Plant.* **6**, 817–29

[62] Kasmati A.R., Töpel M., Khan N.Z., Patel R., Ling Q., Karim S., et al. (2013) Evolutionary, molecular and genetic analyses of Tic22 homologues in Arabidopsis thaliana chloroplasts. *PLoS One.* **8**, e63863

[63] Richter S., Lamppa G.K. (1999) Stromal processing peptidase binds transit peptides and initiates their ATP-dependent turnover in chloroplasts. *J. Cell Biol.* **147**, 33–43

[64] Richter S., Lamppa G.K. (2003) Structural properties of the chloroplast stromal processing peptidase required for its function in transit peptide removal. *J. Biol. Chem.* **278**, 39497–39502

[65] Kmiec B., Teixeira P.F., Glaser E. (2014) Shredding the signal: targeting peptide degradation in mitochondria and chloroplasts. *Trends Plant Sci.* **19**, 771–778

[66] Teixeira P.F., Kmiec B., Branca R.M.M., Murcha M.W., Byzia A., Ivanova A., et al. (2017) A multi-step peptidolytic cascade for amino acid recovery in chloroplasts. *Nat. Chem. Biol.* **13**, 15–17

[67] Trösch R., Jarvis P. (2011) The stromal processing peptidase of chloroplasts is essential in Arabidopsis, with knockout mutations causing embryo arrest after the 16-cell stage. *PLoS One.* **6**, e23039

[68] Kmiec B., Branca R.M.M., Berkowitz O., Li L., Wang Y., Murcha M.W., et al. (2018) Accumulation of endogenous peptides triggers a pathogen stress response in *Arabidopsis thaliana*. *Plant J.* **96**, 705–715

[69] Shi L.X., Theg S.M. (2013) Energetic cost of protein import across the envelope membranes of chloroplasts. *Proc. Natl. Acad. Sci. USA.* **110**, 930–935

[70] Nielsen E., Akita M., Davila-Aponte J., Keegstra K. (1997) Stable association of chloroplastic precursors with protein translocation complexes that contain proteins from both envelope membranes and a stromal Hsp100 molecular chaperone. *EMBO J.* **16**, 935–946

[71] Flores-Pérez Ú., Bédard J., Tanabe N., Lymperopoulos P., Clarke A.K., Jarvis P. (2016) Functional Analysis of the Hsp93/ClpC Chaperone at the Chloroplast Envelope. *Plant Physiol.* **170**, 147–162

[72] Kovacheva S., Bédard J., Patel R., Dudley P., Twell D., Ríos G., et al. (2005) In vivo studies on the roles of Tic110, Tic40 and Hsp93 during chloroplast protein import. *Plant J.* **41**, 412–428

[73] Sjögren L.L.E., Tanabe N., Lymperopoulos P., Khan N.Z., Rodermel S.R., Aronsson H., et al. (2014) Quantitative analysis of the chloroplast molecular chaperone ClpC/Hsp93 in Arabidopsis reveals new insights into its localization, interaction with the Clp proteolytic core, and functional importance. *J. Biol. Chem.* **289**, 11318–11330

[74] Su P.H., Li H.M. (2010) Stromal Hsp70 is important for protein translocation into pea and Arabidopsis chloroplasts. *Plant Cell.* **22**, 1516–1531

[75] Shi L.X., Theg S.M. (2010) A stromal heat shock protein 70 system functions in protein import into chloroplasts in the moss Physcomitrella patens. *Plant Cell.* **22**, 205–220

[76] Huang P.-K., Chan P.-T., Su P.-H., Chen L.-J., Li H. (2016) Chloroplast Hsp93 Directly Binds to Transit Peptides at an Early Stage of the Preprotein Import

Process. *Plant Physiol.* **170**, 857–866

[77] Liu L., McNeilage R.T., Shi L., Theg S.M. (2014) ATP Requirement for Chloroplast Protein Import Is Set by the K_m for ATP Hydrolysis of Stromal Hsp70 in *Physcomitrella patens*. *Plant Cell.* **26**, 1246–1255

[78] Kikuchi S., Asakura Y., Imai M., Nakahira Y., Kotani Y., Hashiguchi Y., et al. (2018) A Ycf2-FtsHi Heteromeric AAA-ATPase Complex Is Required for Chloroplast Protein Import. *Plant Cell.* **30**, 2677–2703

[79] Bae W., Lee Y.J., Kim D.H., Lee J., Kim S., Sohn E.J., et al. (2008) AKR2A-mediated import of chloroplast outer membrane proteins is essential for chloroplast biogenesis. *Nat. Cell Biol.* **10**, 220–227

[80] Kim D.H., Park M.J., Gwon G.H., Silkov A., Xu Z.Y., Yang E.C., et al. (2014) An ankyrin repeat domain of AKR2 drives chloroplast targeting through coincident binding of two chloroplast lipids. *Dev. Cell.* **30**, 598–609

[81] Tu S.L., Chen L.J., Smith M.D., Su Y.S., Schnell D.J., Li H.M. (2004) Import pathways of chloroplast interior proteins and the outer-membrane protein OEP14 converge at Toc75. *Plant Cell.* **16**, 2078–2088

[82] Dhanoa P.K., Richardson L.G., Smith M.D., Gidda S.K., Henderson M.P., Andrews D.W., et al. (2010) Distinct pathways mediate the sorting of tail-anchored proteins to the plastid outer envelope. *PLoS One.* **5**, e10098

[83] Tripp J., Inoue K., Keegstra K., Froehlich J.E. (2007) A novel serine/proline-rich domain in combination with a transmembrane domain is required for the insertion of AtTic40 into the inner envelope membrane of chloroplasts. *Plant J.* **52**, 824–838

[84] Li Y., Martin J.R., Aldama G.A., Fernandez D.E., Cline K. (2017) Identification of Putative Substrates of SEC2, a Chloroplast Inner Envelope Translocase. *Plant Physiol.* **173**, 2121–2137

[85] Viana A.A., Li M., Schnell D.J. (2010) Determinants for stop-transfer and post-import pathways for protein targeting to the chloroplast inner envelope membrane. *J. Biol. Chem.* **285**, 12948–12960

[86] Spiess M., Junne T., Janoschke M. (2019) Membrane Protein Integration and Topogenesis at the ER. *Protein J.* **33**, 306–316

[87] Neupert W., Herrmann J.M. (2007) Translocation of Proteins into Mitochondria. *Annu. Rev. Biochem.* **76**, 723–749

[88] Stuart R.A. (2002) Insertion of proteins into the inner membrane of mitochondria: the role of the Oxa1 complex. *Biochim. Biophys. Acta - Mol. Cell Res.* **1592**, 79–87

[89] Hennon S.W., Soman R., Zhu L., Dalbey R.E. (2015) YidC/Alb3/Oxa1 family of insertases. *J. Biol. Chem.* **290**, 14866–14874

[90] Gerdes L., Bals T., Klostermann E., Karl M., Philippar K., Hunken M., et al. (2006) A second thylakoid membrane-localized Alb3/OxaI/YidC homologue is involved in proper chloroplast biogenesis in Arabidopsis thaliana. *J. Biol. Chem.* **281**, 16632–16642

[91] Nada A., Soll J. (2004) Inner envelope protein 32 is imported into chloroplasts by a novel pathway. *J. Cell Sci.* **117**, 3975–3982

[92] Miras S., Salvi D., Ferro M., Grunwald D., Garin J., Joyard J., et al. (2002) Non-canonical transit peptide for import into the chloroplast. *J. Biol. Chem.* **277**, 47770–8

[93] Miras S., Salvi D., Piette L., Seigneurin-Berny D., Grunwald D., Reinbothe C., et al. (2007) Toc159- and Toc75-independent import of a transit sequence-less precursor into the inner envelope of chloroplasts. *J. Biol. Chem.* **282**, 29482–29492

[94] Villarejo A., Buren S., Larsson S., Dejardin A., Monne M., Rudhe C., et al. (2005) Evidence for a protein transported through the secretory pathway en route to the higher plant chloroplast. *Nat. Cell Biol.* **7**, 1124–1131

[95] Nanjo Y., Oka H., Ikarashi N., Kaneko K., Kitajima A., Mitsui T., et al. (2006) Rice plastidial N-glycosylated nucleotide pyrophosphatase/phosphodiesterase is transported from the ER-golgi to the chloroplast through the secretory pathway. *Plant Cell.* **18**, 2582–2592

[96] Asatsuma S., Sawada C., Itoh K., Okito M., Kitajima A., Mitsui T. (2005) Involvement of alpha-amylase I-1 in starch degradation in rice chloroplasts. *Plant Cell Physiol.* **46**, 858–869

[97] Lehtimäki N., Koskela M.M., Mulo P. (2015) Post-translational modifications of chloroplast proteins: An emerging field. *Plant Physiol.* **168**, pp.00117.2015

[98] Kitajima A., Asatsuma S., Okada H., Hamada Y., Kaneko K., Nanjo Y., et al. (2009) The rice alpha-amylase glycoprotein is targeted from the Golgi apparatus through the secretory pathway to the plastids. *Plant Cell.* **21**, 2844–2858

[99] Radhamony R.N., Theg S.M. (2006) Evidence for an ER to Golgi to chloroplast protein transport pathway. *Trends Cell Biol.* **16**, 385–387

[100] Goldstein G., Scheid M., Hammerling U., Schlesinger D.H., Niall H.D., Boyse E.A. (1975) Isolation of a polypeptide that has lymphocyte-differentiating properties and is probably represented universally in living cells. *Proc. Natl. Acad. Sci. USA.* **72**, 11–5

[101] Hershko A., Ciechanover A. (1998) The Ubiquitin System. *Annu. Rev. Biochem.* **67**, 425–479

[102] Hoppe T. (2005) Multiubiquitylation by E4 enzymes: "One size" doesn't fit all. *Trends Biochem. Sci.* **30**, 183–187

[103] Amerik A.Y., Hochstrasser M. (2004) Mechanism and function of deubiquitinating enzymes. *Biochim. Biophys. Acta - Mol. Cell Res.* **1695**, 189–207

[104] Pickart C.M. (2004) Back to the Future with Ubiquitin. *Cell.* **116**, 181–190

[105] Chen L., Hellmann H. (2013) Plant E3 ligases: Flexible enzymes in a sessile world. *Mol. Plant.* **6**, 1388–1404

[106] Hatfield P.M., Gosink M.M., Carpenter T.B., Vierstra R.D. (1997) The ubiquitin-activating enzyme (E1) gene family in Arabidopsis thaliana. *Plant J.* **11**, 213–226

[107] Kraft E., Stone S.L., Ma L., Su N., Gao Y., Lau O.-S., et al. (2005) Genome analysis and functional characterization of the E2 and RING-type E3 ligase ubiquitination enzymes of Arabidopsis. *Plant Physiol.* **139**, 1597–1611

[108] Brooks C.L., Gu W. (2011) p53 regulation by ubiquitin. *FEBS Lett.* **585**, 2803–2809

[109] Terrell J., Shih S., Dunn R., Hicke L. (1998) A Function for Monoubiquitination in the Internalization of a G Protein–Coupled Receptor. *Mol. Cell.* **1**, 193–202

[110] Spence J., Gali R.R., Dittmar G., Sherman F., Karin M., Finley D. (2000) Cell Cycle–Regulated Modification of the Ribosome by a Variant Multiubiquitin Chain. *Cell.* **102**, 67–76

[111] Nathan J.A., Kim H.T., Ting L., Gygi S.P., Goldberg A.L. (2013) Why do cellular proteins linked to K63-polyubiquitin chains not associate with proteasomes? *EMBO J.* **32**, 552–565

[112] Chen J., Chen Z.J. (2013) Regulation of NF-κB by ubiquitination. *Curr. Opin. Immunol.* **25**, 4–12

[113] Schwertman P., Bekker-Jensen S., Mailand N. (2016) Regulation of DNA double-strand break repair by ubiquitin and ubiquitin-like modifiers. *Nat. Rev. Mol. Cell Biol.* **17**, 379–394

[114] Piper R.C., Dikic I., Lukacs G.L. (2014) Ubiquitin-dependent sorting in endocytosis. *Cold Spring Harb. Perspect. Biol.* **6**

[115] Komander D., Rape M. (2012) The Ubiquitin Code. *Annu. Rev. Biochem.* **81**, 203–229

[116] Finley D. (2009) Recognition and processing of ubiquitin-protein conjugates by

the proteasome. *Annu. Rev. Biochem.* **78**, 477–513

[117] Chen S., Wu J., Lu Y., Ma Y.-B., Lee B.-H., Yu Z., et al. (2016) Structural basis for dynamic regulation of the human 26S proteasome. *Proc. Natl. Acad. Sci. USA.* **113**, 12991–12996

[118] Kleijnen M.F., Roelofs J., Park S., Hathaway N.A., Glickman M., King R.W., et al. (2007) Stability of the proteasome can be regulated allosterically through engagement of its proteolytic active sites. *Nat. Struct. Mol. Biol.* **14**, 1180–1188

[119] Livneh I., Cohen-Kaplan V., Cohen-Rosenzweig C., Avni N., Ciechanover A. (2016) The life cycle of the 26S proteasome: from birth, through regulation and function, and onto its death. *Cell Res.* **26**, 869–885

[120] Rousseau A., Bertolotti A. (2018) Regulation of proteasome assembly and activity in health and disease. *Nat. Rev. Mol. Cell Biol.* **19**, 697–712

[121] VerPlank J.J.S., Goldberg A.L. (2018) Exploring the Regulation of Proteasome Function by Subunit Phosphorylation. In: Methods in molecular biology (Clifton, N.J.). 2018. p. 309–319.

[122] Shen G., Adam Z., Zhang H. (2007) The E3 ligase AtCHIP ubiquitylates FtsH1, a component of the chloroplast FtsH protease, and affects protein degradation in chloroplasts. *Plant J.* **52**, 309–321

[123] Shen G., Yan J., Pasapula V., Luo J., He C., Clarke A.K., et al. (2007) The chloroplast protease subunit ClpP4 is a substrate of the E3 ligase AtCHIP and plays an important role in chloroplast function. *Plant J.* **49**, 228–237

[124] Lee S.S., Lee D.W., Lee Y., Mayer U., Stierhof Y.-D.D., Jurgens G., et al. (2009) Heat shock protein cognate 70-4 and an E3 ubiquitin ligase, CHIP, mediate plastid-destined precursor degradation through the ubiquitin-26S proteasome system in Arabidopsis. *Plant Cell.* **21**, 3984–4001

[125] Wei J., Qiu X., Chen L., Hu W., Hu R., Chen J., et al. (2015) The E3 ligase AtCHIP positively regulates Clp proteolytic subunit homeostasis. *J. Exp. Bot.* **66**, 5809–5820

[126] Ling Q., Huang W., Baldwin A., Jarvis P. (2012) Chloroplast biogenesis is regulated by direct action of the ubiquitin-proteasome system. *Science.* **338**, 655–659

[127] Jarvis P., Chen L.J., Li H., Peto C. a, Fankhauser C., Chory J. (1998) An *Arabidopsis* mutant defective in the plastid general protein import apparatus. *Science.* **282**, 100–103

[128] Ling Q., Jarvis P. (2015) Regulation of Chloroplast Protein Import by the Ubiquitin E3 Ligase SP1 Is Important for Stress Tolerance in Plants. *Curr. Biol.* **25**, 2527–2534

[129] Kelley D.R., Estelle M. (2012) Ubiquitin-Mediated Control of Plant Hormone Signaling. *Plant Physiol.* **160**, 47–55

[130] Sadanandom A., Bailey M., Ewan R., Lee J., Nelis S. (2012) The ubiquitin-proteasome system: central modifier of plant signalling. *New Phytol.* **196**, 13–28

[131] Dong O.X., Ao K., Xu F., Johnson K.C.M., Wu Y., Li L., et al. (2018) Individual components of paired typical NLR immune receptors are regulated by distinct E3 ligases. *Nat. Plants.* **4**, 699–710

[132] Wang T., Chang C., Gu C., Tang S., Xie Q., Shen Q.-H. (2016) An E3 Ligase Affects the NLR Receptor Stability and Immunity to Powdery Mildew. *Plant Physiol.* **172**, 2504–2515

[133] Ruggiano A., Foresti O., Carvalho P. (2014) ER-associated degradation: Protein quality control and beyond. *J. Cell Biol.* **204**, 869–879

[134] Schoebel S., Mi W., Stein A., Ovchinnikov S., Pavlovicz R., DiMaio F., et al. (2017) Cryo-EM structure of the protein-conducting ERAD channel Hrd1 in complex with Hrd3. *Nature.* **548**, 352–355

[135] Neal S., Jaeger P.A., Duttke S.H., Benner C., K Glass C., Ideker T., et al. (2018) The Dfm1 Derlin Is Required for ERAD Retrotranslocation of Integral Membrane Proteins. *Mol. Cell.* **69**, 306-320.e4

[136] Heo J.M., Livnat-Levanon N., Taylor E.B., Jones K.T., Dephoure N., Ring J., et al. (2010) A stress-responsive system for mitochondrial protein degradation. *Mol. Cell.* **40**, 465–480

[137] Deruyffelaere C., Purkrtova Z., Bouchez I., Collet B., Cacas J. (2018) PUX10 associates with CDC48A and regulates the dislocation of ubiquitinated oleosins from seed lipid droplets. *Plant Cell.*

[138] Kretzschmar F.K., Mengel L.F., Müller A., Schmitt K., Blersch K.F., Valerius O., et al. (2018) PUX10 is a lipid droplet-localized scaffold protein that interacts with CDC48 and is involved in the degradation of lipid droplet proteins. *Plant Cell.* , tpc.00276.2018

[139] Foresti O., Rodriguez-Vaello V., Funaya C., Carvalho P. (2014) Quality control of inner nuclear membrane proteins by the Asi complex. *Science.* **346**, 751–755

[140] Schmidt O., Weyer Y., Baumann V., Widerin M.A., Eising S., Angelova M., et al. (2019) Endosome and Golgi-associated degradation (EGAD) of membrane proteins regulates sphingolipid metabolism. *EMBO J.* , e101433

[141] Ling Q., Jarvis P. (2013) Dynamic regulation of endosymbiotic organelles by ubiquitination. *Trends Cell Biol.* **23**, 399–408

[142] Geisler S., Vollmer S., Golombek S., Kahle P.J. (2014) The ubiquitin-conjugating enzymes UBE2N, UBE2L3 and UBE2D2/3 are essential for Parkin-dependent mitophagy. *J. Cell Sci.* **127**, 3280–3293

[143] Ambivero C.T., Cilenti L., Main S., Zervos A.S. (2014) Mulan E3 ubiquitin ligase interacts with multiple E2 conjugating enzymes and participates in mitophagy by recruiting GABARAP. *Cell Signal.* **26**, 2921–2929

[144] Nakamura N., Kimura Y., Tokuda M., Honda S., Hirose S. (2006) MARCH-V is a novel mitofusin 2- and Drp1-binding protein able to change mitochondrial morphology. *EMBO Rep.* **7**, 1019–1022

[145] Karbowski M., Neutzner A., Youle R.J. (2007) The mitochondrial E3 ubiquitin ligase MARCH5 is required for Drp1 dependent mitochondrial division. *J. Cell Biol.* **178**, 71–84

[146] Leboucher G.P., Tsai Y.C., Yang M., Shaw K.C., Zhou M., Veenstra T.D., et al. (2012) Stress-induced phosphorylation and proteasomal degradation of mitofusin 2 facilitates mitochondrial fragmentation and apoptosis. *Mol. Cell.* **47**, 547–557

[147] Benard G., Neutzner A., Peng G., Wang C., Livak F., Youle R.J., et al. (2010) IBRDC2, an IBR-type E3 ubiquitin ligase, is a regulatory factor for Bax and apoptosis activation. *EMBO J.* **29**, 1458–1471

[148] Bragoszewski P., Wasilewski M., Sakowska P., Gornicka A., Böttinger L., Qiu J., et al. (2015) Retro-translocation of mitochondrial intermembrane space proteins. *Proc. Natl. Acad. Sci. USA.* **112**, 7713–8

[149] Mårtensson C.U., Priesnitz C., Song J., Ellenrieder L., Doan K.N., Boos F., et al. (2019) Mitochondrial protein translocation-associated degradation. *Nature.* **569**, 679–683

[150] Schuberth C., Buchberger A. (2005) Membrane-bound Ubx2 recruits Cdc48 to ubiquitin ligases and their substrates to ensure efficient ER-associated protein degradation. *Nat. Cell Biol.* **7**, 999–1006

[151] Nishimasu R., Komori H., Higuchi Y., Nishimasu H., Hiroaki H. (2010) Crystal structure of a PFU-PUL domain pair of Saccharomyces cerevisiae Doa1/Ufd3. *Kobe J. Med. Sci.* **56**, E125-39

[152] Wu X., Li L., Jiang H. (2016) Doa1 targets ubiquitinated substrates for mitochondria-associated degradation. *J. Cell Biol.* **213**, 49–63

[153] Esaki M., Ogura T. (2012) Cdc48p/p97-mediated regulation of mitochondrial morphology is Vms1p-independent. *J. Struct. Biol.* **179**, 112–120

[154] Ling Q., Broad W., Trösch R., Töpel M., Demiral Sert T., Lymperopoulos P., et al.

(2019) Ubiquitin-dependent chloroplast-associated protein degradation in plants. *Science*. **363**, eaav4467

[155] Gentle I., Gabriel K., Beech P., Waller R., Lithgow T. (2004) The Omp85 family of proteins is essential for outer membrane biogenesis in mitochondria and bacteria. *J. Cell Biol.* **164**, 19–24

[156] Wallas T.R., Smith M.D., Sanchez-Nieto S., Schnell D.J. (2003) The roles of Toc34 and Toc75 in targeting the Toc159 preprotein receptor to chloroplasts. *J. Biol. Chem.* **278**, 44289–44297

[157] Wrzaczek M., Brosché M., Kangasjärvi J. (2013) ROS signaling loops - production, perception, regulation. *Curr. Opin. Plant Biol.* **16**, 575–582

[158] Gapper C., Dolan L. (2006) Control of Plant Development by Reactive Oxygen Species. *Plant Physiol.* **141**, 341–345

[159] Demidchik V. (2015) Mechanisms of oxidative stress in plants: From classical chemistry to cell biology. *Environ. Exp. Bot.* **109**, 212–228

[160] Asada K. (2006) Production and scavenging of reactive oxygen species in chloroplasts and their functions. *Plant Physiol.* **141**, 391–396

[161] Gill S.S., Tuteja N. (2010) Reactive oxygen species and antioxidant machinery in abiotic stress tolerance in crop plants. *Plant Physiol. Biochem.* **48**, 909–930

[162] Endo T., Uebayashi N., Ishida S., Ikeuchi M., Sato F. (2014) Light energy allocation at PSII under field light conditions: How much energy is lost in NPQ-associated dissipation? *Plant Physiol. Biochem.* **81**, 115–120

[163] de Bianchi S., Ballottari M., Dall'osto L., Bassi R. (2010) Regulation of plant light harvesting by thermal dissipation of excess energy. *Biochem. Soc. Trans.* **38**, 651–660

[164] Ruban A. V. (2016) Nonphotochemical Chlorophyll Fluorescence Quenching: Mechanism and Effectiveness in Protecting Plants from Photodamage. *Plant Physiol.* **170**, 1903–1916

[165] Ling Q., Jarvis P. (2015) Regulation of chloroplast protein import by the ubiquitin E3 ligase SP1 is important for stress tolerance in plants. *Curr. Biol.* **25**, 2527–2534

[166] Taylor N.L., Tan Y.F., Jacoby R.P., Millar A.H. (2009) Abiotic environmental stress induced changes in the *Arabidopsis thaliana* chloroplast, mitochondria and peroxisome proteomes. *J. Proteomics.* **72**, 367–378

[167] Meyer Y., Siala W., Bashandy T., Riondet C., Vignols F., Reichheld J.P. (2008) Glutaredoxins and thioredoxins in plants. *Biochim. Biophys. Acta - Mol. Cell Res.*

1783, 589–600

[168] Nikkanen L., Toivola J., Diaz M.G., Rintamäki E. (2017) Chloroplast thioredoxin systems: prospects for improving photosynthesis. *Philos. Trans. R. Soc. Lond. B. Biol. Sci.* **372**

[169] Gelhaye E., Rouhier N., Navrot N., Jacquot J.P. (2005) The plant thioredoxin system. *Cell. Mol. Life Sci.* **62**, 24–35

[170] König J., Baier M., Horling F., Kahmann U., Harris G., Schürmann P., et al. (2002) The plant-specific function of 2-Cys peroxiredoxin-mediated detoxification of peroxides in the redox-hierarchy of photosynthetic electron flux. *Proc. Natl. Acad. Sci. USA*. **99**, 5738–5743

[171] Szymańska R., Kruk J. (2010) Plastoquinol is the main prenyllipid synthesized during acclimation to high light conditions in *Arabidopsis* and is converted to plastochromanol by tocopherol cyclase. *Plant Cell Physiol.* **51**, 537–545

[172] Munné-Bosch S. (2005) The role of α-tocopherol in plant stress tolerance. *J. Plant Physiol.* **162**, 743–748

[173] Das K., Roychoudhury A. (2014) Reactive oxygen species (ROS) and response of antioxidants as ROS-scavengers during environmental stress in plants. *Front. Environ. Sci.* **2**, 1–13

[174] Pulido P., Llamas E., Rodriguez-Concepcion M. (2017) Both Hsp70 chaperone and Clp protease plastidial systems are required for protection against oxidative stress. *Plant Signal. Behav.* **12**, e129003

[175] Theis J., Schroda M. (2016) Revisiting the Photosystem II Repair Cycle. *Plant Signal. Behav.* **11**, e1218587

[176] Kato Y., Sun X., Zhang L., Sakamoto W. (2012) Cooperative D1 degradation in the photosystem II repair mediated by chloroplastic proteases in *Arabidopsis*. *Plant Physiol.* **159**, 1428–39

[177] Chiba A., Ishida H., Nishizawa N.K., Makino A., Mae T. (2003) Exclusion of ribulose-1,5-bisphosphate carboxylase/oxygenase from chloroplasts by specific bodies in naturally senescing leaves of wheat. *Plant Cell Physiol.* **44**, 914–921

[178] Ishida H., Yoshimoto K., Izumi M., Reisen D., Yano Y., Makino A., et al. (2008) Mobilization of rubisco and stroma-localized fluorescent proteins of chloroplasts to the vacuole by an ATG gene-dependent autophagic process. *Plant Physiol.* **148**, 142–155

[179] Izumi M., Ishida H., Nakamura S., Hidema J. (2017) Entire Photodamaged Chloroplasts Are Transported to the Central Vacuole by Autophagy. *Plant Cell.* **29**,

377–394

[180] Foyer C.H., LopezDelgado H., Dat J.F., Scott I.M. (1997) Hydrogen peroxide- and glutathione-associated mechanisms of acclimatory stress tolerance and signalling. *Physiol. Plant.* **100**, 241–254

[181] Woodson J.D., Joens M.S., Sinson A.B., Gilkerson J., Salomé P. a, Weigel D., et al. (2015) Ubiquitin facilitates a quality-control pathway that removes damaged chloroplasts. *Science.* **350**, 450–454

[182] Thompson A.R., Doelling J.H., Suttangkakul A., Vierstra R.D. (2005) Autophagic nutrient recycling in *Arabidopsis* directed by the ATG8 and ATG12 conjugation pathways. *Plant Physiol.* **138**, 2097–2110

[183] Nakatogawa H. (2013) Two ubiquitin-like conjugation systems that mediate membrane formation during autophagy. *Essays Biochem.* **55**, 39–50

[184] Shpilka T., Weidberg H., Pietrokovski S., Elazar Z. (2011) Atg8: an autophagy-related ubiquitin-like protein family. *Genome Biol.* **12**, 1–11

[185] Izumi M., Hidema J., Wada S., Kondo E., Kurusu T., Kuchitsu K., et al. (2015) Establishment of monitoring methods for autophagy in rice reveals autophagic recycling of chloroplasts and root plastids during energy limitation. *Plant Physiol.* **167**, 1307–1320

[186] Wittenbach V.A., Lin W., Hebert R.R. (1982) Vacuolar localization of proteases and degradation of chloroplasts in mesophyll protoplasts from senescing primary wheat leaves. *Plant Physiol.* **69**, 98–102

[187] Lee K.P., Kim C., Landgraf F., Apel K. (2007) EXECUTER1- and EXECUTER2-dependent transfer of stress-related signals from the plastid to the nucleus of *Arabidopsis thaliana*. *Proc. Natl. Acad. Sci. USA.* **104**, 10270–10275

[188] Choi H.W., Klessig D.F. (2016) DAMPs, MAMPs, and NAMPs in plant innate immunity. *BMC Plant Biol.* **16**, 1–10

[189] Gill U.S., Lee S., Mysore K.S. (2015) Host Versus Nonhost Resistance: Distinct Wars with Similar Arsenals. *Phytopathology.* **105**, 580–587

[190] Chinchilla D., Bauer Z., Regenass M., Boller T., Felix G. (2006) The *Arabidopsis* receptor kinase FLS2 binds flg22 and determines the specificity of flagellin perception. *Plant Cell.* **18**, 465–476

[191] Segonzac C., Zipfel C. (2011) Activation of plant pattern-recognition receptors by bacteria. *Curr. Opin. Microbiol.* **14**, 54–61

[192] Wu S., Shan L., He P. (2014) Microbial signature-triggered plant defense responses

and early signaling mechanisms. *Plant Sci.* **228**, 118–126

[193] Göhre V., Jones A.M.E., Sklenář J., Robatzek S., Weber A.P.M. (2012) Molecular Crosstalk Between PAMP-Triggered Immunity and Photosynthesis. *Mol. Plant. Microbe. Interact.* **25**, 1083–1092

[194] Li B., Meng X., Shan L., He P. (2016) Transcriptional Regulation of Pattern-Triggered Immunity in Plants. *Cell Host Microbe.* **19**, 641–650

[195] Melotto M., Underwood W., He S.Y. (2008) Role of Stomata in Plant Innate Immunity and Foliar Bacterial Diseases. *Annu. Rev. Phytopathol.* **46**, 101–122

[196] Daszkowska-Golec A., Szarejko I. (2013) Open or Close the Gate – Stomata Action Under the Control of Phytohormones in Drought Stress Conditions. *Front. Plant Sci.* **4**, 1–16

[197] Voigt C.A. (2014) Callose-mediated resistance to pathogenic intruders in plant defense-related papillae. *Front. Plant Sci.* **5**, 1–6

[198] Sawada H., Suzuki F., Matsuda I., Saitou N. (1999) Phylogenetic analysis of *Pseudomonas syringae* pathovars suggests the horizontal gene transfer of *argK* and the evolutionary stability of *hrp* gene cluster. *J. Mol. Evol.* **49**, 627–644

[199] Dodds P.N., Rathjen J.P. (2010) Plant immunity: towards an integrated view of plant-pathogen interactions. *Nat. Rev. Genet.* **11**, 539–548

[200] Jia Y., McAdams S.A., Bryan G.T., Hershey H.P., Valent B. (2000) Direct interaction of resistance gene and avirulence gene products confers rice blast resistance. *EMBO J.* **19**, 4004–4014

[201] Chen Y., Liu Z., Halterman D.A. (2012) Molecular Determinants of Resistance Activation and Suppression by Phytophthora infestans Effector IPI-O. *PLoS Pathog.* **8**, e1002595

[202] Lee H.-A., Yeom S.-I. (2015) Plant NB-LRR proteins: tightly regulated sensors in a complex manner. *Brief. Funct. Genomics.* **14**, 233–242

[203] Jones J.D.G., Dangl J.L. (2006) The plant immune system. *Nature.* **444**, 323–329

[204] Van Der Hoorn R.A.L., Kamoun S. (2008) From guard to decoy: A new model for perception of plant pathogen effectors. *Plant Cell.* **20**, 2009–2017

[205] Henry E., Yadeta K.A., Coaker G. (2014) Recognition of bacterial plant pathogens: local, systemic and trangenerational immunity. *Biophys. Chem.* **257**, 2432–2437

[206] Gouveia B.C., Calil I.P., Machado J.P.B., Santos A.A., Fontes E.P.B. (2017) Immune receptors and co-receptors in antiviral innate immunity in plants. *Front. Microbiol.* **7**, 1–14

[207] Katagiri F., Thilmony R., He S.Y. (2002) The *Arabidopsis thaliana-Pseudomonas syringae* Interaction. *Arabidopsis Book.* **1**, e0039

[208] Glazebrook J. (2005) Contrasting Mechanisms of Defense Against Biotrophic and Necrotrophic Pathogens. *Annu. Rev. Phytopathol.* **43**, 205–227

[209] Lee S.-J., Rose J.K.C. (2010) Mediation of the transition from biotrophy to necrotrophy in hemibiotrophic plant pathogens by secreted effector proteins. *Plant Signal. Behav.* **5**, 769–772

[210] Roine E., Wei W., Yuan J., Nurmiaho-Lassila E.L., Kalkkinen N., Romantschuk M., et al. (1997) Hrp pilus: an hrp-dependent bacterial surface appendage produced by *Pseudomonas syringae* pv. *tomato* DC3000. *Proc. Natl. Acad. Sci. USA.* **94**, 3459–3464

[211] Deng W.L., Preston G., Collmer A., Chang C.J., Huang H.C. (1998) Characterization of the hrpC and hrpRS operons of Pseudomonas syringae pathovars syringae, tomato, and glycinea and analysis of the ability of hrpF, hrpG, hrcC, hrpT, and hrpV mutants to elicit the hypersensitive response and disease in plants. *J. Bacteriol.* **180**, 4523–4531

[212] Kim M.G., Geng X., Lee S.Y., Mackey D. (2009) The *Pseudomonas syringae* type III effector AvrRpm1 induces significant defenses by activating the Arabidopsis nucleotide-binding leucine-rich repeat protein RPS2. *Plant J.* **57**, 645–653

[213] Saucet S.B., Ma Y., Sarris P.F., Furzer O.J., Sohn K.H., Jones J.D.G. (2015) Two linked pairs of *Arabidopsis* TNL resistance genes independently confer recognition of bacterial effector AvrRps4. *Nat. Commun.* **6**, 1–12

[214] Finkelstein R. (2013) Abscisic Acid synthesis and response. *Arabidopsis Book.* **11**, e0166

[215] Hedden P., Thomas S.G. (2012) Gibberellin biosynthesis and its regulation. *Biochem. J.* **444**, 11–25

[216] Mano Y., Nemoto K. (2012) The pathway of auxin biosynthesis in plants. *J. Exp. Bot.* **63**, 2853–2872

[217] León J., Sánchez-Serrano J.J. (1999) Molecular biology of jasmonic acid biosynthesis in plants. *Plant Physiol. Biochem.* **37**, 373–380

[218] Hyun Y., Lee I. (2008) Generating and maintaining jasmonic acid in *Arabidopsis*. *Plant Signal. Behav.* **3**, 798–800

[219] Dempsey D.A., Vlot C.A., Wildermuth M.C., Klessig D.F. (2011) Salicylic acid biosynthesis and metabolism. *Arabidopsis Book.* **9**, e0156

[220] Nemhauser J.L., Hong F., Chory J. (2006) Different Plant Hormones Regulate Similar Processes through Largely Nonoverlapping Transcriptional Responses. *Cell.* **126**, 467–475

[221] Jaillais Y., Chory J. (2010) Unraveling the paradoxes of plant hormone signaling integration. *Nat. Struct. Mol. Biol.* **17**, 642–5

[222] Bari R., Jones J.D.G. (2009) Role of plant hormones in plant defence responses. *Plant Mol. Biol.* **69**, 473–488

[223] Yan J., Zhang C., Gu M., Bai Z., Zhang W., Qi T., et al. (2009) The Arabidopsis CORONATINE INSENSITIVE1 Protein Is a Jasmonate Receptor. *Plant Cell.* **21**, 2220–2236

[224] Santner A., Estelle M. (2007) The JAZ proteins link jasmonate perception with transcriptional changes. *Plant Cell.* **19**, 3839–3842

[225] Katsir L., Chung H.S., Koo A.J., Howe G.A. (2008) Jasmonate signaling: a conserved mechanism of hormone sensing. *Curr. Opin. Plant Biol.* **11**, 428–435

[226] Creelman R.A., Mulpuri R. (2002) The Oxylipin Pathway in *Arabidopsis*. *Arabidopsis Book.* **1**, e0012

[227] Chehab E.W., Kaspi R., Savchenko T., Rowe H., Negre-Zakharov F., Kliebenstein D., et al. (2008) Distinct roles of jasmonates and aldehydes in plant-defense responses. *PLoS One.* **3**, 1–10

[228] Savchenko T., Pearse I.S., Ignatia L., Karban R., Dehesh K. (2013) Insect herbivores selectively suppress the HPL branch of the oxylipin pathway in host plants. *Plant J.* **73**, 653–662

[229] Wang K.L., Li H., Ecker J.R. (2002) Ethylene Biosynthesis and Signaling Networks. *Plant Cell.* **14**, 131–152

[230] Spoel S.H., Johnson J.S., Dong X. (2007) Regulation of tradeoffs between plant defenses against pathogens with different lifestyles. *Proc. Natl. Acad. Sci. USA.* **104**, 18842–18847

[231] Caarls L., Pieterse C.M.J., Van Wees S.C.M. (2015) How salicylic acid takes transcriptional control over jasmonic acid signaling. *Front. Plant Sci.* **6**, 1–11

[232] Doares S.H., Narváez-vpsquez J., Conconi A., Ryan C.A. (1995) Salicylic Acid lnhibits Synthesis of Proteinase lnhibitors in Tomato Leaves lnduced by Systemin and Jasmonic Acid. *Plant Physiol.* **108**, 1741–1746

[233] Niki T., Mitsuhara I., Seo S., Ohtsubo N., Ohashi Y. (1998) Antagonistic Effect of Salicylic Acid and Jasmonic Acid on the Expression of Pathogenesis-Related (PR)

Protein Genes in Wounded Mature Tobacco Leaves. *Plant Cell Physiol.* **39**, 500–507

[234] Mur L.A.J., Kenton P., Atzorn R., Miersch O., Wasternack C. (2005) The Outcomes of Concentration-Specific Interactions between Salicylate and Jasmonate Signaling Include Synergy, Antagonism, and Oxidative Stress Leading to Cell Death. *Plant Physiol.* **140**, 249–262

[235] Liu L., Sonbol F.-M., Huot B., Gu Y., Withers J., Mwimba M., et al. (2016) Salicylic acid receptors activate jasmonic acid signalling through a non-canonical pathway to promote effector-triggered immunity. *Nat. Commun.* **7**, 1–10

[236] Lievens L., Pollier J., Goossens A., Beyaert R., Staal J. (2017) Abscisic Acid as Pathogen Effector and Immune Regulator. *Front. Plant Sci.* **8**, 587

[237] De Bruyne L., Höfte M., De Vleesschauwer D. (2014) Connecting growth and defense: The emerging roles of brassinosteroids and gibberellins in plant innate immunity. *Mol. Plant.* **7**, 943–959

[238] Wilson P.B., Estavillo G.M., Field K.J., Pornsiriwong W., Carroll A.J., Howell K.A., et al. (2009) The nucleotidase/phosphatase SAL1 is a negative regulator of drought tolerance in *Arabidopsis*. *Plant J.* **58**, 299–317

[239] Quintero F.J., Garciadeblás B., Rodríguez-Navarro A. (1996) The SAL1 gene of arabidopsis, encoding an enzyme with 3′(2′),5′-bisphosphate nucleotidase and inositol polyphosphate 1-phosphatase activities, increases salt tolerance in yeast. *Plant Cell.* **8**, 529–537

[240] Banerjee A., Sharkey T.D. (2014) Methylerythritol 4-phosphate (MEP) pathway metabolic regulation. *Nat. Prod. Rep.* **31**, 1043–1055

[241] de Souza A., Wang J.-Z., Dehesh K. (2017) Retrograde Signals: Integrators of Interorganellar Communication and Orchestrators of Plant Development. *Annu. Rev. Plant Biol.* **68**, 85–108

[242] El Oirdi M., El Rahman T.A., Rigano L., El Hadrami A., Rodriguez M.C., Daayf F., et al. (2011) *Botrytis cinerea* Manipulates the Antagonistic Effects between Immune Pathways to Promote Disease Development in Tomato. *Plant Cell.* **23**, 2405–2421

[243] Rahman T.A. El, Oirdi M. El, Gonzalez-Lamothe R., Bouarab K. (2012) Necrotrophic pathogens use the salicylic acid signaling pathway to promote disease development in tomato. *Mol. Plant. Microbe. Interact.* **25**, 1584–1593

[244] Navarro L., Bari R., Achard P., Lisón P., Nemri A., Harberd N.P., et al. (2008) DELLAs Control Plant Immune Responses by Modulating the Balance of Jasmonic Acid and Salicylic Acid Signaling. *Curr. Biol.* **18**, 650–655

[245] Geng X., Jin L., Shimada M., Kim M.G., Mackey D. (2014) The phytotoxin coronatine is a multifunctional component of the virulence armament of *Pseudomonas syringae*. *Planta.* **240**, 1149–1165

[246] Thatcher L.F., Manners J.M., Kazan K. (2009) *Fusarium oxysporum* hijacks COI1-mediated jasmonate signaling to promote disease development in *Arabidopsis*. *Plant J.* **58**, 927–939

[247] Thatcher L.F., Gardiner D.M., Kazan K., Manners J.M. (2012) A Highly Conserved Effector in *Fusarium oxysporum* Is Required for Full Virulence on *Arabidopsis*. *Mol. Plant. Microbe. Interact.* **25**, 180–190

[248] Jiang S., Yao J., Ma K.W., Zhou H., Song J., He S.Y., et al. (2013) Bacterial Effector Activates Jasmonate Signaling by Directly Targeting JAZ Transcriptional Repressors. *PLoS Pathog.* **9**, e1003715

[249] Gimenez-Ibanez S., Boter M., Fernández-Barbero G., Chini A., Rathjen J.P., Solano R. (2014) The Bacterial Effector HopX1 Targets JAZ Transcriptional Repressors to Activate Jasmonate Signaling and Promote Infection in Arabidopsis. *PLoS Biol.* **12**, e1001792

[250] Dar N.A., Amin I., Wani W., Wani S.A., Shikari A.B., Wani S.H., et al. (2017) Abscisic acid: A key regulator of abiotic stress tolerance in plants. *Plant Gene.* **11**, 106–111

[251] Mbengue M., Navaud O., Peyraud R., Barascud M., Badet T., Vincent R., et al. (2016) Emerging Trends in Molecular Interactions between Plants and the Broad Host Range Fungal Pathogens Botrytis cinerea and Sclerotinia sclerotiorum. *Front. Plant Sci.* **7**, 1–9

[252] de Torres-Zabala M., Truman W., Bennett M.H.M.H., Lafforgue G., Mansfield J.W.J.W., Rodriguez Egea P., et al. (2007) *Pseudomonas syringae* pv. *tomato* hijacks the *Arabidopsis* abscisic acid signalling pathway to cause disease. *EMBO J.* **26**, 1434–1443

[253] de Torres Zabala M., Littlejohn G., Jayaraman S., Studholme D., Bailey T., Lawson T., et al. (2015) Chloroplasts play a central role in plant defence and are targeted by pathogen effectors. *Nat. Plants.* **1**, 15074

[254] Lamb C., Dixon R.A. (1997) The Oxidative Burst in Plant Disease Resistance. *Annu. Rev. Plant Physiol. Plant Mol. Biol.* **48**, 251–275

[255] Camejo D., Guzmán-Cedeño Á., Moreno A. (2016) Reactive Oxygen Species, essential molecules, during plant-pathogen interactions. *Plant Physiol. Biochem.* **103**, 10–23

[256] Kadota Y., Shirasu K., Zipfel C. (2015) Regulation of the NADPH Oxidase RBOHD during Plant Immunity. *Plant Cell Physiol.* **56**, 1472–1480

[257] Baxter A., Mittler R., Suzuki N. (2014) ROS as key players in plant stress signalling. *J. Exp. Bot.* **65**, 1229–1240

[258] Mitchell K., Brown I., Knox P., Mansfield J. (2015) The role of cell wall-based defences in the early restriction of non-pathogenic *hrp* mutant bacteria in Arabidopsis. *Phytochemistry.* **112**, 139–150

[259] Uppalapati S.R., Ayoubi P., Weng H., Palmer D.A., Mitchell R.E., Jones W., et al. (2005) The phytotoxin coronatine and methyl jasmonate impact multiple phytohormone pathways in tomato. *Plant J.* **42**, 201–217

[260] Ishiga Y., Uppalapati S.R., Ishiga T., Elavarthi S., Martin B., Bender C.L. (2009) The phytotoxin coronatine induces light-dependent reactive oxygen species in tomato seedlings. *New Phytol.* **181**, 147–160

[261] Roach T., Krieger-Liszkay A. (2012) The role of the PsbS protein in the protection of photosystems i and II against high light in Arabidopsis thaliana. *Biochim. Biophys. Acta - Bioenerg.* **1817**, 2158–2165

[262] Wang Y., Wu Y., Tang D. (2011) The autophagy gene, ATG18a, plays a negative role in powdery mildew resistance and mildew-induced cell death in *Arabidopsis*. *Plant Signal. Behav.* **6**, 1408–1410

[263] Wang Y., Nishimura M.T., Zhao T., Tang D. (2011) ATG2, an autophagy-related protein, negatively affects powdery mildew resistance and mildew-induced cell death in *Arabidopsis*. *Plant J.* **68**, 74–87

[264] Hedtmann C., Guo W., Reifschneider E., Heiber I., Hiltscher H., van Buer J., et al. (2017) The Plant Immunity Regulating F-Box Protein CPR1 Supports Plastid Function in Absence of Pathogens. *Front. Plant Sci.* **8**, 1–22

[265] Wang X., Gou M., Bu H., Zhang S., Wang G. (2014) Proteomic analysis of *Arabidopsis* constitutive expresser of pathogenesis-related gene1 (Cpr30/cpr1-2) mutant. *Plant Omics.* **7**, 142–151

[266] Dong J., Chen W. (2013) The Role of Autophagy in Chloroplast Degradation and Chlorophagy in Immune Defenses during *Pst* DC3000 (AvrRps4) Infection. *PLoS One.* **8**, e73091

[267] Kadota Y., Sklenar J., Derbyshire P., Stransfeld L., Asai S., Ntoukakis V., et al. (2014) Direct Regulation of the NADPH Oxidase RBOHD by the PRR-Associated Kinase BIK1 during Plant Immunity. *Mol. Cell.* **54**, 43–55

[268] Torres M.A., Dangl J.L., Jones J.D.G. (2002) *Arabidopsis* gp91phox homologues

AtrbohD and AtrbohF are required for accumulation of reactive oxygen intermediates in the plant defense response. *Proc. Natl. Acad. Sci. USA.* **99**, 517–522

[269] Marino D., Dunand C., Puppo A., Pauly N. (2012) A burst of plant NADPH oxidases. *Trends Plant Sci.* **17**, 9–15

[270] Miller G., Schlauch K., Tam R., Cortes D., Torres M.A., Shulaev V., et al. (2009) The plant NADPH oxidase RBOHD mediates rapid systemic signaling in response to diverse stimuli. *Sci. Signal.* **2**, ra45

[271] Wang C., El-Shetehy M., Shine M.B., Yu K., Navarre D., Wendehenne D., et al. (2014) Free Radicals Mediate Systemic Acquired Resistance. *Cell Rep.* **7**, 348–355

[272] Liu Y., Ren D., Pike S., Pallardy S., Gassmann W., Zhang S. (2007) Chloroplast-generated reactive oxygen species are involved in hypersensitive response-like cell death mediated by a mitogen-activated protein kinase cascade. *Plant J.* **51**, 941–954

[273] Zurbriggen M.D., Carrillo N., Tognetti V.B., Melzer M., Peisker M., Hause B., et al. (2009) Chloroplast-generated reactive oxygen species play a major role in localized cell death during the non-host interaction between tobacco and *Xanthomonas campestris* pv. *vesicatoria. Plant J.* **60**, 962–973

[274] Tena G., Boudsocq M., Sheen J. (2011) Protein kinase signaling networks in plant innate immunity. *Curr. Opin. Plant Biol.* **14**, 519–529

[275] Boudsocq M., Willmann M.R., McCormack M., Lee H., Shan L., He P., et al. (2010) Differential innate immune signalling via Ca^{2+} sensor protein kinases. *Nature.* **464**, 418–422

[276] Xie K., Chen J., Wang Q., Yang Y. (2014) Direct Phosphorylation and Activation of a Mitogen-Activated Protein Kinase by a Calcium-Dependent Protein Kinase in Rice. *Plant Cell.* **26**, 1–14

[277] Romeis T., Piedras P., Jones J.D. (2000) Resistance gene-dependent activation of a calcium-dependent protein kinase in the plant defense response. *Plant Cell.* **12**, 803–816

[278] Lewis L.A., Polanski K., de Torres-Zabala M., Jayaraman S., Bowden L., Moore J., et al. (2015) Transcriptional Dynamics Driving MAMP-Triggered Immunity and Pathogen Effector-Mediated Immunosuppression in Arabidopsis Leaves Following Infection with *Pseudomonas syringae* pv *tomato* DC3000. *Plant Cell.* **27**, 3038–3064

[279] Zhou J., Wu S., Chen X., Liu C., Sheen J., Shan L., et al. (2014) The *Pseudomonas syringae* effector HopF2 suppresses *Arabidopsis* immunity by targeting BAK1.

Plant J. **77**, 235–245

[280] Wang Y., Li J., Hou S., Wang X., Li Y., Ren D., et al. (2010) A *Pseudomonas syringae* ADP-Ribosyltransferase Inhibits *Arabidopsis* Mitogen-Activated Protein Kinase Kinases. *Plant Cell.* **22**, 2033–2044

[281] Zhang J., Shao F., Li Y., Cui H., Chen L., Li H., et al. (2007) A Pseudomonas syringae Effector Inactivates MAPKs to Suppress PAMP-Induced Immunity in Plants. *Cell Host Microbe.* **1**, 175–185

[282] Cui H., Wang Y., Xue L., Chu J., Yan C., Fu J., et al. (2010) Pseudomonas syringae Effector Protein AvrB Perturbs Arabidopsis Hormone Signaling by Activating MAP Kinase 4. *Cell Host Microbe.* **7**, 164–175

[283] Canonne J., Rivas S. (2012) Bacterial effectors target the plant cell nucleus to subvert host transcription. *Plant Signal. Behav.* **7**, 217–221

[284] Block A., Toruño T.Y., Elowsky C.G., Zhang C., Steinbrenner J., Beynon J., et al. (2014) The *Pseudomonas syringae* type III effector HopD1 suppresses effector-triggered immunity, localizes to the endoplasmic reticulum, and targets the *Arabidopsis* transcription factor NTL9. *New Phytol.* **201**, 1358–1370

[285] Kay S., Hahn S., Marois E., Hause G., Bonas U. (2007) A Bacterial Effector Acts as a Plant Transcription Factor and Induces a Cell Size Regulator. *Science.* **318**, 648–651

[286] Cai L., Cao Y., Xu Z., Ma W., Zakria M., Zou L., et al. (2017) A Transcription Activator-Like Effector Tal7 of Xanthomonas oryzae pv. oryzicola Activates Rice Gene Os09g29100 to Suppress Rice Immunity. *Sci. Rep.* **7**, 5089

[287] Ma K.-W., Flores C., Ma W. (2011) Chromatin Configuration as a Battlefield in Plant-Bacteria Interactions. *Plant Physiol.* **157**, 535–543

[288] Hicks S.W., Galán J.E. (2013) Exploitation of eukaryotic subcellular targeting mechanisms by bacterial effectors. *Nat. Rev. Microbiol.* **11**, 316–326

[289] Escoll P., Mondino S., Rolando M., Buchrieser C. (2015) Targeting of host organelles by pathogenic bacteria: a sophisticated subversion strategy. *Nat. Rev. Microbiol.* **14**, 5–19

[290] Li G., Froehlich J.E., Elowsky C., Msanne J., Ostosh A.C., Zhang C., et al. (2014) Distinct *Pseudomonas type*-III effectors use a cleavable transit peptide to target chloroplasts. *Plant J.* **77**, 310–321

[291] Petre B., Lorrain C., Saunders D.G.O., Win J., Sklenar J., Duplessis S., et al. (2016) Rust fungal effectors mimic host transit peptides to translocate into chloroplasts. *Cell. Microbiol.* **18**, 453–465

[292] Petre B., Saunders D.G.O., Sklenar J., Lorrain C., Win J., Duplessis S., et al. (2015) Candidate Effector Proteins of the Rust Pathogen *Melampsora larici-populina* Target Diverse Plant Cell Compartments. *Mol. Plant. Microbe. Interact.* **28**, 689–700

[293] Xiang Y., Kakani K., Reade R., Hui E., Rochon D. (2006) A 38-amino-acid sequence encompassing the arm domain of the cucumber necrosis virus coat protein functions as a chloroplast transit peptide in infected plants. *J. Virol.* **80**, 7952–64

[294] Emanuelsson O., Nielsen H., von Heijne G. (1999) ChloroP, a neural network-based method for predicting chloroplast transit peptides and their cleavage sites. *Protein Sci.* **8**, 978–984

[295] Jelenska J., Yao N., Vinatzer B.A., Wright C.M., Brodsky J.L., Greenberg J.T. (2007) A J-domain Virulence Effector of *Pseudomonas syringae* Remodels Host Chloroplasts and Suppresses Defenses. *Curr. Biol.* **17**, 499–508

[296] Rodríguez-Herva J.J., González-Melendi P., Cuartas-Lanza R., Antúnez-Lamas M., Río-Alvarez I., Li Z., et al. (2012) A bacterial cysteine protease effector protein interferes with photosynthesis to suppress plant innate immune responses. *Cell. Microbiol.* **14**, 669–681

[297] Jelenska J., van Hal J.A., Greenberg J.T. (2010) *Pseudomonas syringae* hijacks plant stress chaperone machinery for virulence. *Proc. Natl. Acad. Sci. USA.* **107**, 13177–13182

[298] Qiao Y., Li H.F., Wong S.M., Fan Z.F. (2009) Plastocyanin transit peptide interacts with Potato virus X coat protein, while silencing of plastocyanin reduces coat protein accumulation in chloroplasts and symptom severity in host plants. *Mol. Plant. Microbe. Interact.* **22**, 1523–1534

[299] Chotewutmontri P., Bruce B.D. (2015) Non-native, N-terminal Hsp70 molecular motor recognition elements in transit peptides support plastid protein translocation. *J. Biol. Chem.* **290**, 7602–7621

[300] Yalovsky S., Paulsen H., Michaeli D., Chitnis P.R., Nechushtai R. (1992) Involvement of a chloroplast HSP70 heat shock protein in the integration of a protein (light-harvesting complex protein precursor) into the thylakoid membrane. *Proc. Natl. Acad. Sci. USA.* **89**, 5616–5619

[301] Schroda M., Vallon O., Wollman F. a, Beck C.F. (1999) A chloroplast-targeted heat shock protein 70 (HSP70) contributes to the photoprotection and repair of photosystem II during and after photoinhibition. *Plant Cell.* **11**, 1165–78

[302] Hurley B., Lee D., Mott A., Wilton M., Liu J., Liu Y.C., et al. (2014) The Pseudomonas syringae type III effector HopF2 suppresses arabidopsis stomatal

immunity. *PLoS One.* **9**, 1–20

[303] Nomura H., Komori T., Kobori M., Nakahira Y., Shiina T. (2008) Evidence for chloroplast control of external Ca2+-induced cytosolic Ca2+ transients and stomatal closure. *Plant J.* **53**, 988–998

[304] Bernoux M., Timmers T., Jauneau A., Briere C., de Wit P.J.G.M., Marco Y., et al. (2008) RD19, an *Arabidopsis* cysteine protease required for RRS1-R-mediated resistance, is relocalized to the nucleus by the *Ralstonia solanacearum* PopP2 effector. *Plant Cell.* **20**, 2252–2264

[305] Engelhardt S., Boevink P.C., Armstrong M.R., Ramos M.B., Hein I., Birch P.R.J. (2012) Relocalization of late blight resistance protein R3a to endosomal compartments is associated with effector recognition and required for the immune response. *Plant Cell.* **24**, 5142–5158

[306] Rico A., Preston G.M. (2008) *Pseudomonas syringae* pv. *tomato* DC3000 Uses Constitutive and Apoplast-Induced Nutrient Assimilation Pathways to Catabolize Nutrients That Are Abundant in the Tomato Apoplast. *Mol. Plant. Microbe. Interact.* **21**, 269–282

[307] Nomura H., Komori T., Uemura S., Kanda Y., Shimotani K., Nakai K., et al. (2012) Chloroplast-mediated activation of plant immune signalling in Arabidopsis. *Nat. Commun.*

[308] Schwarzländer M., Fricker M.D., Müller C., Marty L., Brach T., Novak J., et al. (2008) Confocal imaging of glutathione redox potential in living plant cells. *J. Microsc.* **231**, 299–316

[309] Schwarzländer M., Dick T.P., Meyer A.J., Morgan B. (2016) Dissecting Redox Biology Using Fluorescent Protein Sensors. *Antioxid. Redox Signal.* **24**, 680–712

[310] Law M.Y., Charles S.A., Halliwell B. (1983) Glutathione and ascorbic acid in spinach (Spinacia oleracea) chloroplasts. The effect of hydrogen peroxide and of Paraquat. *Biochem. J.* **210**, 899–903

[311] Espinoza C., Medina C., Somerville S., Arce-Johnson P. (2007) Senescence-associated genes induced during compatible viral interactions with grapevine and Arabidopsis. *J. Exp. Bot.* **58**, 3197–3212

[312] Rosenvasser S., Mayak S., Friedman H. (2006) Increase in reactive oxygen species (ROS) and in senescence-associated gene transcript (SAG) levels during dark-induced senescence of Pelargonium cuttings, and the effect of gibberellic acid. *Plant Sci.* **170**, 873–879

[313] Khanna-Chopra R. (2012) Leaf senescence and abiotic stresses share reactive

oxygen species-mediated chloroplast degradation. *Protoplasma.* **249**, 469–481

[314] Mubarakshina M.M., Ivanov B.N., Naydov I.A., Hillier W., Badger M.R., Krieger-Liszkay A. (2010) Production and diffusion of chloroplastic H2O2 and its implication to signalling. *J. Exp. Bot.* **61**, 3577–3587

[315] Shirano Y., Kachroo P., Shah J., Klessig D.F. (2002) A Gain-of-Function Mutation in an Arabidopsis Toll Interleukin1 Receptor-Nucleotide Binding Site-Leucine-Rich Repeat Type R Gene Triggers Defense Responses and Results in Enhanced Disease Resistance. *Plant Cell.* **14**, 3149–3162

[316] Li X., Clarke J.D., Zhang Y., Dong X. (2001) Activation of an EDS1-Mediated *R* -Gene Pathway in the *snc1* Mutant Leads to Constitutive, NPR1-Independent Pathogen Resistance. *Mol. Plant. Microbe. Interact.* **14**, 1131–1139

[317] Belkhadir Y., Nimchuk Z., Hubert D.A., Mackey D., Dangl J.L. (2004) Arabidopsis RIN4 Negatively Regulates Disease Resistance Mediated by RPS2 and RPM1 Downstream or Independent of the NDR1 Signal Modulator and Is Not Required for the Virulence Functions of Bacterial Type III Effectors AvrRpt2 or AvrRpm1. *Plant Cell.* **16**, 2822–2835

[318] Zhu Z., Xu F., Zhang Y., Cheng Y.T., Wiermer M., Li X., et al. (2010) Arabidopsis resistance protein SNC1 activates immune responses through association with a transcriptional corepressor. *Proc. Natl. Acad. Sci. USA.* **107**, 13960–13965

[319] Cheng Y.T., Li Y., Huang S., Huang Y., Dong X., Zhang Y., et al. (2011) Stability of plant immune-receptor resistance proteins is controlled by SKP1-CULLIN1-F-box (SCF)-mediated protein degradation. *Proc. Natl. Acad. Sci. USA.* **108**, 14694–9

[320] Boyes D.C., Nam J., Dangl J.L. (1998) The Arabidopsis thaliana RPM1 disease resistance gene product is a peripheral plasma membrane protein that is degraded coincident with the hypersensitive response. *Proc. Natl. Acad. Sci. USA.* **95**, 15849–54

[321] Mackey D., Holt B.F., Wiig A., Dangl J.L. (2002) RIN4 interacts with Pseudomonas syringae type III effector molecules and is required for RPM1-mediated resistance in Arabidopsis. *Cell.* **108**, 743–54

[322] Liu J., Elmore J.M., Fuglsang A.T., Palmgren M.G., Staskawicz B.J., Coaker G. (2009) RIN4 Functions with Plasma Membrane H+-ATPases to Regulate Stomatal Apertures during Pathogen Attack. *PLoS Biol.* **7**, e1000139

[323] van Wersch R., Li X., Zhang Y. (2016) Mighty Dwarfs: Arabidopsis Autoimmune Mutants and Their Usages in Genetic Dissection of Plant Immunity. *Front. Plant Sci.* **7**, 1717

[324] Bruggeman Q., Raynaud C., Benhamed M., Delarue M. (2015) To die or not to die? Lessons from lesion mimic mutants. *Front. Plant Sci.* **6**, 24

[325] Block A., Guo M., Li G., Elowsky C., Clemente T.E., Alfano J.R. (2010) The Pseudomonas syringae type III effector HopG1 targets mitochondria, alters plant development and suppresses plant innate immunity. *Cell. Microbiol.* **12**, 318–30

[326] Preston G.M. (2017) Profiling the extended phenotype of plant pathogens. *Mol. Plant Pathol.* **18**, 443–456

[327] Xin X.-F., Nomura K., Aung K., Velásquez A.C., Yao J., Boutrot F., et al. (2016) Bacteria establish an aqueous living space in plants crucial for virulence. *Nature.* **539**, 524–529

[328] Malhotra J.D., Miao H., Zhang K., Wolfson A., Pennathur S., Pipe S.W., et al. (2008) Antioxidants reduce endoplasmic reticulum stress and improve protein secretion. *Proc. Natl. Acad. Sci. USA.* **105**, 18525–18530

[329] Liu Y., Li J. (2014) Endoplasmic reticulum-mediated protein quality control in Arabidopsis. *Front. Plant Sci.* **5**, 162

[330] Hwang J., Qi L. (2018) Quality Control in the Endoplasmic Reticulum: Crosstalk between ERAD and UPR pathways. *Trends Biochem. Sci.* **43**, 593–605

[331] Shpilka T., Haynes C.M. (2018) The mitochondrial UPR: mechanisms, physiological functions and implications in ageing. *Nat. Rev. Mol. Cell Biol.* **19**, 109–120

[332] Boos F., Krämer L., Groh C., Jung F., Haberkant P., Stein F., et al. (2019) Mitochondrial protein-induced stress triggers a global adaptive transcriptional programme. *Nat. Cell Biol.* **21**, 442–451

[333] Callegari S., Dennerlein S. (2018) Sensing the Stress: A Role for the UPRmt and UPRam in the Quality Control of Mitochondria. *Front. Cell Dev. Biol.* **6**, 31

[334] Ramundo S., Casero D., Mühlhaus T., Hemme D., Sommer F., Crèvecoeur M., et al. (2014) Conditional Depletion of the Chlamydomonas Chloroplast ClpP Protease Activates Nuclear Genes Involved in Autophagy and Plastid Protein Quality Control. *Plant Cell.* **26**, 2201–2222

[335] Dogra V., Duan J., Lee K.P., Kim C. (2019) Impaired PSII proteostasis triggers a UPR-like response in the var2 mutant of Arabidopsis. *J. Exp. Bot.* **70**, 3075–3088

[336] do Amaral M.N., Arge L.W.P., Benitez L.C., Danielowski R., da Silveira Silveira S.F., da Rosa Farias D., et al. (2016) Differential expression of photosynthesis-related genes and quantification of gas exchange in rice plants under abiotic stress. *Acta Physiol. Plant.* **38**, 153

[337] Berry J.O., Yerramsetty P., Zielinski A.M., Mure C.M. (2013) Photosynthetic gene expression in higher plants. *Photosynth. Res.* **117**, 91–120

[338] Saijo Y., Loo E.P. (2019) Plant immunity in signal integration between biotic and abiotic stress responses. *New Phytol.* , nph.15989

[339] Sinha R., Irulappan V., Mohan-Raju B., Suganthi A., Senthil-Kumar M. (2019) Impact of drought stress on simultaneously occurring pathogen infection in field-grown chickpea. *Sci. Rep.* **9**, 5577

[340] Dangi A.K., Sharma B., Khangwal I., Shukla P. (2018) Combinatorial Interactions of Biotic and Abiotic Stresses in Plants and Their Molecular Mechanisms: Systems Biology Approach. *Mol. Biotechnol.* **60**, 636–650

[341] Chojak-Koźniewska J., Kuźniak E., Zimny J. (2018) The Effects of Combined Abiotic and Pathogen Stress in Plants: Insights From Salinity and *Pseudomonas syringae* pv *lachrymans* Interaction in Cucumber. *Front. Plant Sci.* **9**, 1691

[342] Ariga H., Katori T., Tsuchimatsu T., Hirase T., Tajima Y., Parker J.E., et al. (2017) NLR locus-mediated trade-off between abiotic and biotic stress adaptation in Arabidopsis. *Nat. Plants.* **3**, 17072

[343] Zhu Y., Qian W., Hua J. (2010) Temperature Modulates Plant Defense Responses through NB-LRR Proteins. *PLoS Pathog.* **6**, e1000844

[344] Chini A., Grant J.J., Seki M., Shinozaki K., Loake G.J. (2004) Drought tolerance established by enhanced expression of the *CC-NBS-LRR* gene, *ADR1* , requires salicylic acid, EDS1 and ABI1. *Plant J.* **38**, 810–822

[345] Li X., Huang L., Zhang Y., Ouyang Z., Hong Y., Zhang H., et al. (2014) Tomato SR/CAMTA transcription factors SlSR1 and SlSR3L negatively regulate disease resistance response and SlSR1L positively modulates drought stress tolerance. *BMC Plant Biol.* **14**, 286

[346] Prasad K.V.S.K., Abdel-Hameed A.A.E., Xing D., Reddy A.S.N. (2016) Global gene expression analysis using RNA-seq uncovered a new role for SR1/CAMTA3 transcription factor in salt stress. *Sci. Rep.* **6**, 27021

[347] Chen L., Zou W., Fei C., Wu G., Li X., Lin H., et al. (2018) α-Expansin EXPA4 Positively Regulates Abiotic Stress Tolerance but Negatively Regulates Pathogen Resistance in Nicotiana tabacum. *Plant Cell Physiol.* **59**, 2317–2330

[348] Mine A., Berens M.L., Nobori T., Anver S., Fukumoto K., Winkelmüller T.M., et al. (2017) Pathogen exploitation of an abscisic acid- and jasmonate-inducible MAPK phosphatase and its interception by *Arabidopsis* immunity. *Proc. Natl. Acad. Sci. USA.* **114**, 7456–7461

[349] Liao Y., Bai Q., Xu P., Wu T., Guo D., Peng Y., et al. (2018) Mutation in Rice Abscisic Acid2 Results in Cell Death, Enhanced Disease-Resistance, Altered Seed Dormancy and Development. *Front. Plant Sci.* **9**, 405

[350] Watson S.J., Sowden R.G., Jarvis P. (2018) Abiotic stress-induced chloroplast proteome remodelling: a mechanistic overview. *J. Exp. Bot.* **69**, 2773–2781

[351] Bauer J., Chen K., Hiltbrunner A., Wehrli E., Eugster M., Schnell D., et al. (2000) The major protein import receptor of plastids is essential for chloroplast biogenesis. *Nature.* **403**, 203–207

[352] Baldwin A., Wardle A., Patel R., Dudley P., Park S.K., Twell D., et al. (2005) A molecular-genetic study of the Arabidopsis Toc75 gene family. *Plant Physiol.* **138**, 715–733

[353] Olinares P.D., Kim J., van Wijk K.J. (2011) The Clp protease system; a central component of the chloroplast protease network. *Biochim. Biophys. Acta.* **1807**, 999–1011

[354] Nishimura K., Kato Y., Sakamoto W. (2016) Chloroplast Proteases: Updates on Proteolysis within and across Suborganellar Compartments. *Plant Physiol.* **171**, 2280–93

[355] Nishimura K., Kato Y., Sakamoto W. (2016) Essentials of proteolytic machineries in chloroplasts. *Mol. Plant.* **10**, 4–19

[356] Pike S.M., Zhang X.-C., Gassmann W. (2005) Electrophysiological characterization of the Arabidopsis avrRpt2-specific hypersensitive response in the absence of other bacterial signals. *Plant Physiol.* **138**, 1009–17

[357] Keppler L.D., Novacky A. (1987) The initiation of membrane lipid peroxidation during bacteria-induced hypersensitive reaction. *Physiol. Mol. Plant Pathol.* **30**, 233–245

[358] Schulz A., Knoetzel J., Scheller H. V., Mant A. (2004) Uptake of a Fluorescent Dye as a Swift and Simple Indicator of Organelle Intactness: Import-competent Chloroplasts from Soil-grown Arabidopsis. *J. Histochem. Cytochem.* **52**, 701–704

[359] Ishiga Y., Ishiga T., Uppalapati S.R., Mysore K.S. (2011) *Arabidopsis* seedling flood-inoculation technique: a rapid and reliable assay for studying plant-bacterial interactions. *Plant Methods.* **7**, 32

[360] Hanson M.R., Sattarzadeh A. (2011) Stromules: recent insights into a long neglected feature of plastid morphology and function. *Plant Physiol.* **155**, 1486–92

[361] Hanson M.R., Sattarzadeh A. (2013) Trafficking of proteins through plastid stromules. *Plant Cell.* **25**, 2774–82

[362] Hanson M.R., Köhler R.H. (2001) GFP imaging: methodology and application to investigate cellular compartmentation in plants. *J. Exp. Bot.* **52**, 529–539

[363] Hanson M.R., Sattarzadeh A. (2008) Dynamic morphology of plastids and stromules in angiosperm plants. *Plant Cell Env.* **31**, 646–657

[364] Vladimirou E., Li M., Aldridge C.P., Frigerio L., Kirkilionis M., Robinson C. (2009) Diffusion of a membrane protein, Tat subunit Hcf106, is highly restricted within the chloroplast thylakoid network. *FEBS Lett.* **583**, 3690–3696

[365] Craggs T.D. (2009) Green fluorescent protein: structure, folding and chromophore maturation. *Chem. Soc. Rev.* **38**, 2865

[366] Li W., Li J., Bao J. (2012) Microautophagy: lesser-known self-eating. *Cell. Mol. Life Sci.* **69**, 1125–1136

[367] Pincet F., Adrien V., Yang R., Delacotte J., Rothman J.E., Urbach W., et al. (2016) FRAP to Characterize Molecular Diffusion and Interaction in Various Membrane Environments. *PLoS One.* **11**, e0158457

[368] Iizuka R., Yamagishi-Shirasaki M., Funatsu T. (2011) Kinetic study of de novo chromophore maturation of fluorescent proteins. *Anal. Biochem.* **414**, 173–178

[369] Kohler R.H., Zipfel W.R., Webb W.W., Hanson M.R. (1997) The green fluorescent protein as a marker to visualize plant mitochondria in vivo. *Plant J.* **11**, 613–621

[370] Caplan J.L., Kumar A.S., Park E., Padmanabhan M.S., Hoban K., Modla S., et al. (2015) Chloroplast Stromules Function during Innate Immunity. *Dev. Cell.* **34**, 45–57

[371] Luu D.-T., Martinière A., Sorieul M., Runions J., Maurel C. (2012) Fluorescence recovery after photobleaching reveals high cycling dynamics of plasma membrane aquaporins in Arabidopsis roots under salt stress. *Plant J.* **69**, 894–905

[372] Lukyanov K.A., Chudakov D.M., Lukyanov S., Verkhusha V. V. (2005) Photoactivatable fluorescent proteins. *Nat. Rev. Mol. Cell Biol.* **6**, 885–890

[373] Mathur J., Radhamony R., Sinclair A.M., Donoso A., Dunn N., Roach E., et al. (2010) mEosFP-based green-to-red photoconvertible subcellular probes for plants. *Plant Physiol.* **154**, 1573–87

[374] Penaloza-Vazquez A., Preston G.M., Collmer A., Bender C.L. (2000) Regulatory interactions between the Hrp type III protein secretion system and coronatine biosynthesis in *Pseudomonas syringae* pv. *tomato* DC3000. *Microbiology.* **146**, 2447–2456

[375] Hill R., Bendall F. (1960) Function of the Two Cytochrome Components in

Chloroplasts: A Working Hypothesis. *Nature.* **186**, 136–137

[376] Govindjee, Van Rensen J.J.S. (1978) Bicarbonate effects on the electron flow in isolated broken chloroplasts. *Biochim. Biophys. Acta - Rev. Bioenerg.* **505**, 183–213

[377] Bassham J.A., Benson A.A., Calvin M. (1950) The path of carbon in photosynthesis. *J. Biol. Chem.* **185**, 781–7

[378] Mehler A.H. (1951) Studies on reactions of illuminated chloroplasts: I. Mechanism of the reduction of oxygen and other hill reagents. *Arch. Biochem. Biophys.* **33**, 65–77

[379] Niyogi K.K., Truong T.B. (2013) Evolution of flexible non-photochemical quenching mechanisms that regulate light harvesting in oxygenic photosynthesis. *Curr. Opin. Plant Biol.* **16**, 307–314

[380] Goss R., Lepetit B. (2015) Biodiversity of NPQ. *J. Plant Physiol.* **172**, 13–32

[381] Baker N.R. (2008) Chlorophyll Fluorescence: A Probe of Photosynthesis In Vivo. *Annu. Rev. Plant Biol.* **59**, 89–113

[382] Kramer D.M., Johnson G., Kiirats O., Edwards G.E. (2004) New fluorescence parameters for the determination of Q_A redox state and excitation energy fluxes. *Photosynth. Res.* **79**, 209–218

[383] Klughammer C., Schreiber U. (2008) Complementary PS II quantum yields calculated from simple fluorescence parameters measured by PAM fluorometry and the Saturation Pulse method. *PAM Appl. Notes.* **1**, 27–35

[384] Bonfig K.B., Schreiber U., Gabler A., Roitsch T., Berger S. (2006) Infection with virulent and avirulent P. syringae strains differentially affects photosynthesis and sink metabolism in Arabidopsis leaves. *Planta.* **225**, 1–12

[385] Nohales M.A., Kay S.A. (2016) Molecular mechanisms at the core of the plant circadian oscillator. *Nat. Struct. Mol. Biol.* **23**, 1061–1069

[386] Lu H., McClung C.R., Zhang C. (2017) Tick Tock: Circadian Regulation of Plant Innate Immunity. *Annu. Rev. Phytopathol.* **55**, 287–311

[387] Bhardwaj V., Meier S., Petersen L.N., Ingle R.A., Roden L.C. (2011) Defence Responses of Arabidopsis thaliana to Infection by Pseudomonas syringae Are Regulated by the Circadian Clock. *PLoS One.* **6**, e26968

[388] Zhang C., Xie Q., Anderson R.G., Ng G., Seitz N.C., Peterson T., et al. (2013) Crosstalk between the Circadian Clock and Innate Immunity in Arabidopsis. *PLoS Pathog.* **9**, e1003370

[389] Fu Z.Q., Guo M., Jeong B., Tian F., Elthon T.E., Cerny R.L., et al. (2007) A type III

effector ADP-ribosylates RNA-binding proteins and quells plant immunity. *Nature.* **447**, 284–288

[390] Fukuda H., Murase H., Tokuda I.T. (2013) Controlling Circadian Rhythms by Dark-Pulse Perturbations in Arabidopsis thaliana. *Sci. Rep.* **3**, 1533

[391] Maxwell K., Johnson G.N. (2000) Chlorophyll fluorescence—a practical guide. *J. Exp. Bot.* **51**, 659–668

[392] Spoel S.H., Loake G.J. (2011) Redox-based protein modifications: the missing link in plant immune signalling. *Curr. Opin. Plant Biol.* **14**, 358–364

[393] McConnell E.W., Berg P., Westlake T.J., Wilson K.M., Popescu G. V, Hicks L.M., et al. (2019) Proteome-Wide Analysis of Cysteine Reactivity during Effector-Triggered Immunity. *Plant Physiol.* **179**, 1248–1264

[394] Xia X.-J., Zhou Y.-H., Shi K., Zhou J., Foyer C.H., Yu J.-Q. (2015) Interplay between reactive oxygen species and hormones in the control of plant development and stress tolerance. *J. Exp. Bot.* **66**, 2839–56

[395] Chan K.X., Mabbitt P.D., Phua S.Y., Mueller J.W., Nisar N., Gigolashvili T., et al. (2016) Sensing and signaling of oxidative stress in chloroplasts by inactivation of the SAL1 phosphoadenosine phosphatase. *Proc. Natl. Acad. Sci. USA.* **113**, E4567–E4576

[396] French E., Kim B.-S., Iyer-Pascuzzi A.S. (2016) Mechanisms of quantitative disease resistance in plants. *Semin. Cell Dev. Biol.* **56**, 201–208

[397] Boyd L.A., Ridout C., O'Sullivan D.M., Leach J.E., Leung H. (2013) Plant–pathogen interactions: disease resistance in modern agriculture. *Trends Genet.* **29**, 233–240

[398] Huang P.-Y., Zimmerli L. (2014) Enhancing crop innate immunity: new promising trends. *Front. Plant Sci.* **5**, 624

[399] Wishart D.S., Feunang Y.D., Marcu A., Guo A.C., Liang K., Vázquez-Fresno R., et al. (2018) HMDB 4.0: the human metabolome database for 2018. *Nucleic Acids Res.* **46**, D608–D617

[400] Hanson A.D., Beaudoin G.A., McCarty D.R., Gregory J.F. (2016) Does Abiotic Stress Cause Functional B Vitamin Deficiency in Plants? *Plant Physiol.* **172**, 2082–2097

[401] Sprenger H., Kurowsky C., Horn R., Erban A., Seddig S., Rudack K., et al. (2016) The drought response of potato reference cultivars with contrasting tolerance. *Plant. Cell Environ.* **39**, 2370–2389

[402] Isherwood F.A., Mapson L.W. (1956) Biological synthesis of ascorbic acid: the

conversion of derivatives of D-galacturonic acid into L-ascorbic acid by plant extracts. *Biochem. J.* **64**, 13–22

[403] Agius F., González-Lamothe R., Caballero J.L., Muñoz-Blanco J., Botella M.A., Valpuesta V. (2003) Engineering increased vitamin C levels in plants by overexpression of a D-galacturonic acid reductase. *Nat. Biotechnol.* **21**, 177–181

[404] Castelluccio C., Paganga G., Melikian N., Paul Bolwell G., Pridham J., Sampson J., et al. (1995) Antioxidant potential of intermediates in phenylpropanoid metabolism in higher plants. *FEBS Lett.* **368**, 188–192

[405] Nishizawa A., Yabuta Y., Shigeoka S. (2008) Galactinol and raffinose constitute a novel function to protect plants from oxidative damage. *Plant Physiol.* **147**, 1251–63

[406] O'Leary B.M., Neale H.C., Geilfus C.-M., Jackson R.W., Arnold D.L., Preston G.M. (2016) Early changes in apoplast composition associated with defence and disease in interactions between *Phaseolus vulgaris* and the halo blight pathogen *Pseudomonas syringae* Pv. phaseolicola. *Plant. Cell Environ.* **39**, 2172–2184

[407] Kaur R., Macleod J., Foley W., Nayudu M. (2006) Gluconic acid: An antifungal agent produced by Pseudomonas species in biological control of take-all. *Phytochemistry.* **67**, 595–604

[408] de Werra P., Pechy-Tarr M., Keel C., Maurhofer M. (2009) Role of Gluconic Acid Production in the Regulation of Biocontrol Traits of Pseudomonas fluorescens CHA0. *Appl. Environ. Microbiol.* **75**, 4162–4174

[409] Ward J.L., Forcat S., Beckmann M., Bennett M., Miller S.J., Baker J.M., et al. (2010) The metabolic transition during disease following infection of Arabidopsis thaliana by Pseudomonas syringae pv. tomato. *Plant J.* **63**, 443–457

[410] Chaouch S., Noctor G. (2010) Myo-inositol abolishes salicylic acid-dependent cell death and pathogen defence responses triggered by peroxisomal hydrogen peroxide. *New Phytol.* **188**, 711–718

[411] Meng P.H., Raynaud C., Tcherkez G., Blanchet S., Massoud K., Domenichini S., et al. (2009) Crosstalks between Myo-Inositol Metabolism, Programmed Cell Death and Basal Immunity in Arabidopsis. *PLoS One.* **4**, e7364

[412] Donahue J.L., Alford S.R., Torabinejad J., Kerwin R.E., Nourbakhsh A., Ray W.K., et al. (2010) The *Arabidopsis thaliana Myo-* Inositol 1-Phosphate Synthase1 Gene Is Required for *Myo* -inositol Synthesis and Suppression of Cell Death. *Plant Cell.* **22**, 888–903

[413] Torabinejad J., Donahue J.L., Gunesekera B.N., Allen-Daniels M.J., Gillaspy G.E.

(2009) VTC4 is a bifunctional enzyme that affects myoinositol and ascorbate biosynthesis in plants 1, 2[W][OA]. *Plant Physiol.* **150**, 951–961

[414] Nourbakhsh A., Collakova E., Gillaspy G.E. (2015) Characterization of the inositol monophosphatase gene family in Arabidopsis. *Front. Plant Sci.* **5**, 725

[415] Browse J., Somerville C. (1991) Glycerolipid synthesis: biochemistry and regulation. *Annu. Rev. Plant Physiol. Plant Mol. Biol.* **42**, 467–506

[416] Hölzl G., Dörmann P. (2019) Chloroplast Lipids and Their Biosynthesis. *Annu. Rev. Plant Biol.* **70**, 51–81

[417] Lim G.-H., Singhal R., Kachroo A., Kachroo P. (2017) Fatty Acid– and Lipid-Mediated Signaling in Plant Defense. *Annu. Rev. Phytopathol.* **55**, 505–536

[418] Chanda B., Venugopal S.C., Kulshrestha S., Navarre D.A., Downie B., Vaillancourt L., et al. (2008) Glycerol-3-phosphate levels are associated with basal resistance to the hemibiotrophic fungus *Colletotrichum higginsianum* in Arabidopsis. *Plant Physiol.* **147**, 2017–29

[419] Kachroo P., Shanklin J., Shah J., Whittle E.J., Klessig D.F. (2001) A fatty acid desaturase modulates the activation of defense signaling pathways in plants. *Proc. Natl. Acad. Sci. USA.* **98**, 9448–53

[420] Kachroo A., Fu D.-Q., Havens W., Navarre D., Kachroo P., Ghabrial S.A. (2008) An Oleic Acid–Mediated Pathway Induces Constitutive Defense Signaling and Enhanced Resistance to Multiple Pathogens in Soybean. *Mol. Plant. Microbe. Interact.* **21**, 564–575

[421] Chandra-Shekara A.C., Venugopal S.C., Barman S.R., Kachroo A., Kachroo P. (2007) Plastidial fatty acid levels regulate resistance gene-dependent defense signaling in Arabidopsis. *Proc. Natl. Acad. Sci. USA.* **104**, 7277–82

[422] Schnurr J.A., Shockey J.M., De Boer G.J., Browse J.A. (2002) Fatty acid export from the chloroplast. Molecular characterization of a major plastidial acyl-coenzyme A synthetase from Arabidopsis. *Plant Physiol.* **129**, 1700–1709

[423] Yaeno T., Matsuda O., Iba K. (2004) Role of chloroplast trienoic fatty acids in plaint disease defense responses. *Plant J.* **40**, 931–941

[424] Andersson M.X., Kourtchenko O., Dangl J.L., Mackey D., Ellerström M. (2006) Phospholipase-dependent signalling during the AvrRpm1- and AvrRpt2-induced disease resistance responses in *Arabidopsis thaliana*. *Plant J.* **47**, 947–959

[425] Xing J., Chin C.-K. (2000) Modification of fatty acids in eggplant affects its resistance to Verticilliumdahliae. *Physiol. Mol. Plant Pathol.* **56**, 217–225

[426] Wang C., Chin C.K., Chen A. (1998) Expression of the yeast Δ-9 desaturase gene in tomato enhances its resistance to powdery mildew. *Physiol. Mol. Plant Pathol.* **52**, 371–383

[427] Zheng N., Shabek N. (2017) Ubiquitin Ligases: Structure, Function, and Regulation. *Annu. Rev. Biochem.* **86**, 129–157

[428] Dou H., Buetow L., Hock A., Sibbet G.J., Vousden K.H., Huang D.T. (2012) Structural basis for autoinhibition and phosphorylation-dependent activation of c-Cbl. *Nat. Struct. Mol. Biol.* **19**, 184–192

[429] Ranaweera R.S., Yang X. (2013) Auto-ubiquitination of Mdm2 enhances its substrate ubiquitin ligase activity. *J. Biol. Chem.* **288**, 18939–46

[430] Chen A., Kleiman F.E., Manley J.L., Ouchi T., Pan Z.-Q. (2002) Autoubiquitination of the BRCA1·BARD1 RING Ubiquitin Ligase. *J. Biol. Chem.* **277**, 22085–22092

[431] Mergner J., Schwechheimer C. (2014) The NEDD8 modification pathway in plants. *Front. Plant Sci.* **5**, 1–15

[432] Merlet J., Burger J., Gomes J.-E., Pintard L. (2009) Regulation of cullin-RING E3 ubiquitin-ligases by neddylation and dimerization. *Cell. Mol. Life Sci.* **66**, 1924–1938

[433] Jiang M., Chiu S.-Y., Hsu W. (2011) SUMO-specific protease 2 in Mdm2-mediated regulation of p53. *Cell Death Differ.* **18**, 1005–15

[434] Buschmann T., Fuchs S.Y., Lee C.-G., Pan Z.-Q., Ronai Z. (2000) SUMO-1 Modification of Mdm2 Prevents Its Self-Ubiquitination and Increases Mdm2 Ability to Ubiquitinate p53. *Cell.* **101**, 753–762

[435] Salomon D., Orth K. (2013) Lost after translation: post-translational modifications by bacterial type III effectors. *Curr. Opin. Microbiol.* **16**, 213–20

[436] Janjusevic R., Abramovitch R.B., Martin G.B., Stebbins C.E. (2006) A Bacterial Inhibitor of Host Programmed Cell Death Defenses Is an E3 Ubiquitin Ligase. *Science*. **311**, 222–226

[437] Rosebrock T.R., Zeng L., Brady J.J., Abramovitch R.B., Xiao F., Martin G.B. (2007) A bacterial E3 ubiquitin ligase targets a host protein kinase to disrupt plant immunity. *Nature.* **448**, 370–374

[438] Gimenez-Ibanez S., Hann D.R., Ntoukakis V., Petutschnig E., Lipka V., Rathjen J.P. (2009) AvrPtoB Targets the LysM Receptor Kinase CERK1 to Promote Bacterial Virulence on Plants. *Curr. Biol.* **19**, 423–429

[439] Maculins T., Fiskin E., Bhogaraju S., Dikic I. (2016) Bacteria-host relationship:

ubiquitin ligases as weapons of invasion. *Cell Res.* **26**, 499–510

[440] Pisano A., Albano F., Vecchio E., Renna M., Scala G., Quinto I., et al. (2018) Revisiting Bacterial Ubiquitin Ligase Effectors: Weapons for Host Exploitation. *Int. J. Mol. Sci.* **19**

[441] Misaghi S., Balsara Z.R., Catic A., Spooner E., Ploegh H.L., Starnbach M.N. (2006) *Chlamydia trachomatis* -derived deubiquitinating enzymes in mammalian cells during infection. *Mol. Microbiol.* **61**, 142–150

[442] Deshaies R.J., Joazeiro C.A.P. (2009) RING Domain E3 Ubiquitin Ligases. *Annu. Rev. Biochem.* **78**, 399–434

[443] Agne B., Andrès C., Montandon C., Christ B., Ertan A., Jung F., et al. (2010) The acidic A-domain of Arabidopsis TOC159 occurs as a hyperphosphorylated protein. *Plant Physiol.* **153**, 1016–1030

[444] Oreb M., Höfle A., Mirus O., Schleiff E. (2008) Phosphorylation regulates the assembly of chloroplast import machinery. *J. Exp. Bot.* **59**, 2309–2316

[445] Witze E.S., Old W.M., Resing K.A., Ahn N.G. (2007) Mapping protein post-translational modifications with mass spectrometry. *Nat. Methods.* **4**, 798–806

[446] Kaiser P., Meierhofer D., Wang X., Huang L. (2008) Tandem Affinity Purification Combined with Mass Spectrometry to Identify Components of Protein Complexes http://www.ncbi.nlm.nih.gov/pubmed/18370112. In: Methods in molecular biology (Clifton, N.J.). 2008 [cited 2019 Oct 5]. p. 309–326.

[447] Schenk S., Schikora A. (2015) Staining of Callose Depositions in Root and Leaf Tissues. *Bio-protocol.* **5**, e1429

[448] Schindelin J., Arganda-Carreras I., Frise E., Kaynig V., Longair M., Pietzsch T., et al. (2012) Fiji: an open-source platform for biological-image analysis. *Nat. Methods.* **9**, 676–682

[449] Rueden C.T., Schindelin J., Hiner M.C., DeZonia B.E., Walter A.E., Arena E.T., et al. (2017) ImageJ2: ImageJ for the next generation of scientific image data. *BMC Bioinformatics.* **18**, 529

[450] Ridler T.W., Calvard S. (1978) Picture Thresholding Using an Iterative Selection Method. *IEEE Trans. Syst. Man. Cybern.* **8**, 630–632

[451] Littlejohn G.R., Gouveia J.D., Edner C., Smirnoff N., Love J. (2010) Perfluorodecalin enhances in vivo confocal microscopy resolution of Arabidopsis thaliana mesophyll. *New Phytol.* **186**, 1018–1025

[452] Lowe D.G. (2004) Distinctive Image Features from Scale-Invariant Keypoints. *Int.*

J. Comput. Vis. **60**, 91–110

[453] R Core Team. (2019) R: A language and environment for statistical computing. https://www.r-project.org/.

[454] R Studio Team. (2018) RStudio: Integrated Development Environment for R. http://www.rstudio.com.

[455] Mendiburu F. de. (2019) agricolae: Statistical Procedures for Agricultural Research. R package version 1.3-1 https://cran.r-project.org/package=agricolae.

[456] Fox J., Weisberg S. (2019) An R Companion to Applied Regression https://socialsciences.mcmaster.ca/jfox/Books/Companion. 3rd Editio. Thousand Oaks CA: Sage; 2019.

[457] Chen H. (2018) VennDiagram: Generate High-Resolution Venn and Euler Plots. R package version 1.6.20 https://cran.r-project.org/package=VennDiagram.